Perineuronal nets and their role in cognitive impairment in central nervous system diseases

by

John Wesley Paylor

A thesis submitted in partial fulfillment of the requirements for the degree of

Doctor of Philosophy

Department of Psychiatry

University of Alberta

Abstract

Perineuronal nets (PNNs) are organized components of the extracellular matrix that surround mature neurons of the central nervous system (CNS). These structures have neuroprotective properties for host cells, provide structural and functional stability, and have been implicated in brain functions such as learning and memory. This is particularly relevant given that the loss of PNNs is observed in diseases of the CNS, such as schizophrenia and Alzheimer's disease, which also feature cognitive impairment. Given these observations, there is great interest into identifying animal models of disease which feature similar PNN deficits as the human condition, as they could be utilized to further evaluate the significance of their loss.

In my first experiment, I evaluated PNN deficits in the 5xFAD mouse model of Alzheimer's disease. This model features amyloid-β deposition, neuroinflammation, cell loss, and cognitive impairments in tests of memory. I show that 7- and 11-month-old animals have PNN deficits in three of five brain regions examined, including the primary motor cortex, CA1 of the hippocampus, and retrosplenial cortex. I also present data showing that 7-month-old animals have an impairment in memory function. A strength of this work is its evaluation of PNN integrity across numerous brain regions, whereas a focus on a single region is a limitation of other studies in this field. Together, our findings and others indicate that the 5xFAD model exhibits PNN deficits and support is use in evaluating the mechanisms of PNN loss in AD.

In my second experiment, I address a limitation of PNN studies in animal models of disease, which is the presence of the confounding factors of disease pathophysiology. Joint observations of PNN deficits and cognitive impairment in these models cannot provide causative evidence that PNN loss contributes to these impairments. Thus, in this study I sought to degrade PNNs locally within the medial prefrontal cortex of rats to evaluate the impact on cognitive function. My results show that PNN degradation within the mPFC results in impairment in two tests of working memory. PNN degradation however did not impact behavioural flexibility or sensorimotor gating, and the integrity of PV+ interneurons or local inhibitory connectivity was unaltered. These results demonstrate that outside of the confounds of disease models, localized disruption of PNNs within the medial prefrontal cortex can impact cognitive function.

Finally, I evaluate the impact of PNN degradation in the medial prefrontal cortex and retrosplenial cortex of mice on four behavioural assessments designed to assess memory function. To degrade PNNs, I utilized a viral vector system called dox-i-ChABC which expressed ChABC under the control of a dietary trigger. This design enabled behavioural assessments at baseline, after 30 days of ChABC expression, and a subsequent 30 days after the trigger for ChABC had been withdrawn. My results indicate that PNN degradation at either site had minimal impact on cognitive performance. In animals with PNN degradation in the RSC, there was subtle impairments in performance on the crossmodal object recognition task and a loss of PV+ interneurons, although these animals also exhibited changes in exploratory behaviour which could have impacted their performance. I also evaluate the impact of PNN degradation on cortical activity patterns using wide field calcium imaging. PNN degradation left cortical activity and connectivity largely unaltered, although there were decreases in the power of low frequency activity within the RSC. Together, these experiments show that PNN degradation in the RSC of mice has subtle impacts on cognition and cortical activity.

In summary, my work shows PNN deficits in a prominent animal model of AD and shows that it may be useful in further evaluations into PNN deficits and AD. I show mixed evidence of PNNs involvement in several tests of cognitive function, which varies by the region affected and animal species. I demonstrate that PNN loss does not have an immediate effect on the integrity of closely associated PV+ cells, but that prolonged degradation can. PNN degradation also decreased the power of low frequency activity generated from the RSC. These works offer added description to the impacts of PNN degradation on cognition, PV+ interneurons, and broader patterns of cellular activity. These findings are particularly relevant for diseases such as Alzheimer's and schizophrenia, which feature both PNN loss and cognitive impairment.

Preface

This thesis is an original work of John W. Paylor. All animal research was conducted in accordance with Canadian Council on Animal Care guidelines. All animal use protocols were approved by the University of Alberta Animal Care and Use Committee (AUP361).

For data presented in Chapter 2, I was involved in the experimental design, data collection, analysis, and manuscript composition.

Chapter 3 of this thesis has been published as John W. Paylor, Eszter Wendlandt, Tara S. Freeman, Wendie N. Marks, John G. Howland, and Ian R. Winship (2018), 'Impaired Cognitive Function after Perineuronal Net Degradation in the Medial Prefrontal Cortex". eNeuro: 5(6): ENEURO.0253-18. doi: 10.1523/ENEURO.0253-18.2018. Author contributions: J.G.H. and I.R.W. designed research; J.W.P., T.S.F., Q.G., W.N.M. performed research; J.W.P., E.W., W.N.M. analyzed data; J.W.P., J.G.H., and I.R.W. wrote the paper.

For data presented in Chapter 4, I was involved in the experimental design, data collection, analysis, and manuscript composition.

Acknowledgements

This thesis could not have been done without the perpetual support of my supervisor, Dr. Ian Winship. I complete this thesis not only as a student but also a husband to my wife, a father to my daughter, and a survivor of a global pandemic. None of those things would have been possible without your steady support for your students having a life beyond just their work. To my parents, thank you for instilling me with a love for learning and a curiosity for the world. To my wife, you inspire me endlessly. Your ceaseless determination, selflessness and compassion are a gift in my life and every community of people that you touch. Thank you for continuing to make sure that this part of my life didn't get left behind despite all the challenges we took on together. And lastly to my young daughter, you put the colour into every picture my eyes see. You are outspoken and bold and curious, never change. Don't stop questioning and challenging this world. I hope I can give you every chance to experience its majesty and curiosity.

Table of Contents

List of Figures

List of Tables

Glossary of Terms

Aβ = Amyloid-beta

AD = Alzheimer's Disease

ADAMTS = a disintegrin with thrombospondin motifs

AMPA = α-amino-3-hydroxy-5-methyl-4-isoxazolepropionic acid

AMPAR = α-amino-3-hydroxy-5-methyl-4-isoxazolepropionic acid receptor

APP = Amyloid precursor protein

C4S = Chondrotin-4-sulfate

C6S = Chondroitin-6-sulfate

ChABC = Chondroitinase-ABC

CMOR = Crossmodal object recognition

CNS = Central nervous system

CS-GAG = Chondroitin-sulfate glycosaminoglycans

CSPG = Chondroitin sulfate proteoglycan

ECM = Extracellular matrix

EPSP = Excitatory post-synaptic potential

GABA = Gamma-aminobutyric acid

LTD = Long-term depression

LTP = Long-term potentiation

MMP = Matrix metalloproteinase

mPFC = Medial prefrontal cortex

NMDA = N-methyl-d-asparate

NMDAR = N-methyl-d-aspartate receptor

OSST = Operant set-shifting task

PNN = Perineuronal net

PPI = Prepulse inhibition

PS1 = Presenilin-1

PV+ = Parvalbumin-positive

RMS = Root Mean Square

RSC = Retrosplenial cortex

SEM = Standard error of the mean

SZ = Schizophrenia

TOR = Tactile object recognition

VOR = Visual object recognition

WFA = Wisteria floribunda agglutinin

Chapter 1: An introduction to perineuronal nets, their structure and function, and the consequences of their loss in diseases of the central nervous system such as schizophrenia and Alzheimer's

1.1 Perineuronal Nets

Perineuronal nets (PNNs) are complex, reticular assemblies that surround mature neurons of the central nervous system (CNS). Their discovery dates to some of the very first advances in the identification of neurons by Camillo Golgi and Ramón y Cajal in 1983. Golgi first identified them, where he described the presence of a non-neuronal 'corset of neurokeratin' or, "a delicate covering, mainly reticular in structure… which surrounds the cell body of nerve cells" (Golgi, 1893; 1898). However, Cajal disagreed, arguing that they were simply a staining artifact and given his powerful influence in the field of neuroanatomy, interest into these structures waned.

More than a century later we now know that PNNs are critical structures in neurodevelopment, they support and protect mature neurons of the CNS, they restrict neuronal plasticity, and they contribute to behavioural outputs of the brain. PNNs are a part of the broader extracellular matrix (ECM), which comprises approximately 20% of the brains total volume and includes the interstitial matrix, which is loosely distributed throughout the parenchyma, the basal lamina, PNNs, and perinodal matrices at nodes of Ranvier (Dityatev et al., 2010; Fawcett et al., 2019; Nicholson & Syková, 1998; Rauch, 2007). Among these, PNNs are the most organized presentation. They surround the cell body, dendrites, and axon initial segments of the neurons that host them. Synaptic inputs intended for neurons surrounded by these matrices are thought to penetrate the net, which provides structural support for their connection and creates a permissive site for transmission (Sigal et al., 2019; Tsien, 2013). PNNs are present in almost all mammalian CNS tissues, although they can vary significantly in the neuronal types they surround, their distribution, and composition (Galtrey et al., 2008; Hendry et al., 1988; Jäger et al., 2013; Lupori et al., 2023; Seeger et al., 1994). In the brain, PNNs are most often found surrounding inhibitory interneurons, whereas in the spinal cord, many motor neurons within ventral and intermediate

horns possess them. In the neocortex, PNNs are most frequently observed surrounding parvalbumin-positive (PV+) inhibitory interneurons, although they have been identified sparsely surrounding some pyramidal cells (Matthews et al., 2002). In some areas of the brain, up to 70% of PV+ interneurons co-localize with *wisteria floribunda agglutinin* (WFA) labelled PNNs, the most common immunohistochemical stain used to identify them (Lupori et al., 2023). Over the last several decades, PNNs have gained increasing appreciation for their role in the 'tetrapartite synapse' which also includes astrocytes and the traditional presynaptic and postsynaptic elements of chemical synapses within the CNS (Dityatev et al., 2006; Dityatev & Rusakov, 2011; Song & Dityatev, 2018).

1.2 Structure of PNNs

The primary components of PNNs include hyaluronan, chondroitin sulfate proteoglycans (CSPGs), link proteins, and tenascins (Carulli & Verhaagen, 2021; Kwok et al., 2010; Yamaguchi, 2000). Hyaluronan is the backbone of PNN structure and the foundation upon which other components assemble. It is synthesized by hyaluronan synthase, a plasma-membrane bound enzyme primarily expressed in neurons. During synthesis, hyaluronan can be bound to the membrane of a cell by hyaluronan synthase, which is thought be the mechanism by which PNNs are anchored to host cells (Kwok et al., 2010). Consistent with its foundational role in PNNs, degradation of hyaluronan with hyaluronidase completely disrupts PNNs (Deepa et al., 2006; Happel et al., 2014; Sun et al., 2018). While hyaluronan serves the backbone of PNN structure, CSPGs are the primary constituent that condense around this scaffold. CSPGs found in PNNs are members of the letican family of proteoglycans, including aggrecan, versican, neurocan, phosphocan, and brevican. Among these, aggrecan appears consistently in nearly all PNNs, while the other CSPGs are present in varying degrees based on the cell type of the host and

region examined (Dauth et al., 2016; Miyata et al., 2018; Zimmermann & Dours-Zimmermann, 2008). CSPGs consist of a core protein and varying numbers of chondroitin-sulfate glycosaminoglycan chains (CS-GAG) attached to the core protein. CS-GAG chains are comprised of disaccharide units of glucuronic acid and N-acetylgalactosamine. Both N-acetylgalactosamine and glucuronic acid can be sulfated at various positions, which can impact their function. This is notable when comparing the unique functions of PNNs relative to the broader interstitial matrix as they exhibit differently sulfated CS chains which confer them with differing functions (Deepa et al., 2006). The most widely utilized marker for PNN detection with immunostaining, WFA, binds to an unknown sulfation motif within CS-GAG chains. However, not all PNNs are labelled with WFA, likely due to the significant heterogeneity in sulfation patterns (Matthews et al., 2002). Numerous growth-modulating molecules also bind to CS-GAG chains, such as neurotrophins, semaphorin 3A, reelin, and the transcription factor orthodenticle homeobox 2 (OTX2; (Beurdeley et al., 2012; Dick et al., 2013; Lensjø et al., 2017; Martínez-Cerdeño & Clascá, 2002; Pesold et al., 1999). Interestingly, the sulfation patterns of CS-GAG chains also differ throughout development. Chondroitin-6-sulfate (C6S) is most prominent during development and has growth-promoting properties whereas chondroitin-4-sulfate (C4S) upregulates throughout the lifespan and has growth-inhibiting properties (Foscarin et al., 2017; Kitagawa et al., 1997; Miyata et al., 2018; Wang et al., 2008). The additional components of PNNs, link proteins and tenascins, facilitate binding of CSPGs to hyaluronan and to other CSPGs, respectively (Kwok et al., 2015; Oohashi et al., 2015). Genetic knockouts of either tenascins or link proteins has been shown to impair PNN formation and can elicit similar plasticity-enhancing properties within neurons and larger cortical networks (Bekku et al., 2012; Brückner et al., 2000; Carulli et al., 2010; Weber et al., 1999). While these knockouts can impair

PNN formation, total CSPG levels in the brain are typically unchanged, demonstrating their unique contribution to the assembly of PNNs. While the cellular origins of the components for PNN formation are not completely described, they are thought to be generated primarily by neurons and glia. Glial cells have been shown to produce hyaluronan, tenascins, and several CSPGs while neurons have primarily been shown to produce CSPGs such as aggrecan, phosphocan, and brevican (Lander et al., 1998; Miyata et al., 2005; Seidenbecher et al., 2002). However, PNNs have been shown to assemble even without the presence of glial cells, although in atypical presentation suggesting they are capable of synthesizing all PNN components (Dityatev et al., 2007; Frischknecht et al., 2009; John et al., 2006; Miyata et al., 2005).

1.3 PNN Formation

Diversity among the components of PNNs confers them with dramatically differing functional roles as an assembled structure. This is readily demonstrated throughout development where PNNs exhibit significant growth and change during the post-natal lifespan. During early embryonic development PNNs are largely absent but their components such as hyaluronan and neurocan are readily detectable in the CNS (Milev et al., 1998). Neurocan is primarily expressed early in development and serves as an axonal guidance cue for the developing nervous system (Miller et al., 1995; Pearlman & Sheppard, 1996). During the post-natal lifespan, the upregulation of link proteins seems to initiate the congregation of PNN components into a structured assembly (Carulli et al., 2006, 2007) . In cells that do not typically produce pericellular hyaluronan, overexpressing hyaluronan synthase 3 causes them to secrete hyaluronan (Kwok et al., 2010). If these cells are also able to secrete cartilage link protein 1 (Ctrl1) and aggrecan, they will organically condense into a compact PNN-like matrix. This role for link proteins appears to be tailored specifically towards PNN formation, as animals lacking Ctrl1

have attenuated PNN formation, but levels of CSGPs within the brain are still similar (Carulli et al., 2010). Unique isoforms of link proteins also appear to be suited to binding specific CSPGs to PNNs. In animals lacking *Bral2*, the presence of brevican is significantly reduced in PNNs, but aggrecan is unaltered (Bekku et al., 2012). By contrast, Ctrl1 appears to primarily bind aggrecan and versican to hyaluronan (Binette et al., 1994; S. Shi et al., 2004; Shibata et al., 2003). Genetic knockout studies have also demonstrated that components such as aggrecan are not only required for PNN formation, but also maintenance. In animals lacking *Acan*, a gene encoding for aggrecan, animals display brain-wide disruption of PNN formation (Rowlands et al., 2018). Notably, acute knockout of *Acan* within the visual cortex of mature mice also disrupts the accumulation of CSPGs and link proteins into their structure, supporting the suggestion of a role in ongoing PNN maintenance.

The developmental trajectories of PNNs have been described primarily based on rodent studies. In the mouse brainstem PNNs are first apparent between postnatal day (PND) 7 and 14. In subcortical structures and cortical areas they are identifiable by PND 14 and PND 21, respectively (Brückner et al., 2000; Nakagawa et al., 1987; Ueno et al., 2017). The most significant increase in PNN markers was generally observed between PND 21 and 40 in one characterization of mouse PNN development (Brückner et al., 2000). However, other studies have demonstrated that these trajectories can differ vastly by region. For example, PNNs in the somatosensory cortex of mice PNNs see the most significant growth between PND 14 to 28, whereas in the medial prefrontal cortex (mPFC) continued growth is observed until PND 56 (Lipachev et al., 2019; Ueno et al., 2017). In rats, our lab has previously shown steady increases in PNN growth in the mPFC until PND 90 (Paylor et al., 2016). Observations from human post-mortem studies indicate that PNNs in the mPFC are faintly detectable as early as 54 days of age

(Mauney et al., 2013; Rogers et al., 2018). However, more typical presentations were not apparent until 2 years of age in the mPFC or hippocampus, and these steadily increased until 8 years of age. The formation of PNNs appears to be an activity-dependent process. Suppression of neuronal activity with tetrodotoxin inhibits PNN formation (Reimers et al., 2007). Similarly, in animal studies utilizing sensory deprivation such as dark rearing which restricts the necessary light stimuli for early maturation of the visual cortex, PNN formation is diminished (Pizzorusso et al., 2002). Whisker trimming and auditory deprivation have similar effects on PNN formation in the somatosensory and auditory cortices, respectively (McRae et al., 2007; Reinhard et al., 2019; Ueno et al., 2017). This activity-dependent formation of PNNs is integral to their involvement in the closure of so called "critical periods of plasticity". This process was described in the context of the visual cortex in seminal work by Pizzorusso et al. (2002). In response to light, the visual cortex undergoes dramatic reorganization of its cortical neurons which results in the formation of ocular dominance columns, which preferentially respond to input from the left or right eye. Dark rearing, by which sensory input to one eye is deprived, results in ocular dominance columns with a heavy skew in their response towards the eye receiving input. However, after maturation of the visual cortex, dark rearing no longer impacts the stability of ocular dominance columns. PNNs were considered as one possible mechanism for this resiliency to dark rearing during maturity, as their formation coincides with the closure of this critical period of plasticity. This was readily demonstrated in additional experiments showing that degradation of PNNs in the mature visual cortex with chondroitinase ABC (ChABC), a commonly used enzyme for degrading CS-GAG chains within PNNs, can revert ocular dominance columns to a more plastic state which are sensitive to sensory deprivation. Since this discovery similar relationships between PNNs and critical periods of plasticity have

been demonstrated for fear memories in the amygdala and sensory processing in the barrel cortex of rodents, as well as vocal learning in the auditory nuclei of songbirds (Balmer et al., 2009; Cornez et al., 2020; Cornez, Collignon, et al., 2020; Gogolla et al., 2009; Nowicka et al., 2009). Recent work has also described a critical period for episodic memory encoding within CA1 of the hippocampus (Ramsaran et al., 2023). Importantly, genetic knockout studies specifically targeted PNN components such as tenascin-R or aggrecan also show similar effects of persistent ocular dominance plasticity (Bekku et al., 2012; Carulli et al., 2010; Rowlands et al., 2018). Given that total CSPG levels within the brain are similar despite diminished PNN formation in these animals, it suggests that PNNs specifically play a role in the closure of critical periods of plasticity. Together, the studies described here demonstrate that PNNs play a critical role in the developmentally regulated maturation of both primary sensory areas as well as regions of the brain associated with more complex functions, such as fear and memory. It has been suggested that PNNs could even play similar roles in the maturation of more complex cognitive domains such as the frontal cortex and executive control, although putative critical periods for these have yet to be defined.

1.4 Function of PNNs

The functions of PNNs have been most readily described by studies that destabilize PNNs or utilize genetic knockouts of PNN components to exhibit the consequences of their loss. Firstly, PNNs and their components have a variety of direct interactions with other molecules and cellular receptors. During development, PNNs show numerous interactions that suggest an involvement in synapse formation and receptor clustering. They facilitate synapse formation and clustering of AMPA receptors through their interactions with pentraxins, which are secreted at presynaptic terminals of synapses targeting PNN-surrounded neurons (Chang et al., 2010; Lee et

al., 2017; Xu et al., 2003). PNNs also interact with integrins, via which they can influence dendritic spine motility, which is consistent with studies showing that enzymatic degradation of PNNs can increase spine motility (de Vivo et al., 2013; Majewska & Sur, 2003; Orlando et al., 2012; Pizzorusso et al., 2006). Aggrecan-immunoreactive puncta can be detected at extrasynaptic sites on cell surfaces prior to synapse formation, indicating they may even play a role in pre-patterning neurons for synapse formation (Dino et al., 2006). Some support for this could also be drawn from studies showing that genetic knockouts of PNN components results in fewer synapses formed onto PV+ interneurons, which typically express a PNN (Favuzzi et al., 2017). The binding of signaling molecules within PNNs structure is not restricted to development either. In mature synapses, CSPGs interact with AMPA receptors and potassium channels to restrict their mobility and extra synaptic diffusion (Favuzzi et al., 2017; Frischknecht et al., 2009). In this role PNNs affect synaptic depression by restricting the exchange of desensitized receptors for naïve ones during periods of high-frequency stimulation. Developed PNNs also show interactions with chemorepulsive axon guidance proteins such as semaphorin 3A, which may repulse impinging synaptic connections onto mature neurons (de Winter et al., 2016; Orlando et al., 2012). Reelin, which plays a role in NMDA receptor organization within synapses is also integrated into PNNs structure (Campo et al., 2009; Iafrati et al., 2014; Pesold et al., 1998). In addition to these molecular interactions PNNs play an important role in regulating neuronal physiology, although this can vary significantly by region and cell type. Generally, PNN loss appears to alter the balance of excitation and inhibition by reducing inhibitory activity (Wingert & Sorg, 2021). This is supported by studies showing that enzymatic degradation of PNNs can reduce inhibitory activity and revert affected networks to a more juvenile state of electrophysiological activity (Christensen et al., 2021; Lensjø et al., 2017). Other common

observations within PV+ cells after PNN degradation are decreased firing rates, reduced firing thresholds, and increased firing variability (Balmer, 2016; Dityatev et al., 2007; Hayani et al., 2018; Liu et al., 2023; Wingert & Sorg, 2021). PNN degradation has also been shown to impact synaptic physiology although often with contrasting effects. PNN disruption within the visual cortex or perirhinal cortex can enhance long-term depression (LTD) but impairs early-phase LTP and LTD in CA1 of the hippocampus (Bukalo et al., 2007; Romberg et al., 2013). LTP within the visual cortex is also enhanced by ChABC administration (de Vivo et al., 2013). Even within regions such as the hippocampus, PNN degradation can have differing consequences. Pyramidal cells within CA2 of the hippocampus show a loss of LTP after PNN formation and ChABC treatment can restore it (Carstens et al., 2016). In contrast, within the CA1 region ChABC treatment suppresses LTP (Bukalo et al., 2007). These contrasting effects cannot be reconciled in simplistic manner which is reflective of the diversity of neural types surrounded by PNNs and their own unique compositions. Nonetheless, these findings reflect that PNNs have an impact on neuronal and synaptic physiology, which warrants consideration in any context where they are disrupted.

PNNs also have important neuroprotective properties and provide critical support to the physiological demand of highly active neurons. CS-GAG chains within PNNs are highly charged structures that contribute to PNNs forming a polyanionic environment in the pericellular space around neurons. This environment can act as a buffering system for calcium (Ca^{2+}), potassium (K^{+}), and sodium (Na^{+}), which are necessary for cellular function (Brückner et al., 1993, 1996; Härtig et al., 1999). PNNs have been shown to buffer bivalent cations such as Ca^{2+} by contributing to local diffusion properties in the pericellular space (Hrabětová et al., 2009; Okamoto et al., 1994). In addition to these supports of ogoing cellular demand PNNs can bind

high amounts of cations such as iron (Fe^{2+}) which can contribute to oxidative stress (Morawski et al., 2004; Reinert et al., 2022). Other studies have shown that during development when PV+ interneurons are not yet surrounded by a PNN, they are more vulnerable to oxidative stress than mature PV+ cells that are bearing them (Cabungcal et al., 2013). Similarly, in mature PV+ cells treatment with ChABC to degrade PNNs renders them vulnerable to oxidative stress. Interventional studies also suggest that antioxidant therapies such as N-acetylcysteine can diminish oxidative stress and prevent its effects on PV+ cell health and PNN disruption (Cardis et al., 2018; Dwir et al., 2021; Hameed et al., 2023). This neuroprotective role is also indicated by observations in the context of disease. In AD, neurons surrounded by PNNs are less likely to accumulate lipofuscin, an intralysosomal pigment produced by Fe^{2+}-induced oxidative stress (Morawski, et al., 2004). In animal models featuring excessive oxidative stress, such as *Glcm* knockout mice, PNN surrounded neurons appear less affected (Suttkus et al., 2014). PNNs have also been shown to protect neurons against excitotoxicity induced by high concentrations of glutamate or trimethyltin intoxication (Okamoto et al., 1994; Schüppel et al., 2002). Interestingly, this neuroprotective role may shield more than just host neurons. Under normal conditions CSPGs within PNNs are largely resilient to proteolytic degradation by trypsin, chymotrypsin, or pepsin, but after ChABC treatment CSPGs are readily digested by these same enzymes (Koppe et al., 1997). In addition to these studies demonstrating PNNs neuroprotective roles, there is a broader body of literature also describes similar neuroprotective properties for individual PNN components such as tenascin-R (Angelov et al., 1998; Egea et al., 2010; Liao et al., 2005). Together, these findings present strong evidence that PNNs provide both local support for the physiological demands of host neurons and protect against stressors on cell function. The

importance of this function is doubly important when considering that a significant proportion of PNNs surround highly active PV+ interneurons which have incredible metabolic demand.

1.5 PNNs and PV+ Interneurons

Any consideration of the functional roles of PNNs or the impact of their loss is inextricably tied to their close association with PV+ interneurons. These interneurons are defined by their expression of the calcium-binding protein parvalbumin (Hu et al., 2014; Lim et al., 2018). Nearly all PV+ interneurons are GABAergic, and they are typically classified as either chandelier or basket type cells. These interneurons are highly active and fast-spiking, and are found throughout the cortex, thalamus, striatum, cerebellum, and hippocampus. Within the cerebral cortex, approximately 10-20% of neurons express GABA and among those 30-50% express PV+, making them the largest category of inhibitory interneurons (Cowan et al., 1990; Rudy et al., 2011; Tamamaki et al., 2003). This cell type can exert remarkable influence over local cortical circuits. A sampling of the connectivity between individual PV+ cells and their local environment shows that in some areas up to 75% of pyramidal cells within a 200 μm distance of a particular PV+ interneuron make connections (Packer & Yuste, 2011). Their most distal synapses can be over 300 μm from their soma. PV+ interneurons are the primary source of perisomatic inhibition onto pyramidal cells, giving them a high degree of influence on target neurons (Carceller et al., 2020; Freund & Katona, 2007). Studies have shown that PV+ cells synapse primarily onto cell bodies of pyramidal cells at sites with densely accumulated α1-GABA receptors (Nusser, 1996). This innervation near to sites of action potential initiation enable them to exert significant inhibitory influence over cells upon which they synapse.

Functionally, PV+ interneurons are thought to play a critical role in the regulation of network activity, and they display unique firing properties that allow for this. Their defining

marker, PV protein, rapidly sequesters calcium and attenuates post-spike hyperpolarization (Caillard et al., 2000). They also possess high levels of the voltage-dependent potassium channels KV3.1 and KV3.2 which facilitate narrow spiking patterns and sustained high-frequency activity. Together, these unique properties enable them to maintain fast-spiking action potentials with limited fatigue. Several studies have demonstrated the impact that PNN degradation can have on these functional properties. In brevican-deficient mice, the clustering of KV3.1b channels and AMPA receptors are significantly reduced (Du et al., 1996; Goldberg et al., 2008). Brevican-deficit mice have also been shown to have PV interneurons that are hyperexcitable, with decreased firing thresholds and diminished firing frequencies (Favuzzi et al., 2017). PNN degradation studies have shown that ChABC treatment decreases the mean spiking activity of PV+ interneurons and increases their spiking variability (Christensen et al., 2021; Lensjø et al., 2017). PV+ interneurons also display structural attributes which enable them to integrate information broadly within cortical circuits. They can receive input from numerous afferent pathways as they typically exhibit dendrites that cross multiple cortical layers (Gulyás et al., 1999; Kubota et al., 2016; Nörenberg et al., 2010; Tukker et al., 2013). They possess lengthy axons, which can have cumulative lengths of 30 to 50 mm and extensive arborization, enabling them to exert wide inhibitory influence (Karube et al., 2004; Nörenberg et al., 2010; Sik et al., 1995). These unique properties enable PV+ cells to contribute more broadly to a variety of complex neural circuit functions. For example, PV+ interneurons are thought to contribute to blanket inhibition, which is a form of widespread, non-specific inhibition of cortical networks (Karnani et al., 2014). The excitatory post synaptic potentials (EPSPs) from a single action potential in a pyramidal cell is sufficient to reliably produce an action potential in a connected PV+ interneuron (Jouhanneau et al., 2018). Given the immense sphere of influence of PV+ cells,

this indicates that the activation of a single pyramidal cell which synapses onto a PV+ interneuron could result in blanket inhibition of a large proportion of neurons in their local area. In the context of PNN degradation, it follows that the impact of PNN loss could disrupt the contributions of PV+ interneurons to blanket inhibition. Support for this could be drawn from studies showing that PNN degradation alters the balance between excitation and inhibition by reducing inhibitory activity in local cortical circuits (Donato et al., 2013; Fawcett et al., 2019; Lensjø et al., 2017).

While PV+ interneurons have been suggested to play roles in a variety of other inhibitory circuit functions including sparse encoding, modulation, and pattern separation, they have been most extensively studied for their contributions to the generation of high frequency activity (40-100 Hz), called gamma oscillatory activity. Gamma activity is thought to be involved in sensory processes and integration, and coherence in gamma activity between regions is thought to facilitate complex cognition functions (Buzsáki & Wang, 2012; Fries, 2005, 2009; Lesh et al., 2011). Support for PV+ involvement in gamma oscillatory activity can be drawn from a wide variety of studies. During neurodevelopment gamma oscillatory activity increases throughout postnatal development and stabilizes in ~4 weeks in the rodent mPFC, which is coincident with the maturation of PV+ interneurons in this region (Bitzenhofer et al., 2020). PV+ interneuron activity shows a strong coupling with gamma oscillations and manipulations to reduce or stimulate PV activity can attenuate or generate gamma oscillatory activity, respectively (Buzsáki & Wang, 2012; Klausberger & Somogyi, 2008; Sohal et al., 2009; Tukker et al., 2013). Direct support of PV+ cell involvement in gamma activity can also be drawn from optogenetic studies showing increases in gamma oscillatory activity after PV+ stimulation (Cho et al., 2020; Kim et al., 2015; Liu et al., 2020; McNally et al., 2021). While the mechanism underlying gamma

oscillations is not fully understood, conventional models such as the pyramidal-interneuron network gamma (PING) model, suggest that PV+ interneurons play a regulatory role by synchronizing the activity of pyramidal cells through rhythmic inhibition (Gonzalez-Burgos & Lewis, 2012; Whittington et al., 2000). Consistent with this, disruption of glutamatergic signaling onto PV+ cells decreases excitation of PV+ cells and disrupts gamma activity (Fuchs et al., 2007). The close relationship of PV+ cells with PNNs and the impacts of PNN disruption are also readily shown in studies of evaluating gamma oscillatory activity, although these can vary by brain region. In the mouse visual cortex or anterior cingulate cortex, PNN degradation can result in increases in gamma power, but in the prefrontal cortex, it reduces it (Carceller et al., 2020; Lensjø al., 2017; Steullet et al., 2014). While these findings differ, direct PV+ inhibition can lead to increases in spontaneous gamma power but reduced evoked gamma oscillatory, suggesting that these effects may be dependent on brain-state (Cho et al., 2015; Guyon et al., 2021; Sohal et al., 2009). Together, these studies demonstrate an important role for PV+ cells and PNNs in the generation of gamma activity, which is thought to underlie complex cognitive functions such as attentional control, sensory integration, and working memory (Basar-Eroglu et al., 2007; Buzsáki & Wang, 2012; Fries, 2005, 2009; Haig et al., 2000; Lesh et al., 2011).

1.6 PNNs in Cognition

While the discovery of PNNs role in critical periods of visual plasticity renewed interest into their function, it was a seminal work by Gogolla et al., (2009) that demonstrated their contributions to plasticity can also have important roles beyond primary sensory development. In this case it is PNNs involvement in the maturation of fear extinction phenotypes. In adult animals conditioned fear memories are resilient to extinction following nonreinforced exposure to a condition fear stimulus, but in younger animals, extinction results in the erasure of these

memories. In the work of Gogolla et al. (2009) they firstly demonstrated that this developmental switch between the juvenile and mature fear extinction phenotype coincides with the maturation of PNNs in the amygdala. Secondly, when PNNs are degraded within amygdala of adult animals they revert to a more juvenile state of plasticity and their fear memories subject to erasure (Gogolla et al., 2009). Since this initial discovery additional studies have indicated a broader role for PNNs in fear memories. PNN depletion in the hippocampus, medial prefrontal cortex, and anterior cingulate cortex can all impair fear memory (Hylin et al., 2013; Shi et al., 2019). Other studies have demonstrated modality specific involvement, where PNN degradation within the auditory or visual cortex impairs auditory and visual fear conditioning, respectively (Banerjee et al., 2017; Thompson et al., 2018). While these studies suggest a significant role for PNNs in the formation of fear memories, others have demonstrated a much more general function in memory. A rapidly growing body of research suggests an involvement of PNNs in the acquisition and consolidation of drug-associated memories (Brown & Sorg, 2023; Lasek et al., 2018; Slaker et al., 2016). PNN disruption in the cerebellum disrupts motor-associative memories and in the medial entorhinal cortex, can impair the representations of new environments and render previously stable representations subject to interference (Carulli et al., 2020; Christensen et al., 2021). Conversely, some studies have shown PNN degradation can have beneficial effects on memory. PNN degradation in the perirhinal cortex can enhance object recognition memories and in the medial prefrontal cortex, PNN degradation improves performance on the touchscreen trial unique, non-matching to location (TUNL) task (Anderson et al., 2020; Carulli et al., 2020; Donato et al., 2013; Romberg et al., 2013; Rowlands et al., 2018). In addition to their contributions to memory, PNNs have a demonstrated involvement in learning tasks. Within hours of fear conditioning, CSGP mRNA and PNN levels increase, before returning to baseline

24 hours later, suggesting they play a role in encoding these learned behaviours (Banerjee et al., 2017). The degradation of PNNs in the auditory cortex enhances reversal learning and in the cerebellum expedites motor-associative learning (Carulli et al., 2020; Happel et al., 2014; Hirono et al., 2018). Similarly, aging-related declines in motor learning correlate with PNN levels in the striatum and PNN degradation restores this learning capacity (Richard et al., 2018). Support for their role in learning can also be drawn from knockout studies showing that animals lacking tenascin-R have enhanced reversal learning in the Morris Water Maze (Morellini et al., 2010).

While these observations vary based on the method of disruption and the region within which they affected, they demonstrate a clear role for PNNs in cognition, learning and memory. The question of how PNNs affect memory and learning is still not fully described, however. A recent model suggests that these effects are mediated through PV+ interneuron activity (Fawcett et al., 2019). After degradation with ChABC, the restrictive barrier surrounding PV+ is removed and there is an increase in inhibitory synapses on the dendrites of PV+ cells (Caroni, 2015; Donato et al., 2013). Increased inhibition of PV+ cells decreases their activity, which is reflected in reductions in GAD67 and PV expression within PV cells (Donato et al., 2013, 2015). Reduced inhibitory output from PV+ cells in turn can increase excitability within cortical circuits to facilitate learning and memory. While intriguing, aspects of this model still require experimental validation and the impacts of PNN degradation are not always consistent by region. Continued study into the effects of targeted PNN depletion within localized areas in otherwise healthy animals are ideal for isolating out these unique contributions that PNNs make to learning and memory.

1.7 PNNs in Schizophrenia

At the beginning of the century numerous studies identified that PNN loss is a feature of the post-mortem tissue of patients who suffered from SZ in their lifetime. This deficit was first demonstrated in the amygdala and entorhinal cortex where significantly reduced numbers of PNNs and massive increases in CSPG-positive glial cells were detected (Pantazopoulos, 2010). Notably, the PNN deficits observed clearly differentiated post-mortem tissue of people that suffered from SZ from those that suffered from bipolar disorder, which can share certain symptoms such as psychosis. Subsequent studies demonstrated similar PNN deficits in the prefrontal cortex, inferior colliculus, reticular thalamic nucleus, olfactory epithelium, and superior temporal cortex in SZ (Alcaide et al., 2019; Enwright et al., 2016; Kilonzo et al., 2020; Mauney et al., 2013; Pantazopoulos et al., 2013, 2015; Pietersen et al., 2014; Steullet et al., 2018). The deficit in the prefrontal cortex is particularly notable as the trajectory of PNN development follows prolonged post-natal growth with the most significant increases in the peri-pubertal period before stabilizing into adulthood. Coincidentally, this developmental period is also when the overt symptoms of SZ first begin to appear. The mPFC is also a region of significant interest in SZ pathophysiology given its contributions to dopaminergic signaling and its role in cognitive functions which are frequently impaired in the people suffering from this disease (Ellenbroek et al., 1996; Gariano & Groves, 1988; Sekiguchi et al., 2019; Sesack & Carr, 2002). Other regions with PNN deficits also bear significance within SZ symptomatology. For example, the superior temporal cortex plays a role in auditory processing and hallucinations in SZ are most frequently auditory in nature (Mueser et al., 1990). More recent reports have also described PNN deficits within the reticular thalamic nucleus and inferior colliculus. Deficits within these areas indicate that PNN deficits are not restricted to cortical areas and could impact primary sensory processing (Kilonzo et al., 2020; Steullet et al., 2018). While these descriptions

were informative, human post-mortem studies are limited in their ability to determine what contributions PNNs make to the progression of diseases such as SZ, if any. This issue is keenly suited to scientific discovery using animal models of disease, which offer significantly more investigative utility.

While there is significant debate over the validity of animal models to capture aspects of a complex, poorly understood, and neurodevelopmental disease like SZ, animal models have nonetheless proven to be able to recapitulate some of the features of SZ. With regards to PNNs, the first of these was utilizing a maternal immune activation (MIA) model of SZ where during gestation the mother is treated with a controlled infection. In healthy animals, PNNs within the PFC follow as similar developmental trajectory throughout the postnatal lifespan as shown in people, where they increase until late adolescence and adulthood. However, in animals whose mothers had MIA, these offspring develop PNN deficits. The PNN development of MIA animals followed a similar trajectory to those of healthy animals until late adolescence and early adulthood, where a PNN deficit first emerges in the PFC. This developmental period is also when this rodent model first demonstrates behavioural symptoms consistent with a SZ-like phenotype (Vorhees et al., 2015; Wolff et al., 2011; Wolff & Bilkey, 2008; Zhang et al., 2012). A subsequent study demonstrated that PNN deficits (and PV impairment) in the mPFC are a common feature across 12 out of 14 of the models evaluated, which included both genetic and environmental models (Steullet et al., 2018). These findings suggest that animal models are effective in modeling PNN deficits and that among them, PNN deficits are a remarkably common feature. Another finding within these studies was that most models also exhibited significant impairments in PV+ interneurons and elevated oxidative stress. These features of animal models also appear to capture endophenotypes of the human condition, where PV+

interneuron abnormalities and excessive oxidative stress are observed (Bitanihirwe et al., 2009; Bitanihirwe & Woo, 2011; Cuenod et al., 2022; Do et al., 2015; Hashimoto et al., 2003; Yao & Reddy, 2011). Given the high-frequency activity of PV+ interneurons they are particularly vulnerable to environmental stressors such as oxidative stress (Cabungcal et al., 2013; Ruden et al., 2021). Together, these studies demonstrate a potential mechanism that could underlie dysfunction within SZ and its models, whereby PNN loss renders PV+ interneurons susceptible to environmental stressors such as oxidative stress, which in turn drives their dysregulation (Berretta et al., 2015; Do et al., 2015; Perkins et al., 2020).

Given the commonality of PNN deficits among both human post-mortem studies and a wide variety of animal models of the disease, interest has since shifted towards describing the mechanisms by which PNNs are lost and the implications that this has for the disease. Foremost among these is their relationship with PV+ interneurons which are also disturbed in SZ. Numerous studies have demonstrated reductions in PV+ messenger RNA (mRNA) and protein levels in SZ, although neuronal density is typically spared (Curley et al., 2011; Gonzalez-Burgos et al., 2010; Guidotti et al., 2000; Impagnatiello et al., 1998; Kilonzo et al., 2020; Thompson et al., 2009; Woo et al., 2004). The expression of GAD67 mRNA and protein is reduced in SZ and GAD67 mRNA are entirely absent in up to 50% of PV interneurons (Hashimoto et al., 2003). Given that GAD67 and PV expression are highly correlated, this loss suggests that PV+ interneurons are a possible focal point of dysfunction within SZ (Donato et al., 2013). Other features of the disease also implicate PV+ interneurons. Cortical hyperexcitability is a common feature of SZ, which is consistent with the decreases in inhibitory output seen from PV+ interneurons after PNN degradation (Daskalakis et al., 2007; Eichhammer et al., 2004; Hoffman & Cavus, 2002; Lakatos et al., 2013; Spencer et al., 2009). Abnormalities in gamma oscillations,

which are largely thought to be driven by PV+ interneuron activity, are common in recordings from people suffering from SZ. Given this it is unsurprising that numerous cognitive behaviours that have been shown to require gamma synchronization, such as working memory, attention, and sensorimotor gating, are impaired SZ (Dickerson et al., 2010; Forbes et al., 2009; Leung & Ma, 2018; Senkowski & Gallinat, 2015; Swerdlow et al., 2014). However, in many studies of gamma activity deficits are only observed during engagement with cognitive tasks and conversely, during periods of spontaneous activity, gamma activity is increased (Uhlhaas & Singer, 2015). These alterations in signal-to-noise ratio are very similar to what is observed in PV+ interneurons after PNN degradation, where broadband spontaneous activity of gamma is often increased but during narrow band evoked activity, gamma is impaired (Cho et al., 2015; Guyon et al., 2021; Sohal et al., 2009). These results provide strong support that PV+ interneurons are an important feature of SZ pathology. When paired with observations of PNN deficits, gamma asynchrony, cortical hyperexcitability, and disruption of the inhibitory system in SZ, it becomes apparent that PNN and PV cells are part of a larger and perhaps significant locus of dysfunction within the disease.

In addition to these converging lines of evidence, other aspects of SZ dysfunction offer further support PV+ interneurons having a central role in SZ pathophysiology. In the last several decades, the N-methyl-d-aspartate receptor (NMDAR) hypofunction hypothesis of SZ has gained significant interest to explain commonalities among the positive, negative, and cognitive symptoms of SZ. It is derived from observations that NMDAR antagonists such as ketamine and phencyclidine can induce symptoms reminiscent of each of these three domains. Interestingly, NMDAR hypofunction hypothesis can integrate well with numerous other observations about PNNs and PV+ interneurons. In modern models of the circuitry underlying gamma oscillations,

interneuron activity is driven by excitatory glutamate-mediated input from pyramidal cells, which in turn inhibited rhythmically via feedback inhibition from PV+ interneurons (called the PING model). Thus, glutamatergic input and glutamatergic receptors for AMPA and NMDA are essential to drive the rhythmic inhibition from PV+ interneurons and NMDAR hypofunction could reduce excitatory drive onto PV cells. Consistent with this, NMDAR antagonists have been shown to decrease GABAergic interneuron activity and subsequently disinhibit pyramidal cells, increasing their activity (Homayoun & Moghaddam, 2007). However, other studies have indicated that NMDAR contributions to glutamatergic transmission in PV cells are relatively small compared to AMPARs (Hull et al., 2009; NyÍri et al., 2003; Rotaru et al., 2011; Wang & Gao, 2009). Consistent with this, gamma oscillatory activity is largely unaffected by NMDAR antagonism, but is reduced by AMPAR antagonism, although these findings vary by region (Buhl et al., 1998; LeBeau et al., 2002; Roopun et al., 2008; Traub et al., 1996). Another angle by which NMDA hypofunction might impact PV+ cells is during development. The maturation of PV+ cells is an activity dependent process as demonstrated in critical periods of plasticity and NMDAR dysfunction may disturb this maturation process. In line with this, the inhibition of NMDARs during development can result in persistent impairments in PV+ cell density (Powell et al., 2012). Other studies have shown that the high-firing rates of PV+ interneurons are in part due to a developmental switch in NMDAR subunits (NR2B to NR2A) and disrupting this switch impairs synaptic plasticity and produces deficits in cognitive function (Matta et al., 2011; McGlothan et al., 2008; Nihei et al., 2000). NMDAR activation has also been shown to enhance antioxidant systems such as glutathione, thioredoxin, and peroxiredoxin (Baxter et al., 2015; Papadia et al., 2008). Given the susceptibility of PV+ interneurons to stressors such as redox dysregulation, NMDAR activation might serve a protective role in this regard. In support of this,

deletion of the NR1 subunit of NMDARs in PV+ interneurons results in PV and GAD67+ deficits and elevated levels of oxidative stress within these cells (Belforte et al., 2010; Jiang et al., 2013). Although not conclusive, these studies demonstrate evidence of a relationship between NMDAR function and PV+ interneurons, which links them with another major hypothesis within the SZ literature. Further studies are required to better describe the relationship between excitation and inhibition in the generation of gamma oscillations, and the role that PV+ interneurons and NMDARs may play.

A final aspect of SZ pathology that might implicate PNN/PV abnormalities is deficits in myelination. Myelination abnormalities are observed extensively in SZ pathology, which has been demonstrated through human in vivo brain imaging studies, but also in post-mortem studies (Alvarado-Alanis et al., 2015; Aston et al., 2004; Cheung et al., 2008; Fitzsimmons et al., 2013; Harris et al., 2009; Lener et al., 2015; Pérez-Iglesias et al., 2010; White et al., 2011). Like PNN development, the time course of myelination within people shows significant overlap with the onset of SZ, typically in late adolescence and early adulthood (Do et al., 2015). While not readily recognized, PV+ interneurons are one of the most heavily myelinated types of interneurons in the CNS. Among all myelinated cortical neurons in humans, 25-50% are GABAergic, and among these, almost all express PV (Micheva et al., 2016). Similar findings have been demonstrated in the mouse visual cortex after myelination occurs throughout adolescence (McGee et al., 2005). Given the fast-spiking dynamics of PV+ interneurons their myelination is perhaps not surprising. PV+ interneurons axonal arborizations are significant in both complexity and length and their regulatory function within local cortical networks demands high precision in the firing of their action potentials (Fino et al., 2013; Packer & Yuste, 2011; Pajevic et al., 2014). Myelination would support these functions given that it can increase conduction velocities and enhance long-

range coherence (Salami et al., 2003). Myelination could also support the immense physiological stress that PV+ interneurons experience during periods of high activity, such as gamma oscillations. It has been shown that during gamma oscillatory activity, mitochondrial oxidative capacity is pushed nearly to its limit and oxygen consumption rates are similar to that of seizure activity (Kann et al., 2014). Given this, myelination could contribute to managing these significant energy demands (Funfschilling et al., 2012; Lee et al., 2012). The presence of the ECM is also important for myelination in the form of the perinodal matrix, which are structurally similar to PNNs but surround nodes of Ranvier (Bekku et al., 2009). Like PNNs, they are thought to act as a cation buffer against the exchange of ions at nodes of Ranvier. Given the shared structural composition of PNNs and perinodal matrices, disruption of PNNs in SZ is suggestive of shared impairment of perinodal matrices. In support of this, brevican deficient mice have disrupted perinodal matrices around their nodes of Ranvier and exhibit abnormal nerve conduction properties (Bekku et al., 2012). Interestingly, comparing this strain with wild-type animals shows no difference in the clustering of their ion channels at nodes of Ranvier but does show differences in the extracellular diffusion of ions, which is indicative of their role in cation buffering. Together, these studies demonstrate yet another pathological alteration thought to be central to SZ dysfunction that shares significant overlap with PNNs and PV interneurons.

Despite the wealth of evidence implicating PNNs in the pathophysiology of schizophrenia and its symptoms, there remain numerous obstacles to interpreting their significance in the disease. Observations that PNNs are reduced in SZ are informative but do not necessarily implicate PNNs as a core feature of the disease. PNN deficits could be an epiphenomenon of other pathophysiological disease processes or could even serve a compensatory mechanism to combat against pathological changes during the disease. Similarly,

while animal models can be informative for replicating these PNN deficits and offer utility in studying mechanisms, they present numerous confounding factors when attempting to make causative conclusions about what role PNNs play in SZ. These issues warrant further investigation into the role of PNN degradation outside of the contexts of disease, where more direct relationships between PNN loss and the symptoms or pathology of the disease can be evaluated.

1.8 PNNs in Alzheimer's Disease

In addition to their involvement in SZ, PNNs have also been implicated in other CNS disease such as AD, autism, bipolar disorder, epilepsy, fragile X syndrome, and multiple sclerosis (Alcaide et al., 2019; Baig et al., 2005; Brandenburg & Blatt, 2022; Crapser et al., 2020; Gray et al., 2008; Pantazopoulos et al., 2015; Pollock et al., 2014; Wen et al., 2018; Yutsudo & Kitagawa, 2015). Among these, the contributions of PNNs to memory and cognition are particularly relevant to the symptoms of AD. Post-mortem studies of AD have offered mix results with regards to PNN changes. PNN deficits have been observed in the cingulate, entorhinal, frontal and temporal cortices of patients that suffered from AD (Baig et al., 2005; Crapser et al., 2020; Kobayashi et al., 1989; Pantazopoulos & Berretta, 2016). In contrast, one study which broadly evaluated PNNs within the frontal and temporal cortices, striatum, and thalamus showed no alterations to PNNs in AD (Morawski et al., 2012). While this could be taken as mixed evidence, these differing results could be attributed to the inherent diversity present in human post-mortem samples and the detection methods used to label PNNs in these studies varied. Transgenic mouse models of AD have also offered utility in evaluating PNN alterations after genetic manipulation of familial-AD genes. In the 5xFAD model which overexpresses amyloid precursor protein (APP) and presenilin-1 (PS1) with 5 mutant genes,

PNNs are reduced in the subiculum and visual cortex of 4-month old animals and these deficits persist until 18-months (Crapser et al., 2020). Similar deficits are shown in the subiculum in the 3xTG animal model, although the visual cortex is spared (Javonillo et al., 2022). In the Tg2576 model, two studies have demonstrated reductions in neurons dual-labelled WFA+/PV+ neurons in the hippocampus, and another has described deficits in the CSPG core protein brevican (Ajmo et al., 2010; Cattaud et al., 2018; Rey et al., 2022). Recent investigations into the rTg4510 mice which feature tauopathy have also shown PNN deficits and PV+ interneuron dysfunction within the somatosensory cortex at 6-months of age (Kudo et al., 2023). Other studies in AD models including Tg2576, APP^{NL-F}, and P301S animals have reported negative results of PNN deficits, although evaluations in these models focused only on the parietal cortex, hippocampus, and perirhinal cortex (Morawski et al., 2010; Sos et al., 2020; Yang et al., 2015). Together, the human and animal model studies demonstrate evidence of PNN loss within AD pathology, however these deficits are not global and vary by the region examined. Future studies would benefit from a more systematic and broader characterization of PNN deficits, particularly in animal models where such a design is feasible.

Given descriptions of their loss in AD in specific areas of the brain, it warrants consideration what the impact of PNN loss in these areas could mean. While PNNs have been implicated in cognitive impairment, memory function, and learning in other CNS diseases like SZ, their role in AD is not as well studied. Similarly, only a small number of studies have evaluated PNN deficits in animal models of AD. In the P301S model, which overexpresses a mutant form of tau, memory impairments are observable in object recognition tasks (Yang et al., 2015). Interestingly however, object recognition performance is restored after injections of ChABC into the perirhinal cortex, an area critical for object recognition tasks. Subsequent

experiments demonstrated that administering antibodies against C4S, the more inhibitory form of CS, extended the retention of long-term object recognition in WT animals and rescued deficits in in the P301S model (Yang et al., 2017). These findings are particularly interesting because they suggest that PNN depletion could serve a beneficial role in alleviating cognitive impairments in AD. Similar results have been demonstrated in otherwise healthy animals, where PNN reductions within the perirhinal cortex can enhance object recognition memory (Romberg et al., 2013; Rowlands et al., 2018). However, in the broader context of studies into PNN depletion where many describe memory impairments after PNN degradation, this suggests that that PNNs within the perirhinal cortex could have a unique relationship with memory in this task (Banerjee et al., 2017; Christensen et al., 2021; Hylin et al., 2013; Kochlamazashvili et al., 2010).

An additional consideration of PNNs in AD is their neuroprotective properties on host neurons. This is particularly relevant in AD which features significant oxidative stress, the expression of factors involved in cell toxicity, and significant cell death (Christen, 2000; Fricker et al., 2018; Yang et al., 2003). One consistent observation across brain regions within post-mortem AD tissue was that cells with PNNs rarely exhibited phosphorylated tau (Morawski et al., 2012). When looking more broadly at the cortical distribution of PNNs, it is also notable that areas relatively dense in PNNs are largely spared from AD pathology (Brückner et al., 1999). Together, these results might suggest that PNNs play a neuroprotective role against AD. Direct evidence of this was shown in cultured cortical neurons where the presence of PNNs was protective against Aβ toxicity and treatment with ChABC removed this protection (Miyata et al., 2007). Similarly, PNN-associated neurons in slice cultures rarely observed to internalize tau protein and after ChABC treatment these neurons internalize it as similar rates as non-PNN bearing cells (Suttkus et al., 2016). In addition to Aβ accumulation, AD also features significant

oxidative stress like as is seen in SZ, which can readily impact PV+ interneuron function if unmitigated (Cabungcal et al., 2013; Solodkin et al., 1996). The impacts of AD on PV+ interneurons however are unclear. In human post-mortem studies, some have observed impairment in PV+ interneurons and others show apparent preservation, although deficits are a feature in numerous animal models of the disease (Ali et al., 2019; Baig et al., 2005; Saiz-Sanchez et al., 2013, 2015; Takahashi et al., 2010; Zallo et al., 2018). Despite these mixed observations, a recent study in the APP/PS1 model of AD showed that PV interneuron activity might have a more central role in AD pathogenesis (Hijazi et al., 2020). Within this model, hippocampal PV interneurons become hyperexcitable prior to any observed changes in excitatory pyramidal neurons. These alterations in PV+ hyperexcitability also coincide with the onset of impairments in spatial learning and memory. Inhibition of PV+ cells reduced this hyperexcitability to restore normal levels of PV+ cell activity and rescued memory impairments. Most notably, this dampening of PV+ interneuron hyperexcitability also reduced Aβ-plaque deposition. This study demonstrates not only an involvement of PV+ interneurons in the cognitive deficits exhibited in this model but that alterations in PV+ activity could be a contributing factor to Aβ-plaque deposition, which is considered a hallmark of AD pathology (Goedert et al., 1991; Hardy & Allsop, 1991). Linking this to PNNs, consistent observations that their degradation increases the excitability of PV+ interneurons could suggest that their loss in AD disrupts PV+ activity which in turn contributes to cognitive impairment and exacerbation of Aβ pathology (Dityatev et al., 2007).

In summary, PNNs are implicated in human AD and as a feature of numerous animal models of the disease, although these deficits vary by region. These observations are particularly relevant given the prominent memory and cognition impairments seen in AD and the role that

PNNs can play in those functions. While PNNs may confer protective properties against the pathology of AD, that makes their disruption only more consequential in the context of a disease that features significant cellular toxicity and metabolic stress. Further study is required to provide more thorough characterizations of PNN deficits through the brains of both AD patients and animal models of the disease. Such information could be used as a foundation upon which to further evaluate the effects of PNN degradation within these regions to determine their impact on the cognitive symptoms of AD.

1.9 Thesis Outline and Aims

The goals of this thesis were to evaluate the role of PNNs in CNS diseases and cognition. PNN loss and cognitive impairment are a shared feature of several CNS diseases, including SZ and AD (Baig et al., 2005; Crapser et al., 2020; Kilonzo et al., 2020; Mauney et al., 2013; Pantazopoulos et al., 2010; 2013; Steullet et al., 2018). Previous work from our laboratory has shown that PNN deficits are also apparent in a prominent animal model of SZ, a finding which has since been demonstrated as a common feature among numerous animal models of the disease (Paylor et al., 2016; Steullet et al., 2017). Studies into other CNS diseases such as autism multiple sclerosis, epilepsy, bipolar disorder, and fragile X syndrome have also indicated that PNN loss could be a consequence of their pathophysiology (Alcaide et al., 2019; Brandenburg & Blatt, 2022; Gray et al., 2008; Pantazopoulos et al., 2015; Pollock et al., 2014; Wen et al., 2018; Yutsudo & Kitagawa, 2015). However, the implications of their loss in these diseases are not clear. To address this, evaluating PNN deficits in prominent animal models of disease allows us to determine whether animal models can recapitulate aspects of PNN loss. By identifying appropriate models to study this phenomenon, we provide opportunities to investigate the mechanisms of their loss, the consequences for symptomatology and pathophysiology, and

evaluate potential treatments against disease driven PNN loss. The evaluation of PNN deficits in animal models alone can also be problematic however, as models typically feature complex pathophysiology of their own. Like CNS diseases, the observation of PNN loss in animal models of disease does not necessarily implicate them as a core feature of their pathology, as their degradation could be an epiphenomenon of other pathophysiological processes. Alternatively, their downregulation could be a compensatory mechanism. Thus, investigations into the impact of PNN loss on cognition outside of disease models are also valuable to better isolate out their unique contributions.

Chapter 2 Aims – Evaluating PNN deficits in the 5xFAD mouse model of AD

In this chapter, I sought to utilize my previous experience in characterizing PNN deficits in a SZ model by applying similar techniques to an animal model of AD. Like in SZ, cognitive impairment is a prominent feature of AD symptomatology and post-mortem studies indicate a loss of PNNs in several regions of the brain in AD (Baig et al., 2005; Crapser et al., 2020; Kobayashi et al., 1989). However, other reports have demonstrated negative results of PNN loss in the disease (Morawski et al., 2010). PNN integrity in animal models of the disease has also been sparsely evaluated and in only limited regions of the brain. Given the significant overlap between the effects of PNN disruption on cognition and memory, and impairment in those functions within AD, more thorough investigations of PNN loss in the disease are necessary. Given better descriptions of when and where PNN disruption occurs within AD and animal models of the disease, future investigations could better target the specific consequences of PNN disruption with these areas.

Within this chapter, I utilized 5xFAD mouse model of AD which overexpresses amyloid-precursor protein 695 (APP695) and presenilin-1 (PS1) with 5 mutant genes (APP: S-K670N, S-

M671L, F-176V, L-V7171; PSEN1: M146L, L286V). This model features an aggressive AD-like presentation with significant Aβ-plaque accumulation, neuroinflammation, synaptic disruption, and neuronal cell death, all of which are features of AD (Akhtar et al., 2022; Forner et al., 2021; Oakley et al., 2006). These animals also display deficits in spatial working memory, novel object recognition, fear conditioning, and social recognition with varying onsets (Griñán-Ferré et al., 2016; Jawhar et al., 2012; Kimura & Ohno, 2009; Oakley et al., 2006). I evaluated PNN deficits in the immunohistochemical staining of the CNS of 5xFAD mice across 5 different brain areas: the mPFC, primary motor cortex, hippocampus, entorhinal cortex, and retrosplenial cortex (RSC). Additionally, I sought to evaluate the temporal progression of any deficits by evaluating both 7-month and 11-month-old animals. While these animals have shown to have cognitive impairments on some tasks by 7-months of age, these deficits are often observed to worsen with age, which correlates with the severity of their disease (Bouter et al., 2014; Jawhar et al., 2012; Oakley et al., 2006; Schneider et al., 2014; Urano & Tohda, 2010).

In addition to this characterization of PNN deficits, I evaluated several other markers of disease progression in AD. Firstly, I stained for Aβ-plaque deposition, which is a hallmark feature of AD pathology, to measure disease severity (LaFerla et al., 2007; Murphy & LeVine, 2010; D.-S. Wang et al., 2006). I evaluated IBA1+ microglia as a marker to assess the degree of neuroinflammation within animals. Microglia have been shown to play a prominent role in both AD (and 5xFAD) pathology and help to regulate the integrity of PNNs in otherwise healthy animals (Cameron & Landreth, 2010; Crapser et al., 2020; Hansen et al., 2018; Hong et al., 2016). Lastly, I evaluated the presence of PV+ interneurons, which are closely associated with PNNs, and fluorojade-C, a stain for identifying cell death within the mPFC and RSC. I also tested animals' performance on two tests of memory, a spontaneous alternation task and novel

object recognition, as a measure of cognitive impairment. In this case, previous studies would predict that cognitive impairment in these tasks would already be present by 7-months of age, but replicating this here would allow us to contrast these deficits against any observed PNN deficits.

Chapter 2 Hypothesis: 5xFAD animals will exhibit cognitive impairment in spatial memory and object recognition and will have corresponding reductions in PNNs in five regions of the brain: the mPFC, primary motor cortex, CA1 of the dorsal hippocampus, entorhinal cortex and retrosplenial cortex. PNN deficits will worsen with age and all these regions will demonstrate significant accumulation of Aβ deposition, microglial reactivity, and markers of cell death, which is characteristic of this animal model of AD.

Chapter 3 Aims – Evaluating cognitive impairment after targeted depletion of PNNs within the mPFC of rats

This experiment intended to build upon previous findings from our laboratory that demonstrated that in a MIA model of SZ in rats (polyI:C), PNN deficits emerge within the medial prefrontal cortex in late adolescence and early adulthood (Paylor et al., 2016). These results demonstrated that the polyI:C model was effective at recapitulating some of the PNN deficits observed in the post-mortem tissue from patients who suffered from schizophrenia. Notably, in animals from MIA mothers' their PNN development followed a typical trajectory until late adolescence and early adulthood. The appearance of this deficit also coincided with the typical onset of cognitive impairment in this animal model, some of which are though to be dependent on the mPFC (Ballendine et al., 2015; Vorhees et al., 2015; Wolff et al., 2011; Wolff & Bilkey, 2008). While a characterization of the timeline of PNN loss and the presentation of symptoms within these animals is informative, linking PNN deficits to cognitive impairment is difficult. Like the limitations of human post-mortem studies, the observation of PNN loss and development of SZ

symptoms could be concurrent but unrelated phenomenon. Thus, in chapter 3 the experiment was designed to isolate the impact of PNN loss within the mPFC, the same region within which our lab had observed PNN deficits in the maternal immune activation model of SZ.

To evaluate the impact of PNN loss, I treated rats with bilateral injections of ChABC, an enzyme which degrades PNNs, within the same developmental window that we had previously observed PNN deficits in our MIA model. Using immunohistochemistry, I evaluated the efficacy of ChABC to degrade PNNs and look for potential changes within PV interneurons using three markers: PV fluorescence, GAD67 fluorescence, and Gephyrin+ puncta. Both PV+ and GAD67+ are commonly expressed markers within PV+ inhibitory interneurons and previous studies have demonstrated that a loss in their fluorescence might be indicative of alterations within these cell types (Enwright et al., 2016; Kinney et al., 2006; Zallo et al., 2018). The third stain, gephyrin, is a major scaffolding protein at inhibitory synapses. As such, I evaluated its density on mature neuronal cells within the mPFC to evaluate potential changes in inhibitory connectivity. I also assessed any potential neuroinflammation as a result of PNN degradation by labeling IBA1+ microglia and GFAP+ astrocytes. Two weeks after ChABC injections I evaluated animals across a battery of four tests of cognition including prepulse inhibition, operant set shifting, oddity preference task, and the crossmodal object recognition task. These tests offered a broad assessment of sensorimotor gating, behavioural flexibility, working memory, and multisensory integration. Impairment in these functions is common in schizophrenia and importantly for the present study, deficits in them have been shown in the MIA model of SZ we previously observed PNN deficits in (Ballendine et al., 2015; Vorhees et al., 2015; Wolff et al., 2011; Wolff & Bilkey, 2008). By utilizing common behavioural measures, this allowed comparisons against the broader impact of the MIA model of SZ on cognition against localized disruptions of PNNs.

Chapter 3 Hypothesis: Treatment with ChABC will degrade PNNs within the mPFC and diminish the expression of PV+ and GAD67+ fluorescence within PV+ interneurons but will not have significant impact on local inflammation. PNN degradation within the mPFC will impair cognitive performance, as measured on four unique cognitive tests: prepulse inhibition, operant set-shifting, oddity preference, and crossmodal object recognition.

Chapter 4 Aims – Evaluating the impact of transient PNN degradation within either the mPFC or RSC on cognition and memory in healthy mice

In this chapter I planned to build upon the findings of chapter 3, which demonstrated the PNN degradation within the mPFC outside of the confounds of disease models, can result in cognitive impairment (Paylor et al., 2018). To advance upon my previous work, I first sought to evaluate whether these deficits in rats also translated into mice. While mice typically are considered less suited to cognitive testing than rats, they also offer significant utility in terms of genetic manipulations and in vivo imaging opportunities. Thus, the potential to harness the utility of mice necessitated that we first characterize the cognitive profile of mice and the impacts of PNN degradation. Rather than utilize ChABC, I utilized a dual viral vector that enables for localized expression of ChABC under the control of a dietary trigger (Burnside et al., 2018). This design enabled evaluation of animals' cognitive performance at baseline, after 30 days of ChABC expression, and 30 days after the dietary trigger for ChABC expression had been withdrawn. Additionally, given emerging evidence and our observations of dense PNN expression within the RSC, I chose to include this along with the mPFC as a second region of interest in our study. The RSC is a highly interconnected region of cortex that has demonstrated involvement in working memory, spatial cognition, and the default mode network (Buckner & DiNicola, 2019; Monko & Heilbronner, 2021; Morris et al., 1999; Raichle, 2015; Raichle et al., 2001; Vann et al., 2009).

Moreover, numerous recent studies have implicated RSC dysfunction in SZ (Bluhm et al., 2009; Liang et al., 2006; Whitfield-Gabrieli et al., 2009).

First, I evaluated animals' performance on four cognitive tests: open field behaviour, spontaneous alternation, the oddity preference task, and crossmodal object recognition. I utilized these tests to evaluate general motor activity, working memory, and multisensory integration. After baseline behavioural assessments, I followed these animals for 30 days of sustained ChABC progression, after which I against tested them on the same battery of cognitive assessments. The dietary trigger for ChABC was then withdrawn and animals were evaluated in a final behavioural session after an additional 30 days. At the end of the experiment animals were euthanized to confirm the efficacy of ChABC expression to degrade PNNs within the mPFC and RSC. I also evaluated the impact of PNN degradation on PV+ interneurons at both sites and assessed any inflammatory reactivity to the expression of ChABC within these animals. Lastly, I included an additional cohort of control and ChABC animals underwent wide field optical imaging to evaluate patterns of cortical activity (spontaneous and sensory evoked) after PNN degradation within the RSC.

Chapter 4 Hypothesis: ChABC expression will result in PNN deficits in the mPFC or RSC but will not affect the integrity of PV+ interneurons at either location. PNN degradation within the mPFC will impact performance on oddity object preference and the crossmodal object recognition task, but not open field behaviours or spontaneous alternation. Animals with PNNs degraded in the RSC will have impaired spontaneous alternation, oddity object preference, and crossmodal object recognition, but not open field behaviours. PNN degradation within the RSC will impact activity patterns generated from the RSC and its interconnectivity with other cortical areas.

Chapter 2 – Perineuronal net loss, amyloid-β deposition, and cognitive deficits in the brains of 5xFAD-transgenic mice

Abstract

Perineuronal nets are organized components of the extracellular matrix that sheathe mature neurons of the CNS. These structures play a critical role in limiting neuronal plasticity and providing structural and functional support to the neurons that host them. The loss of PNNs in the context of disease can cause dysregulation in plasticity, the excitatory/inhibitory balance of the cortex, and can result in impairment in cognitive functions such as memory. Here, we investigate the integrity of PNNs in the 5xFAD model of Alzheimer's disease, which reflects cognitive deficits and β-amyloid (Aβ)-containing neuropathology associated with the disease. We evaluated animals across five brain regions at time points representative of moderate (7-months) and later stages of disease (11-months). Concurrently, we evaluated Aβ deposition, microglial activation, markers of cell death, and the presence of parvalbumin-positive inhibitory interneurons. We also evaluated animals in the earlier stage of disease on two cognitive tests of memory, spontaneous alternation and novel object recognition. Our data show that cognitive deficits in spontaneous alternation and novel object recognition are present in animals at 7-months of age. We also show significant extracellular matrix loss throughout the brains of 5xFAD animals. PNN deficits were observed in the retrosplenial cortex, CA1 region of the dorsal hippocampus, and primary motor cortex – but not in the medial prefrontal cortex or entorhinal cortex. All brain regions investigated had significant Aβ deposition, elevated markets of neuroinflammation and cell death, but normal levels of parvalbumin positive inhibitory interneurons. This data suggests that the extracellular matrix and PNNs are significantly altered in 5xFAD animals as early as 7-months of age. The loss of PNNs in selected brain regions could contribute to cognitive impairment observed in 5xFAD animals and warrants further investigation in human AD brains.

Introduction

Alzheimer's Disease (AD) is the most common form of dementia. Its symptoms include progressive memory loss and cognitive decline that can affect multiple cognitive domains. Globally, 55 million people suffer from AD and there are 10 million new cases each year. This number is expected to increase in coming years with an increase in the aging population in our society (Alzheimer's Association, 2019). In Canada, where 600 thousand people suffer from AD, the estimated healthcare costs associated with the illness are $10.4 billion (Alzheimer's Society of Canada, 2016; 2022). These projections only account for direct healthcare costs and do not include the costs of diminished quality of life, productivity lost, and dependence on informal care. Between 2000 and 2012, disability-adjusted life years (DALYs), years of life lost (YYL), and years lived with disability (YLD) attributed to AD and other dementias grew globally by 65%, 148%, and 40%, respectively (WHO, Global Burden of Disease Study). Given that AD has a progressive but delayed onset, and the immense societal burden of the disease, it is essential to better understand it's etiology and pathophysiology.

The primary neurological features of AD are intracellular neurofibrillary tangles (NFT) enriched with hyperphosphorylated tau protein and extracellular neuritic plaques containing amyloid-beta (Aβ) peptides. The early development of the disease is characterized by the extracellular deposition of Aβ in the entorhinal cortex (Braak & Braak, 1991; Lehéricy et al., 1989; Nardone et al., 2008; Whitehouse et al., 1982). As the disease progresses, Aβ spreads throughout the neocortex and NFT through medial and inferior regions of the brain. In late-stage AD, both extracellular Aβ deposits and/or NFT can be found throughout the cortex and hippocampus as well as some subcortical nuclei of the brain. In addition to the development of Aβ-containing neuritic plaques and NFT, AD-affected brains typically exhibit decreased synaptic

density, neuronal loss, as well as increased gliosis and neuroinflammatory activity (Brun et al., 1995; Bussière et al., 2003; Davies et al., 1987; Lorke et al., 2006; Masliah et al., 2001; Nordberg & Winblad, 1986).

Etiologically, two forms of AD have been identified, familial AD (FAD) and sporadic AD. FAD is far less common (less than 5% of cases of AD) but presents with an earlier onset. The pathology and symptoms of both forms of the disease are otherwise indistinguishable from each other. FAD cases are caused by mutations of three known genes i.e., amyloid precursor protein (APP) gene location on chromosome 21, presenilin-1 (PSEN) gene located on chromosome 14 and presenilin-2 gene located on chromosome 1. The PSEN1/2 genes are essential to the cleavage of APP and the subsequent generation of Aβ. The identification of gene mutations in APP and PSEN1/2 are the foundation of generating transgenic models of AD which are now being utilized to study its pathophysiology. One such model is the 5xFAD transgenic mouse model which co-express three APP (Swedish mutation: K670N, M671L, Florida mutation: I716V; London mutation: V717I) and two PS1 (M146L and L286V) Familial AD mutations resulting in the development of AD-related pathology. The gene mutations drive excessive accumulation of Aβ plaques in specific brain regions. Anatomical observations in 5xFAD mice also have demonstrated the presence of significant neuroinflammatory activity, synaptic disruption, and neuronal cell death, all of which are characteristic of AD (Akhtar et al., 2022; Forner et al., 2021; Oakley et al., 2006).

In addition to its cellular and anatomical presentation, 5xFAD mutant mice display behavioural and cognitive impairments that are consistent with AD (Griñán-Ferré et al., 2016; Oakley et al., 2006). Deficits in spatial working memory have been demonstrated in both Y-maze and cross-maze designs in 5xFAD mice, beginning as early as 6 months of age (Jawhar et

al., 2012; Oakley et al., 2006). Importantly, while studies have shown that 5xFAD mice do develop motor impairments, in these tasks' animals had similar motor behaviour to controls but impaired working memory performance, suggesting this deficit is not due to confounding motor impairment. Similarly, spatial working memory deficits have been demonstrated in the Morris Water maze, where impaired spatial memory is present as early as 6 months of age, and impaired learning shown in 9 month and 1 year old animals (Bouter et al., 2014; Ohno et al., 2006; O'Leary & Brown, 2022; Schneider et al., 2014; Urano & Tohda, 2010). Across numerous behavioural testing paradigms, 5xFAD animals' deficits have been shown to increase with age, which is thought to be reflective of the progressive neuropathological development of an AD-like phenotype in 5xFAD animals. In addition to their spatial working memory deficits, 5xFAD mice also present with other cognitive impairments in fear conditioning, novel object recognition, and social recognition tasks (Griñán-Ferré et al., 2016; Kimura & Ohno, 2009; Locci et al., 2021).

One dimension of AD that has gained significant interest in recent years is the role that neuroplasticity might play in both the progression of the disease pathology and its symptoms, such as cognitive decline (Mercerón-Martínez et al., 2021; Mesulam, 2000; Spires-Jones & Knafo, 2011). Cognitive functions such as learning and memory are dependent on neuroplasticity and deficits in this capacity could underlie impairments observed in AD. Therapeutic interventions designed to enhance plasticity might also be able to counteract the progressive cognitive decline seen in AD. One anatomical substrate with significant contributions to neural plasticity that has been considered is the extracellular matrix (ECM). The ECM exists in three primary forms in the brain: a loose form of the ECM which exists throughout the entire

interstitial space between cells, the basal lamina, and perineuronal nets (PNNs), which are organized ECM composites that surround certain cell types (Kwok et al., 2011; Lau et al., 2013).

PNNs play a critical role in regulating plasticity in the brain (Fawcett et al., 2019; Sorg et al., 2016; Wang & Fawcett, 2012). The development of PNNs in primary sensory regions typically coincides with the closure of critical windows of plasticity (Pizzorusso et al., 2002). Within these windows, cortical tissue undergoes dramatic reorganization in response to external stimuli. Manipulations which delay the formation of PNNs can extend these critical windows, and enzymatic degradation of PNNs after a critical window has closed can re-establish a period of elevated plasticity (Carulli et al., 2010; Lander et al., 1997; Pizzorusso et al., 2002). Like primary sensory regions, the amygdala also has a critical window during development within which learned fear memories resulting from fear conditioning become permanent and resilient to extinction. This development shift occurs in parallel to a significant upregulation in PNN density within the amygdala (Gogolla et al., 2009). Degradation of mature PNNs in the amygdala via injections of the enzyme chondroitinase ABC (ChABC), which degrades perineuronal nets, restores the ability to extinguish or unlearn these fear memories.

While a broad body of research describes PNNs role in learning, memory, and cognitive impairment in the context of other CNS diseases (e.g. schizophrenia, addictions), there is less available data investigating their contributions in AD (Sorg et al., 2016; Testa et al., 2019). Animal models have been more widely utilized to investigate how the ECM, and in some cases PNNs, might be impacted by AD pathophysiology and what their role might be in the development of disease pathology. In a transgenic line of mice expressing a mutant form of tau protein (P301S), resulting in tauopathy and cognitive impairments such as diminished object recognition, ChABC injections into the perirhinal cortex restores object memory to normal levels

(S. Yang et al., 2015). Similarly, transgenic attenuation of PNNs delayed the onset of memory loss by several weeks in this model of tauopathy. Subsequent studies showed that administering antibodies specifically targeting chondroitin-4-sulfate (C4S), the more inhibitory form of CSPG present in PNNs, extended long-term object recognition in wild-type animals and reversed deficits when administered to animals with an AD-like phenotype (S. Yang et al., 2017). Taken together, these studies might suggest that PNN depletion could serve a beneficial role in alleviating cognitive impairments in AD.

In contrast to behavioural studies showing improved cognitive performance after PNN degradation, neuroanatomical investigations suggest that maintaining PNN integrity may play an important role in protecting neurons from AD-related pathology. Firstly, cortical regions densely populated with PNNs appear to be relatively spared by AD pathology compared to other cortices (Brückner et al., 1999a). In cultured cortical neurons, the presence of PNNs is directly protective against Aβ toxicity and if pre-treated with ChABC to degrade PNNs, these neurons are no longer spared (Miyata et al., 2007). This protective role is particularly relevant when considering the close relationship between PNNs and their most common host neuronal type, parvalbumin+ (PV) inhibitory interneurons. PNNs are supportive of the high energy demands of these highly active neurons and their dissolution makes PV+ interneurons particularly vulnerable to the reactive oxygen species produced seen in AD (Cabungcal et al., 2013; Solodkin et al., 1996). A loss of PV+ cells has been shown in numerous AD models but observations from human post-mortem tissue are less clear, with decreases in PV+ cells in the dentate gyrus but increases in piriform cortex (Ali et al., 2019; Baig et al., 2005; Saiz-Sanchez et al., 2013, 2015; Takahashi et al., 2010; Zallo et al., 2018). Functionally, the disruption of PV+ cellular activity has shown to lead to imbalances in excitatory and inhibitory activity in the cortex that contributes to AD-pathology

(Hijazi et al., 2020; Verret et al., 2012). One mechanistic link that could underlie the loss of PNNs and PV+ disruption in AD is the activity of microglia, which modify and regulate the integrity of PNNs (Crapser et al., 2020).

Microglia are important regulators of PNN integrity in both the healthy and diseased brain. Like PNNs, microglia have direct roles in modulating neuronal and synaptic elements and contribute to learning and memory (Elmore et al., 2018; Rice et al., 2015; Tremblay et al., 2011). In damaged or diseased states microglia can remodel the ECM including PNNs, via their activation and secretion of matrix metalloproteinases which degrade ECM components (Gottschall & Deb, 1996; Patel et al., 2013; Wen et al., 2018). A relationship between microglia and PNN integrity was recently demonstrated in the subiculum of 5xFAD animals, where chronic activation of microglia and PNN loss are both observed (Crapser et al., 2020). Pharmacologically depleting microglia prevented 5xFAD PNN loss in the subiculum, even though Aβ-plaques were unaltered. Notably, many microglia in this study were also positive for intracellular markers of PNNs, supporting their putative role in phagocytic clearance of cellular debris and their capacity to digest PNN components. Similar results were found when PNNs were examined in human post-mortem tissue from the subiculum, which had significant PNN loss that correlated inversely with plaque burden (Crapser et al., 2020).

While disturbances in the ECM, PNNs, and microglia have been described in AD, the progression and breadth of this degradation is not entirely clear. In the present study, we sought to examine the integrity of PNNs in 5xFAD mice across five brain regions: the medial prefrontal cortex, primary motor cortex, dorsal hippocampus, entorhinal cortex, and retrosplenial cortex. Within these regions, we evaluated the brains of mice at 7 and 11-months of age to determine whether PNN changes might parallel or differ with age accompanying the progressive

development of Aβ-related pathology in 5xFAD animals. We took particular interest in the progression of AD and the potential loss of PNNs within the mPFC and RSC, two regions of the brain that might contribute to memory impairments seen in AD. The mPFC has been widely studied in AD and other disease contexts for its role in working memory and its contributions to integrating diverse sensory information (Gisquet-Verrier & Delatour, 2006; Granon et al., 1994; Jobson et al., 2021; Mu et al., 2022; Shin et al., 2020). Direct infusion of Aβ into the mPFC induces permanent deficits in working memory and reversal learning and impacts excitability and plasticity within the region (Bai et al., 2016; Torres-Flores & Peña-Ortega, 2022). Numerous other studies have linked mPFC related dysfunction in animal models of AD, including 5xFAD, to the memory impairments these models present with (Girard et al., 2012; Q. Sun et al., 2022; Tian et al., 2018). Similar to the mPFC, healthy functioning of the RSC has been shown to be involved in spatial and working memory processes (Kim et al., 2020; Stacho & Manahan-Vaughan, 2022; Trask & Fournier, 2022). Given the high density of PNNs in this region, we took interest to determine whether it would be particularly resilient to AD-related pathology (Carceller et al., 2022; Seeger et al., 1994).

We also evaluated a cohort of 5xFAD animals with at 7-months of age on two cognitive tasks, novel object recognition and spontaneous alternation, to determine whether PNN changes within these task-associated regions might show common impairment. Manipulations of the mPFC have previously been shown to impact performance on spontaneous alternation tasks, but the consequences for novel object recognition are less clear (Delatour & Gisquet-Verrier, 1996; Divac et al., 1975). Numerous studies have shown that in single trial novel object recognition, manipulations of the mPFC may not impact performance, but more complex versions of the task such as cross-modal object recognition can be impacted (Barker et al., 2007; Mitchell &

Laiacona, 1998; Paylor et al., 2018). In the case of the RSC, manipulations have previously shown to impact alternation behaviour and novel object recognition performance (de Landeta et al., 2021, 2022; Kim et al., 2020; Nelson et al., 2015; Pothuizen et al., 2010).

Our results indicate that the loss of ECM integrity is widespread throughout the cortex of 5xFAD animals by 7 months of age, but that PNN deficits are region-specific. In the moderate (i.e., 7-month) and later stages of disease (i.e., 11-month), the primary motor cortex, CA1 of the dorsal hippocampus, and retrosplenial cortex, unlike the mPFC and entorhinal cortex, had significant loss of PNNs. In every region we observed significant Aβ-plaque deposition and activation of microglia. Within the mPFC and RSC, there was no significant loss of PV+ cells despite their close association with PNNs, but there were elevated markers of cell death, particularly in later stages of disease. Behaviourally, animals with moderate pathology presented with significant impairments in both spontaneous alternation and novel object recognition memory when compared to WT controls.

Methods

Subjects. We utilized 5xFAD mice and age-matched WT mice (The Jackson Laboratory) on a C57BL/6xSJLbackground. The phenotype and 5xFAD presentation of these animals has been described previously (Oakley et al., 2006). After arrival, animals were housed in ventilated plastic cages with food and water at libitum, on a 12-hour light/dark cycle. All animal procedures were performed in accordance with the University of Alberta animal care committee's regulations. A total of n = 33 animals were utilized for these experiments. For the immunohistochemistry experiments, a total of n = 23 animals were utilized, n = 15 animals were euthanized at 7-months of age cohort and n = 8 were utilized for the 11-month cohort. Among those 23 animals, n = 12 animals were wild-type genotype (7-mo, n = 8; 11-mo, n = 4) and n =

11 were 5xFAD mutant genotype (7-mo, n = 7; 11-mo, n = 4). For the behavioural studies, a total of n = 10 animals were utilized. All animals in the behavioural cohort were euthanized at 7-months of age (WT, n = 5; 5xFAD, n = 5)

Novel Object Recognition Task. To investigate non-spatial cognitive memory, we performed the novel object recognition (NOR) memory test. This task was performed in a white acryl plastic chamber (40cm × 40 cm × 40 cm). In brief, a habituation trial was conducted one day prior to the training where all the mice were exposed to the open field arena in the plastic box without objects for 10mins for acclimatization. During the training session, mice were allowed to explore freely and get acquainted with two identical objects for 8min. After 24h post-familiarization, one of the familiar objects was replaced with a novel object and the interactions of the animals with these objects were recorded for 8mins. Only active exploration, defined as direct interaction with the nose or vibrissae towards the object but not circling around the object, was included in the analysis. The time spent exploring each object was recorded to evaluate the relative exploration of the novel vs familiar object and was calculated as the discrimination ratio: $DR = (t_{nov}\text{-}t_{fam}/ t_{tot})$, wherein "$t_{nov}$" represents time exploring the novel object, "t_{fam}" the familiar object, and "t_{tot}" represents total time spent exploring both objects.

Spontaneous alternation. Spontaneous alternation performance was conducted using a symmetrical Y shaped maze composed of three arms with groove and wall (35L x 7W x 15H cm). This test was conducted to investigate the willingness of an animal to explore a new environment and spontaneous behavior of alternating to a new arm without entering the previously visited arm utilizing spatial memory. In brief, each animal was introduced into the center of the maze and allowed to explore freely for 8min during which the acquisition of total number and pattern of arm entries were recorded using a video camera and analyzed. Arm entry

was complete when the hind paws of the mouse had been completely placed in the arm. Percentage of spontaneous alternation was calculated based on the number of triads "T_{not}" containing entries into all three arms divided by the maximum number of possible alternations (total arm entries minus 2, T_{na-2}) i.e., percentage of spontaneous alternation= $T_{not}/(T_{na-2})$.

Tissue Collection. Following behavioral testing, mice were deeply anesthetized with isoflurane and transcardially perfused with PBS followed by 4% paraformaldehyde using infusion pumps. After perfusion, brains were extracted and stored in 4% paraformaldehyde at 4°C. One-day later, brains were transferred to 30% sucrose for several days and then frozen in isopentane and optimal cutting temperature (OCT) gel. Frozen brains were sectioned at 25 μm on a cryostat.

Immunohistochemistry. Slides were warmed to room temperature for 20 min and then given three washes in 1X PBS for 10 min each. After which slides were incubated for 1 hour with 10% Protein Block, Serum-Free (Dako, Missisauga, ON) in 1X PBS. Slides were then incubated overnight at room temperature with a primary antibody in a solution of 1% Protein Block, 1% Bovine Serum Albumin, and 99.9% 1X PBS with 0.1% Triton X-100. Primary antibodies were as follows: mouse anti-4G8 (1:500, Biolegend), rabbit anti-IBA1 (1:200; Dako), *Wisteria floribunda* agglutinin (WFA; 1:1000; Vector Labs), rabbit anti-parvalbumin (1:1000; Swant); mouse anti-NeuN (1:500, Millipore). After overnight incubation, slides were washed three times, twice in 1X PBS with 1% tween-20 and once in 1X PBS. Slides were then incubated for 1h with secondary antibodies in antibody solution (as above). Secondary antibodies were as follows: streptavidin 647 (1:200; Invitrogen), donkey anti-mouse Alexa Fluor 488 (1:200; Invitrogen), donkey anti-rabbit Alexa Fluor 647 (1:200; Invitrogen), and donkey anti-mouse 647 (1:200; Invitrogen). After 1 hour incubation slides were washed again three times. For slides stained with Fluorojade-C (FJC), after secondary antibody incubation slides were transferred to a 1% NaOH

and 80% ethanol solution for 5 minutes. After that, they soaked in 70% ethanol for 5 minutes, and then lastly distilled water for 5 minutes. Slides were then transferred to an FJC solution (10mL stock solution of 0.01% FJC in distilled water) and 90 mL of 0.2% acetic acid) for 30 minutes. Slides were then washed a final time in distilled water for 2 minutes. After the staining process was complete (for all slides including those subjected to FJC), slides were mounted with DAPI (4',6-diamidino-2-phenylindole) in vectashield mounting medium (Vector Labs, Philadelphia, PA) and coverslipped.

Microscopy. Images were acquired using a Leica DMI6000B Microscope with LAS AF computer software. Regions of interest were identified using Allen Mouse Brain Atlas (Allen Reference Atlas – Mouse Brain. Available from atlas.brain-map.org) and selected based on landmarks in the DAPI nuclear staining pattern. The coordinates for each region were as follows: Medial Prefrontal Cortex (+1.5 to +1.8 AP, 0.5 ML, 2.5 DV; with the imaging window aligned to the midline and extending laterally through all cortical layers); Primary Motor Cortex (+0.4 to +0.8 AP, 1.5 ML, 1.0 DV; with the imaging window aligned to the dorsal surface of the brain and extending down through all cortical layers); Dorsal Hippocampus (-1.6 to -1.9 AP, 1.5 DV; with the imaging window centered over the hippocampus); Entorhinal Cortex (-2.9 to -3.2 AP, 3.5 ML, 4.5 DV; with the imaging window aligned to the lateral and ventral surfaces of the brain extending in towards the midline); Retrosplenial Cortex (-2.9 to -3.2 AP, 0.5 ML, 1.0 DV; with the imaging window aligned to the dorsal midline of the brain, extending laterally). All images were captured at 5X magnification except for the dorsal hippocampus, which was captured at 10X magnification. For each animal, a total of 6 images were taken bilaterally in adjacent sections. A constant gain, exposure, and light intensity was used across all animals for each region and stain.

Image Analysis. Analysis was completed on unmodified images by an observer blind to the experimental condition of the tissue analyzed. For each region of interest, an imaging rectangle was drawn over the target area and the measurement area quantified for comparison. For all stains mean brightness within the measurement area was captured. Mean brightness values were normalized to the mean of each staining set to control for separate staining cohorts. Cell counts for DAPI+, FJC+ cells, and PV+ cells were performed using the Image-based Tool for Counting Nuclei (Centre for Bio-image Informatics, UC Santa Barbara, CA, USA) plugin for NIH ImageJ software. PNN counts were conducted manually and identified based on an evaluation of three criteria: brightness, shape, and the presence of dendrites or an initial axon segment.

Statistical Analyses. All data are presented as mean ± SEM. Statistical analyses were conducted in PRISM Software (Prism Software, Irvine, CA) and significance was set at $p < 0.05$. For all immunohistochemistry, 2-way ANOVAs were conducted on the dependent variables with animal age (7 month or 11 month) and strain (WT or 5FAD) as independent variables. Post-hoc analyses utilized Bonferroni corrected t-tests. For the behavioural tasks, unpaired t-tests were utilized to compare outcomes between WT and 5xFAD animals at 7 months of age.

Results

In the present study, we utilized immunohistochemistry to evaluate the integrity of PNNs in 5xFAD mice in five brain regions over two time-points, 7-months, and 11-months of age, which are representative of moderate and later stages of disease (Devi et al., 2015; Devi & Ohno, 2016). Simultaneously, we assessed the degree of Aβ build-up to determine disease progression across these same brain regions and IBA1+ microglia as a marker of neuroinflammatory activity. We further probed two regions, the medial prefrontal cortex and retrosplenial cortex to assess markers of cellular death and for the presence of PV+ inhibitory interneurons, which are closely

associated with PNNs. To determine whether PNN deficits within these regions was associated with cognitive performance, we assessed animals on two behavioural measures, spontaneous alternation and novel object recognition.

Behavioural tasks. To test animals' memory performance at 7-months of age, we evaluated them on two tasks: novel object recognition and a spontaneous alternation task. For the novel object recognition task (Figure 1), we first evaluated total exploration time during the testing phase which was unaffected by group ($t_{(8)}$=0.12, $p > 0.05$). However, 5xFAD animals did show a significant decrease in discrimination ratio for the novel object when compared to WT animals ($t_{(8)}$=6.33, $p < 0.01$). For the spontaneous alternation task we evaluated total number of arm entries and spontaneous alternation events as a percentage of total entries (Figure 2). The total number of arm entries did not differ significantly between WT and 5xFAD animals ($t_{(8)}$=1.73, $p > 0.05$) but 5xFAD animals did have a significant decrease in spontaneous alternation percentage (Figure 2, bottom right; $t_{(8)}$=4.85, $p < 0.01$). This confirms that 7-month-old 5xFAD animals had significant impairments on both tests of working memory.

Medial Prefrontal Cortex Immunostaining. Here we describe observations from our immunostaining within the mPFC (Figure 3A) which included 4G8 (green), IBA1 (red), WFA, and PNN counts (both purple).

First, to evaluate the extent of amyloid plaque deposition we evaluated mean brightness of 4G8 (Figure 3B). A 2-way ANOVA to analyze the effect of age and strain on 4G8-staining intensity showed a main effect of strain ($F_{(1, 18)}$ = 18.22, $p < 0.001$) but no main effect of age on 4G8 staining intensity ($F_{(1, 18)}$ = 0.004 p = 0.94). There was no interaction between age and strain ($F_{(1, 18)}$ = 0.66, p = 0.43). A post-hoc comparison showed a significant increase in 4G8 staining intensity in 5xFAD animals compared to WT at 7-months of age ($t_{(13)}$ = 4.21, $p < 0.01$). While

5xFAD animals also showed an increase in 4G8 staining intensity at 11-months, this difference was not significant ($t_{(7)} = 2.17$, $p > 0.05$).

Next, we evaluated IBA1+ microglia within the mPFC (Figure 3C). A 2-way ANOVA of age and strain on IBA1 staining intensity showed a significant main effect of strain ($F_{(1, 18)} = 4.94$, $p = 0.04$) but no main effect of age ($F_{(1, 18)} = 0.14$, $p = 0.71$), and no interaction ($F_{(1, 18)} = 0.002$, $p = 0.99$). Post-hoc comparisons did not show any significant differences at either 7-months ($t_{(13)}=1.83$, $p = 0.16$) or 11-months ($t_{(7)}=1.39$, $p = 0.36$) of age.

Lastly, to assess the integrity of the ECM, we evaluated WFA staining intensity and PNN counts in medial prefrontal cortex. A 2-way ANOVA of age and strain on WFA staining intensity (Figure 3D) showed a significant main effect of strain ($F_{(1, 18)} = 6.78$, $p = 0.02$) but no main effect of age ($F_{(1, 18)} = 0.01$, $p = 0.93$), and no interaction ($F_{(1, 18)} = 0.50$, $p = 0.49$). Post-hoc comparisons showed a significant decrease in WFA-staining in 5xFAD animals at 7 months compared to WT ($t_{(13)} = 2.74$, $p = 0.02$). While there was a decrease in WFA at 11-months of age in 5xFAD animals, this difference was not significant ($t_{(7)} = 1.19$, $p = 0.50$). Next, we evaluated PNNs (Figure 3E) within the same region. A 2-way ANOVA of age and strain on PNN count showed no main effect of strain ($F_{(1, 18)} = 0.31$, $p = 0.58$) or age ($F_{(1, 18)} = 1.36$, $p = 0.26$), and no interaction ($F_{(1, 18)} = 0.36$, $p = 0.55$).

Primary Motor Cortex Immunostaining. Here we describe our immunostaining within the primary motor cortex (Figure 4A), which included 4G8 (green), IBA1 (red), WFA, and PNN counts (both purple).

First, we evaluated 4G8 mean brightness as a measure of amyloid plaque deposition (Figure 4B). A 2-way ANOVA of age and strain on 4G8-staining intensity (Figure 4) showed a significant

main effect of age ($F_{(1, 18)} = 5.92$, $p = 0.03$) and strain ($F_{(1, 18)} = 129.10$, $p < 0.001$) but no interaction ($F_{(1, 18)} = 3.28$, $p = 0.09$). Post-hoc comparisons showed significant increases in 4G8 staining intensity in 5xFAD animals at 7-months ($t_{(13)} = 7.920$, $p < 0.01$) and 11-months of age ($t_{(7)} = 8.26$, $p < 0.01$). There was also a significant increase in 4G8 staining intensity from 7 to 11-months of age in 5xFAD animals ($t_{(18)} = 3.000$, $p = 0.046$).

Next, we evaluated mean brightness for IBA1+ microglia (Figure 4C). A 2-way ANOVA of age and strain on IBA1 staining intensity showed a significant main effect of strain ($F_{(1, 18)} = 22.00$, $p < 0.01$) on IBA1 staining intensity but no main effect of age ($F_{(1, 18)} = 2.36$ $p = 0.14$). There was no statistically significant interaction ($F_{(1, 18)} = 0.88$, $p = 0.39$). Post-hoc comparisons showed significant increases in IBA1 staining intensity in 5xFAD animals at 7-months ($t_{(13)} = 3.11$, $p < 0.05$) and 11-months of age ($t_{(7)} = 3.53$, $p < 0.01$).

Lastly, we assessed both WFA mean brightness as a measure of ECM integrity and PNN counts. A 2-way ANOVA to analyze the effect of age and strain on WFA staining intensity (Figure 4D) showed a significant main effect of strain ($F_{(1, 18)} = 28.27$, $p < 0.01$) but no main effect of age ($F_{(1, 18)} = 0.01$, $p = 0.93$) and no significant interaction ($F_{(1, 18)} = 0.68$, $p = 0.42$). Post-hoc comparisons showed a significant decrease in WFA staining intensity in 5xFAD animals compared to WT at 7-months of age ($t_{(13)} = 3.73$, $p < 0.01$) and 11-months of age ($t_{(7)} = 3.85$, $p < 0.01$). A 2-way ANOVA of age and strain on PNN count (Figure 4E) in the primary motor cortex showed a main effect of strain ($F_{(1, 18)} = 14.81$, $p < 0.01$) but not age ($F_{(1, 18)} = 1.89$, $p = 0.18$). There was no statistically significant interaction ($F_{(1, 18)} = 0.83$, $p = 0.37$). Post-hoc comparisons showed a significant decrease in PNN number in 5xFAD animals compared to WT at 7-months of age ($t_{(13)} = 4.03$, $p < 0.01$). While there was a decrease in the number of PNNs in primary

motor cortex of 5xFAD animals compared to WT at 11-months of age, this difference was not significant ($t_{(7)} = 1.81$, $p > 0.05$).

CA1 of the Hippocampus Immunostaining. Here we describe immunostaining within the CA1 region of the hippocampus (Figure 5A), which included 4G8 (green), IBA1 (red), WFA, and PNN counts (both purple).

Firstly, we measured 4G8 mean brightness to evaluate amyloid plaque deposition (Figure 5B). A 2-way ANOVA of age and strain on 4G8-staining intensity showed a significant main effect of strain ($F_{(1, 18)} = 41.66$, $p < 0.01$) on 4G8 staining intensity but no main effect of age ($F_{(1, 18)} = 2.99$ $p = 0.10$) and no interaction ($F_{(1, 18)} = 0.58$, $p = 0.45$). Post-hoc comparisons showed significant increases in 4G8 staining intensity in 5xFAD animals at 7-months ($t_{(13)} = 4.82$, $p < 0.01$) and 11-months of age ($t_{(7)} = 4.47$, $p < 0.01$).

Next, we evaluated the mean brightness of IBA1+ staining to assess neuroinflammation (Figure 5C). A 2-way ANOVA to analyze the effect of age and strain on IBA1 staining intensity (Figure 5) showed a significant main effect of strain ($F_{(1, 18)} = 51.41$, $p < 0.01$) and age ($F_{(1, 18)} = 6.85$, $p = 0.02$) on IBA1 staining intensity but no interaction ($F_{(1, 18)} = 3.65$, $p = 0.07$). Post-hoc comparisons showed a significant increase in IBA1 staining intensity in 5xFAD animals compared to WT at 7-months of age ($t_{(13)} = 4.45$, $p < 0.01$) and 11-months of age ($t_{(7)}=5.62$, $p < 0.01$). We also observed a significant increase in IBA1 staining intensity from 7-months to 11-months of age in 5xFAD animals ($t_{(19)} = 3.16$, $p = 0.03$).

Lastly, we assessed ECM integrity by measuring WFA mean brightness and evaluated PNN counts within CA1 of the hippocampus. A 2-way ANOVA of age and strain on WFA staining intensity (Figure 5D) showed a significant main effect of strain ($F_{(1, 18)} = 19.50$, $p < 0.01$) but no

main effect of age ($F_{(1, 18)} = 0.37$, $p = 0.55$) and no interaction ($F_{(1, 18)} = 1.06$, $p = 0.32$). Post-hoc comparisons showed a significant decrease in WFA staining intensity in 5xFAD animals compared to WT at 7-months of age ($t_{(13)} = 2.86$, $p = 0.02$) and 11-months of age ($t_{(7)} = 3.38$, $p < 0.01$). A 2-way ANOVA of age and strain on PNN count (Figure 5E) in the CA1 region of the dorsal hippocampus showed a main effect of strain ($F_{(1, 18)} = 11.08$, $p < 0.01$) but not age ($F_{(1, 18)} = 1.58$, $p = 0.22$) on PNN count. There was no statistically significant interaction ($F_{(1, 18)} = 0.30$, $p = 0.59$). Post-hoc comparisons showed a significant decrease in PNN number in 5xFAD animals compared to WT at 7-months of age ($t_{(13)} = 3.28$, $p < 0.01$). While there was a decrease in the number of PNNs in the CA1 region of the dorsal hippocampus of 5xFAD animals compared to WT at 11-months of age, this difference was not significant ($t_{(7)} = 1.72$, $p = 0.20$).

Entorhinal Cortex Immunostaining. Here we describe measures from our immunostaining within the entorhinal cortex (Figure 6A), which included 4G8 (green), IBA1 (red), WFA, and PNN counts (both purple).

First, we report measures from our 4G8 staining. A 2-way ANOVA of age and strain on 4G8-staining intensity (Figure 6B) showed a significant main effect of strain ($F_{(1, 18)} = 38.49$, $p < 0.01$) but no main effect of age ($F_{(1, 18)} = 0.77$, $p = 0.39$) and no interaction ($F_{(1, 18)} = 3.61$, $p = 0.07$). Post-hoc comparisons showed significant increases in 4G8 staining intensity in 5xFAD animals at 7-months ($t_{(13)} = 3.57$, $p < 0.01$) and 11-months of age ($t_{(7)} = 5.08$, $p < 0.001$).

We next evaluated IBA1+ staining for mean brightness. A 2-way ANOVA to analyze the effect of age and strain on IBA1 staining intensity (Figure 6C) showed a significant main effect of strain ($F_{(1, 18)} = 15.09$, $p < 0.01$) on IBA1 staining intensity but no main effect of age ($F_{(1, 18)} = 1.36$ $p = 0.26$) and no significant interaction ($F_{(1, 18)} = 1.37$, $p = 0.26$). Post-hoc comparisons showed no statistically significant change in IBA1 staining intensity in 5xFAD animals

compared to WT at 7 months ($t_{(13)} = 2.25$, $p = 0.07$), but a significant increase in 5xFAD animals at 11-month ($t_{(7)} = 3.17$, $p = 0.01$) animals.

Lastly, we evaluated WFA mean brightness and PNN counts (Figure 7D, E). In the entorhinal cortex, a 2-way ANOVA to analyze the effect of age and strain on WFA staining intensity (Figure 7D) showed a significant main effect of strain ($F_{(1, 18)} = 13.47$, $p < 0.01$) on WFA staining intensity but no main effect of age ($F_{(1, 18)} = 0.01$ $p = 0.92$) and no interaction ($F_{(1, 18)} = 0.19$, $p = 0.67$). Post-hoc comparisons showed a significant decrease in WFA staining intensity in 5xFAD animals compared to WT at 7-months of age ($t_{(13)}$=2.68, $p = 0.03$) and 11-months of age ($t_{(7)} = 2.57$, $p = 0.03$). A 2-way ANOVA of age and strain on PNN count (Figure 7E) in the entorhinal cortex showed no main effect of strain ($F_{(1, 18)} = 0.43$, $p = 0.52$), age ($F_{(1, 18)} = 0.07$, $p = 0.78$), and no interaction ($F_{(1, 18)} = 0.74$, $p = 0.40$).

Retrosplenial Cortex Immunostaining. Here we describe measures from our immunostaining within the retrosplenial cortex (Figure 7A) which included 4G8 (green), IBA1 (red), WFA, and PNN counts (both purple).

Within the retrosplenial cortex, a 2-way ANOVA to analyze the effect of age and strain on 4G8-staining intensity (Figure 7B) showed a significant main effect of strain ($F_{(1, 18)} = 68.35$, $p < 0.01$) on 4G8 staining intensity but no main effect of age ($F_{(1, 18)} = 2.87$, $p = 0.11$). There was also a statistically significant interaction between strain and age ($F_{(1, 18)} = 5.92$, $p = 0.03$). Post-hoc comparisons showed a significant increase in 4G8 staining intensity in 5xFAD animals compared to WT at 7-months of age ($t_{(13)} = 4.94$, $p < 0.001$) and 11-months of age ($t_{(7)} = 6.63$, $p < 0.0001$).

For IBA1+, a 2-way ANOVA of age and strain on staining intensity (Figure 7C) showed a significant main effect of strain ($F_{(1, 18)} = 12.57$, $p < 0.01$) but no main effect of age ($F_{(1, 18)} = 0.41$ $p = 0.53$) and no significant interaction ($F_{(1, 18)} = 0.97$, $p = 0.34$). Post-hoc comparisons revealed no change in IBA1 staining intensity in 5xFAD animals compared to WT at 7 months ($t_{(13)} = 2.16$, $p = 0.08$) of age, but a significant increase in 11-month ($t_{(7)} = 2.81$, $p = 0.02$) animals.

Within the retrosplenial cortex, a 2-way ANOVA of age and strain on WFA staining intensity (Figure 7D) showed was a significant main effect of strain ($F_{(1, 18)} = 42.87$, $p < 0.01$) on WFA staining intensity but no main effect of age ($F_{(1, 18)} = 0.36$, $p = 0.56$). There was no significant interaction ($F_{(1, 18)} = 1.22$, $p = 0.28$). Post-hoc comparisons revealed significant decreases in WFA staining intensity in 5xFAD animals compared to WT at 7 months ($t_{(13)} = 4.61$, $p > 0.001$) and 11-months of age ($t_{(7)} = 4.74$, $p < 0.001$). A 2-way ANOVA of age and strain on PNN count (Figure 7E) in the RSC showed a main effect of strain ($F_{(1, 18)} = 10.13$, $p = 0.004$) but no main effect of age ($F_{(1, 18)} = 0.81$, $p = 0.38$) and no interaction ($F_{(1, 18)} = 0.06$, $p = 0.82$). Post-hoc comparisons showed a significant decrease in PNN number in 5xFAD animals compared to WT at 7-months of age ($t_{(13)} = 2.56$, $p = 0.04$). While there was a decrease in the number of PNNs in the retrosplenial cortex of 5xFAD animals compared to WT at 11-months of age, this difference was not significant ($t_{(7)} = 2.09$, $p = 0.09$).

Parvalbumin And Fluorojade-C Immunostaining (mPFC and RSC). To further probe two regions of interest, the mPFC and RSC, we stained for PV+ inhibitory interneurons which are closely associated with PNNs and fluorojade-C, a marker for cell death.

Within the mPFC, a 2-way ANOVA of age and strain on PV cell count (Figure 8B) showed no significant main effect of strain ($F_{(1, 14)} = 0.53$, $p = 0.48$) or age ($F_{(1, 18)} = 3.35$ $p = 0.09$) and no

interaction ($F_{(1, 14)} = 0.05$, $p = 0.82$) between strain and age on PV+ cell count. A 2-way ANOVA of age and strain on FJC+ cell count (Figure 8C) showed a main effect of strain ($F_{(1, 18)} = 6.89$, $p = 0.02$) on FJC+ cell count but no main effect of age ($F_{(1, 18)} = 1.77$, $p = 0.20$) and no significant interaction ($F_{(1, 18)} = 1.74$, $p = 0.21$). Post-hoc comparisons showed no significant differences in FJC+ cell count in 5xFAD animals at 7-months ($t_{(13)} = 1.07$, $p = 0.59$) or 11-months of age ($t_{(7)} = 2.49$, $p = 0.051$) despite showing increases in counts at both time points.

Within the retrosplenial cortex, a 2-way ANOVA of age and strain on PV+ cell count (Figure 8E) showed no main effect of strain ($F_{(1, 14)} = 0.06$, $p = 0.81$) or age ($F_{(1, 18)} = 0.21$ $p = 0.65$) on PV+ cell count. There was also no interaction ($F_{(1, 14)} = 0.24$, $p = 0.63$). A 2-way ANOVA of age and strain on FJC+ cell count (Figure 8F) showed a main effect of strain ($F_{(1, 18)} = 27.52$, $p < 0.001$) and a main effect of age ($F_{(1, 18)} = 15.12$, $p < 0.01$) on FJC+ cell count. There was also a statistically significant interaction ($F_{(1, 18)} = 17.08$, $p < 0.001$). Post-hoc comparisons showed a significant difference between WT and 5xFAD animals at 11-months of age ($t(7) = 6.024$, $p < 0.01$). There was also a significant difference between 5xFAD animals at 7 months and 11 months ($t_{(13)} = 5.95$, $p < 0.01$).

Confocal Imaging

To probe qualitative relationships between cell death, amyloid deposition, and inflammation, we co-stained and performed high resolution confocal imaging within the RSC. A common pattern among our observations was that 4G8+ plaques also featured an FJC+ cell within their core (Figure 9A), suggesting amyloid accumulation and cell death are associated. This pattern was inversely related to the distribution of NeuN+ cells, which were absent from areas with plaque accumulation. We also evaluated the relationship between amyloid deposition and WFA+ PNNs (Figure 9B). PNNs rarely featured 4G8 accumulation within them, and inversely, patterns of

4G8+ accumulation within cells were rarely surrounded by a PNN. These observations are consistent with prior literature indicating that PNNs can be neuroprotective against Aβ accumulation (Miyata et al., 2007).

Discussion

In the present study we utilized the 5xFAD mouse model of AD to determine the integrity of PNNs in five regions of the brain at 7- and 11-months of age, which are representative of moderate and severe stages of disease in these animals (Devi et al., 2015; Devi & Ohno, 2016). In parallel, we evaluated markers of Aβ deposition, microglial inflammation, cell death, and parvalbumin interneurons. We also conducted two behavioural assays of memory in the moderate disease cohort. Our behavioural data suggests that by 7-months of age, 5xFAD animals present with significant impairment in novel object recognition and spontaneous alternation. Throughout the brains of 5xFAD animals, we identified PNN reductions animals that were apparent at 7-months of age in the primary motor cortex, CA1 region of the dorsal hippocampus, and retrosplenial cortex – but were unchanged in the medial prefrontal cortex or entorhinal cortex. We observed significant elevations of Aβ deposition and reductions in WFA labelling in all five regions. Significant microglial reactivity was also detected in the primary motor cortex, CA1 region of the hippocampus, entorhinal cortex, and retrosplenial cortex. We also show elevated cell death markers in 5xFAD animals in both the medial prefrontal cortex and retrosplenial cortex. Interestingly, PV+ inhibitory interneurons, which are closely associated with PNNs were not altered in 5xFAD animals at either time point.

Behavioural Observations

Our behavioural assays show that at 7-months of age, 5xFAD transgenic animals had significant impairment in novel object recognition and spontaneous alternation. This result is consistent with previous literature reporting deficits in novel object recognition as early as 4-months of age in 5xFAD animals (Frydman-Marom et al., 2011; Grayson et al., 2015; Kim et al., 2020; Kim et al., 2019; Kubota et al., 2016; Son et al., 2018). Similarly, previous studies have shown deficits in the spontaneous alternation task with 5xFAD animals as early as 5 months old, which progressively worsen with age (de Pins et al., 2019; Devi et al., 2015; El Gaamouch et al., 2020; Jawhar et al., 2012; Oakley et al., 2006). These memory impairments are likely reflective of disrupted processing in task-associated regions of the brain. In the context of the 5xFAD model, it is difficult to directly tie PNN deficits within certain regions of the brain to deficits in cognitive performance given the significant and widespread burden of disease. Nonetheless, the fact that we observed behavioural deficits in parallel to PNN deficits in the primary motor cortex, dorsal hippocampus, and retrosplenial cortex, but not the medial prefrontal cortex or entorhinal cortex is informative. To better discern the relationship between PNN deficits within specific regions of the brain and cognitive performance, more targeted approaches to degrading PNNs in an otherwise healthy state are far more informative.

Among the regional PNN deficits observed here, the deficits in the hippocampus and retrosplenial cortex are particularly notable when considering our behavioural observations. Hippocampal lesion studies have readily demonstrated its importance for successful discrimination in object recognition tasks (Cohen et al., 2013; Cohen & Stackman Jr., 2015; de Lima et al., 2006; Haijima & Ichitani, 2012). Similarly, inactivation of the dorsal hippocampus, including focal inactivation of the CA1 region of the dorsal hippocampus, can impair object recognition memory at 24 hours (Cohen et al., 2013; Hammond et al., 2004). Interestingly, recent

work has demonstrated a role for PNNs along with PV+ interneurons in a newly identified critical period for episodic memory formation within CA1 of the hippocampus (Ramsaran et al., 2023). In this context, the maturation of PNNs facilitates a development switch in PV+ cells towards sparse encoding that facilities competitive neuronal allocation and memory precision. Depleting PNNs via genetic knockout or enzymatic degradation reverted PV+ activity to a more juvenile activity pattern and impaired memory precision in both fear conditioning and spatial foraging tasks. These results would suggest that the PNN deficits observed here within CA1 could have a significant role in the cognitive deficits we observed. By contrast, the role of the RSC in object recognition tasks has mixed evidence. Lesions of the RSC have been shown to spare object recognition, whilst impairing object-in-place discrimination, which suggests it has more involvement in allocentric memory (Ennaceur et al., 1997; Vann & Aggleton, 2002). However, another study has shown that inactivation of the RSC can impair object recognition memory at 24 hours and that the RSC shows elevated levels of c-fos following the task (de Landeta et al., 2020). Evaluating the specific role of PNN loss within either the retrosplenial cortex or dorsal hippocampus on memory is more difficult, given a lack of study within the literature. However, PNN manipulation within other regions of the brain has been shown to impact object recognition memory, often with improved task performance. In a mouse model of AD with excessive tau phosphorylation and impaired object recognition, injection of ChABC into the perirhinal cortex to degrade PNNs improved object recognition (Yang et al., 2015). Similarly, in mice lacking Ctrl1, which is involved in PNN assembly, mature PNNs fail to develop and long-term object recognition memory is enhanced (Romberg et al., 2013). The same study showed similar effects after depleting PNNs in the perirhinal cortex with direct infusions of ChABC. Genetic ablation of the gene *Acan*, which encodes the CSPG aggrecan, also results in

depleted PNN levels brain-wide and enhanced object recognition memory (Rowlands et al., 2018). Together, these studies indicate that decreased PNN levels could improve object recognition memory. In the context of 5xFAD, this might mean that PNN loss unrelated to memory dysfunction or even that PNN decreases are compensatory for diminished memory function.

Studies investigating the relationship between PNN integrity and performance on spontaneous alternation are limited compared to those evaluating object recognition. To our knowledge, there are no studies demonstrating a direct effect on spontaneous alternation after targeted depletion of PNNs. However, numerous studies have observed changes in performance in contexts where reduced PNNs are also observed. Animal models of chronic stress, chronic pain, and sepsis all present with impaired spontaneous alternation paired and have decreased PNN levels in certain regions of the brain (de Araújo Costa Folha et al., 2017; Tajerian et al., 2018; Zhang et al., 2023). Other studies utilizing lesion or inactivation models have probed the neuroanatomical basis of spontaneous alternation and found it to require interaction across numerous brain areas (Lalonde, 2002; Nelson et al., 2015). With respect to the regions assessed here, lesion and inactivation studies have consistently shown that damage to the hippocampus results in impaired spontaneous alternation (Johnson et al., 1977; Kirkby et al., 1967; Means et al., 1971; Stevens & Cowey, 1973). Other studies have highlighted the contributions of the prefrontal, entorhinal, and retrosplenial cortices. In the mPFC, direct lesions to the cortical region impair spontaneous alternation (Delatour & Gisquet-Verrier, 1996; Divac et al., 1975). In the RSC, temporary inactivation with muscimol results in significant impairment of spontaneous alternation, but permanent lesions only result in mild impairment (Nelson et al., 2015; Pothuizen et al., 2008). And in the entorhinal cortex lesions impair learned alternation, a form of the task

where alternation is reinforced with rewards, but no effect is seen after combined excitotoxic lesions of the entorhinal and adjacent perirhinal cortex (Aggleton et al., 1997; Ramirez & Stein, 1984). These studies highlight the distributed processing involved in spontaneous alternation, which extends beyond just those regions discussed. With regards to our data, it is difficult to attribute deficits in spontaneous alternation to any specific region with a PNN deficit, or directly to PNNs themselves. Further studies examining targeted degradation of PNNs combined with assessments of spontaneous alternation could better localize PNNs contribution to the behaviour. Nonetheless, our data are consistent with prior reports of impaired spontaneous alternation in 5xFAD animals. Our results join a growing body of evidence that observes PNN deficits and impaired spontaneous alternation in parallel in contexts of disease (de Pins et al., 2019; El Gaamouch et al., 2020; Jawhar et al., 2012; Oakley et al., 2006).

Anatomical observations

Our data provide novel insight into the breadth and extent of PNN loss in the 5xFAD animal model of AD. Across all five brain regions examined we saw reductions in WFA-labelled ECM staining and in the primary motor cortex, CA1 of the dorsal hippocampus, and retrosplenial cortex, we saw significant decreases in PNN counts. Our observations join a limited set of studies which have evaluated PNN densities in AD and models of the disease, often with mixed results. In human AD, three prior studies have demonstrated decreased PNN levels in the cingulate, entorhinal, frontal and temporal cortices of human post-mortem tissue (Baig et al., 2005; Crapser et al., 2020; Kobayashi et al., 1989; Pantazopoulos & Berretta, 2016). In contrast to those, other studies evaluating PNN levels determined there was no change in PNN density in the frontal or temporal cortex, similar to negative results reported from the cortex, striatum, and thalamus (Brückner et al., 1999; Morawski et al., 2010; Morawski et al., 2012). One possible

explanation for this inconsistency is the varied labelling methods for detecting PNNs used in these studies (e.g., Wisteria floribunda agglutinin, Vicia villosa lectin, CSPG-specific antibodies). Another factor could the inherent diversity present in human post-mortem samples. Interestingly, one consistent observation across human post-mortem studies was that phosphorylated tau+ neurons were rarely surrounded by a PNN (Morawski et al., 2012). While we did not evaluate tau+ as it is not a feature of the 5xFAD model, our qualitative observations were that PNNs rarely featured amyloid-deposition within them, which is consistent with prior studies showing neuroprotective properties of PNNs against Aβ.

In animal models of AD, observations of PNNs have also been mixed. Studies have typically focused on the hippocampal formation and results vary by the model, age, and region utilized. Our data adds a broader evaluation, showing PNN deficits in the primary motor cortex, CA1 region, and retrosplenial cortex. These results join previous observations in the 5xFAD animal model that PNNs are reduced in the subiculum and visual cortex as early as 4-months of age, which persisted until 18-months of age (Crapser et al., 2020). In other models of AD, the impact on PNN integrity has been less clear. In the 3xTg-AD model, PNN deficits are observed in the subiculum of 18-month old mice, but there is no change in the visual cortex (Javonillo et al., 2022). In the Tg2576 model, two studies have shown decreases in dual PV+/WFA+ neurons in regions of the hippocampus and another study has shown reductions in brevican, a CSPG core protein, and the amount of CS-GAG chains present on brevican (Ajmo et al., 2010; Cattaud et al., 2018; Rey et al., 2022). However, a fourth study using Tg2576 mice showed no change in WFA-labelling found in the parietal cortex between 14-18 months of age (Morawski et al., 2010). PNN loss has also been reported in the somatosensory cortex of rTg4510 mouse modal of tauopathy at 6-months of age, and this occurs in parallel to dysfunction within PV+ interneurons

and elevated expression of ECM-degrading enzymes expressed by microglia (Kudo et al., 2023). Negative results of PNN changes have been reported in the APP^{NL-F} mouse model of AD, where PNNs in the hippocampus are unaffected at 21-months of age, and in the perirhinal cortex at 3-months of age in the P301S model. In the APP/PS1 model, significant increases in ECM proteins were detected in the hippocampus at 3-months of age. These changes preceded any amyloid plaque formation and paralleled the presentation of memory deficits in the transgenic animals (Végh et al., 2014). Interestingly, direct injections of ChABC into the hippocampus to show that this could restore activity levels and memory performance in these animals. While there is a significant diversity in the discussed results, our data and others establish that the 5xFAD model presents with broad, but not global PNN deficits, with utility for investigating PNN deficits in AD pathology.

It is of interest that in our study that despite reductions in WFA-labelled ECM throughout all five regions examined they did not always exhibit parallel reductions in PNNs. This discrepancy could suggest that PNNs are in fact resilient to AD-related pathology and less affected than the broader WFA-labelled ECM. This suggestion would be supported within the literature by studies demonstrating protective effects of PNNs against AD-pathology (Crapser et al., 2020; Miyata et al., 2007). PNN-surrounded neurons rarely exhibit tau accumulation and areas dense in PNNs are have been shown to be less affected by AD (Brückner et al., 1999; Morawski et al., 2012). More direct evidence for these protective effects were shown in hippocampal slice cultures, where neurons rarely internalize tau if surrounded by PNNs, but this protective effect is removed by digestion of PNNs with ChABC (Suttkus et al., 2016). Similarly effects have been shown in cultured cortical neurons with Aβ toxicity (Miyata et al., 2007). An alternative explanation could be the temporal progression of 5xFAD animal's neuropathology.

The progression of Aβ deposition in 5xFAD typically affects subcortical and hippocampal structures first, before spreading throughout interconnected networks as the disease progresses (Gail Canter et al., 2019; Oblak et al., 2021). As such, seeing less severe markers of disease in anterior regions like the medial prefrontal cortex relative to the hippocampus is not surprising. Given this, the broader reductions in WFA-labeling we observed might be a preceding step to PNN loss, which show some resiliency in AD. It is possible that in later disease time points, PNN disruption could progress into the mPFC as was demonstrated in other areas. Future studies with greater temporal resolution of the two time-points utilized here would be useful in determining the resiliency of PNNs against AD pathology in the 5xFAD model.

PNNs are most frequently observed surrounding PV+ inhibitory interneurons. These neurons are a fast-spiking and metabolically demanding cell type that are thought to be critical in regulating local cortical circuits. Here, data from 7-month and 11-month-old animals indicate that PV+ interneuron densities were not affected by 5xFAD pathology, but there are numerous caveats to interpreting these observations. Firstly, densities alone may not be reflective of overall PV+ neuron function as our outcomes were not sensitive to changes in cellular activity, plasticity, or expression. This discrepancy between activity and expression profiles is demonstrated in a recent study of the rTg4510 mouse model of tauopathy showed that PNN disruption was paralleled by dysfunctional activity of PV+ interneurons, but no alterations in the expression of the sodium channel NaV1.1 or potassium channel Kv3.1b (Kudo et al., 2023). Secondly, in other disease contexts it has been demonstrated that PNN degradation renders PV+ cells vulnerable to subsequent disruption, which is consistent with their protective role on host neurons (Cabungcal et al., 2013; Crapser et al., 2020; Hsieh et al., 2017; Miyata et al., 2007). In a recent study of 5xFAD in the subiculum it was shown that PNN loss preceded PV+ cell loss

and that the latter was not detectable at 11 months but was at 18 months of age, suggesting the time points in our study may have preceded gross PV+ cell loss (Crapser et al., 2020). The reason for the delay between PNN and loss and PV+ cell loss is not yet clear, although prolonged periods without the cellular support and neuroprotective properties provided by PNNs might result in their dysregulation. In human AD, reports on PV+ cell integrity are limited and vary based on the region examined. Studies examining the PFC, inferior temporal cortex, and visual cortex have reported no change in PV+ cell density in post-mortem tissue (Hof et al., 1991; Leuba et al., 1998). Others studies have reported decreases in PV+ cell densities in the dentate gyrus, CA1-CA2 of the hippocampus, as well as the frontal and temporal cortex (Arai et al., 1987; Brady & Mufson, 1997) .

In parallel to our assessments of the ECM we evaluated more typical markers of disease progression in 5xFAD animals, including Aβ deposition, IBA1+ microglia reactivity, and markers of cell death. In prior literature examining 5xFAD animals, Aβ-plaque deposition is detectable as early as 1.5 to 2 months of age, first appearing in deep layers of the cortex, hippocampus, and subcortical structures, and by 9 months of age is present throughout the neocortex (Forner et al., 2021; Gail Canter et al., 2019; Oakley et al., 2006; Oblak et al., 2021). As Aβ-plaques develop, there are proportional increases in microgliosis and astrogliosis and in later stages of disease significant neuronal cell loss occurs. Our data is largely consistent with these prior observations, with significant Aβ deposition, microglial reactivity, and cell death present at 7-months and worsening by 11-months of age. In addition to calculating IBA1+ densities, qualitative observations from our imaging were that IBA1+ microglia presented in a reactive state with more ameboid morphology, including a larger soma size and less-ramified processes. Reactive microglia can secrete a variety of pro-inflammatory factors, such as

interleukin-1β, interleukin-6, Tumor necrosis factor-α, and extracellular matrix degrading enzymes, such as matrix metalloproteinases (Leake et al., 2000; Lorenzl et al., 2003; Oblak et al., 2021; Perry et al., 2010; Wang et al., 2015). A recent study showed that pharmacological inactivation of microglia can prevent the degradation of PNNs in 5xFAD animals but the rate of Aβ deposition remained the same (Crapser et al., 2020). In animals where microglia were not manipulated, IBA1+ microglia had detectable levels of WFA-labelling for ECM markers inside their cell bodies, indicating that microglia had engulfed the cleaved components of PNNs after degradation. Together, these experiments show that microglia play a critical role in driving ECM-degradation in the 5xFAD model. Given that microglia play an important role in human AD progression, the 5xFAD model appears valuable in further exploring the relationship between PNNs and microglia in the disease.

Consequences of PNN loss

PNNs play important roles in supporting ongoing cellular activity. In studies where PNNs are degraded, host neurons undergo increased synaptic turnover and sensitization, increases in excitability, and altered connectivity (Carceller et al., 2022; Dityatev et al., 2007; Favuzzi et al., 2017; Frischknecht et al., 2009). PNNs also form an ionized buffer around neurons, which is thought to contribute to maintaining ion homeostasis around highly-active neurons like PV+ cells (Morawski et al., 2015). PNNs also confer neuroprotective properties onto host neurons. In neurons rich with CSPGs, Aβ has limited toxicity, but these protective properties are eliminated after treatment with ChABC (Miyata et al., 2007). Similarly, PNNs have shown to be protective against the effects of oxidative stress. In younger animals where PV+ cells are less frequently surrounded by PNNs, oxidative stress is more consequential for PV+ cell health that in older animals with mature PNNs (Cabungcal et al., 2013). Given the high degree of oxidative stress

observed in AD this indicates that PNN-surrounded cells are more resilient to his pathology (Christen, 2000; Huang et al., 2016). These studies demonstrate the importance of PNNs in the limiting the effects of notable pathophysiological mechanisms in AD. This is especially important given their close relationship with PV+ interneurons, which a recent study has demonstrated could play a more central role in the progression of AD-pathology. Studies in the hippocampus of APP/PS1 mice or somatosensory cortex of rTg4510 mice have shown that inhibitory interneurons become hyperexcitable prior to any changes in excitatory pyramidal cells (Hijazi et al., 2020; Kudo et al., 2023). These alterations in the hippocampus coincide with initial impairments in spatial learning and memory and chemogenic inhibition of PV+ cells to reduce excitability restores normal levels of PV+ cell activity and prevents memory impairment (Hijazi et al., 2020). Importantly, preventing PV+ cell hyperexcitability in these animals also reduced Aβ-plaque deposition. This latter finding is of significant interest given that PNN degradation can enhance the excitability of PV+ interneurons (Dityatev et al., 2007). These studies justify further investigation into how PNN disruption during AD might affect PV+ cell activity and the progression of the disease.

Conclusion

PNNs are important plasticity-regulating structures in the mature CNS with neuroprotective properties for the neurons they are hosted by. Their loss in the context of injury or disease can result in aberrant neuroplasticity, disrupt the excitatory/inhibitory balance of cortical tissues, and render certain cell types more vulnerable to pathophysiological insult. Our data demonstrates the coincidence of widespread ECM disruption, region-specific PNN disruption, and cognitive impairment in two memory-related tasks in the 5xFAD model of AD. This model could be utilized to further probe the temporal and mechanistic relationships between PNN degradation

and the progression of an AD-like phenotype in these animals. We suggest further investigation in the earliest stages of disease development to discern whether PNN related changes could impact plasticity and excitability in the etiogenic stages of disease.

Figures

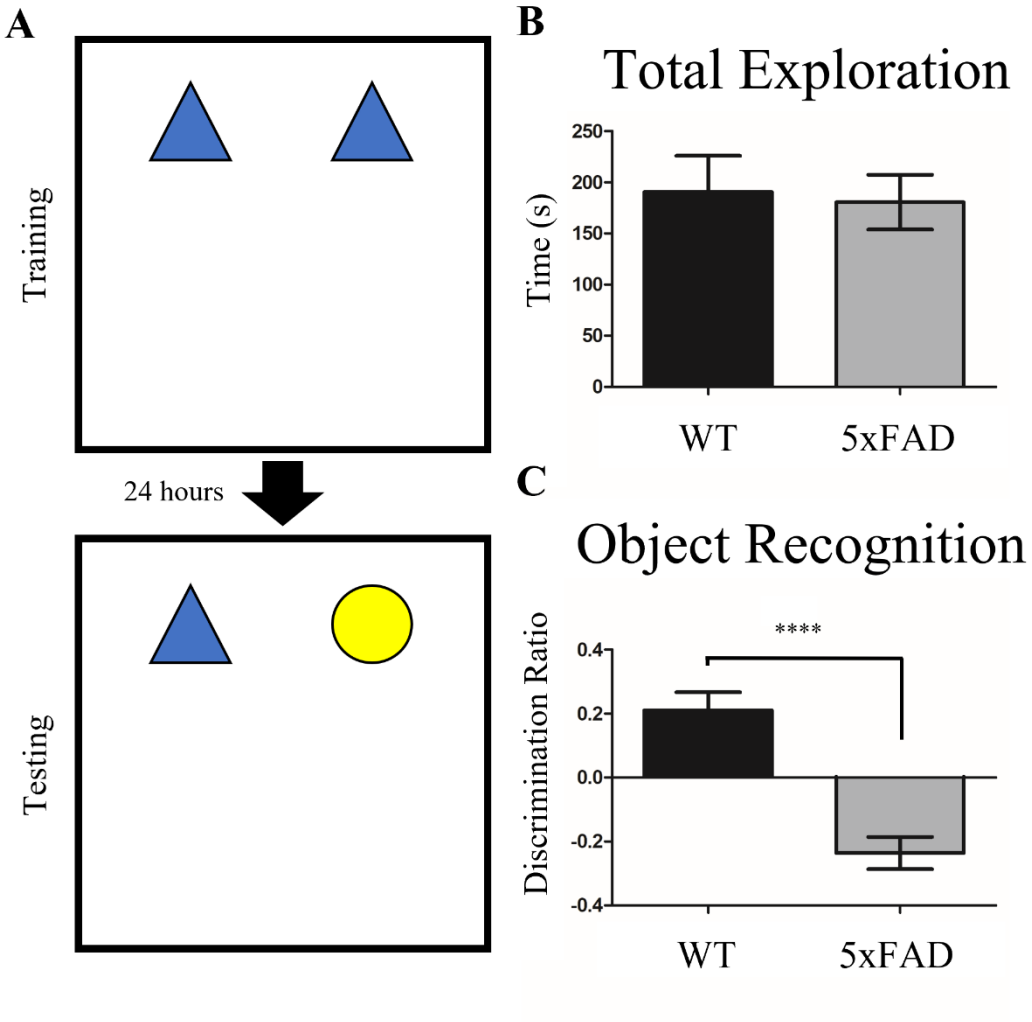
A
Training
24 hours
Testing
B
Total Exploration
Time (s)
250
200
150
100
50
0
WT
5xFAD
C
Object Recognition
Discrimination Ratio
****
0.4
0.2
0.0
-0.2
-0.4
WT
5xFAD

Figure 2.1. Object recognition is impaired in 5xFAD animals. (A) A schematic representation of the novel object recognition task. Animals were placed in an arena with two identical objects and allowed to freely explore for 8 minutes. After 24h post-familiarization, animals were re-introduced into the arena but with one familiar object replaced with a novel one. In healthy animals, a preference to explore the novel object is typically demonstrated. (B) Graphical representation of behaviour for 7-month-old WT and 5xFAD animals. Total exploration time (shown top) did not significantly differ between WT and 5xFAD animals (C) 5xFAD animals had significantly lower discrimination ratios for the novel object after 24 hours ($t_{(8)} = 6.33$, $p < 0.01$). This indicates a deficit in memory performance in 5xFAD animals as assessed on this task.

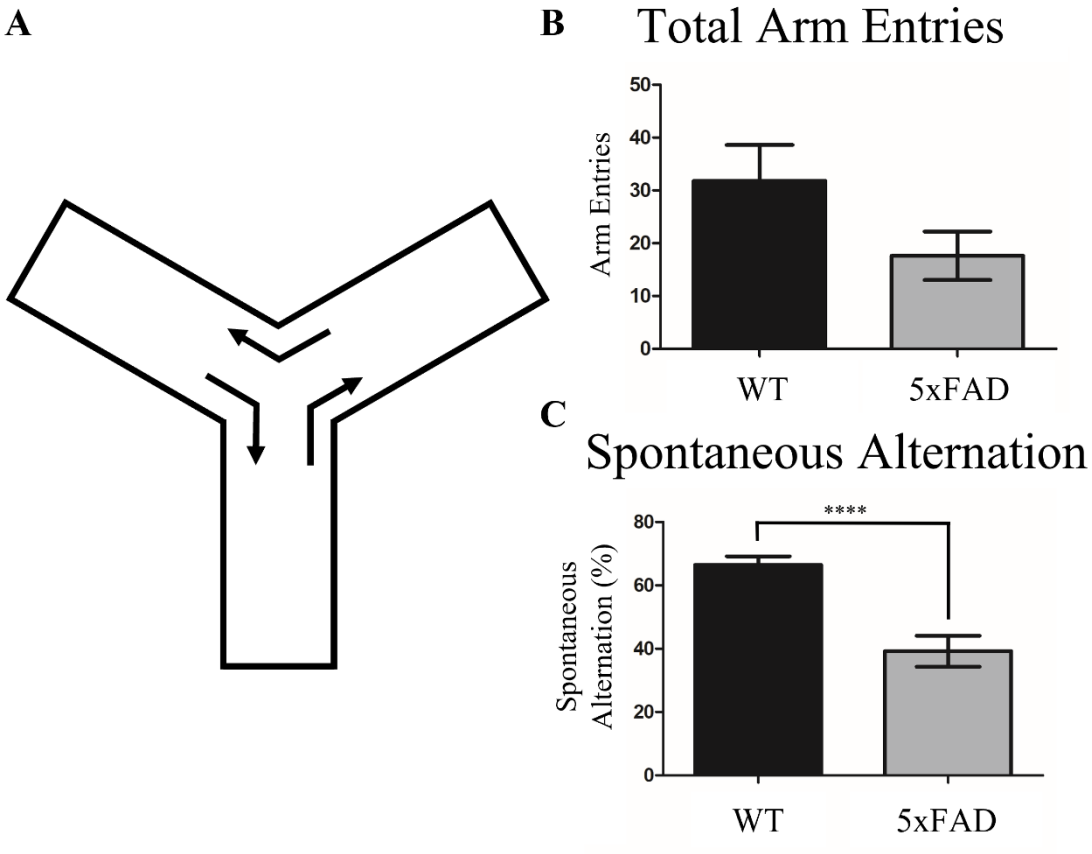
A
B
Total Arm Entries
Arm Entries
50
40
30
20
10
0
WT
5xFAD
C
Spontaneous Alternation
****
Spontaneous Alternation (%)
80
60
40
20
0
WT
5xFAD

Figure 2.2. Spontaneous alternation is impaired in 5xFAD animals. (A) Schematic representation of the spontaneous alternation task. (B) Graphical representation of animal's total number of arm entries. While 5xFAD animals showed less arm entries overall, this difference was not significant. (C) 5xFAD animals did show significantly reduced spontaneous alternation behaviour within the Y-maze ($t_{(8)}$=4.85, $p < 0.01$). This indicates that 5xFAD animals exhibit a deficit in working memory as assessed on this task.

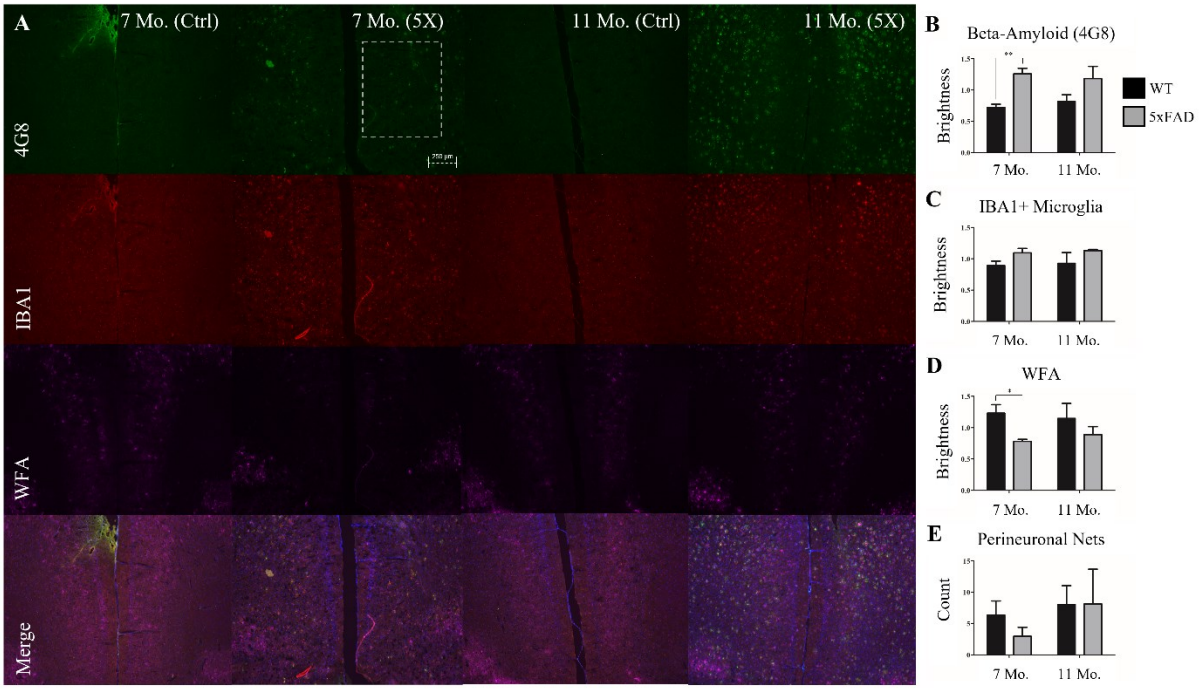
A
7 Mo. (Ctrl)
7 Mo. (5X)
11 Mo. (Ctrl)
11 Mo. (5X)
4G8
IBA1
WFA
Merge
B
Beta-Amyloid (4G8)
Brightness
7 Mo.
11 Mo.
WT
5xFAD
C
IBA1+ Microglia
Brightness
7 Mo.
11 Mo.
D
WFA
Brightness
7 Mo.
11 Mo.
E
Perineuronal Nets
Count
7 Mo.
11 Mo.

Figure 2.3. The medial prefrontal cortex of 5xFAD animals has elevated amyloid deposition, reactive microglia, and reduced WFA staining of the ECM but no deficits in PNNs. (A) Representative images of immunostaining for 4G8 (green), IBA1 (red), and WFA (purple). (B) An ANOVA on 4G8 staining intensity showed a main effect of strain ($F_{(1, 18)} = 0.66$, $p < 0.05$), but no main effect of age and no interaction. Post-hoc comparisons showed a significant increase in 4G8 deposition between WT and 5xFAD animals at 7-months of age ($t_{(13)} = 4.21$, $p < 0.01$). (B) An ANOVA on IBA1 staining intensity show a main effect of strain ($F_{(1, 18)} = 4.94$, $p < 0.05$) but no main effect of age and no interaction. However, post-hoc comparisons did not show significant differences between groups at either time point. (D) An ANOVA on WFA staining intensity showed a main effect of strain ($F_{(1, 18)} = 6.78$, $p < 0.05$) but no main effect of age and no interaction. Comparisons showed a significant decrease in 5xFAD animals at 7-months of age ($t_{(13)} = 2.74$, $p < 0.05$). (E) Lastly, we assessed PNN counts which showed no main effect of strain or age, and no interaction. Data presentation as Mean ± SEM. Scale bar represents 250 μm (*, $p < 0.05$, **, $p < 0.01$).

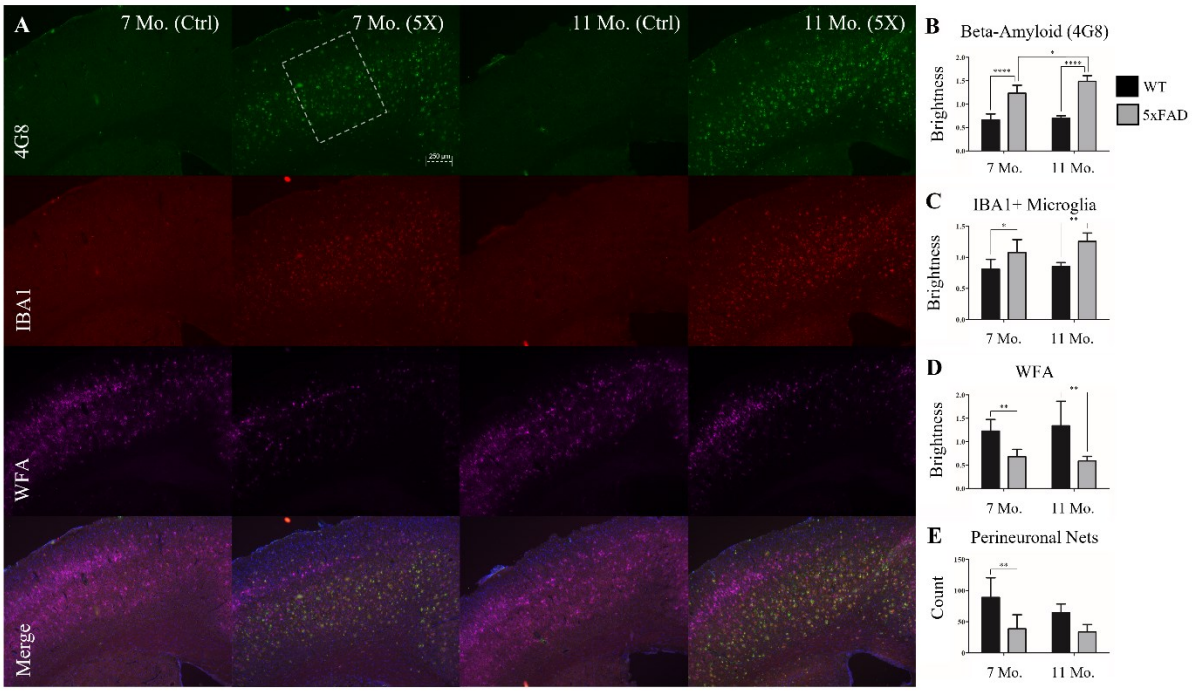
A
7 Mo. (Ctrl)
7 Mo. (5X)
11 Mo. (Ctrl)
11 Mo. (5X)
4G8
IBA1
WFA
Merge
B
Beta-Amyloid (4G8)
Brightness
WT
5xFAD
7 Mo.
11 Mo.
C
IBA1+ Microglia
Brightness
7 Mo.
11 Mo.
D
WFA
Brightness
7 Mo.
11 Mo.
E
Perineuronal Nets
Count
7 Mo.
11 Mo.

Figure 2.4. The primary motor cortex of 5xFAD animals has elevated 4G8 staining, inflamed microglia, and reduced WFA staining and PNNs. (A) Representative images of immunostaining for 4G8 (green), IBA1 (red), and WFA (purple). (B) An ANOVA on 4G8 staining intensity showed a main effect of strain ($F_{(1, 18)} = 129.10$, $p < 0.001$) and a main effect of age ($F_{(1, 18)} = 5.92$, $p < 0.05$) but no interaction. Post-hoc comparisons showed significant increases in 4G8 staining intensity in 5xFAD animals at 7-months ($t_{(13)} = 7.920$, $p < 0.01$) and 11-months of age ($t_{(7)}= 8.26$, $p < 0.01$). There was also a significant increase in 4G8 staining intensity from 7 to 11-months of age in 5xFAD animals ($t_{(18)} = 3.000$, $p < 0.05$). (C) An ANOVA on IBA1 staining intensity showed a main effect of strain ($F_{(1, 18)} = 22.00$, $p < 0.01$) but no main effect of age and no interaction. Subsequent comparisons showed significant increases in IBA1 staining intensity in 5xFAD animals at 7-months ($t_{(13)}= 3.11$, $p < 0.05$) and 11-months of age ($t_{(7)} = 3.53$, $p < 0.01$). (D) An ANOVA on WFA staining intensity showed a main effect of strain ($F_{(1, 18)} = 28.27$, $p < 0.01$) but no main effect of age and no interaction. Post-hoc comparisons showed a significant decrease in WFA staining intensity in 5xFAD animals compared to WT at 7-months of age ($t_{(13)} = 3.73$, $p < 0.01$) and 11-months of age ($t_{(7)} = 3.85$, $p < 0.01$). (E) Lastly, we compared PNNs between the groups which showed a main effect of strain ($F_{(1, 18)} = 14.81$, $p < 0.01$) but no main effect of age and no interaction. Data presentation as Mean ± SEM. Scale bar represents 250 μm (*, $p < 0.05$, **, $p < 0.01$, ****, $p < 0.0001$).

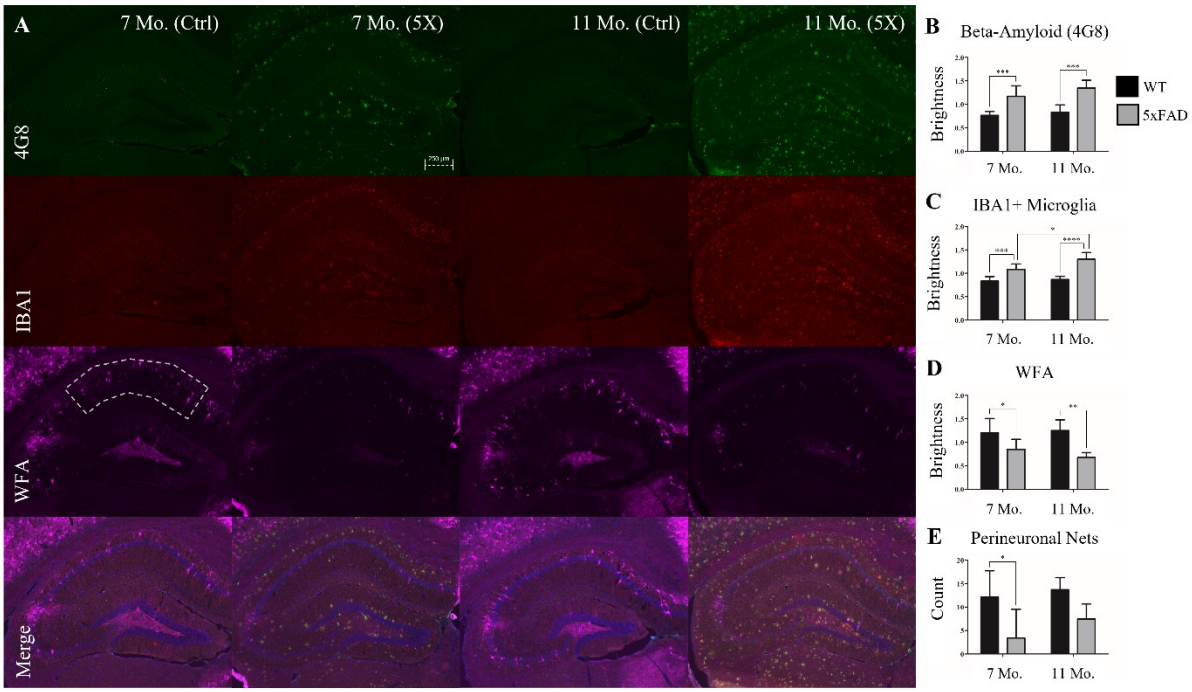
A
7 Mo. (Ctrl)
7 Mo. (5X)
11 Mo. (Ctrl)
11 Mo. (5X)
4G8
IBA1
WFA
Merge
B
Beta-Amyloid (4G8)
Brightness
WT
5xFAD
7 Mo.
11 Mo.
C
IBA1+ Microglia
Brightness
7 Mo.
11 Mo.
D
WFA
Brightness
7 Mo.
11 Mo.
E
Perineuronal Nets
Count
7 Mo.
11 Mo.

Figure 2.5. Within CA1, 5xFAD animals have elevated amyloid deposition, inflamed microglia and exhibit a loss of WFA straining and PNNs. (A) Representative images of immunostaining for 4G8 (green), IBA1 (red), and WFA (purple). (B) Comparing 4G8 staining intensity within the CA1 with an ANOVA showed a main effect of strain ($F_{(1, 18)} = 41.66$, $p < 0.01$) but no main effect of age and no interaction. Post-hoc comparisons showed significant increases in 4G8 staining intensity in 5xFAD animals at 7-months ($t_{(13)} = 4.82$, $p < 0.001$) and 11-months of age ($t_{(7)} = 4.47$, $p < 0.001$). (C) Analysis of IBA1 staining showed a main effect of strain ($F_{(1, 18)} = 51.41$, $p < 0.01$) and age ($F_{(1, 18)} = 6.85$, $p < 0.05$), but no statistically significant interaction. Post-hoc comparisons showed a significant increase in IBA1 staining intensity in 5xFAD animals compared to WT at 7-months of age ($t_{(13)} = 4.45$, $p < 0.001$) and 11-months of age ($t_{(7)}$=5.62, $p < 0.0001$). We also observed a significant increase in IBA1 staining intensity from 7-months to 11-months of age in 5xFAD animals ($t_{(19)} = 3.16$, $p < 0.05$). (D) A comparison of WFA labelling showed a main effect of strain ($F_{(1, 18)} = 19.50$, $p < 0.01$) but no main effect of age and no interaction. Post-hoc comparisons showed a significant decrease in WFA staining intensity in 5xFAD animals compared to WT at 7-months of age ($t_{(13)} = 2.86$, $p < 0.05$) and 11-months of age ($t_{(7)} = 3.38$, $p < 0.01$). (E) Lastly, we assessed PNNs where an ANOVA showed a main effect of strain ($F_{(1, 18)} = 11.08$, $p < 0.01$) but no main effect of age and no interaction. Post-hoc comparisons showed a significant decrease in PNN number in 5xFAD animals compared to WT at 7-months of age ($t_{(13)} = 3.28$, $p < 0.01$). Data presentation as Mean ± SEM. Scale bar represents 250 µm (*, $p < 0.05$, **, $p < 0.01$, ***, $p < 0.001$, ****, $p < 0.0001$).

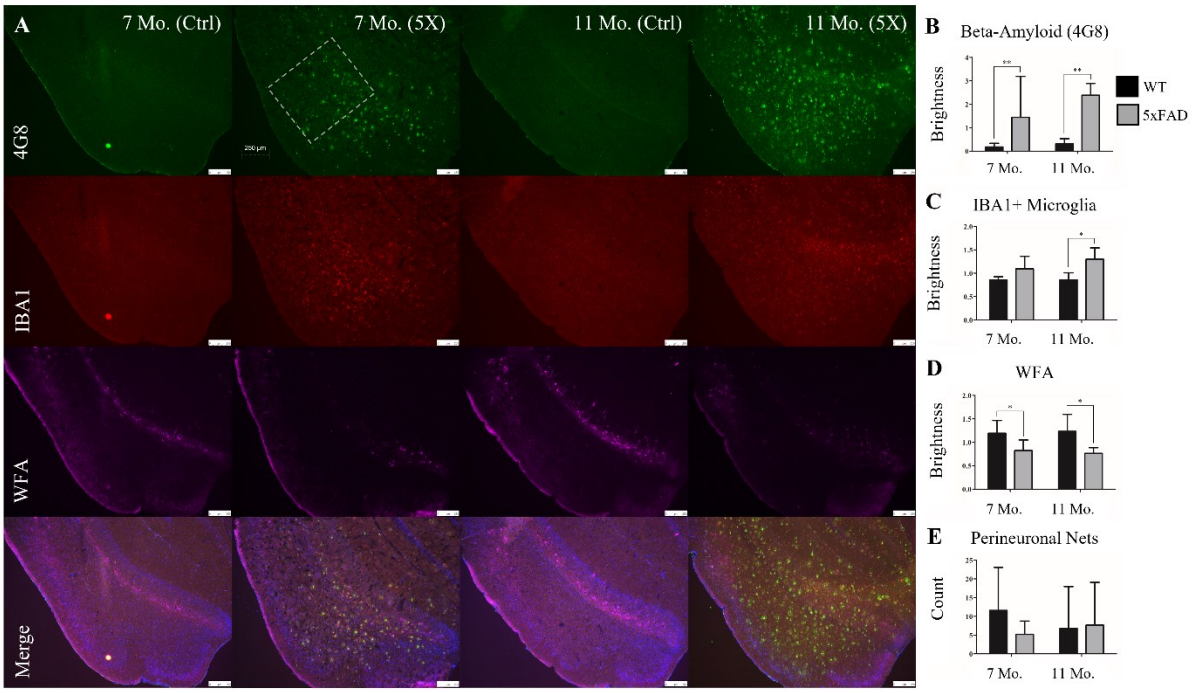
A
7 Mo. (Ctrl)
7 Mo. (5X)
11 Mo. (Ctrl)
11 Mo. (5X)
4G8
IBA1
WFA
Merge
B
Beta-Amyloid (4G8)
Brightness
WT
5xFAD
7 Mo.
11 Mo.
C
IBA1+ Microglia
Brightness
7 Mo.
11 Mo.
D
WFA
Brightness
7 Mo.
11 Mo.
E
Perineuronal Nets
Count
7 Mo.
11 Mo.

Figure 2.6. The entorhinal cortex of 5xFAD exhibits increased amyloid deposition, reactive microglia, and reduced WFA labeling of the extracellular matrix but no change in PNN density. (A) Representative images of immunostaining for 4G8 (green), IBA1 (red), and WFA (purple) within the entorhinal cortex. (B) An ANOVA on 4G8 staining intensity showed a main effect of strain ($F_{(1, 18)} = 38.49$, $p < 0.01$) but no main effect of age and no interaction. Post-hoc comparisons showed significant increases in 4G8 staining intensity in 5xFAD animals at 7-months ($t_{(13)} = 3.57$, $p < 0.01$) and 11-months of age ($t_{(7)} = 5.08$, $p < 0.01$). (C) An ANOVA on IBA1 staining intensity showed a main effect of strain ($F_{(1, 18)} = 15.09$, $p < 0.01$) but no main effect of age and no interaction. (D) An ANOVA on WFA straining intensity showed a main effect of strain ($F_{(1, 18)} = 13.47$, $p < 0.01$) but no main effect of age and no interaction. Post-hoc comparisons showed a significant decrease in WFA staining intensity in 5xFAD animals compared to WT at 7-months of age ($t_{(13)}=2.68$, $p < 0.05$) and 11-months of age ($t_{(7)} = 2.57$, $p < 0.05$). (E) Lastly, we evaluated PNNs, where an ANOVA showed no main effect of strain, age, and no interaction. Data presentation as Mean ± SEM. Scale bar represents 250 μm (*, $p < 0.05$, **, $p < 0.01$).

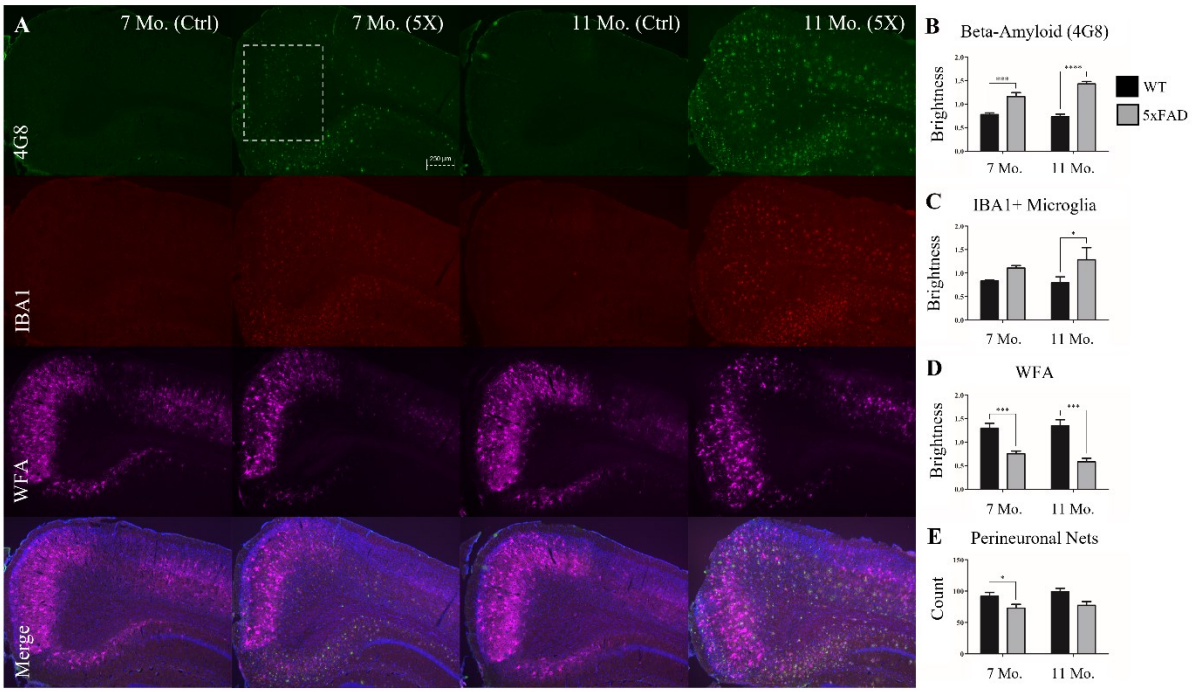
A
7 Mo. (Ctrl)
7 Mo. (5X)
11 Mo. (Ctrl)
11 Mo. (5X)
4G8
IBA1
WFA
Merge
B
Beta-Amyloid (4G8)
Brightness
WT
5xFAD
7 Mo.
11 Mo.
C
IBA1+ Microglia
Brightness
7 Mo.
11 Mo.
D
WFA
Brightness
7 Mo.
11 Mo.
E
Perineuronal Nets
Count
7 Mo.
11 Mo.

Figure 2.7. The RSC of 5xFAD animals display elevated amyloid deposition and reactive microglia and decreased WFA labeling and PNNs. (A) Representative images of immunostaining for 4G8 (green), IBA1 (red), and WFA (purple) within the entorhinal cortex. (B) An ANOVA on 4G8 staining intensity within the RSC showed a main effect of strain ($F_{(1, 18)}$ = 68.35, $p < 0.01$), but no main effect of age and no interaction. Post-hoc comparisons showed a significant increase in 4G8 staining intensity in 5xFAD animals compared to WT at 7-months of age ($t_{(13)} = 4.94$, $p < 0.001$) and 11-months of age ($t_{(7)} = 6.63$, $p < 0.0001$). (C) Next we compared IBA1 staining with an ANOVA which showed a main effect of strain ($F_{(1, 18)} = 12.57$, $p < 0.01$) but no main effect of age and no interaction. Post-hoc comparisons revealed no change in IBA1 staining intensity in 5xFAD animals compared to WT at 7 months ($t_{(13)} = 2.16$, $p > 0.05$) of age. (D) An ANOVA on WFA staining showed main effect of strain ($F_{(1, 18)} = 42.87$, $p < 0.01$) but no main effect of age and no interaction. Post-hoc comparisons revealed significant decreases in WFA staining intensity in 5xFAD animals compared to WT at 7 months ($t_{(13)} = 4.61$, $p > 0.001$) and 11-months of age ($t_{(7)} = 4.74$, $p < 0.0001$). (E) Lastly, we assessed PNNs where an ANOVA showed a main effect of strain ($F_{(1, 18)} = 10.13$, $p < 0.01$) but no main effect of age and no interaction. Post-hoc comparisons showed a significant decrease in PNN number in 5xFAD animals compared to WT at 7-months of age ($t_{(13)} = 2.56$, $p < 0.05$). Data presentation as Mean ± SEM. Scale bar represents 250 µm (*, $p < 0.05$, ***, $p < 0.001$, ****, $p < 0.0001$).

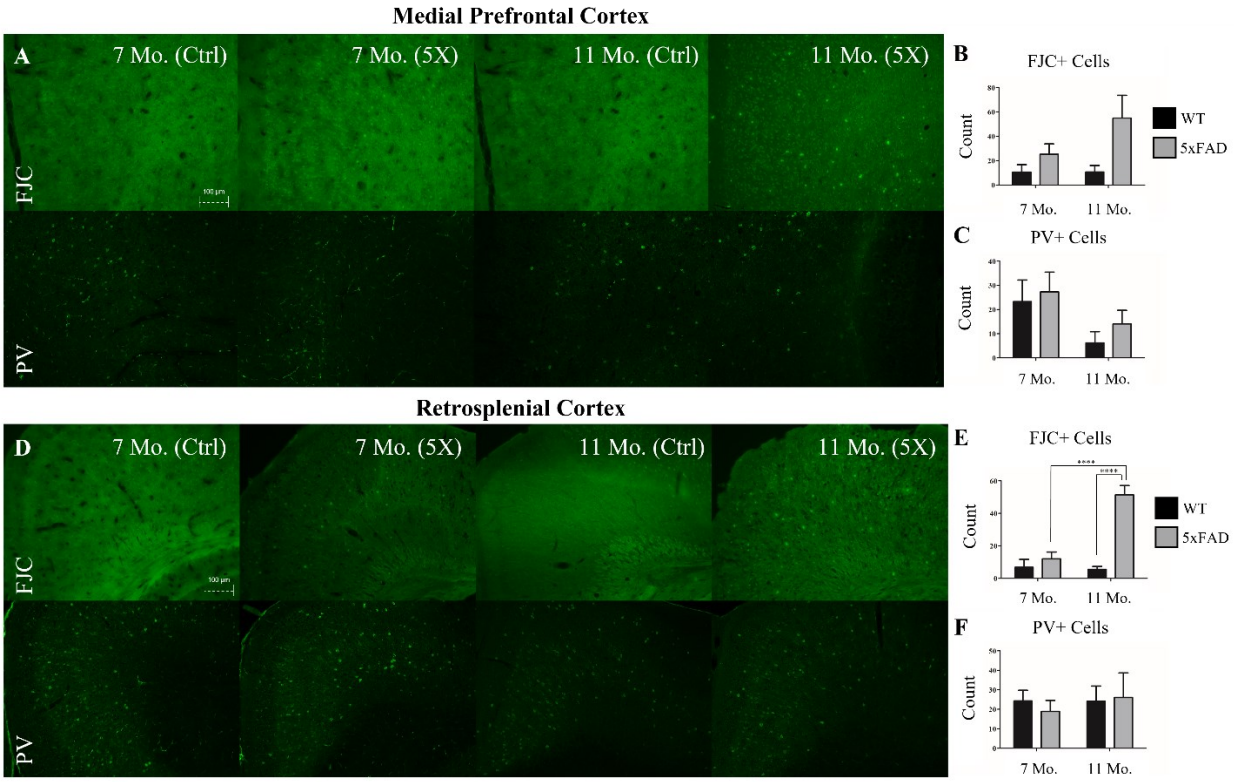
Medial Prefrontal Cortex
A
7 Mo. (Ctrl)
7 Mo. (5X)
11 Mo. (Ctrl)
11 Mo. (5X)
FJC
PV
B
FJC+ Cells
Count
WT
5xFAD
7 Mo.
11 Mo.
C
PV+ Cells
Count
7 Mo.
11 Mo.
Retrosplenial Cortex
D
7 Mo. (Ctrl)
7 Mo. (5X)
11 Mo. (Ctrl)
11 Mo. (5X)
FJC
PV
E
FJC+ Cells
Count
WT
5xFAD
7 Mo.
11 Mo.
F
PV+ Cells
Count
7 Mo.
11 Mo.

Figure 2.8. Evaluation of cell death and PV+ interneurons in the mPFC and RSC. (A) Representative immunostaining of FJC (top) and PV+ (bottom) in the mPFC. (B) An ANOVA on FJC+ cells identified with the mPFC showed a significant main effect of strain ($F_{(1, 18)} = 6.89$, $p = 0.02$) but no main effect of age and no interaction. Despite a noticeable increase in FJC+ cells in 11-month-old 5xFAD animals, this difference was not significant. (C) An ANOVA on PV+ interneurons showed no main effect of strain or age, and no interaction, although PV+ interneurons did appear to decrease with age in both groups. Data presentation as Mean ± SEM. Scale bar represents 100 µm. (D) Representative immunostaining of FJC (top) and PV+ (bottom) in the RSC. (F) Within the RSC, an ANOVA showed significant main effect of strain ($F_{(1, 18)} = 27.52$, $p < 0.01$) and age ($F_{(1, 18)} = 15.12$, $p < 0.01$), and a significant interaction ($F_{(1, 18)} = 17.08$, $p < 0.01$). Post-hoc comparisons showed a significant difference between WT and 5xFAD animals at 11-months of age ($t_{(7)} = 6.024$, $p < 0.01$). There was also a significant difference between 5xFAD animals at 7 months and 11 months ($t_{(13)} = 5.95$, $p < 0.01$). (F) Across all groups animals appeared to show similar amounts of PV+ interneuron labeling. An ANOVA on PV+ cell counts showed no main effect of age, strain, and no interaction. Data presentation as Mean ± SEM. Scale bar represents 100 µm (****, $p < 0.0001$).

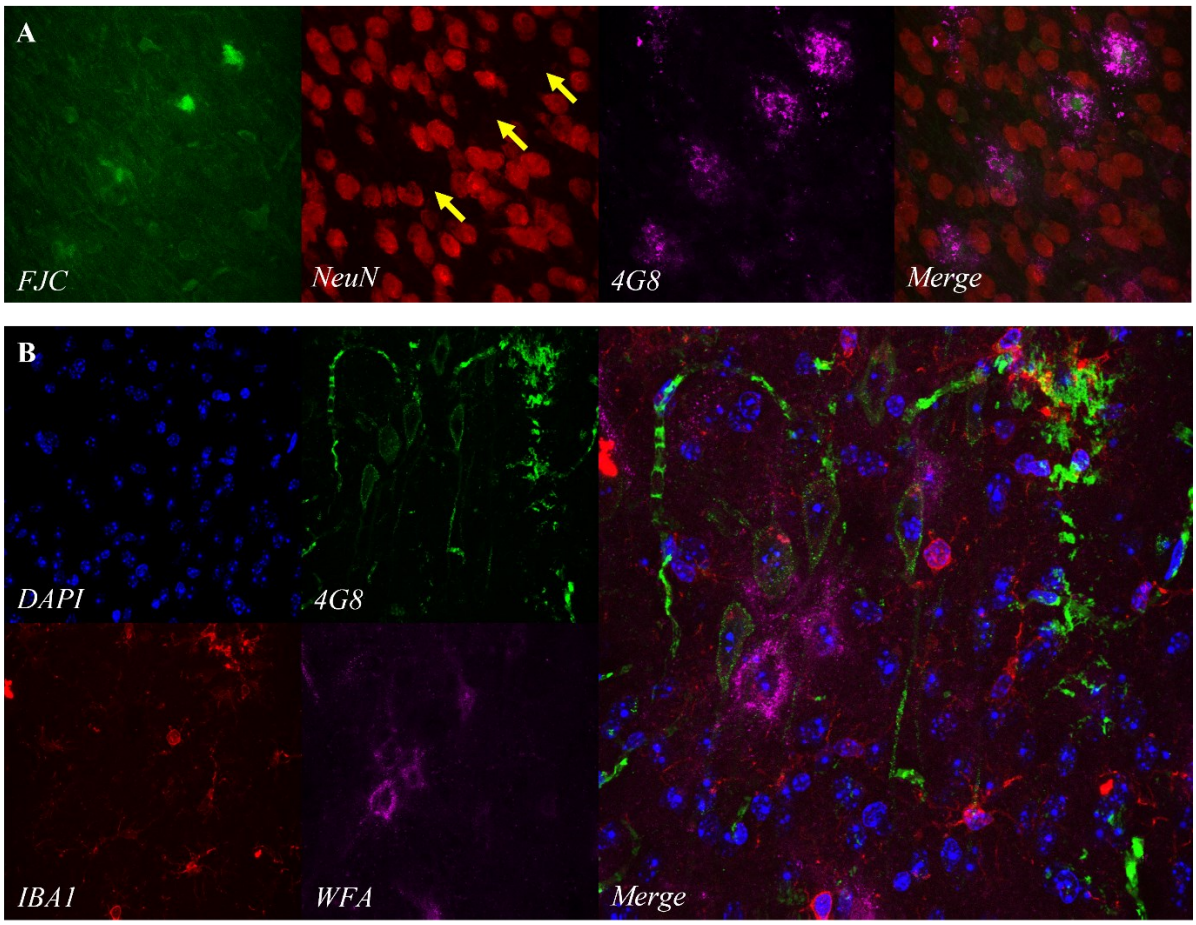
A
FJC
NeuN
4G8
Merge
B
DAPI
4G8
IBA1
WFA
Merge

Figure 2.9. Qualitative evaluation of immunostaining. (A) Representative immunostaining of FJC (green) for cell death, NeuN (red) for neurons, and 4G8 (purple) for amyloid plaque deposition. Qualitative observations showed that dying cells were frequently identifiable in the central mass of amyloid plaques. Amyloid plaques also appeared to carve out spaces devoid of NeuN+ staining (yellow bars indicate the positions of FJC+ cells). (B) Representative immunostaining for DAPI cell nuclei (blue), IBA1+ microglia (red), amyloid-deposits (green) and WFA (purple). PNNs rarely featured amyloid-β accumulation within them. Conversely, 4G8+ cells were rarely observed to be surrounded by a PNN. Plaques did often exhibit proximity to IBA1+ microglia, however.

Chapter 3 – Impaired cognitive function after perineuronal net degradation in the medial prefrontal cortex

Abstract

Perineuronal nets (PNNs) are highly organized components of the extracellular matrix that surround a subset of mature neurons in the central nervous system. These structures play a critical role in regulating neuronal plasticity, particularly during neurodevelopment. Consistent with this role, their presence is associated with functional and structural stability of the neurons they ensheath. A loss of PNNs in the prefrontal cortex has been suggested to contribute to cognitive impairment in disorders such as schizophrenia. However, the direct consequences of PNN loss in medial prefrontal cortex (mPFC) on cognition has not been demonstrated. Here, we examined behavior after disruption of PNNs in mPFC of Long-Evans rats following injection of the enzyme Chondroitinase ABC (ChABC). Our data show that ChABC-treated animals were impaired on tests of object oddity perception. Performance in the cross-modal object recognition task was not significantly different for ChABC-treated rats, although ChABC-treated rats were not able to perform above chance levels whereas control rats were. ChABC treated animals were not significantly different from controls on tests of prepulse inhibition, set-shifting, reversal learning, or tactile and visual object recognition memory. Posthumous immunohistochemistry confirmed significantly reduced PNNs in mPFC due to ChABC treatment. Moreover, PNN density in the mPFC predicted performance on the oddity task, where higher PNN density was associated with better performance. These findings suggest that PNN loss within the mPFC impairs some aspects of object oddity perception and recognition and that PNNs contribute to cognitive function in young adulthood.

Introduction

Perineuronal nets (PNNs) are highly organized components of the extracellular matrix that surround the cell body, proximal dendrites, and initial axon segment of mature central nervous system (CNS) neurons (Hockfield & McKay, 1983; Wang & Fawcett, 2012). These structures play a critical role in the regulation of neuronal plasticity in the CNS (Pizzorusso et al., 2002; Sorg et al., 2016). PNNs act as a physical barrier to structural changes in the neurons and also stabilize the functional properties of these neurons. Consistent with this, PNNs are sparse early in development when plasticity is generally at its highest and increase throughout the postnatal lifespan, particularly following critical periods of plasticity (Mauney et al., 2013; Pizzorusso et al., 2002). Within these periods, cortical tissue undergoes dramatic structural reorganization of neural connectivity in response to the appropriate stimulus (Hensch, 2005). These changes are followed by a period of synaptic pruning, and then stabilization of the network long-term. In line with a role in regulating plasticity, PNN expression increases at the closure of these critical periods and degradation of PNNs can re-open these windows of heightened plasticity in adulthood (Lensjø et al., 2017; Pizzorusso et al., 2002).

Several recent studies suggest that PNNs are reduced in the post-mortem tissue of patients suffering from CNS disorders such as schizophrenia, epilepsy, and Alzheimer's disease (Baig et al., 2005; Berretta et al., 2015; Bitanihirwe & Woo, 2014; McRae & Porter, 2012; Okamoto et al., 1994; Pollock et al., 2014). In schizophrenia, post-mortem analyses of the prefrontal cortex, amygdala, and superior temporal cortex suggest reduced PNN density (Enwright et al., 2016; Mauney et al., 2013; Pantazopoulos et al., 2010). This finding has been replicated in animal models of the disease and coincides with the development of cognitive impairment (Paylor et al., 2016; Steullet et al., 2017). Post-mortem analysis of Alzheimer's

patients has also revealed deficits in PNNs in the frontal lobe (Baig et al., 2005; Brückner et al., 1999; Morawski et al., 2010). Moreover, PNNs protect against Alzheimer's pathology and their loss may render neurons particularly vulnerable to the disease pathology (Okamoto, Mori, & Endo, 1994). PNN loss and the degradation of extracellular matrix components have also been implicated in epileptogenesis and the maintenance of seizures in epilepsy (McRae & Porter, 2012; Pollock et al., 2014). While this observational evidence is a compelling indicator that PNNs are involved in CNS disorders, our current understanding of their functional significance is limited. Studies that show coincidental PNN loss and behavioral disturbances are intriguing, but do not necessarily implicate the loss of PNNs as sufficient for causing cognitive dysfunction.

We have previously observed a reduction of PNNs in medial prefrontal cortex (mPFC) of the offspring of rats exposed to polyI:C during pregnancy (Paylor et al., 2016). As an extension of these findings, the present study examined cognitive function after targeted reduction of PNNs in the mPFC of rats using Chondroitinase ABC (ChABC). ChABC catalyzes the breakdown to glycosaminoglycan subunits of chondroitin sulfate proteoglycans (CSPGs), which are the primary component of PNNs (Brückner et al., 1998; Crespo et al., 2007). This treatment has been used extensively to degrade CSPGs in PNNs and the surrounding interstitial matrix (Fawcett, 2015). After injection, we assessed cognitive function using tasks where performance is impaired in the offspring of rats subjected to polyI:C during pregnancy, including altered object oddity preference, recognition memory, sensorimotor gating, and cognitive flexibility (set-shifting and reversal learning; Ballendine et al., 2015; Bissonette et al., 2013; Kamiński et al., 2017; Latif-Hernandez et al., 2016; Lins et al., 2018; Yang et al., 2014). We found that ChABC treatment reduced overall extracellular matrix staining within the mPFC as well as a reduced density of PNNs. These cellular changes were associated with impaired performance on an object oddity

task, and performance at chance levels in a task measuring cross-modal object recognition. Interestingly, linear regression showed that PNN density predicted performance on the oddity task. Conversely, PNN digestion did not affect performance on measures of prepulse inhibition, set-shifting, reversal learning, or tactile and visual object recognition memory. Thus, our findings support a nuanced effect of degrading mPFC PNNs on cognitive functions related to schizophrenia.

Methods

Subjects. Adult male Long Evans rats (n = 80; 300-350 g; Charles River Laboratories, Kingston, NY, USA) were used for all experiments. After their arrival, animals were pair-housed in ventilated plastic cages and left undisturbed for 1 week with food and water *ad libitum* (Purina Rat Chow). A 12:12-h lighting cycle was used with lights on at 7:00am. Animals were given environmental enrichment in their home cage in the form of a plastic tube throughout the experiment. Following acclimatization, animals used for operant conditioning were maintained at 90% of free feeding weight and singly housed to ensure the appropriate amount of food was consumed by each rat in the home cage after behavioral testing. All animal procedures were performed in accordance with the University of Saskatchewan animal care committee's regulations.

Behavioral Measures.

All rats were handled for at least 5 min/day for 3 days before behavioral testing. They were also habituated to transport in an elevator from the vivarium to the testing rooms. Rats were randomly assigned to one of two groups for behavioral testing. Group 1 had ChABC or PEN infused into mPFC prior to testing two weeks later on prepulse inhibition (PPI), the cross-modal object

recognition (CMOR) battery, and the oddity task. Group 2 was food restricted and then trained to press levers for food reward in the operant conditioning chambers. After passing set-shifting (SS) Train (see below), ChABC or PEN was infused into mPFC. Two weeks later, the rats were retrained on the SS Train (3-4 days) and then tested on visual cue discrimination, set-shifting, and reversal learning.

Prepulse Inhibition (PPI): PPI measures the percent attenuation of motor response to a startling tone when that tone is preceded by a brief prepulse. Two SR-LAB startle boxes (San Diego Instruments, San Diego, CA, USA) were used. Each session had a constant background noise (70 dB) and began with 5 min of acclimatization, followed by 6 pulse-alone trials (120 dB, 40 ms). Pulse-alone (6 trials), prepulse alone (18), prepulse + pulse (72), and no stimulus (6) trials were then presented in a pseudorandom order, followed by 6 additional pulse-alone trials. Prepulse + pulse trials began with a 20 ms prepulse of 3, 6, or 12 dB above background (70 dB). Prepulse–pulse intervals (time between the onset of the prepulse and the 120 dB pulse) were short (30 ms) or long (50, 80, or 140 ms). The inter-trial interval varied randomly from 3 to 14 s (Howland et al., 2012; Lins et al., 2017).

Cross-Modal Object Recognition (CMOR) Battery: This task uses spontaneous exploratory behavior to assess visual memory, tactile memory, and visual-tactile sensory integration (Ballendine et al., 2015; Winters & Reid, 2010). The testing apparatus was a Y-shaped maze with 1 start arm and 2 object arms (10 × 27 cm) made of white corrugated plastic. A white plastic guillotine-style door separated the start arm from the object arms, and Velcro at the distal end of the object arms fixed objects in place. A removable, clear Plexiglas barrier could be inserted in front of the objects. A tripod positioned above the apparatus held a video camera that recorded the task activity. Rats were habituated to the apparatus twice for 10 min. Lighting alternated

during habituation between white light (used during visual phases) and red light (used during tactile phases) for 5 min each with the order counterbalanced, and the clear barriers were in place for one day of habituation and removed for the other with order counterbalanced between all rats. Test days consisted of a 3 min sample phase with two identical copies of an object attached with Velcro to the maze, a 60 min delay, and then a 2 min test phase with a third copy of the original object and a novel object placed in the maze. Rats began each phase in the start arm; the guillotine door was opened and closed once the rat entered the object arms. This task consisted of 3 distinct tests performed on 3 separate days: tactile memory (day 1), visual memory (day 2) and cross-modal memory (day 3). Red light illuminated the tactile phases allowing the rats' behavior to be recorded while preventing the rats' visual assessment of the objects and the removal of the clear barriers allowed for tactile exploration. White light was used during visual phases, but clear Plexiglas barriers in front of the objects prevented tactile exploration. CMOR had a tactile sample phase (red light, no barriers) and a visual test phase (white light, clear barriers). Recognition memory was defined as significantly greater exploration of the novel object than the familiar object. Video recordings of behavior were manually scored by investigators blind to the treatment status of the rats and identity of the objects. Novel object preference was reported as a discrimination ratio (time exploring novel object – time exploring familiar object)/(total time exploring both objects) of the first minute of the test phase.

Oddity Discrimination: The oddity discrimination test measures object perception using presentation of 3 copies of one object and a fourth distinct or 'odd' object (Bartko et al., 2007). The testing apparatus was a square arena (60 x 60 x 60 cm) constructed of white corrugated plastic with Velcro in each of the 4 corners. Following two days of habituation to the arena (10 min sessions), the test day was conducted. On test day, 3 identical objects and one different or

'odd' object made of glazed ceramic (a round 'owl' statue, 9.5 cm in diameter x 8 cm tall) or plastic (a square Lego statue, 5.5 cm (w) x 7 cm (h)) were fixed to the Velcro and the rats' activity were recorded for 5 min using a video camera mounted to the ceiling. The odd object and its location was counterbalanced among the rats in both treatment groups. Object exploration times were hand scored by an investigator blind to the treatment status of the rats. Object examination was counted when a rat's face was oriented toward the object at a maximum distance of 2 cm. Odd object preference was reported as a percentage of the total time exploring the odd object. Note that 25% is chance performance in this task (Lins et al., 2018).

Operant Set-Shifting Task (OSST): Eight operant conditioning chambers (MedAssociates Systems, St. Albans, VT, USA) in sound-attenuating cubicles were used. The chambers contained two retractable levers and two stimulus lights positioned on either side of a food port used to deliver food rewards (Dustless Precision Pellets, 45 mg, Rodent Purified Diet; BioServ, Frenchtown, NJ). A 100 mA house light illuminated the chamber. Sessions began with levers retracted and the chamber in darkness (inter-trial state), with the exception of lever training days in which the trial began with levers exposed to allow for baiting with ground reward pellets. Rats were tested once each day. *Lever training*. Rats were trained to press the levers as described previously and immediately after reaching criterion, side preference was determined (Floresco et al., 2008; Thai et al., 2013; Y. Zhang et al., 2012). *Visual-cue discrimination*. Rats were trained to press the lever indicated by a stimulus light illuminated above it. Trials (every 20 s) began with an illumination of one stimulus light, followed 3 s later by the house light and insertion of both levers. A correct press of the lever underneath the illuminated stimulus light caused retraction of both levers and the delivery of a reward pellet. The house light remained illuminated for an additional 4 s before the chamber returned to the inter-trial state. An incorrect

press returned the chamber to the inter-trial state (all lights off) with no reward. Failure to press a lever within 10 s of their initial insertion was scored as an omission and the immediate return of the chamber to the inter-trial state. *Strategy set-shift (shift to response discrimination)*. The visual-cue rule from the previous stage was reinforced with 20 trials where the rat was required to press the lever below the illuminated stimulus light. Subsequently, rats were required to change their response from the visual cue to a spatial cue (the lever opposite to their side preference, regardless of whether the stimulus light was illuminated) to receive a reward pellet. *Reversal learning*. Rats were required to press the lever opposite to the one rewarded during set-shifting. Criterion was 10 consecutive correct responses for each testing day and errors for each testing day were coded as described previously (Floresco et al., 2008; Thai et al., 2013; Zhang et al. 2012). Rats were tested for a minimum of 30 trials per day and a maximum of 150 trials per day. If a second day of testing was required, trials per criterion were calculated as the sum of the trials completed on all testing days for a given discrimination.

mPFC Infusions of ChABC or Penicillinase (PEN). Prior to and during the procedure, rats were anesthetized with the inhalant anesthetic isoflurane (Janssen, Toronto, ON). Pre-operatively, all rats were administered a 0.5 mg/kg subcutaneous dose of the analgesic Anafen (Merial Canada Inc, QC). After animals were positioned in the stereotaxic apparatus, the scalp was cut and retracted to expose the skull. Holes were drilled above mPFC and injectors made from 35Ga silica tubing (WPI, Sarasota, FL) glued to PE-50 tubing were inserted bilaterally to the following coordinates: anteroposterior (AP) +3.0 mm; lateral (L) 0.7 mm; dorsoventral (DV) 4.4 mm relative to bregma. Either ChABC (100 units/ml) or PEN (100 units/ml) was infused (0.1 ul/min) for 2 min at DV coordinates -4.4 mm, -4.2 mm, and -3.9 mm (total infusion volume 0.6 ul/side). Injectors were left in place for an additional 6 min to allow for diffusion of the solution away

from the last infusion site. Injectors were then slowly removed, the holes filled with bone wax, and wound was closed with stitches.

Tissue Collection. Following behavioral testing, rats were deeply anesthetized with isoflurane and transcardially perfused with PBS followed by 4% paraformaldehyde using infusion pumps. After perfusion, brains were extracted and stored in 4% paraformaldehyde at 4°C. One-day later, brains were transferred to 30% sucrose for several days and then frozen in isopentane and optimal cutting temperature (OCT) gel. Frozen brains were sectioned at 25 µm on a cryostat. For cFos staining, animals (PEN = 8, ChABC = 8) were time-perfused 100 minutes after assessment on the oddity object task.

Immunohistochemistry. Slides were warmed to room temperature for 20 min and then given three washes in 1X PBS for 10 min each. After which slides were incubated for 1 hour with 10% Protein Block, Serum-Free (Dako, Missisauga, ON) in 1X PBS. Slides were then incubated overnight at room temperature with a primary antibody in a solution of 1% Protein Block, 1% Bovine Serum Albumin, and 99.9% 1X PBS with 0.1% Triton X-100. Primary antibodies were as follows: Mouse anti-Chondroitin-4-Sulfate (C4S; 1:400; Millipore, Etobicoke, ON), Wisteria Floribunda Agglutinin (WFA; 1:1000; Vector Labs, Philadelphia, PA), mouse anti-Parvalbumin (1:1000; Swant, Switzerland), rabbit anti-Parvalbumin (1:1000; Swant, Switzerland); rabbit anti-IBA1 (1:200; Dako, Mississauga, ON); mouse anti-GFAP (1:200; Sigma-Aldrich, Oakville, ON); c-Fos (1:400; Cell Signaling, Whitby, ON); mouse anti-GAD67 (1:400; Millipore, Etobicoke, ON); anti-Gephryin (1:500; ThermoFisher; Rockford, IL). After overnight incubation, slides were washed three times, twice in 1X PBS with 1% tween-20 and once in 1X PBS. Slides were then incubated for 1h with secondary antibodies in antibody solution (as above). Secondary antibodies were as follows: Streptavidin 647 (1:200; Invitrogen, Burling,

ON), Donkey anti-Mouse Alexa Fluor 488 (1:200; Molecular Probes, Eugene, OR), Donkey anti-Rabbit Alexa Fluor 647 (1:200; Molecular Probes, Eugene, OR), and Donkey anti-Mouse 647 (1:200, Molecular Probes, Eugene, OR). After 1 hour incubation slides were washed again three times and mounted with DAPI (4',6-diamidino-2-phenylindole) in vectashield mounting medium (Vector Labs, Philadelphia, PA).

Microscopy. Images were acquired using a Leica DMI6000B Microscope with LAS AF computer software. The mPFC was identified using The Rat Brain in Stereotaxic Coordinates and selected based on landmarks in the DAPI nuclear staining pattern (Paxinos & Watson, 2007). The mPFC was identified between +2.76mm and +3.24mm anterior to Bregma with the imaging window aligned to the midline and extending through cortical layers 1-6. All imaging was captured at 10X magnification with a total of 6 images taken bilaterally in adjacent sections (~250μm apart). Images from the primary somatosensory jaw (S1J) area were also taken from within the same slices (directly lateral) as images of the mPFC, as a control region outside of the targeted injection area. A constant gain, exposure, and light intensity was used across all animals. Gephyrin and Neuronal Nuclei (NeuN) confocal imaging was conducted on a LEICA SP5 Confocal microscope. For each animal, four 2x2 tile scans were conducted at 25X magnification over the mPFC.

Image analysis. Analysis was completed on unmodified images by an observer blind to the experimental condition of the tissue analyzed. Cell counts for DAPI+, IBA+, PV+, c-Fos+ cells and Gephyrin+ puncta were performed using the Image-based Tool for Counting Nuclei (Centre for Bio-image Informatics, UC Santa Barbara, CA, USA) plugin for NIH ImageJ software. PNNs were counted manually using ImageJ Cell Counter function. For cell specific Gephryin+ puncta, 4 cells were selected per image from each quadrant (total number of cells analyzed = 229). For

PV+ immunofluorescence and GAD67 colocalization, an overlay for all PV+ cells were generated using the ImageJ Analyze Particles function and mean brightness values taken from both PV+ and GAD67+ channels within cell marked areas. A second analysis for PV+ and c-Fos+ cell density and colocalization was conducted using a custom automated detection script in Python (Python Software Foundation. Python Language Reference, version 2.7. Available at http://www.python.org). For all images a standard rectangular area was drawn over the region of interest, spanning cortical layers 1-6, within which cells were identified and measurement parameters kept constant. For each stain measurements of mean brightness within the area were also taken. Quantification of densities are expressed as a 100x100 micron square (10000μm^2).

Statistical Analyses. All data are presented as mean ± SEM. Statistical analyses were conducted in PRISM Software (Prism Software, Irvine, CA) and significance was set at $p < 0.05$. For experiments in Figure 1-3 and 6-7, unpaired students t-tests were used to compare PEN to ChABC. Simple linear regressions were used to examine the predictive value of behavioural performance on PNN densities. For Figure 4, a two-way ANOVA of Treatment Group and Prepulse Intensity was conducted to probe deficits in prepulse inhibition. In Figure 5, in addition to unpaired students t-tests, we utilized one-sample t-tests against chance performance to probe animals performance on object recognition. One sample t-tests to chance performance are frequently used in behavioral neuroscience to determine whether performance of a given group differs significantly from chance (Gervais et al., 2016; Jacklin et al., 2016; Lins et al., 2018).

Results

Perineuronal Nets & Interstitial Matrix. To confirm the degradation of CSPGs and PNNs after treatment with ChABC, we stained with Chondroitin-4-Sulfate (C-4-S), a marker for cleaved components of CSPGs, and Wisteria Floribunda Agglutinin (WFA), a marker for the CSPGs that

preferentially labels PNNs (PEN = 40, ChABC = 40). Treatment with ChABC did not alter total cellular density (Figure 1. E) in the mPFC ($t_{(77)}$=0.37, p = 0.72). Staining intensity for C-4-S was significantly greater in ChABC treated animals than controls (Figure 1. F; $t_{(76)}$=12.56, p < 0.0001). ChABC treatment induced a significant reduction in WFA staining intensity (Figure 1. G; $t_{(77)}$=4.83, p < 0.0001) and a reduction in PNN density within the mPFC (Figure 2. E; $t_{(77)}$=6.403, p < 0.0001). As a control to demonstrate selective digestion of PNNs at the site of injection, we assessed the same measures in the S1J, lateral from the mPFC, from within the same tissue slices. Within the S1J, total cellular density was not altered by ChABC treatment (Figure 1. E; $t_{(76)}$=1.327, p = 0.19). C4S staining intensity (Figure 1. F; $t_{(76)}$=0.07, p = 0.94) and WFA staining intensity (Figure 1. G; $t_{(76)}$=1.03, p = 0.30) within the S1J were also unaffected by ChABC treatment. We also visually inspected slides anterior of the mPFC, including the frontal association cortex and regions of the orbitofrontal cortex and found no signs of elevated C4S or reduced WFA staining intensity. Similarly, there was no overt C4S or WFA alterations posterior in regions such as the hippocampus (data not shown).

Parvalbumin-expressing (PV+) Interneurons. PNNs most frequently surround PV+ inhibitory interneurons (Härtig et al., 1992). To assess whether changes in PNNs were paralleled by cellular loss of these inhibitory interneurons, immunostaining for an antibody specific to PV+ was performed (PEN = 40, ChABC = 40). Despite the close association between PNNs and PV+ inhibitory interneurons, the total density of PV+ cells was unchanged (Figure 2. F; $t_{(77)}$=0.74, p = 0.46). However, the percentage of PV+ cells surrounded by a PNN was significantly reduced in ChABC treated animals (Figure 2. G; $t_{(77)}$=2.71, p < 0.01).

GAD67 Expression. To assess whether ChABC affected the integrity of PV+ cells, immunostaining for GAD67+, a critical GABA synthesis enzyme present in PV+ cells, was

performed along with PV+ staining (PEN = 16, ChABC = 16). Across all images there was no difference between PEN and ChABC groups in terms of the number of cells analyzed ($t_{(29)}$=1.28, p = 0.21). PV+ fluorescence within PV+ cells did not differ between groups (Figure 3. F; $t_{(29)}$=1.17, p = 0.25). Similarly, ChABC treatment did not result in an overall change in GAD67+ fluorescence from within PV+ cells (Figure 3. G; $t_{(29)}$=0.99, p = 0.33).

Gephryin+ Puncta. To further examine the cellular consequences of ChABC treatment, we assessed Gephryin, a major scaffolding protein at inhibitory synapses, to determine whether PNN loss resulted in changes in inhibitory connectivity (PEN = 8, ChABC = 8). Within the mPFC, the total number of Gephryin+ puncta was not affected by ChABC treatment ($t_{(14)=}$1.30, p = 0.22). Next, we assessed Gephryin+ puncta colocalized with NeuN, a marker for neuronal cells. A total of 229 cells were analyzed (avg = 14.31 per animal) and measured cell size did not differ between PEN or ChABC animals ($t_{(14)}$=0.27, p = 0.82). The number of Gephyrin+ puncta colocalized with NeuN did not differ between groups (Figure 3. H; $t_{(14)}$=0.67, p = 0.51)

Immune Cell Labeling. To assess the degree of reactive inflammation to the injection of ChABC or PEN, immunostaining for IBA1+ microglia and GFAP+ astrocytes was performed (PEN = 16, ChABC = 16). Intensity of IBA1+ immunofluorescence was not altered by ChABC, (Figure 4. C; $t_{(30)}$=0.50, p = 0.61) but IBA1+ microglia cell density was significantly increased in treated animals (Figure 4. D; $t_{(30)}$=2.31, p < 0.05). Treatment with ChABC did not significantly alter GFAP+ immunoreactivity (Figure 4. E; $t_{(30)}$=0.28, p = 0.79).

Prepulse Inhibition. To assess whether PNN degradation resulted in deficits in sensorimotor gating, rats were tested on a (PPI) task using the presentation of acoustic stimuli. Rats showed a robust startle response to presentation of 120-db tones in all treatment groups (PEN = 25, ChABC = 24). We observed a main effect of pulse block ($F_{(2,141)}$ = 56.65, p < 0.0001) indicating

habituation of the startle response over the testing session. ChABC treatment resulted in a marginally increased startle response but this effect was not significant ($F_{(1,141)} = 3.20$, $p = 0.08$). Rats in both treatment groups displayed greater PPI for trials with louder prepulses (Figure 4. B). A main effect of prepulse intensity ($F_{(2,141)} = 35.44$, $p < 0.0001$) confirmed this observation (Figure 4. B). There was no main effect of treatment with ChABC on prepulse inhibition ($F_{(1,141)} = 0.01$, $p = 0.93$) and no interaction between prepulse intensity and treatment ($F_{(2,141)} = 0.25$, $p = 0.78$). Linear regression was used to investigate the relationship between PNN density and prepulse inhibition for 12 dB prepulses but no significant relationship was detected ($R^2 < 0.01$, $p = 0.91$)

CMOR. To assess whether PNN degradation affected recognition memory we assessed rats on a CMOR task (PEN = 20, ChABC = 23). Both groups showed similar levels of total object exploration during the sample phases of all three tests (tactile: PEN=43.02±2.44 s, ChABC=47.57±3.12 s; visual: PEN=7.92±0.68 s, ChABC=7.92±0.50 s; cross-modal: PEN=46.14±3.69 s, ChABC=42.74±3.12 s; statistics not shown). In the tactile object recognition testing phase, both groups had similar total exploration time of the objects (Figure 6. B; $t_{(46)}=1.31$, $p = 0.26$) and discrimination ratio for the novel object was not affected by treatment ($t_{(46)}=0.32$, $p = 0.75$). One sample t-tests revealed that rats in both groups displayed a preference for the novel object significantly greater than expected by chance (PEN $t_{(23)}=6.80$, $p<0.001$; ChABC $t_{(23)}=8.59$, $p<0.001$). In the visual object recognition testing phase, both groups had similar total exploration time of the objects (Figure 6. C; ($t_{(46)}=0.21$, $p = 0.83$) and discrimination ratio for the novel object was not affected by treatment ($t_{(46)}=0.19$, $p = 0.85$). Rats in both groups displayed a preference for the novel object significantly greater than expected by chance (one sample t-tests, PEN $t_{(23)}=1.97$, p=0.03; ChABC $t_{(23)}=2.35$, $p = 0.01$). In the CMOR testing phase,

both groups had similar total exploration time of the objects ($t_{(41)}$=1.54, p = 0.87). When comparing the discrimination ratio for the novel object, rats treated with ChABC were not significantly different than control rats (Figure 6. D; $t_{(41)}$=0.86, p = 0.39). However, a comparison against chance showed that PEN rats performed significantly better than to be expected if rats had no recollection of the objects (one sample t-test: $t_{(19)}$ = 2.80, p = 0.01) whereas rats treated with ChABC did not perform significantly better than chance ($t_{(22)}$ = 1.39, p = 0.09). Linear regression did not reveal significant relationships between PNN density and performance on visual, tactile, or cross modal object recognition (Figure 6. E-G; visual: R^2 = 0.02, p = 0.37; tactile: R^2 = 0.01, p = 0.62; CMOR: R^2 = 0.02, p = 0.44).

Oddity Task. As a second assessment of recognition memory function, rats (PEN = 8, ChABC = 8) were tested on an oddity task to determine if ChABC treatment impaired the ability to perceive and maintain representations of odd stimuli in their environment. There was no difference between total time exploring the objects for PEN or ChABC groups ($t_{(14)}$=0.04, p = 0.96). When the percentage of exploration for the odd object was evaluated, ChABC-treated rats spent significantly less time inspecting the odd object compared to the duplicate objects than PEN-treated rats (Figure 7. B; $t_{(14)}$=2.55, $p < 0.05$). Linear regression analysis identified a significant relationship between PNN density and the odd object preference in both groups (Figure 6. C; R^2 = 0.36, $p < 0.05$).

Rats evaluated on the oddity task were perfused 100 minutes after completion of the test to permit analysis of c-Fos immunoreactivity as a marker of neuronal activity in the mPFC (PEN = 8, ChABC = 8). Treatment with ChABC did not significantly alter the total number of c-Fos+ cells (Figure 8. F; $t_{(14)}$=0.33, p = 0.75) nor was there a change in the intensity of c-Fos+ immunofluorescence in the cell soma (Figure 8. H, $t_{(14)}$=0.56, p = 0.59). However, a comparison

of the number of PV+ cells that co-localized with c-Fos+ immunoreactivity in ChABC animals relative to controls approached statistical significance (Figure 8. G, $t_{(14)}$=2.10, p = 0.054).

Set-Shifting & Reversal Learning. To determine if animals treated with ChABC had deficits in cognitive flexibility and learning, rats were assessed in set-shifting and reversal learning paradigms. Rats in both groups (PEN, n=15; ChABC, n=16) had similar trials to reach criterion for the set-shifting task ($t_{(29)}$=0.16, p = 0.87) and a similar number of total errors ($t_{(29)}$=0.16, p = 0.87). Comparison of perseverative errors only revealed no significant differences between treatment groups ($t_{(29)}$=0.51, p = 0.61) nor did they differ statistically in regressive errors (t(29)=0.83, p = 0.42). A simple linear regression was utilized to determine the relationship between PNN density and total errors committed in the set-shifting task but no relationship was found (R^2 = 0.03, p = 0.34)

With regards to reversal learning, both PEN (n=16) and ChABC (n=16) rats required a similar number of trials to reach criterion ($t_{(29)}$=0.34, p = 0.74) and committed a similar number of total errors ($t_{(29)}$=0.04, p = 0.97). Errors committed by the two groups also did not differ when subdivided into perseverative errors ($t_{(29)}$=0.57, p = 0.57) or regressive errors ($t_{(29)}$=1.22, p = 0.23). A simple linear regression was utilized to determine the relationship between PNN density and total errors committed. There was a weak negative relationship between PNN density and total errors, but this effect was not significant (R^2 = 0.10, p = 0.08).

Discussion

Here, targeted delivery of ChABC was used to degrade CSPGs and PNNs in the mPFC of adult rats. Immunohistochemistry confirmed that ChABC treatment elevated staining for C-4-S stubs, the cleaved disaccharide components of PNNs, and decreased WFA staining, a marker for

CSPGs in the extracellular matrix. The density of PNNs was significantly decreased in mPFC by ChABC treatment. There was no change in the density of PV+ inhibitory interneurons, but the number of PV+ cells surrounded by a PNN was reduced. Furthermore, PV+ cells also had no change in the fluorescence of PV+ protein, c-Fos+, gephyrin or GAD67. ChABC treatment significantly increased the density of IBA1+ microglia within the mPFC. Notably, PNN loss in the mPFC was accompanied by behavioral impairments in an oddity task and in CMOR, whereas prepulse inhibition, set-shifting, and reversal learning were unaffected.

Perineuronal Nets & Cognitive Function

The battery of tasks used in the present study was developed from previous research conducted to assess behavioral effects in the offspring of rats subjected to treatment with polyI:C during pregnancy. As the offspring of polyI:C-treated dams display altered behavior in these tasks (Howland et al. 2012; Zhang et al. 2012; Ballendine et al. 2015; Lins et al. 2018) and have reduced PNNs in mPFC (Paylor et al. 2016), we reasoned it would be valuable to assess behavior in the same tasks following ChABC infusions in young adulthood. In general, behavior of the PEN-treated rats was similar to that previously reported for these tasks (Ballendine et al. 2015; Marks et al. 2016; Lins et al. 2018); thus, we are confident in our testing protocols for these groups of rats. ChABC did not significantly affect PPI or alter the startle response. Although the mPFC is involved in the modulation of PPI in rats, an array of other brain areas are also involved (Swerdlow et al., 2001). Therefore, it is likely that the relatively subtle manipulation of mPFC PNNs we performed was insufficient to disturb the global activity of this circuit. Previously, deficits in frontal-dependent object recognition tasks, including object-in-place and CMOR, were observed in the male offspring of polyI:C treated dams (Howland et al. 2012; Ballendine et al. 2015). Other tasks, such as object recognition or the tactile and visual variants of the CMOR

battery, were unaffected (Howland et al. 2012; Ballendine et al. 2015). Lesions of the orbitofrontal, but not mPFC, cortex impair performance of the CMOR task (Reid et al., 2014). As a result, it was somewhat unexpected that injections of ChABC into mPFC impaired performance of CMOR. Reconciling the effect of mPFC ChABC injections on CMOR with the lack of effect on the operant conditioning-based discrimination, set-shifting, and reversal learning task battery is also difficult. In particular, temporary inactivation of the mPFC impairs the set-shifting aspect of the task (Floresco et al. 2008). Thus, given the relatively subtle nature of the observed impairment of CMOR following mPFC ChABC injection, replication in future studies is important. The circuitry involved in the object oddity task is incompletely characterized, although no study to our knowledge has directly implicated the mPFC in this task. Previous work has shown the involvement of lateral cortical regions including perirhinal cortex in object oddity tasks (Bartko et al. 2007). As mPFC interactions with the perirhinal cortex are necessary for some object memory tasks (Hannesson, 2004), it is possible that interactions between these areas are also involved in the oddity task. However, this speculation will need to be tested directly.

These data contribute to a growing body of literature that suggests PNNs play an important role in cognitive function. PNN loss is associated with behavioral changes in several brain disorders (Pantazopoulos & Berretta, 2016), but relatively few studies have directly examined the effect of targeted PNN degradation on cognition. PNN degradation in the mPFC was recently shown to decrease the frequency of inhibitory currents onto mPFC pyramidal cells and impair cocaine-induced conditioned-place preference memory (Slaker et al., 2015). Consistent with our findings, PNN degradation was not associated with elevated network activity as indicated by the density of c-Fos+ cells, but the number of c-Fos+ cells ensheathed by a PNN

was decreased. These findings differ from the trend towards elevated c-Fos+ expression in PV+ inhibitory interneurons observed in our data. Elevated c-Fos in PV+ neurons is consistent, however, with recent data showing ChABC treatment in the anterior cingulate cortex increased the fast rhythmic activity of GABAergic interneurons (Steullet t al., 2014). Interestingly, PNN degradation by genetic knockout of the PNN component Cartilage-link-1 protein or with ChABC treatment into the perirhinal cortex enhanced object recognition (Romberg et al., 2013). Similarly, genetic depletion of Tenascin-R, a PNN component, improved performance in reversal learning and working memory paradigms (Morellini et al., 2010). In contrast, genetic knockout of Tenascin-C produced deficits in hippocampal-dependent contextual memory (Strekalova, 2002). These discrepancies may be explained by differences in the method and location of PNN manipulation, the memory task studied, and the time course of degradation and behavioral assessment. Memory impairment due to PNN disruption using ChABC depends on the timing of treatment in relation to memory formation. For example, removal of PNNs within the basolateral amygdala impairs conditioned fear memories but only if given prior to fear conditioning and extinction (Gogolla et al., 2009). Conversely, removal of PNNs within the basolateral amygdala impairs drug-associated memories, but only if given after memory formation but prior to extinction (Xue et al., 2014). Slaker et al. (2015) found that that WFA intensity after ChABC injection into the mPFC was reduced 3, 9, and 13 days following treatment but not at 30 days (Slaker et al., 2015), whereas PNN density was only significantly reduced 3 days post-injection and returned to control levels by 9 days. Conversely, our data shows that PNN density and WFA labelling intensity is still significantly reduced ~ 25 days post-injection. These differences might be explained by animal strain differences (Sprague Dawley vs Long-Evans rats in our study) or

injection volume (0.6 µl total volume vs. 0.6 µl/side in our study) as ChABC concentration used were similar (0.09 units/µl vs 0.1 units/µl in our study).

Functional Consequences of PNN Degradation

The effects of PNN degradation on neuronal structure and function are still poorly understood but can be considered in light of known PNN functions, including: (1) the regulation of GABAergic transmission, (2) restriction of neural plasticity, and (3) protection from oxidative stress and other environmental factors. PNNs are most frequently associated with PV+ fast-spiking GABAergic inhibitory interneurons. PV+ cells typically express the potassium channel KV3.1b, which is thought to give rise to their rapidly repolarizing action potentials. PNNs are thought to support these highly metabolically active neurons by acting as a buffers of excess cation changes in the local extracellular space (Härtig et al., 1999). The loss of PNNs has also been suggested to disrupt ion homeostasis and contribute to changes in functional activity of host neurons (e.g., hyperexcitability; Brückner et al., 1993). PNNs are important regulators of receptor function and localization on interneurons. During periods of elevated activity, synaptic glutamate AMPA receptors become desensitized and are exchanged for naïve receptors from the extrasynaptic pool (Heine et al., 2008). PNNs restrict this process, allowing for desensitization of synapses (Frischknecht et al., 2009). Degradation of PNNs might contribute to the hyper-excitability in neuronal cells that previously hosted PNNs. This is consistent with previous findings that ChABC treatment increases the firing rate of inhibitory interneurons (Dityatev et al., 2007; L. Liu et al., 2023). Our c-Fos immunolabeling did not conclusively identify increased immediate early gene activity in PV+ cells in ChABC-treated rats following the oddity task, but a comparison of the number of PV+ cells expressing c-Fos (relative to controls) approached statistical significance ($p = 0.054$).

PNNs also play a critical role in the regulation of neural plasticity, as evidenced by their role regulating critical periods of heightened plasticity during development (Sorg et al., 2016; Takesian & Hensch, 2013). Notably, PV upregulation denotes the onset of critical periods and the appearance of PNNs expression indicates the closure of critical periods (del Rio et al., 1994; Hensch, 2005; McRae et al., 2007; Takesian & Hensch, 2013). In maturity, the degradation of PNNs can re-open critical periods of elevated structural and functional plasticity (Gogolla et al., 2009; Pizzorusso et al., 2002). Moreover, genetic knockouts that disrupt PNNs (e.g. Cartilage-link protein 1) can permanently delay the closure of the critical period and maintain a juvenile state of elevated plasticity well into adulthood (Carulli et al., 2010). Outside of critical periods, PNNs maintain similar plasticity-restricting properties. The degradation of PNNs with microinjections of ChABC enhances spine dynamics in hippocampal pyramidal cells (Orlando et al., 2012). Similarly, injections of ChABC into the visual cortex of adult mice can enhance spine dynamics and contribute to long term functional synaptic plasticity (de Vivo et al., 2013; Pizzorusso et al., 2006). While digestion of PNNs in mPFC in our study was associated with varying degrees of impairment on cognitive tasks, we did not evaluate markers of neuroplasticity and it remains to be determined if CSPG digestion induced aberrant neuroplasticity that contributed to these deficits.

Finally, PNNs may be protective against oxidative stress and other pathological processes in CNS disease (Morawski et al., 2004; Suttkus, Morawski, et al., 2016). Fast-spiking PV+ interneurons are highly susceptible to oxidative stress and their association with PNNs is protective in immature and mature PV cells (Cabungcal et al., 2013; Suttkus et al., 2012) Suttkus et al., 2012). While it has not been directly demonstrated that PNN degradation in otherwise healthy animals results in oxidative stress injury, their loss may render neurons more susceptible

to insult or disease. A recent study analyzed numerous genetic and environmental animal models of schizophrenia and identified oxidative stress in PV+ interneurons as a common feature in 12 of 14 models evaluated (Steullet et al., 2017). PNN loss was also present in 12 out of 14 of those models. While we did not detect overt loss of PV+ interneurons, increased oxidative stress in PV+ cells after PNN digestion could contribute to altered cognitive performance.

PNNs in CNS Disease

Our findings contribute to a growing body of literature that implicates PNNs and their loss in the symptomatology of CNS disorders such as schizophrenia, epilepsy, and Alzheimer's (Baig et al., 2005; Berretta et al., 2015; Bitanihirwe & Woo, 2014; McRae & Porter, 2012; Okamoto et al., 1994; Pantazopoulos & Berretta, 2016; Pollock et al., 2014; Winship et al., 2018). Decreased PNN density in the prefrontal cortex, superior temporal cortex, and amygdala has been reported in post-mortem tissue from patients diagnosed with schizophrenia (Enwright et al., 2016; Mauney et al., 2013; Pantazopoulos et al., 2010). The loss of PNNs in the mPFC has also been recapitulated in animal models of schizophrenia (Paylor et al., 2016; Steullet et al., 2017). Our finding that PNN loss can disrupt performance on the CMOR task are of particular importance in this context, as polyI:C affected animals present with a CMOR deficit (Ballendine et al., 2015). In schizophrenia, disturbances to the inhibitory system have been reported, including loss of PV+ expression and GAD67, the GABA synthesis enzyme (Enwright et al., 2016; Glausier et al., 2014; Kimoto et al., 2014; Volk et al., 2000). CSPG digestions with ChABC did not induce significant changes in PV+ or GAD67+ fluorescence within PV+ cells. ChABC digestion induces a transient loss of CSPGs and PNNs, and it may be that altered PV and GAD67 expression in schizophrenia may results from chronic absence of PNNs around PV+ cells. Conversely, PNN decreases in schizophrenia may be the result of long term, developmental

dysregulation of PV+ cells which also disrupts the healthy expression of PV and GAD67. Similarly, we did not detect significant changes in the density of Gephyrin+ puncta, which can be used to identify the presynaptic terminals of inhibitory synapses in the CNS. This suggests that our ChABC injections did not grossly modify the number of inhibitory synapses. However, our measurements are only sensitive to a net gain or loss of inhibitory synaptic contacts, and not changes to the turnover rate. Previous studies using in vivo imaging have shown that ChABC can destabilize dendritic spines and increase their motility while not affecting the net number, length, or volume (de Vivo et al., 2013).

Conclusion

Our findings demonstrate that ChABC degrades PNNs and the interstitial matrix of the extracellular matrix in the mPFC. The loss of PNNs was associated with impairment in oddity object identification and object recognition memory. These findings contribute to growing body of literature suggesting that PNNs play an important role in healthy cognitive function and may have relevance for brain disorders (e.g., schizophrenia) where the pathology includes a loss of PNNs. While the mechanisms by which PNNs are reduced in these diseases is not well understood, interventions that target the loss of PNNs or stimulate their development could reduce cognitive impairment in neurodevelopmental or neurodegenerative diseases.

Figures

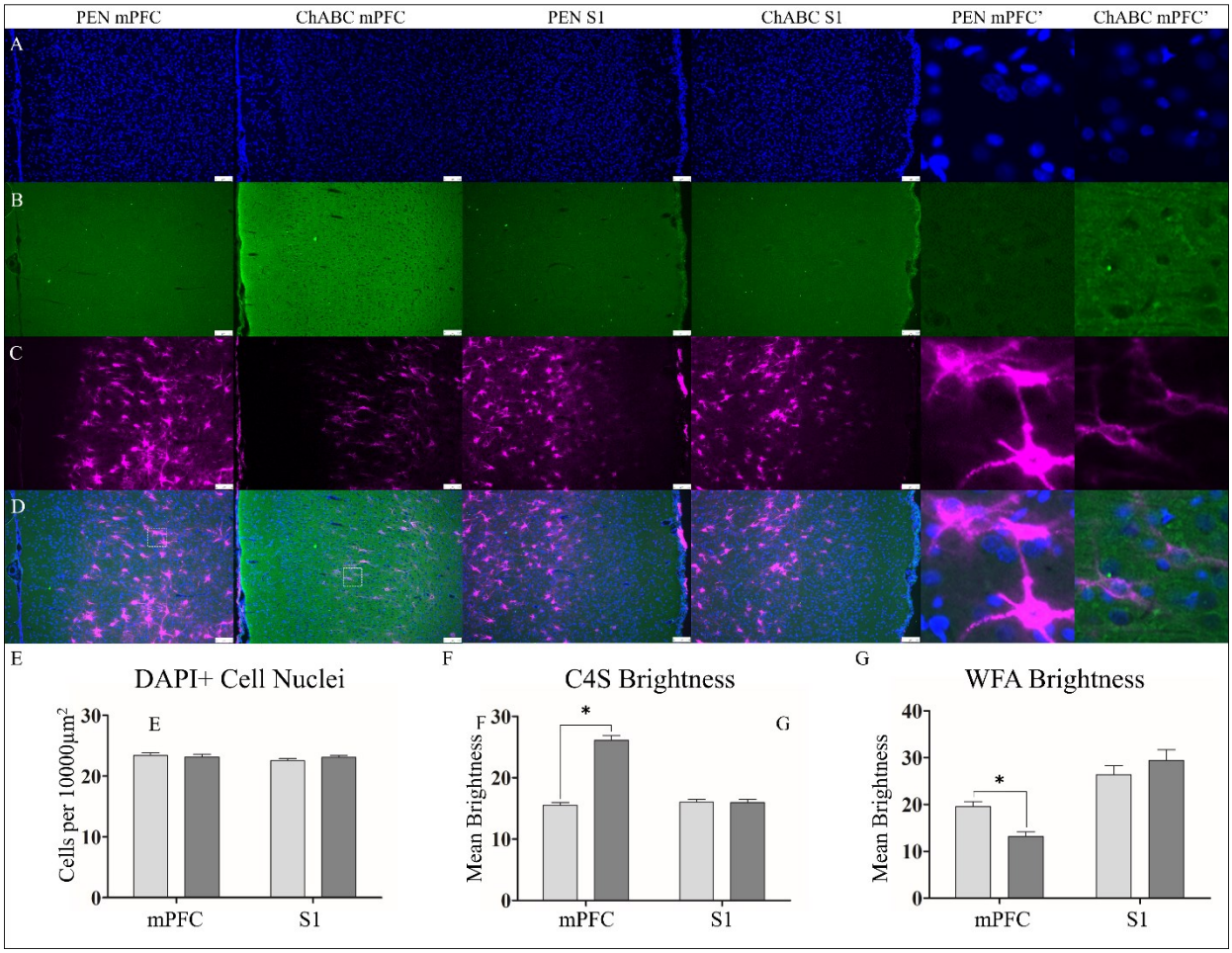
PEN mPFC
ChABC mPFC
PEN S1
ChABC S1
PEN mPFC'
ChABC mPFC'
A
B
C
D
E
DAPI+ Cell Nuclei
Cells per 10000µm²
mPFC
S1
F
C4S Brightness
Mean Brightness
*
G
WFA Brightness

Figure 3.1. ChABC treatment increases C4S staining for cleaved CSPG stubs and decreases WFA expression of the extracellular matrix. Representative images of DAPI (A), C4S (B), WFA (C), and merges images (D). Within the mPFC, PEN-treated and ChABC-treated animals had no difference in total cellular density (E). PEN animals had minimal expression of C4S for cleaved CSPG stubs but after ChABC treatment this significantly increased (F). There was also a significant reduction in WFA expression in ChABC treated animals (G). Similar analysis of the S1 (middle panels) of the same tissue slices from PEN-treated and ChABC-treated animals revealed no differences in C4S or WFA consistent with the localized injection and degradation we observed. Higher magnification images (left) images are 100x100 um (10000um^2) insets taken from white-lined boxes (D, left). Scale bar (white) is 100 microns. PEN, n=40; ChABC, n=40. * = $p < 0.05$

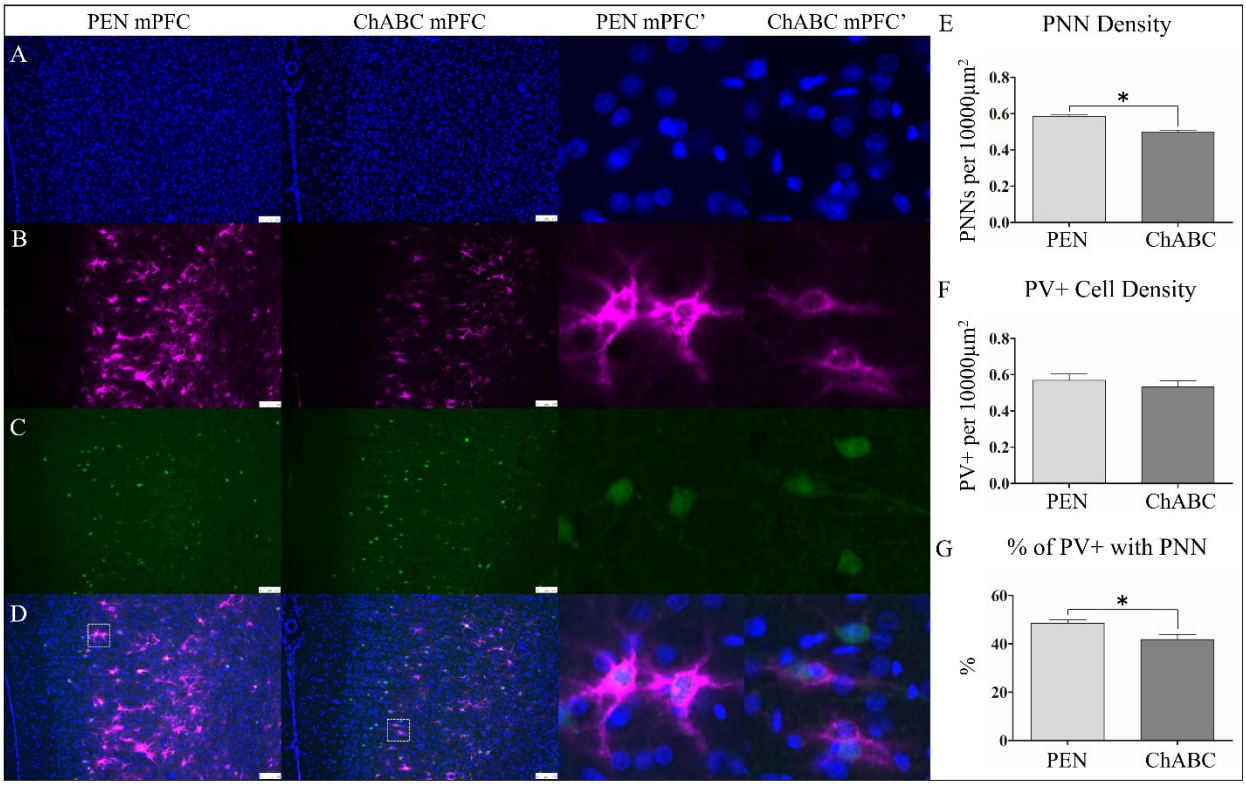
PEN mPFC
ChABC mPFC
PEN mPFC'
ChABC mPFC'
A
B
C
D
E
PNN Density
PNNs per 10000µm²
0.8
0.6
0.4
0.2
0.0
*
PEN
ChABC
F
PV+ Cell Density
PV+ per 10000µm²
0.8
0.6
0.4
0.2
0.0
PEN
ChABC
G
% of PV+ with PNN
%
60
40
20
0
*
PEN
ChABC

Figure 3.2. ChABC treatment reduced PNN density but did not affect PV+ interneurons. Representative images of DAPI (A), WFA (B), PV+ (C), and merges images (D). An examination of PNN density (E) showed that ChABC-treated animals had a significant reduction in PNNs. The density of PV+ interneurons was unchanged after PNN degradation (F). Higher magnification images (middle right) from the mPFC of PEN and ChABC showed that significantly less PV+ cells were surrounded by a PNN in ChABC treated animals (G). Higher magnification images are 100x100 um (10000um^2) insets taken from white-lined boxes (D, left). Scale bar (white) is 100 microns. PEN, n=40; ChABC, n=40. * = $p < 0.05$

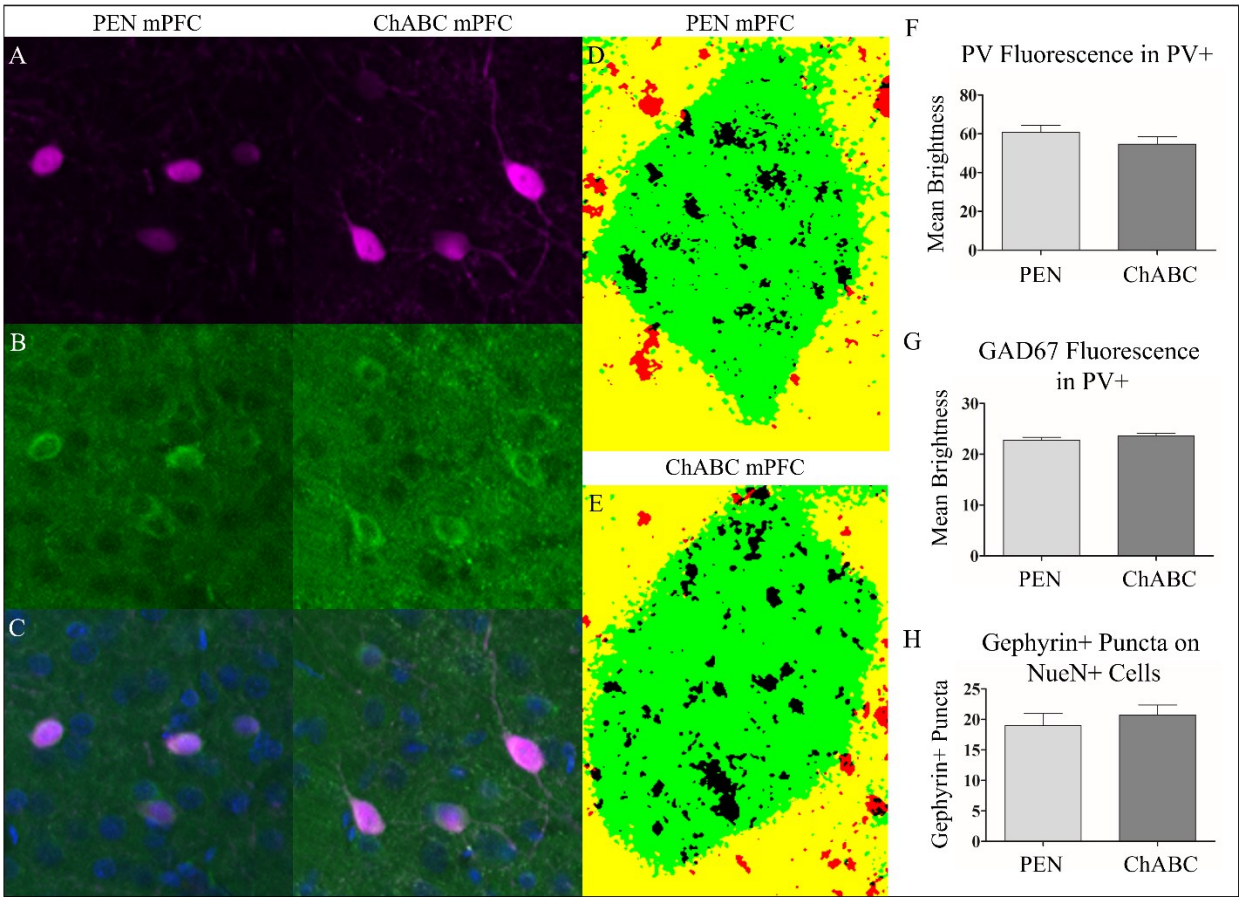
PEN mPFC
ChABC mPFC
PEN mPFC
A
B
C
D
ChABC mPFC
E
F
PV Fluorescence in PV+
Mean Brightness
80
60
40
20
0
PEN
ChABC
G
GAD67 Fluorescence in PV+
Mean Brightness
30
20
10
0
PEN
ChABC
H
Gephyrin+ Puncta on NueN+ Cells
Gephyrin+ Puncta
25
20
15
10
5
0
PEN
ChABC

Figure 3.3. Expression profile of PV+ cells is unaltered after ChABC treatment. To evaluate the effect of ChABC treatment on PV+ cells (A), we examined PV+ and GAD67+ (B), cell fluorescence (merged in C). Additionally, we examined the number of Gephryin+ puncta on neuronal cells labelled with NeuN (D,E; NeuN+ cell = green, colocalized Gephyrin+ puncta = black, puncta not colocalized with NeuN = red). ChABC treatment did not result in any change in PV+ fluorescence within PV+ cells (F). Similarly, GAD67+ expression in PV+ was not affected by ChABC. The number of Gephyrin+ puncta colocalized with NeuN+ cells was also unaffected by ChABC treatment. Images are 100x100 um (10000um^2) in size. PEN, n=16; ChABC, n=16. * = $p < 0.05$.

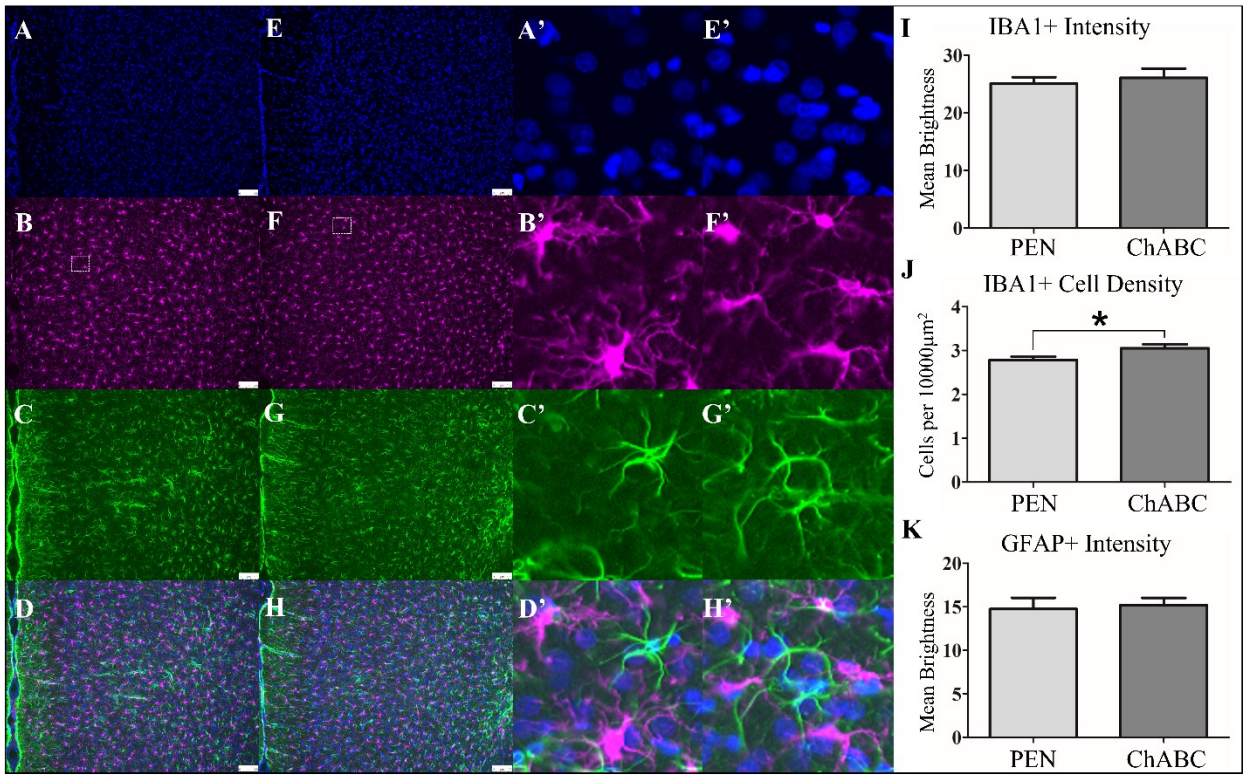
A
E
A'
E'
B
F
B'
F'
C
G
C'
G'
D
H
D'
H'
I
IBA1+ Intensity
Mean Brightness
30
20
10
0
PEN
ChABC
J
IBA1+ Cell Density
Cells per 10000μm²
4
3
2
1
0
*
PEN
ChABC
K
GFAP+ Intensity
Mean Brightness
20
15
10
5
0
PEN
ChABC

Figure 3.4. ChABC treatment increased microglial density but did not result in a robust immune response over PEN-treated control animals. Representative images are shown for DAPI (A), IBA1 (B), GFAP (C), and merged images (D). ChABC treatment did not result in overall changes in IBA1 staining intensity (C), but did cause a small but significant increase in IBA1+ cell density (D). Similar to IBA1, ChABC injection did not result in overt changes in GFAP staining intensity for astrocytes (E). Higher magnification images (middle right) are 100x100 um (10000um^2) insets taken from white-lined boxes (D, left). Scale bar (white) is 100 microns. * = $p < 0.05$ Scale bar (white) is 100 microns. PEN, n=16; ChABC, n=16. * = $p < 0.05$.

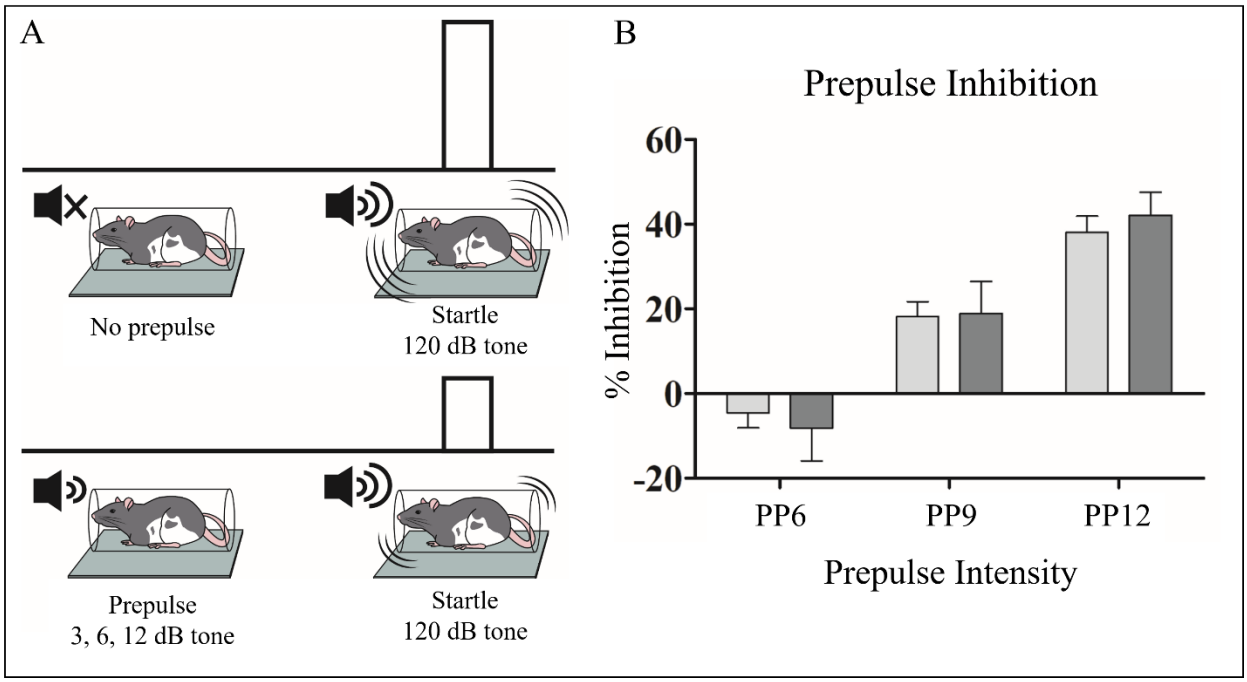
A
No prepulse
Startle
120 dB tone
Prepulse
3, 6, 12 dB tone
Startle
120 dB tone
B
Prepulse Inhibition
% Inhibition
60
40
20
0
-20
PP6
PP9
PP12
Prepulse Intensity

Figure 3.5. PNN degradation did not affect PPI. (A) Graphic representation of the behavioral assay. (B) Rats showed greater PPI for trials with increasingly loud prepulses. However, ChABC treatment did not affect PPI at any prepulse intensity. PEN, n=25; ChABC, n=24.

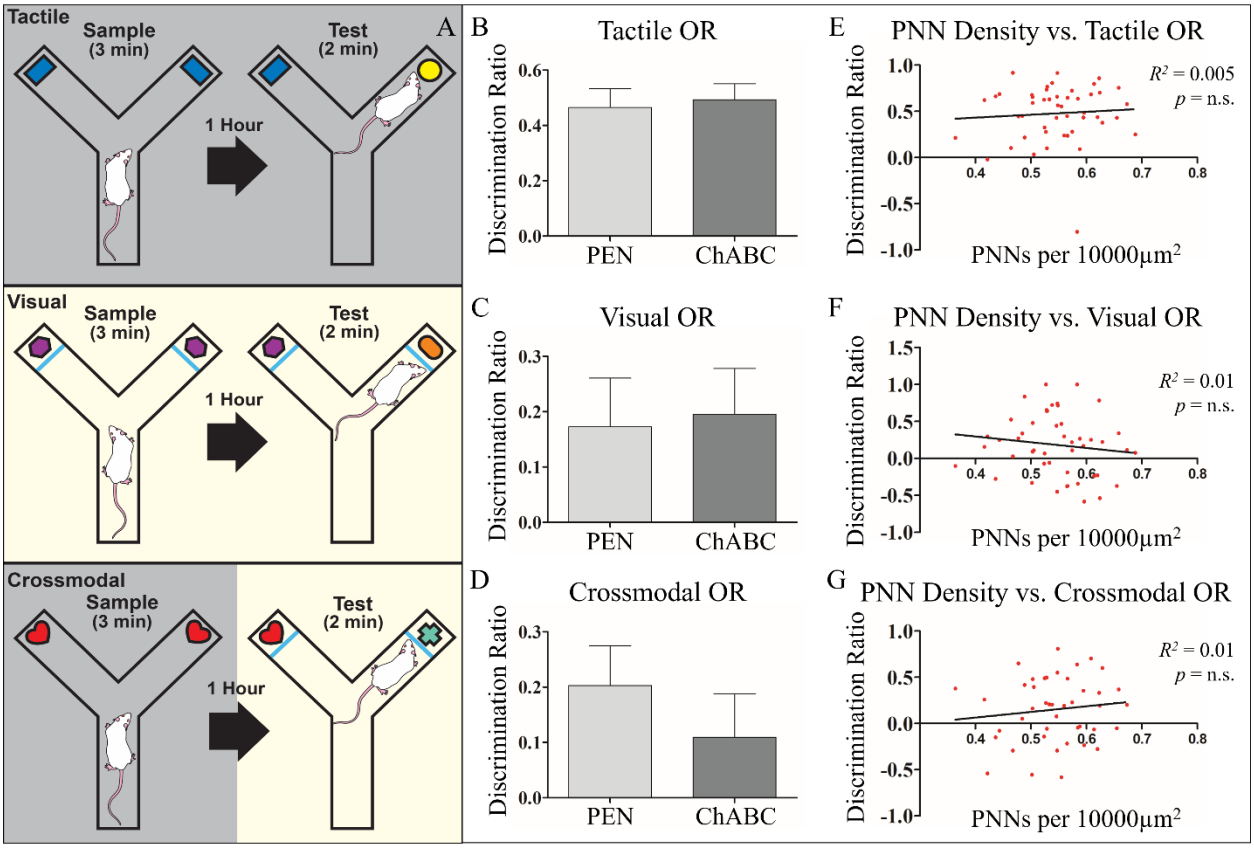
Tactile
Sample
(3 min)
Test
(2 min)
A
1 Hour
Visual
Sample
(3 min)
Test
(2 min)
1 Hour
Crossmodal
Sample
(3 min)
Test
(2 min)
1 Hour
B
Tactile OR
Discrimination Ratio
0.6
0.4
0.2
0.0
PEN
ChABC
C
Visual OR
Discrimination Ratio
0.3
0.2
0.1
0.0
PEN
ChABC
D
Crossmodal OR
Discrimination Ratio
0.3
0.2
0.1
0.0
PEN
ChABC
E
PNN Density vs. Tactile OR
Discrimination Ratio
1.0
0.5
0.0
-0.5
-1.0
0.4
0.5
0.6
0.7
0.8
R² = 0.005
p = n.s.
PNNs per 10000µm²
F
PNN Density vs. Visual OR
Discrimination Ratio
1.5
1.0
0.5
0.0
-0.5
-1.0
0.4
0.5
0.6
0.7
0.8
R² = 0.01
p = n.s.
PNNs per 10000µm²
G
PNN Density vs. Crossmodal OR
Discrimination Ratio
1.0
0.5
0.0
-0.5
-1.0
0.4
0.5
0.6
0.7
0.8
R² = 0.01
p = n.s.
PNNs per 10000µm²

Figure 3.6. PNN degradation resulted impaired cross-modal recognition memory. (A) Graphic illustration of the behavioral assay. To emphasize the tactile modality (top) in object recognition, the lights are turned off during the task to limit rat's ability to gather visual information about the object. In the visual phase (middle), the lights are on but the glass pane is positioned between the rat and the object, preventing them from gathering tactical information about the object. In the cross-modal phase (lower), animals are trained in one modality (e.g. tactile) and tested in the other (e.g. visual) to challenge integration across sensory modalities. ChABC treatment did not result in any changes in performance in tactile (B) or visual OR (C) and after ChABC treatment, animals still performed significantly better than chance. In the cross-modal OR (D) phase, animals treated with ChABC were not able to perform at better than chance levels whereas PEN treated animals were. Linear regression were conducted to determine the predictive value of animals performance on the task of their PNN density, but no relationship was observed for the tactile (E), visual (F), or cross-modal (G) components of the task. PEN, n=20; ChABC, n=23. * = $p < 0.05$.

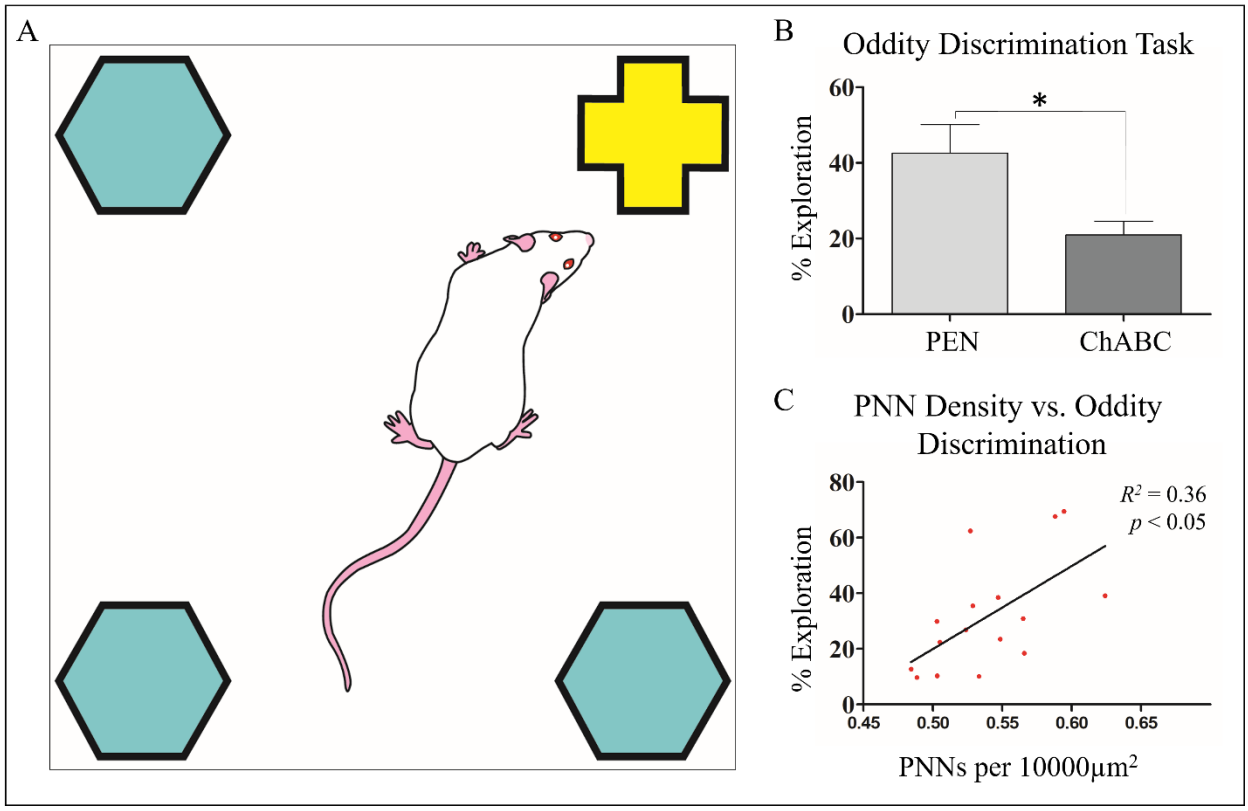
A
B
Oddity Discrimination Task
% Exploration
60
40
20
0
*
PEN
ChABC
C
PNN Density vs. Oddity Discrimination
% Exploration
80
60
40
20
0
$R^2 = 0.36$
$p < 0.05$
0.45
0.50
0.55
0.60
0.65
PNNs per 10000µm²

Figure 3.7. PNN degradation impaired performance on the oddity task and performance was predictive of PNN density. (A) Graphic illustration of the oddity task. Animals are presented with 4 objects, 3 of which are common and 1 of which is odd. (B) Animals treated with ChABC had a significant impairment in % exploration for the odd object compared to PEN animals. (C) Linear regression showed that animal's PNN density, irrespective of treatment group, was predictive of performance on the oddity task. PEN, n=8; ChABC, n=8. * = $p < 0.05$.

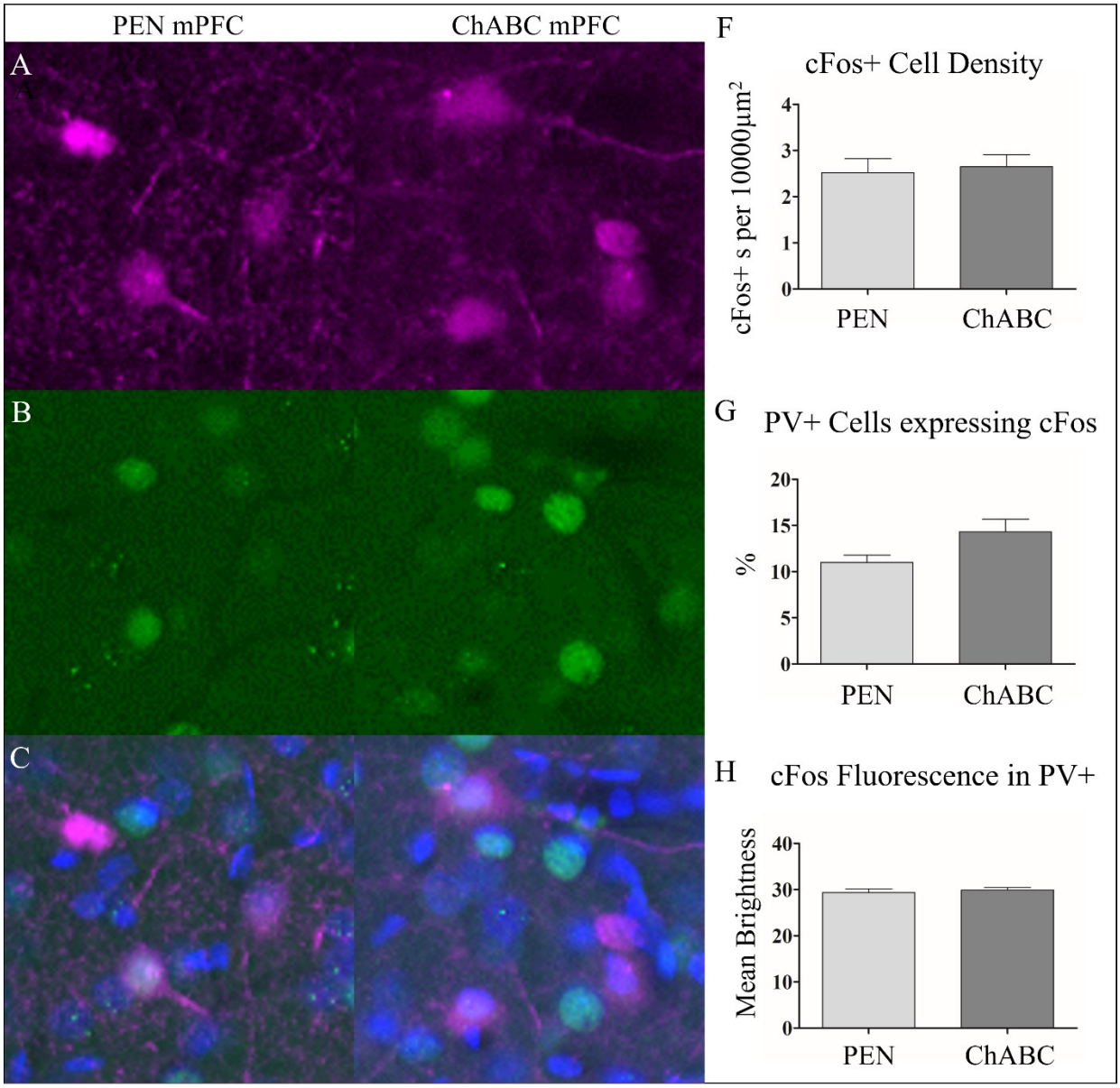
PEN mPFC
ChABC mPFC
A
B
C
F
cFos+ Cell Density
cFos+ s per 10000µm²
4
3
2
1
0
PEN
ChABC
G
PV+ Cells expressing cFos
%
20
15
10
5
0
PEN
ChABC
H
cFos Fluorescence in PV+
Mean Brightness
40
30
20
10
0
PEN
ChABC

Figure 3.8. PNN degradation did not alter the cFos activity in PV+ cells. To evaluate the effect of behavioural testing on cellular activity, we time-perfused (100-minutes) a subset (n=16) of animals after the oddity object experiment and examined c-Fos+ expression, a marker of heightened neuronal activity. Representative images for PV+ cells (A), c-Fos (B), and merged images (C). ChABC treatment did not result in a change in the total number of c-Fos+ cells within the mPFC, (F) it did however result in a slight increase in the number c-Fos+ colocalized with PV+, but this effect did not reach statistical significance (G). ChABC treatment did not affect c-Fos+ fluorescence within PV+ cells (H). Images are 100x100 um (10000um^2). PEN, n=8; ChABC, n=8. * = $p < 0.05$.

Chapter 4 – Comparing the impact of perineuronal net depletion in the medial prefrontal cortex or retrosplenial cortex on working memory performance and mesoscale brain activity

Abstract

Perineuronal net (PNNs) are organized extracellular matrices that surround mature neurons of the central nervous system (CNS) and help stabilize neuronal connectivity. The loss of PNNs because of injury or disease can result in aberrant synaptic connectivity and can disturb the contributions of host neurons, most often inhibitory interneurons, to local cortical networks. PNN loss in defined cortical regions can impact cognition and memory. These deficits are relevant for CNS diseases like schizophrenia, where PNN loss and cognitive impairment are both present. Here, we evaluated the impact of 30 days of PNN degradation in either of the medial prefrontal cortex (mPFC) or retrosplenial cortex (RSC) on several tasks involving working memory and utilize mesoscale imaging to evaluate broader cortical changes. We utilized an immune-evasive dual viral vector system, dox-i-ChABC, under the control of a doxycycline trigger to express chondroitinase ABC (ChABC) within the two target regions. PNN degradation in the medial prefrontal cortex was not associated with cognitive impairment in any task. Degradation of PNNs in retrosplenial cortex induced moderate impairment of object recognition memory in the crossmodal object recognition task. Interestingly, PNN degradation resulted in reduced parvalbumin+ interneurons density in the RSC. Wide-field optical imaging was used to evaluate broader changes in cortical connectivity after PNN degradation in the RSC. We found that cortical functional connectivity (spontaneous and sensory evoked) was largely unaltered but identified a significant decrease in power at low frequencies of activity in RSC. These data suggest that PNN degradation in RSC can impair performance in tests of working memory, potentially via the loss of parvalbumin+ interneurons and alterations in low frequency cortical activity. These findings encourage further investigation into the contributions that PNN loss makes to cognitive impairment and cortical interconnectivity, all of which are disturbed in CNS diseases like schizophrenia.

Introduction

Perineuronal nets (PNNs) are critical regulators of neuronal plasticity within the central nervous system (CNS). They restrict the capacity for host neurons to modify their neuronal connections, provide neuroprotection against reactive oxygen species and other stressors, and their presence stabilizes ongoing functional activity both locally and within larger cortical networks (Fawcett et al., 2019; Reichelt et al., 2019; Sorg et al., 2016; Wang & Fawcett, 2012). In recent years, numerous studies have highlighted the impact of CNS injuries and disease on PNN integrity within the brain. Post-mortem samples from patients who suffered from schizophrenia, bipolar disorder, epilepsy, multiple sclerosis, and Alzheimer's disease have shown to have PNN deficits (Alcaide et al., 2019; Baig et al., 2005; Berretta et al., 2015; Enwright et al., 2016; Gray et al., 2008; Kobayashi et al., 1989; Mauney et al., 2013; McRae & Porter, 2012; Steullet et al., 2018). Animal models utilized to study these disorders have also demonstrated that PNN loss is a common feature across a wide variety of models, even those with unique etiological origins (Crapser et al., 2020; Paylor et al., 2016; Steullet et al., 2017) . Given that PNN deficits appear as a common feature among numerous CNS diseases and their models, there is significant interest into how the loss of perineuronal nets impacts CNS function. More specifically, how the loss of PNNs impacts the activity of the cortex and how this in turn affects behaviour and cognition requires further exploration.

Studies evaluating the role of PNNs have typically utilized enzymatic degradation of their components, such as chondroitin sulfate proteoglycans (CSPGs), to evaluate the consequences of their loss. While endogenous enzymes like matrix metalloproteinases or a disintegrin with thrombospondin motifs (ADAMTSs) do exist, most commonly Chondroitinase-ABC (ChABC) which degrades the glycosaminoglycan side chains of CSPGs is administered. This treatment has

been broadly utilized in investigation of PNN depletion and in the context of CNS injuries or disease where CSPGs are frequently deposited. Degradation studies have provided immense insight into the importance of PNNs within the CNS. Functionally, PNNs are known to restrict synaptic turnover which limits the exchange of sensitized receptors for naïve ones (Frischknecht et al., 2009). They limit the motility of dendritic spines and when degraded, new spine formation is increased (Orlando et al., 2012). The presence of PNNs also supports the balance between excitatory and inhibitory spiking and contributes to ion homeostasis around highly active inhibitory interneurons (Lensjø et al., 2017). Within this balance, the degradation of PNNs reduces inhibitory activity and reverts cortical networks to a more juvenile, excited state. The depletion of PNNs can also alter inhibitory and excitatory inputs onto inhibitory cell types (Caroni, 2015; Donato et al., 2013; Fawcett et al., 2019; Takesian & Hensch, 2013). Despite these generalized phenomena, the functional consequences of PNN loss and reduced GABAergic inhibition are less clear and appear to vary by the region affected. For example, PNN depletion with chondroitinase ABC (ChABC) in the hippocampus can impair long term potentiation (LTP) and long term depression (LTD), but the same treatment administered to the perirhinal cortex enhances LTD (Lensjø et al., 2017). Other means of depleting PNNs such as genetic knockout of PNN components like brevican or neurocan have also demonstrated PNNs impact on neuronal transmission. In mice deficient in brevican, early-phase hippocampal LTP is impaired and in mice lacking neurocan, late-phase hippocampal LTP is impaired (Brakebusch et al., 2002; Zhou et al., 2001). The differences between these results are likely due to regional heterogeneity, as PNNs are not a homogenous structure nor are the cellular types they surround (Matthews et al., 2002; Ojima et al., 1998). Still, these studies demonstrate a clear impact of PNN degradation on synaptic transmission.

PNNs are most typically associated with parvalbumin positive (PV) inhibitory interneurons. Depending on the region examined, up to 70% of PV+ interneurons can be surrounded by a PNN (Enwright et al., 2016; Pantazopoulos et al., 2006). PV+ interneurons play important roles in aspects of neuronal transmission such as gain control, lateral inhibition, and pattern separation and they are the primary source of perisomatic inhibitory input on cortical neurons (Bartos & Elgueta, 2012; Carceller et al., 2020; Takesian & Hensch, 2013). On a larger scale, PV+ interneurons are essential to the generation of gamma oscillatory activity which is thought to contribute to sensory integration and feature-binding across broad brain domains (Lodge et al., 2009; Sohal et al., 2009). This rhythm is generated as the high-frequency action potentials of fast-spiking PV+ interneurons synchronize the activity pyramidal cells via inhibition (Kann et al., 2014). Interestingly, a prominent feature of EEG recordings from patients suffering from schizophrenia is disrupted gamma synchrony, and this is coincident with numerous reports of PV+ dysfunction and PNN loss in the post-mortem brain tissue of patients who suffered from the disease (Enwright et al., 2016; Gonzalez-Burgos & Lewis, 2012; Kilonzo et al., 2020; Mauney et al., 2013; Pantazopoulos et al., 2010; Steullet et al., 2018; Y. Sun et al., 2011). Similarly in animal models of SZ such as those induced by maternal immune activation, PNN loss and gamma asynchrony are both observed (Canetta et al., 2016; Dickerson et al., 2010; Jadi et al., 2016; Paylor et al., 2016). Notably, SZ and animal models of the disease also exhibit alterations at other frequency ranges, including theta and low frequency activity (Hunt et al., 2017; Speers & Bilkey, 2021; Uhlhaas et al., 2008). PV+ interneurons have been shown to contribute to activity within these frequency ranges as well (Christensen et al., 2021; Lensjø et al., 2017; Shi et al., 2019). Together, these studies demonstrate the broader cortical impact of PNN disruption and its impact on PV+ interneurons activity and implicate PNNs in

schizophrenia related dysfunction of PV+ interneurons, plasticity, and the inhibitory/excitatory balance of the cortex (Berretta et al., 2015; Bucher et al., 2021; Do et al., 2015; Lewis, 2014)

PNNs make contributions to both the ongoing functional and structural maintenance of brain function. Thus, it is not surprising that another means by which PNN disruption could impact broader cortical networks is through structural changes or cortical reorganization. PNNs are perhaps best studied for their role in critical periods of plasticity, within which unique cortical regions undergo significant remodeling in response to an external stimulus (Reh et al., 2020; Reichelt et al., 2019; Takesian & Hensch, 2013). This is readily demonstrated in the visual system, where in response to light, the visual cortex undergoes dramatic reorganization. The result of this remodeling is ocular dominance columns which are stabilized long-term at the closure of the critical window of plasticity. The degradation of PNNs, often achieved by application of an enzyme like ChABC, which cleaves apart PNN components, can reopen these critical windows of plasticity and allow for further remodeling of cortical tissue (Pizzorusso et al., 2002). Similar phenomena have been observed in the somatosensory cortex with the development of the barrel cortex, in the amygdala with the development of a mature fear extinction phenotype, and in CA1 of the hippocampus for episodic memory (Gogolla et al., 2009; McRae et al., 2007; Ramsaran et al., 2023). Another means to deplete PNNs is by preventing their formation via genetic knockouts of essential components such as chondroitin sulfate proteoglycans, hyaluronan, or link proteins. Two studies utilizing genetic knockouts of *Ctrl1* and *Acan* which encode for cartilage link protein and aggrecan, respectively, show that these knockouts attenuate PNN formation and that these animals display persistent ocular dominance plasticity and aberrant axonal sprouting in sensory pathways (Carulli et al., 2010; Rowlands et al., 2018). These studies demonstrate that PNNs are an important limiting factor on

structural plasticity, and that their presence supports stable, long-term organization of cortical tissues. Together, these findings, and those of abnormal brain activity where PNNs integrity is disrupted, clearly show that PNN loss can have deleterious effects within larger cortical areas and not just at the cellular or synaptic level. One further step would be to evaluate the impact of PNN loss on broader, brain-wide connectivity and communication. Diseases like schizophrenia which feature significant PNN loss also exhibit disturbances in the human 'connectome', which is the more comprehensive connectivity map of the human brain (Lavigne et al., 2022; MacKay et al., 2018; Narr & Leaver, 2015; Rubinov & Bullmore, 2013). These studies typically utilize broader mesoscale imaging techniques such as functional magnetic resonance imaging or diffusion tensor imaging. Despite their proven value in clinical investigations into diseases like schizophrenia, these techniques have not been readily utilized to investigate broader connectivity disruptions because of PNN loss.

PNN loss has demonstrated effects on cognition and behaviour. In CNS diseases, PNN deficits have been most widely reported in the post-mortem tissue of people who suffered from schizophrenia, which also presents with significant impairments in working memory (Enwright et al., 2016; Forbes et al., 2009; Lett et al., 2014; Mauney et al., 2013; Pantazopoulos et al., 2013; Pantazopoulos et al., 2010; Pietersen et al., 2014). The observation that PNNs are reduced in brain regions associated with the symptoms of the disease, such as disruptions of the prefrontal cortex and working memory impairments, suggest a link between PNN deficits and impairment (Euston et al., 2012; Paylor et al., 2018; Smucny et al., 2022; Yang et al., 2014). Animal models of schizophrenia support this suggestion. In a prominent maternal immune activation model of schizophrenia in rats, PNN development in the prefrontal cortex follows a typical trajectory until late adolescence or early adulthood, after which their growth plateaus

relative to healthy controls (Paylor et al., 2016). The timing of the emergence of a PNN deficit in the prefrontal cortex of these animals is paralleled by the development of working memory deficits (Ballendine et al., 2015; Howland et al., 2012; Wolff & Bilkey, 2008). Furthermore, direct injections of ChABC to degrade PNNs in prefrontal cortex of otherwise healthy animals impairs performance on novel object recognition tests of working memory (Paylor et al., 2018). Thus, direct PNN manipulation can impact working memory performance outside of the confounds of developmental models or disease. It also specifically implicates the mPFC, a region that is a significant locus for dysfunction in schizophrenia, in working memory impairments (Dienel et al., 2022; Glahn et al., 2005). Interestingly, PNN degradation does not always have consistent effects depending on the region affected. While working memory is impaired after degradation of PNNs in the mPFC, enzymatic attenuation of PNNs within the perirhinal cortex can enhance object recognition, as can brain-wide attenuation of aggrecan (Romberg et al., 2013; Rowlands et al., 2018). The diversity of effects on working memory after PNN degradation across unique brain regions are likely reflective of the distributed processing involved in a complex cognitive function. Support for this is eloquently shown in a recent study where bilateral inactivation in any of the mPFC, medial entorhinal cortex, anteromedial thalamic nucleus, and retrosplenial cortex can impair object recognition, but the same effect is not observed in the anterior cingulate cortex. Unilateral inactivation of any of these regions was insufficient to impair object recognition. However, when unilateral inactivation of the RSC was paired with inactivation of the perirhinal cortex, mPFC, medial entorhinal cortex, or anteromedial cortex in the contralateral hemisphere, object recognition was significantly impaired. The studies described here demonstrate that PNN disruption can have clear

consequences for cognition, but also highlight the need for a more comprehensive understanding of how PNN disruption can impact broader connectivity patterns.

In addition to the mPFC, the retrosplenial cortex (RSC) is an emerging region of interest in studies evaluating cognitive impairment such as is seen in schizophrenia. The RSC is a highly-interconnected, associative region of cortex that shares anatomical connections with the medial temporal lobe, parietal cortex, frontal cortical regions, the thalamus, as well as the hippocampus and hippocampal formation (Bluhm et al., 2009; Monko & Heilbronner, 2021; Morris et al., 1999; Vann et al., 2009). It has been identified as a part of the default-mode network, which is preferentially active when the host is not focused on their external environment (Buckner & DiNicola, 2019; Lu et al., 2012; Raichle, 2015; Raichle et al., 2001). Historically, studies of the RSC have focused largely on its role in spatial navigation and spatial working memory, but more recent reports have revealed much broader and more integrative functions (Mitchell et al., 2018; Troy Harker & Whishaw, 2004; Vann et al., 2009). For example, in the non-spatial Y-maze, an arena that lacks any major spatial cues, object recognition is impaired after inactivation of the RSC (de Landeta et al., 2021). This suggests that the contributions of the RSC to working memory are not only restricted to spatial tasks. In a broader context, a recent meta-analysis demonstrated that the RSC is one of several brain regions that comprise a core network involved in the processing of autobiographical memories, navigation, the theory of mind, and the default mode (Spreng et al., 2009). Connectivity studies indicate that communication between many of these regions, including the RSC, appear to be disturbed in schizophrenia and this might contribute to cognitive impairment in the disorder (Bluhm et al., 2009; Liang et al., 2006; Monko & Heilbronner, 2021; Whitfield-Gabrieli et al., 2009). Despite its potential significance for cognitive impairment in schizophrenia, there is limited research on PNNs in the RSC. In addition

to its described role in cognitive function, two other factors make this region of particular interest for study. Firstly, the RSC has by relative amounts one of the densest expression patterns of perineuronal nets in the cortex in rodents (Carceller et al., 2022; Seeger et al., 1994). This might indicate that PNN loss within the RSC because of pathophysiological processes or after targeted degradation could have significant impacts on its contributions to cognition. And secondly, the RSC's high degree of interconnectivity and anatomical position on the dorsal surface makes it an enticing target for mesoscale imaging techniques which can broadly evaluate connectivity patterns.

In the present study we sought to evaluate how working memory performance and brain activity as assessed by optical imaging were impacted by PNN degradation in either the mPFC or RSC. The healthy functioning of these two regions has been shown to contribute to cognitive tasks such as working memory, and both are regions of interest in disorders featuring cognitive impairment including schizophrenia. To deplete PNNs, we utilized an immune-evasive viral vector called dox-i-ChABC that expresses ChABC under the control of a dietary trigger. This design allowed us to degrade PNNs locally within the mPFC or RSC for a defined period. We subjected animals to a battery of behavioural assessments at three time points: baseline, after 1-month of ChABC expression, and again 1 month after ChABC had been withdrawn. Our data show that 30 days of PNN degradation within the RSC can have a subtle impact in performance on tests of working memory and reduce the density of PV+ interneurons. PNN degradation in the mPFC by contrast had no impact on cognitive performance of PV+ density. To determine the impact on cortical activity patterns, we used wide-field optical imaging to assess spontaneous and auditory evoked activity after 30 days of ChABC expression in the RSC. These data suggest that while broad functional connectivity of RSC during spontaneous or sensory evoked activity

was not significantly altered, there was a significant reduction in in the power of low frequency (i.e., slow wave) activity in the RSC during spontaneous activity. These findings encourage further investigation into how the microscale cellular consequences of PNN degradation translate into mesoscale alterations and broader cognitive impairments seen after PNN loss.

Methods

Subjects. All mice, total n = 77, were utilized from an on-site breeding colony at the University of Alberta. The behavioural experiments included a total of n = 66 animals, approximately 2-months of age, cross-bred from two genetic strains on a BL6 background: Thy1-GCaMP6S and Pvalb-tdTomato. These strains express an activity-dependent green fluorescent protein in Thy1+ neurons or red fluorescent protein (TdTomato) in PV+ interneurons, respectively. Breeding these lines together resulted in 4 unique strains of double-positive (PG), single positive for Thy1-GCaMP6S (G) or Pvalb-TdTomato (P) or expressing neither (WT). Cages of animals with mixed genotypes were randomly assigned to two groups: control (WT = 11, G = 14, P = 6, PG = 7), which included animals that received dox-i-ChABC injections but did not get the doxycycline diet ($Dox^{-}Virus^{+}$) and animals that had no dox-i-ChABC injections but did receive doxycycline diet ($Dox^{+}Virus^{-}$), and the ChABC group (WT =17, G = 12, P = 3, PG = 7), which received both dox-i-ChABC injections and doxycycline administration ($Dox^{+}Virus^{+}$). Animals that received dox-i-ChABC were also randomized to receive viral vector injections at one of two sites: mPFC (control, n = 17; dox, n = 14) or RSC (control, n = 10; dox, n = 18). Both male and female animals were utilized for these experiments (male, n = 27; female, n = 39). Animals were housed in ventilated plastic cages on a 12-hour light/dark cycle. The wide field optical imaging studies included a total of n = 10 adult B6(Thy1-GCaMP6s)4.3 mice. These mice express a genetically-encoded calcium indicator under the *Thy1* promoter (Dana et al., 2014). All the animals received

viral vector injections of dox-i-ChABC bilaterally over the RSC site and were randomly assigned to control (n = 5) or doxycycline (n = 6) dietary conditions. All procedures are conducted in accordance with the Canadian Council for Animal Care and are approved by the University of Alberta Health Sciences Laboratory Animal Services animal care and use committee.

Surgical Preparation. Animals were anesthetised at 4% isoflurane and kept on maintenance anesthesia for surgery between 2-2.5% isoflurane with pure oxygen as the carrier gas. Animals were head fixed on a stereotaxic injection frame and temperature was monitored and maintained at 37 $^{\circ}$C using an electric heating pad with feedback thermistor. Buprivicane (0.25%) was injected into the scalp prior to any surgical procedures. For viral vector injections, the scalp was incised along the dorsal surface of the brain to reveal bregma and the midline suture of the brain and the skull cleared with a scalpel. Burr holes were drilled bilaterally above the mPFC (ML = 0.5, AP = +1.7) or RSC (ML = 0.5, AP = -2.7) and a syringe attached mounted on a stereotaxic frame was inserted into the brain at a depth of 2.0 mm for mPFC injections and 1.0 mm for RSC injections. Viral vectors were injected over 5 minutes at a rate of 0.2 µl/minute (total volume 1.0 µl). The same procedure was the carried out in the opposing hemisphere at the same injection region. After the injection procedure was complete, the scalp was resealed using surgical sutures. For animals intended for wide-field optical imaging (n = 11), the same procedure was followed but a much larger section of scalp was fully removed to accommodate a 10 mm x 10 mm hexagonal glass coverslip. After these animals had received viral injections, a glass coverslip was secured to the skull and surrounding scalp tissue with clear dental cement (C&B – Metabond, Parkell Inc. Edgewood, NY, USA). After either surgical procedure, animals were given subcutaneous injections of buprenorphine (0.1 mg/kg) for pain management and placed in

a recovery cage. After surgical preparation, animals were given at least 5 days of recovery time prior to the start of behavioural assessments.

ChABC Expression. We utilized an immune-evasive dual lentiviral vector system, dox-i-ChABC, where ChABC expression is under control of a doxycycline inducible regulatory switch that utilizes a chimeric transactivator designed to evade T cell recognition (LV.PGK.GARrtTA + LV.TRE.ChABC; described in Burnside et al., 2018). The dox-i-ChABC system allowed us to exert temporal control over ChABC expression with a localized targeting within the cortex, whilst remaining largely immunologically inert. The doxycycline trigger is a broad-spectrum antibiotic that is widely available in clinical contexts and can be administered easily via animal's diet. During initial housing and breeding all animals were provided with ad libitum access to standard chow and water. For the behavioural experiments, after the first battery of baseline behavioural testing had been completed animals, chow was changed to either control (Control Diet, Bio-Serv) or doxycycline (Dox Diet, 200mg/kg, Bio-Serv) chow with ad libitum access for 30 days. After completion of the second behavioral testing session, the remaining available chow was removed, and all animals had access to control diet for an additional 30 days. For animals in the optical imaging experiment, they were switched onto either control or doxycycline diets after their first baseline imaging session had been completed, for a duration of 30 days.

Behavioural Testing. Animals underwent three batteries of behavioural testing that included assessments in the open field, oddity task, spontaneous alternation, and cross-modal object recognition. These sessions, including habituation and testing were spread across 7 days for each set of assessments at three time points: baseline, after 30 days of dietary treatment, and 30 days after the dietary regiment for both groups had been switched to control. The order of tasks for all

animals was as follows: open field, the oddity task, spontaneous alternation, visual object recognition, tactile object recognition, and finally crossmodal object recognition.

Open Field Assessments. The open field recordings were taken a square testing arena (40 x 40 x 15 cm) constructed of white corrugated plastic. Animals were placed in the testing arena for a singular 5-minute session and their behaviour recorded from fixed camera above the arena. Assessments of video recordings were completed in Matlab with the OptiMouse program from animal positional detection (Ben-Shaul, 2017). We made basic assessments of speed and distance travelled while in the arena. Additionally, we designed a basic assessment of anxiety behaviour in the rodents while performing the open field assessment. Mice will typically prefer to remain near walls or corners and in darker areas (lighting in our arena was consistent throughout all areas) of a testing apparatus and this effect is enhanced in mice with anxiety (Seibenhener & Wooten, 2015). To evaluate this parameter, we recorded time spent in the entire area (T_{arena}; 40x40 cm) and within the centre ($T_{centre;}$ 20x20cm) of the arena. We then calculated the percentage of time spent in the exterior of the arena with the formula: (T_{arena} - T_{centre}) / T_{arena} x 100.

Oddity Object Recognition. The oddity object discrimination test measure object perception using three copies of identical objects and a fourth 'odd' object. The testing apparatus was a square arena (40 cm x 40 cm x 15 cm) made of clear corrugated plastic with opaque white wallpaper. The objects could be fastened to any of the four corners of the arena. Mice had one day of habituation in the arena with no objects present for 5 minutes, after which the test day was conducted. On test day, three identical objects and one odd object were fastened to the four corners. Mice were placed in the maze and their behaviour recorded over 4 minutes using a video camera mounted to the ceiling. The location of the odd object within the arena was

counterbalanced among the mice in each treatment group. Object exploration times were hand scored by an investigator blind to the treatment status of the mice performing the task. Object exploration was assessed based on three criteria: the mouse' head must be oriented towards the object, within 2 cm of the object, and not actively grooming. Odd object preference was reported as a percentage ([T_{odd} / T_{tot}] x 100) of the total time exploring the odd object, where "T_{odd}" represents time spent exploring the odd object and "$\underline{T_{tot}}$" the total time spent exploring all four objects during the test trial.

Spontaneous Alternation. Spontaneous alternation performance was assessed using a symmetrical Y shaped maze composed of three arms with groove and wall (35L x 7W x 15H cm). Each animal was introduced into the center of the maze and allowed to explore freely for 5 min during which the acquisition of total number and pattern of arm entries were recorded using a video camera and analyzed. Assessments of video recordings were completed in Matlab with the OptiMouse program from animal positional detection (Ben-Shaul, 2017). Percentage of spontaneous alternation was calculated based on the number of triads "T_{not}" containing entries into all three arms divided by the maximum number of possible alternations (total arm entries minus 2, T_{na-2}) i.e., percentage of spontaneous alternation= T_{not} /(T_{na-2}).

Cross-modal Object Recognition. This task utilized spontaneous exploratory behaviour to assess visual and tactile memory, as well as visual-tactile sensory integration (Winters and Reid, 2010; Ballendine et al., 2015). Animals are placed into symmetrical Y shaped maze composed of a start arm and two object arms (35L x 7W x 15H cm). An opaque white plastic insert was used as a barrier between the start arm and the two object arms. In each of the object arms, an object could be fastened at the distal end of the arm and clear plastic inserts could be placed to prevent animals from interacting with the objects. The objects utilized were a mix of plastic animal

figures, rubber toys, and 3-D printed objects, all 6-8 cm in height. Mice were habituated for two 5-minute sessions, alternating the lighting between white light (for visual phases) and red light (for tactile phases). In the white light habituation session, clear plastic barriers were inserted in the object arms. No objects were present in the habituation sessions. These limitations prevent visual exploration of the objects under red light and prevent tactile exploration of the objects when the clear plastic barrier is present. After habituation, animals were subjected to tactile, visual, and crossmodal object recognition on separate, sequential days. Test days started with a 3-minute sample phase with two identical objects presents in the object arms of the Y-maze. After a 60-minute delay, the animals underwent a test phase with a third copy of the identical object and a novel object present in the object arms. The novel object and the novel object arm were counterbalanced across all animals. Mice began the experiment in the start arm, the door was open and closed once mice entered the object arms. The test phase was 2-minutes in duration. On the crossmodal testing day, tactile conditions (red light, no barriers) were utilized in the sample phase and visual conditions (white light, clear barriers) in the testing phase. Recognition memory was defined as significantly greater exploration of the novel object than the familiar object. Recordings were made from a camera fixed to a frame mounted above the arena and behaviour was manually scored by investigators blind to the treatment status of the mice and identity of the objects. Novel object preference was reported as a discrimination ratio (DR): $(t_{nov}-t_{fam)} / t_{tot}$, wherein "$t_{nov}$" represents time exploring the novel object during the testing phase, "t_{fam}" represents time exploring the familiar object, and "t_{tot}" represents total time spent exploring both objects over the course of the 2-minute trial.

Tissue Collection. Following the final behavioural testing session, mice were deeply anesthetized with isoflurane and perfused transcardially with PBC followed by a 4% paraformaldehyde

solution using infusion pumps. Brains were extracted and subsequent stored in 4% paraformaldehyde in a 4°C fridge. After two days, brains were transferred to a 30% sucrose solution for several days and then frozen in isopentane and optimal cutting temperature gel (OCT). Frozen brains were sectioned on a cryostat at 25 µm.

Immunohistochemistry. Slides were warmed to room temperature for 20 min and then given three washes in 1× PBS for 10 min each. After which slides were incubated for 1 h with 10% Protein Block, serum-free (Dako) in 1× PBS. Slides were then incubated overnight at room temperature with a primary antibody in a solution of 1% Protein Block, 1% bovine serum albumin, and 99.9% 1× PBS with 0.1% Triton X-100. Primary antibodies were as follows: mouse anti-chondroitin-4-sulfate (C4S; 1:400; Millipore), *Wisteria floribunda* agglutinin (WFA; 1:1000; Vector Labs), rabbit anti-parvalbumin (1:1000; Swant); rabbit anti-IBA1 (1:200; Dako); mouse anti-GFAP (1:200; Sigma-Aldrich). After overnight incubation, slides were washed three times, twice in 1× PBS with 1% Tween 20 and once in 1× PBS. Slides were then incubated for 1 h with secondary antibodies in antibody solution (as above). Secondary antibodies were as follows: streptavidin 647 (1:200; Invitrogen), donkey anti-mouse Alexa Fluor 488 (1:200; Invitrogen), donkey anti-rabbit Alexa Fluor 647 (1:200; Invitrogen), and donkey anti-mouse 647 (1:200; Invitrogen). After 1 h of incubation, slides were washed again three times and mounted with 4’,6-diamidino-2-phenylindole (DAPI) in Vectashield mounting medium (Vector Labs).

Epifluorescent Microscopy. Images were acquired using a Leica DMI6000B Microscope with LAS AF computer software. Regions of interest were identified using Allen Mouse Brain Atlas (Allen Reference Atlas – Mouse Brain. Available from atlas.brain-map.org) and selected based on landmarks in the DAPI nuclear staining pattern. The coordinates for each region were as follows: mPFC (+1.5 to +2.0 AP, 2.5 DV; with the imaging window aligned to the midline

and extending laterally through all cortical layers) and the RSC (-2.5 to -3.0 AP, 1.0 DV; with the imaging window aligned to the dorsal midline of the brain, extending laterally). RSC images were captured at 5X magnification and the mPFC at 10X. For each animal, a total of 4 images were taken bilaterally in adjacent sections. A constant gain, exposure, and light intensity was used across all animals for each region and stain.

Immunohistochemistry Quantification. Analysis was completed on unmodified images by an observer blind to the experimental condition of the tissue analyzed. For each region of interest, an imaging rectangle was drawn over the target area and the measurement area quantified for comparison. The region of interest was localized using DAPI immunolabeling. For all stains mean brightness within the measurement area was captured. We also visually inspected adjacent cortical areas and slices to determine the targeting of our injections. While this confirmed the selectivity of our treatment, animals in the ChABC group did show some elevated expression of C4S along the injection path through the motor cortex dorsal to the mPFC. In the RSC group some animals showed C4S expression in the adjacent secondary motor cortex and dorsal hippocampus. Cell counts for PV+ and IBA1+ cells were automated using the Image-based Tool for Counting Nuclei (Centre for Bio-image Informatics, UC Santa Barbara, CA, USA) plugin for NIH ImageJ software. PNN counts were conducted manually and identified based on an evaluation of three criteria: brightness, shape, and the presence of dendrites or an initial axon segment.

Statistical Analyses of Behaviour & Immunohistochemistry. All data are presented displaying mean ± SEM and individual data points. PRISM Software (Prism Software) and MATLAB (Mathworks, Natick, MA, USA), were utilized to conduct statistical analyses and significance was set at $p < 0.05$. Behavioural outcomes were evaluated using two-way repeated measures

ANOVAs were utilized to compare the effects of time (baseline, 30 day, 30-day post diet) and treatment group (control, ChABC) on performance across all animals. Given that the groups were expected to perform similarly on measures at baseline, we determined *a priori* to utilize one-sample t-tests against chance performance at the 30-day timepoint in the oddity preference task and crossmodal object recognition test. Such comparisons are frequently used in behavioural experiments to compare whether group performance differs from chance (Gervais et al., 2016; Jacklin et al., 2016). Otherwise, multiple comparison with Bonferroni's correction were only included where significant main effects were detected in an ANOVA. Two exclusion criteria were included: in the crossmodal task animals that did not explore each of the objects for a minimum of 3-seconds were excluded, and in the oddity task, animals that did not exceed 8s total exploration time were excluded from the analysis. The immunohistochemistry data was all generated from a single time point (30-days after the dietary trigger was withdrawn). Unpaired t-tests were utilized to compare between control and ChABC groups. Simple linear regressions were also included to compare animals' behavioural performance with immunohistochemical measures.

Wide Field Optical Imaging. Widefield optical fluorescence imaging was performed to measure cortical changes intracellular calcium as an indicator of neural activity. Calcium fluorescence data was collected from 12-bit images captured on a Teledyne DALSA (Waterloo, ON, Canada) 1M60 CCD camera and EPIX EL1 frame grabber with XCAP 3.8 imaging software (EPIX, Inc., Buffalo Grove IL). GCaMP6s was excited using a blue LED (Thor Labs (Newton, New Jersey, USA) M470L5) with an excitation filter (Thor Labs (Newton, New Jersey, USA) FB470-10). Images were captured with a macroscope composed of front-to-front lenses (10 mm x 10 mm

field of view) and calcium fluorescence was filtered using a Semrock (New York, NY, USA) Brightline FF01-525/30-25 green light emission filter housed in a 3D printed filter housing.

Spontaneous and Evoked Activity. Recordings of spontaneous and evoked activity were conducted in awake mice, head fixed on a treadmill. Animals were habituated to the apparatus twice, daily for 7 days prior to the baseline imaging session and 1-month imaging time point. Each animal underwent two imaging session: a baseline session after their surgical preparation and viral injection (with at least 10 days of recovery time and habituation to the imaging apparatus) but prior to change in diet administration (control or doxycycline), and a second imaging session after 30 days of ChABC expression. Spontaneous activity was recorded at 30 Hz for a total of 20 minutes. To reduce the impact of fluorescence signal distortions that are sometimes caused by large cortical blood vessels, we focused into the cortex at a depth of ~0.5 mm. For auditory-evoked activity recordings, data was collected at 30 Hz sampling rate. Auditory-evoked recordings consisted of 10s trials that were initiated every 20s, with the stimulus delivered 3s into each trial. Trials and stimulation were initiated using a signal from a Cambridge Electronic Design 1401 mk2 output board controlled by the software Spike2 (v6.18) (Cambridge, United Kingdom). Stimulation signals were generated using a Model 2100 Isolated Pulse Stimulator (AM Systems, Sequim, WA, USA). A 5 ms auditory stimulation was delivered using a broad-spectrum auditory signal from a computer speaker.

Data Analysis. Spontaneous recordings were subjected to bandpass filtering between 0.05-15 Hz, for the initial power spectrum analysis, or 0.5-5 Hz for all subsequent analyses. Areas outside the surgical preparation or off brain were masked out and recordings were processed with a global signal regression to remove global changes. Across the entire spontaneous recording, $\Delta F/F_{\circ}$ was calculated to determine relative changes in fluorescence. Regions of interest were designated by

5x5 pixel boxes with coordinates based on the Allen Mouse Brain Atlas. As our manipulation was bilateral, we expected the hemispheres to have similar values. To confirm this, we compared root mean square (RMS) values from both hemispheres for each condition using a two-way ANOVA with Bonferroni's Test to correct for multiple comparisons. There were no significant differences between ROIs. As such, we averaged left and right hemisphere RMS values together.

Seed pixel Correlation Maps. For each region of interest, we calculated correlation coefficients between the ROI pixel and every other pixel in the field of view, to show areas that are correlated in activity. To quantify functional connectivity within a local area, we calculated area specific thresholds based on the Allen Brain Atlas for the RSC at 4% of the brain area in the field of view. We then used that same threshold for the 30-day recordings for each mouse to determine percent area change in their seed pixel map. To confirm these effects were not specific to the threshold chosen we utilized one additional less-restrictive threshold of 10% to evaluate whether similar trends were observed in the data.

Statistical Analyses of Optical Imaging. For power spectrum analyses, we conducted a Wilcoxon rank-sum test for control and treatment groups between the frequency ranges of 0.1-1 Hz and 1.0-5.0 Hz. Standard deviations and correlations for spontaneous activity were calculated as relative change from the baseline to 1-month time point and probed with two-way ANOVAs with Bonferroni correction for multiple comparisons. Data from seed pixel maps and area under the curve calculations were compared with two-way repeated measures ANOVAs with Bonferroni multiple comparisons corrections. Amplitude and peak delay of auditory evoked responses were compared with paired t-tests of baseline and 1-month data for each condition.

Results

Animal Data. We evaluated animals' total weight and weight change over the course of the experiment. Weight change is reported firstly for the duration of the dietary regiment, and secondly for the total course of the experiment. Animals in both groups increased in weight (Control: $M = 2.532\text{g} \pm 0.195$; Dox: M=$2.716\text{g} \pm 0.326$) over the course of the 30-day diet regiment, but there was no significant difference in total weight change in either dietary condition ($t_{(63)} = 0.123$, $p = 0.902$). Second, we evaluated total weight change from the beginning of the experiment until animals were euthanized. Animals total weight increased over the total course of the experiment (Control: $M = 3.382\text{g} \pm 0.249$; Dox: $M = 3.326 \pm 0.301$) but there was no significant difference in weight change ($t_{(63)} = 0.146$, $p = 0.884$).

Open Field Assessments. To determine whether dox-i-ChABC treatment at either site might alter gross motor activity, we first tested animals' exploratory behaviour in an open-field arena (Figure 1A). Additionally, to evaluate whether PNN degradation had any effects on anxiety, we designed a basic assessment of animals' preference to remain in the perimeter area of an arena (Seibenhener & Wooten, 2015). Our measures of these constructs included total distance travelled and percentage of the time spent in the perimeter of the arena. A repeated-measures ANOVA on total distance travelled (Figure 1B, top left) revealed a significant main effect of time ($F_{(2, 70)} = 5.295$, $p = 0.008$) but no main effect of treatment and a non-significant interaction between time and treatment (Treatment: $F_{(1, 35)} = 1.978$, $p = 0.168$; Interaction: $F_{(2, 70)} = 0.058$, $p = 0.9430$). Post-hoc comparisons showed that control animals had a significant decrease in distance travelled from baseline to 60-days ($t_{(22)} = 2.691$, $p = 0.027$). Generally, the animals in both groups appeared to have slightly lower distances travelled across the experiment, which might be the result of repeated exposure to the task over the course of the experiment. As a measure of anxiety, we compared the two groups preference to stay in the 'exterior' zone of the

arena (near walls and corners) rather than to explore the interior of the arena (Figure 1B, bottom left). In this case, a two-way repeated measures ANOVA showed no main effects of time ($F_{(2, 70)}$ = 0.233, p = 0.756), treatment ($F_{(1, 35)}$ = 0.270, p = 0.566), and no significant interaction ($F_{(2, 70)}$ = 1.439, p = 0.244). These outcomes suggest that ChABC treatment within the mPFC had no impact on anxiety-related behaviours in the open field arena.

The same measures were performed in animals in the RSC cohort. First, we evaluated total distance travelled (Figure 1B, top right) with a repeated measures ANOVA that showed a main effect of time ($F_{(2, 64)}$ = 5.409, p = 0.009), but no main effect treatment ($F_{(1, 32)}$ = 1.587, p = 0.217), and no interaction between the two ($F_{(2, 64)}$ = 0.783, p = 0.461). Post-hoc comparisons between time points did not reveal any significant differences between time points in either of the groups. We then assessed animal's preference to explore the exterior more than the interior of the arena (Figure 1B, bottom right) as a basic test for anxiety. A repeated measures ANOVA showed a main effect of time ($F_{(2, 64)}$ = 8.022, p = 0.001). Post-hoc comparisons revealed that in ChABC treated animals, there was a significant increase from baseline to 60 days ($t_{(16)}$=4.623, p < 0.001). There was no main effect of treatment ($F_{(1, 32)}$ = 0.121, p = 0.731) and no interaction between time and treatment ($F_{(2, 64)}$ = 2.413, p = 0.098). These results suggest that after PNN degradation in the RSC and an additional 30 days without ChABC expression, anxiety-like behaviours in the open field arena increased.

Oddity Object Recognition. Our first test of working memory assessed whether PNN degradation impaired animals' ability to perceive and maintain representations of odd stimuli in their environment (Figure 2A). This test evaluates the preference for an 'odd' object among other objects that are identical to each other (Bartko et al., 2007). Previous work from our lab has

demonstrated a deficit in the performance of this task after PNN degradation with direct infusion of chABC into the mPFC (Paylor et al., 2018).

For this task, we measured total exploration time and oddity preference as a percentage. We first analyzed total exploration times for all four objects among for the mPFC cohort (Figure 2B, top left). A repeated measures ANOVA revealed a significant main effect of time ($F_{(2, 58)}$ = 7.336, p = 0.002), but post-hoc comparisons did not reveal any significant differences between time points for either control or ChABC animals. There was no main effect of treatment ($F_{(1, 29)}$ = 0.820, p = 0.3735) and no interaction between time and treatment ($F_{(2, 58)}$ = 2.651, p = 0.079) on total exploration time. We then compared the animal's preference for the odd object (Figure 2B, bottom left). A two-way repeated measures ANOVA showed no main effect of time ($F_{(2, 58)}$ = 1.963, p = 0.150), no main effect of treatment ($F_{(1, 29)}$ = 3.176, p = 0.085), and no interaction between time and treatment ($F_{(2, 58)}$ = 1.699, p = 0.191). A probe of the 30-day time point with a one sample t-test against chance showed that both control and ChABC animals performed significantly better than chance performance (CTRL: $t_{(21)}$ = 5.630, p < 0.0001; ChABC: $t_{(13)}$ = 4.637, p < 0.001). The absence of an effect after mPFC degradation stands in contrast to previous work from our laboratory demonstrating a deficit in this task after ChABC infusion into the medial prefrontal, although our prior study used rats rather than mice (Paylor et al., 2018).

We also analyzed animals with ChABC expression within the RSC on the oddity object preference task. An evaluation of total exploration times of all four objects (Figure 2B, top right) with a repeated measures ANOVA revealed no main effect of time ($F_{(2, 52)}$ = 0.538, p = 0.583) or treatment ($F_{(1, 26)}$ = 0.559, p = 0.461) on total exploration time, but we did observe a significant interaction between time and treatment ($F_{(2, 52)}$ = 4.519, p = 0.015). Post-hoc comparisons revealed a significant increase in total exploration time for ChABC animals compared to controls

at the 30-day time point ($t_{(26)}$=2.684, p = 0.042). This suggests that PNN degradation within the RSC may alter exploratory behaviour in this task. Next, we evaluated animals' preference for the odd object (Figure 2B, bottom right). A repeated measures ANOVA revealed a significant main effect of time ($F_{(2, 52)}$ = 5.254, p = 0.015), but no main effect of treatment ($F_{(1, 26)}$ = 2.813, p = 0.105), and no interaction between time and treatment ($F_{(2, 52)}$ = 3.065, p = 0.055). Post-hoc comparisons showed that control animals had a significant increase in oddity preference from baseline to 30 days ($t_{(13)}$ = 3.325, p = 0.010), whereas preference for the odd object in ChABC treated animals was not significantly greater at 30 days. We also probed the 30-day time point with one sample t-tests, which showed that both control and ChABC animals performed significantly better than chance performance (CTRL: $t_{(13)}$ = 10.90, p < 0.0001; ChABC: $t_{(13)}$ = 4.610, p < 0.001).

Spontaneous alternation. The second test we utilized to assess working memory performance after PNN degradation was a spontaneous alternation test. This test relies on animals' tendency to explore new environments. This is readily demonstrated in a Y-maze arena (Figure 3A), where animals exiting one of the three open arms will typically choose the less recently explored arm over the previous arm (d'Isa et al., 2021).

We assessed two primary outcomes from this test, both total arm entries and spontaneous alternation expressed as a percentage of total visits. First, to evaluate animals' exploratory activity we tested the total number of arm entries for animals with the mPFC cohort (Figure 3B, top left). This was reflected in a two-way repeated measures ANOVA that showed a significant main effect of time ($F_{(2, 52)}$ = 8.970, p = 0.001) on total number of arm entries. Post-hoc comparisons showed significant decreases in total arm entries for control animals at both 30 days and 60 days compared to baseline (30D: $t_{(22)}$ = 2.445, p = 0.046; 60D: $t_{(22)}$ = 6.538, p < 0.001).

While a similar trend was apparent in ChABC animals, arm entries were not significantly different at 30 or 60D. There was no main effect of treatment ($F_{(1, 26)} = 0.086$, $p = 0.772$) and no significant interaction of time and treatment on total arm entries ($F_{(2, 52)} = 0.294$, $p = 0.747$). Next, we evaluated differences in spontaneous alternation behaviour (Figure 3B, bottom left). A repeated measures ANOVA showed no main effect of time ($F_{(2, 50)} = 2.545$, $p = 0.092$) or treatment ($F_{(1, 25)} = 0.263$, $p = 0.613$), and no interaction between time and treatment ($F_{(2, 50)} = 1.508$, $p = 0.231$). Thus, PNN degradation within the mPFC had minimal impact on spontaneous alternation behaviour.

We next evaluated the same outcomes but for animals that had PNN degradation within the RSC. Again, total number of arm entries seemed to decrease over each of the three time points (Figure 3B, top right). A two-way repeated measure ANOVA showed a main effect of time ($F_{(2, 64)} = 8.242$, $p = 0.001$), but no main effect of treatment ($F_{(1, 32)} = 0.002$, $p = 0.958$), and no interaction between the two ($F_{(2, 64)} = 0.236$, $p = 0.791$). Post-hoc comparisons that in both control and ChABC animals, total arm entries decreased significantly from baseline to the 60-day time point (CTRL: $t_{(16)} = 3.047$, $p = 0.015$; ChABC: $t_{(16)} = 3.711$, $p = 0.004$).We then compared animal's percentage of spontaneous alternation (Figure 3B, bottom right). Both groups of animals exhibited a slight increase in spontaneous alternations across the course of the experiment. This was reflected in a two-way repeated measures ANOVA, which showed a main effect of time ($F_{(2, 64)} = 4.890$, $p = 0.012$) on spontaneous alternation, although post-hoc comparisons showed no differences between time points for either group. There was no main effect of treatment ($F_{(1, 32)} = 0.987$, $p = 0.328$) and no interaction ($F_{(2, 64)} = 2.389$, $p = 0.100$). Thus, PNN degradation within the RSC has no clear impact on spontaneous alternation behaviours.

Cross-modal Object Recognition. Our last test of working memory utilized the cross-modal object recognition task (Figure 4A). This specialized version of the novel object recognition task places further demand on working memory to integrate information across multiple sensory modalities (visual and tactile) which has been shown to be dependent on the function of the PFC (Ballendine et al., 2015; Winters & Reid, 2010). Previous data from our laboratory has demonstrated an impairment in this task after direct infusion of ChABC into the mPFC (Paylor et al., 2018). More recent evidence also indicates that the function of the RSC may contribute to this task as well (Gray et al., 2023; Hindley et al., 2014). Data below is included for testing in each of the three tests in the order that they were assessed (tactile, visual, crossmodal).

Tactile Object Recognition. In the tactile phase, red light conditions are utilized to minimize visual information gathered about the objects, but animals have unrestricted access to gather tactile information about the object. We first compare tactile exploration times for control and ChABC animals from the mPFC cohort (Table 1). A repeated measures ANOVA on time and treatment showed no main effect of time ($F_{(2, 42)} = 1.01$, $p = 0.367$), treatment ($F_{(1, 21)} = 0.265$, $p = 0.612$) and no interaction between time and treatment ($F_{(2, 42)} = 0.253$, $p = 0.778$) on tactile exploration. We next evaluated discrimination ratios for the tactile object recognition component of the task (Figure 4B, top left). A repeated measures ANOVA on time and treatment revealed no significant main effect of time ($F_{(2, 42)} = 0.167$, $p = 0.838$), treatment ($F_{(1, 21)} = 0.079$, $p = 0.780$), and no interaction between the two ($F_{(2, 42)} = 0.004$, $p = 0.996$). A one-sample t-test indicated that both control and ChABC groups performed significantly better than chance at discriminating the novel object (CTRL: $t_{(18)}=3.596$, $p = 0.002$; ChABC: $t_{(3)}=3.268$, $p = 0.047$). These results are consistent with previous work from our laboratory demonstrating that mPFC PNN degradation does not impair unimodal tactile object recognition (Paylor et al., 2018).

We next evaluated animals from the RSC group on their tactile object recognition. First, we compared mean exploration times for two groups with a repeated measures ANOVA on time and treatment (shown Table 1). There was main effect of time ($F_{(2, 52)} = 10.75$, $p < 0.001$) on mean exploration time, but no main effect of treatment ($F_{(1, 26)} = 1.314$, $p = 0.262$) and no interaction between the two ($F_{(2, 52)} = 1.875$, $p = 0.163$). Post-hoc comparisons showed a significant difference in control animals between baseline and both the 30-day and 60-day time points (30D: $t_{(12)} = 5.011$, $p < 0.001$; 60D, $t_{(12)} = 3.496$, $p = 0.009$). While this effect was more pronounced in control animals, both groups appeared to explore the objects more after 30 days and 60 days, relative to baseline, although this comparison was not significant across time points for ChABC animals. Next, we evaluated discrimination ratios for the tactile object recognition phase of the test (Figure 4B, top right). There was no significant main effect of time ($F_{(2, 52)} = 0.400$, $p = 0.670$) or treatment ($F_{(1, 26)} = 0.607$, $p = 0.443$), and no interaction between time and treatment on tactile discrimination ratios ($F_{(2, 52)} = 0.588$, $p = 0.559$). A one-sample t-tests indicated that both control and ChABC groups performed significantly better than chance at discriminating the novel object (CTRL: $t_{(12)}=5.812$, $p < 0.001$; ChABC: $t_{(14)}=3.846$, $p = 0.002$). This suggests that PNN degradation targeted to the RSC is not sufficient to impair performance on this unimodal, tactile object recognition task.

Visual Object Recognition. In the visual phase of the task, animals can gather visual information about the object but are prevented from gathering tactile information by a clear glass pane separating them from the object. First, we compared mean exploration times for animals in the mPFC cohort (all crossmodal task exploration times are shown in Table 1). A repeated-measures ANOVA on time and treatment group revealed a significant main effect of time ($F_{(2, 66)} = 4.434$, $p = 0.017$), but no main effect of treatment ($F_{(1, 33)} = 0.295$, $p = 0.590$) and no interaction

between the two ($F_{(2, 66)} = 0.478$, $p = 0.621$). Over the course of the experiment, both groups mean exploration times were reduced, but post-hoc comparisons revealed no significant differences between time points for either group. Next to test animal's unimodal, visual object recognition, we compared discrimination ratios for the novel object in the visual testing phase for the mPFC cohort (Figure 4B, middle left). A repeated measures ANOVA with time and treatment group as variables revealed no significant main effect of time ($F_{(2, 66)} = 1.988$, $p = 0.146$), treatment ($F_{(1, 33)} = 0.174$, $p = 0.678$), and no significant interaction between time and treatment ($F_{(2, 66)} = 0.751$, $p = 0.470$). We probed the 30-day time point with one-sample t-tests showed that both control and treatment groups performed significantly better than chance at discriminating for the novel object (CTRL: $t_{(20)} = 5.445$, $p < 0.001$; ChABC: $t_{(13)} = 2.893$, $p = 0.013$). These results are consistent with ones from previous work in our lab demonstrating that mPFC PNN digestion does not impair performance on this unimodal, visual object recognition component of the task (Paylor et al., 2018).

Next, we compared visual exploration times for animals the retrosplenial group (shown Table 1). A repeated measures ANOVA revealed a significant main effect of time ($F_{(2, 58)} = 6.020$, $p = 0.007$) and treatment ($F_{(1, 29)} = 4.78$, $p = 0.037$). There was no significant interaction between time and treatment on mean exploration time ($F_{(2, 58)} = 0.180$, $p = 0.836$). Post-hoc comparisons revealed that in ChABC animals, there was a significant increase in exploration times from baseline to 30 days ($t_{(16)} = 2.563$, $p = 0.042$) but there were no significant differences between treatment groups at any time point. We then evaluated animal's visual discrimination ratios during this phase of the test (Figure 4B, middle right). A repeated measures ANOVA on time and treatment showed no main effect of time ($F_{(2, 58)} = 0.051$, $p = 0.944$) or treatment ($F_{(1, 29)} = 0.025$, $p = 0.874$), and no interaction between time and treatment ($F_{(2, 58)} = 0.04$, $p = 0.960$) on

visual discrimination ratios for the RSC group. We probed the 30-day time point with one-sample t-tests which showed that both control and ChABC groups performed significantly better than chance at discriminating for the novel object (CTRL: $t_{(14)}$=5.133, $p < 0.001$; ChABC: $t_{(16)}$=3.943, $p = 0.001$).These outcomes indicate that PNN disruption within the RSC is not sufficient to disrupt unimodal visual object recognition. However, elevated exploration times in the ChABC group might indicate that PNN degradation had some other impact on exploratory behaviour in the visual phase of this task.

Crossmodal Object Recognition. First, we compare total exploration times for animals from the mPFC group (Table 1). A two-way ANOVA on time and treatment group revealed a significant main effect of time ($F_{(2, 62)} = 14.70$, $p < 0.0001$) and a significant main effect of treatment group ($F_{(1, 31)} = 8.06$, $p = 0.008$). There was no interaction between time and treatment group ($F_{(2, 62)} = 0.33$, $p = 0.720$). While there were no differences between treatment groups at any time point, post-hoc comparisons did show that both control and ChABC animals had significant decreases in exploration time from baseline to 60 days (CTRL: $t_{(18)} = 4.018$, $p = 0.002$; ChABC: $t_{(13)} = 2.687$, $p = 0.037$). Given the similar effect seen in both groups, this might be reflective of a decrease in interest in the task over repeated testing sessions or changes in performance of this task with age. Next, we evaluated crossmodal object recognition performance (Figure 4B, bottom left). A comparison of animal's discrimination ratios with a two-way repeated measures ANOVA showed a significant main effect of treatment group ($F_{(1, 31)} = 4.622$, $p = 0.040$), though ChABC animals had lower discrimination ratios at each of the three time points (including baseline). There was no significant main effect of time ($F_{(1, 31)} = 0.125$, $p = 0.8737$) and no significant interaction between time and treatment ($F_{(2, 62)} = 0.567$, $p = 0.570$). Post-hoc comparisons between treatment groups at each time point did not reveal any significant

differences. We probed the 30-day time point with one-sample t-tests against chance, which confirmed that neither control or ChABC animals performed better than chance (CTRL: $t(18)=1.783$, $p = 0.092$; DOX: $t(13)=1.106$, $p = 0.289$). These results are difficult to interpret given that both groups of animals appeared to perform the task poorly at all time points.

Next, we compared total exploration times for animals in the RSC group. A two-way ANOVA on time and treatment group revealed a significant main effect of time ($F_{(2, 58)} = 12.08$, $p < 0.001$) and a significant main effect of treatment ($F_{(1, 29)} = 4.98$, $p = 0.034$). There was no significant interaction between time and treatment on exploration times ($F(2, 58) = 1.11$, $p = 0.336$). While post-hoc comparisons did not reveal any significant differences between the groups at any of the three time points, both control and ChABC animals had increased exploration times after 30 days (CTRL: $t_{(15)} = 3.634$, $p = 0.005$; ChABC: $t_{(16)} = 3.477$, $p = 0.007$). The similarities here suggest that there might have been testing effects between sessions, which could be the result of repeated exposure to the testing arena or other factors that changed between sessions such as age. We next compared discrimination ratios for the RSC group (Figure 4B, bottom right). A two-way ANOVA on time and treatment group revealed no significant main effect of time ($F_{(2, 58)} = 1.046$, $p = 0.356$), treatment ($F_{(1, 29)} = 2.092$, $p = 0.159$), and no interaction between time and treatment group ($F_{(2, 58)} = 0.911$, $p = 0.408$) on animal's discrimination ratios. However, one-sample t-tests at 30 days suggest that ChABC animals' performance did not differ from chance performance ($t_{(14)}= 0.382$, $p = 0.708$), whereas control animals were significantly better than chance at discriminating the novel object ($t_{(15)}=2.823$, $p = 0.013$).

PNN Degradation and Behavioural Correlations. To assess the effectiveness of our dox-i-ChABC expression system to degrade PNNs, we stained animals' tissue with chondroitin-4-

sulfate (C4S), which labels the cleaved components of perineuronal nets after ChABC treatment, and with *wisteria floribunda agglutinin* (WFA), which is a widely utilized label for PNNs. We also labelled for parvalbumin-positive (PV+) inhibitory interneurons, which are closely associated with PNNs and present correlations of PNN counts and PV+ counts with certain behavioural outcomes. All staining measures are reflective of animal's tissue at the 60-day time point, after the full dietary regiment and behavioural testing was complete.

Findings from the mPFC cohort are shown in Figure 5. We observed an increase of 50.3% overall in the mean brightness of C4S labeling for the ChABC treatment group relative to control animals ($t_{(32)} = 3.615$, $p = 0.001$). As expected, we observed the opposite effect with number of PNNs, with a decrease of 27.2% in ChABC treated animals ($t_{(29)} = 2.891$, $p = 0.007$). There was no change in the number of PV+ interneurons ($t_{(22)} = 0.244$, $p = 0.809$). It is worth nothing that in the $Dox^{-}Virus^{+}$ control group, which received dox-i-ChABC injections but no doxycycline diet administration, there was still a faint but noticeable expression pattern of C4S near the injection site. This is likely due to some 'leakage' of ChABC expression which was noted in the original description of dox-i-ChABC (Burnside et al., 2018). A visual inspect of adjacent cortical areas and slices confirmed the targeting of our injections, although there were patterns of C4S expression along the injection path through dorsal portions of the motor cortex. We also evaluated correlations between behavioural outcomes and PNNs or PV+ interneurons. Linear regressions showed a positive relationship between crossmodal object recognition performance and PV+ counts, where performance increased with higher PV+ levels in the mPFC, but this effect was not significant. There was no relationship between PNN counts and performance on the crossmodal task (PNN: $R^2 = 0.008$, $p = 0.653$; PV+: $R^2 = 0.218$, $p = 0.051$). PNNs or PV+ interneurons within the mPFC did not have show any significant relationship with

performance on the oddity task (PNN: $R^2 = 0.044$, $p = 0.351$; PV+: $R^2 = 0.019$, $p = 0.621$). The lack of a relationship between PNN counts and oddity preference contrasts previous work from our lab which demonstrated a relationship between the two after targeted ChABC infusions into the mPFC in rats (Paylor et al., 2018). However, in the present study the relationship between PNNs and oddity preference was evaluated 30 days after the trigger for ChABC expression was withdrawn, whereas in the previous study this relationship was evaluated during active degradation. This difference might also be attributable to differences.

In the RSC, our immunostaining (Figure 6) showed that ChABC expression similarly resulted in a 43.5% increase in C4S labeling at the target area ($t_{(28)} = 2.263$, $p = 0.032$). These was also a 28.8% decrease in PNN counts within the RSC ($t_{(26)}=5.749$, $p < 0.001$). We also evaluated the presence of PV+ interneurons, which were significantly decreased (56.6%) in the RSC of the ChABC group ($t_{(19)} = 3.420$, $p = 0.003$). These results confirm the efficacy of dox-i-ChABC to degrade PNNs within either target area after doxycycline administration. They also suggest that the relationship between PNN degradation and the impact on PV+ interneurons can vary by the region affected. In addition to these measures, we visually inspected adjacent cortical areas and slices to confirm the targeting of our injections. Next, we considered correlations between behavioural performance on immunolabeling for the retrosplenial cohort. There was no significant relationship between crossmodal performance and either of PNN counts or PV+ interneurons (PNN: $R^2 = 0.022$, $p = 0.467$; PV+: $R^2 = 0.095$, $p = 0.186$). Similarly, there was no relationship between PNN counts or PV+ interneurons and oddity performance (PNN: $R^2 = 0.133$, $p = 0.073$; PV+: $R^2 = 0.002$, $p = 0.844$.

Inflammatory Markers. As the dox-i-ChABC vector is supposed to be immune-inert, we also evaluated two inflammatory markers, IBA1 for microglia and GFAP for astrocytes, to assess the

impact of inflammation in animals. Qualitatively, we did not observe consistent signs of overt inflammation reflected in either IBA1 or GFAP labelling at either cortical site. Within the mPFC (Figure 7) a comparison of IBA1+ staining intensity did not reveal any significant differences between ChABC and control animals ($t_{(30)} = 0.134$, $p = 0.124$). A closer inspection of IBA1+ positive microglia in both treatment groups also appeared to show similar morphology. There were also no observable differences in GFAP labeling ($t_{(26)}=1.216$, $p = 0.540$). Similarly, in the RSC group (Figure 8) we did not detect any significant changes in IBA1+ cell counts ($t_{(25)}=1.473$, $p = 0.337$), and IBA1+ microglia appeared to show similarly ramified, morphological states on visual inspection. A comparison of GFAP mean brightness in the RSC did not reveal a significant change between the two groups ($t_{(25)} = 1.869$, $p = 0.079$). These results indicate that our ChABC expression system did not result in ongoing inflammatory activity.

Spontaneous Activity. First, we conducted a power spectrum analysis of activity from the RSC for control and treatment groups (Figure 9B). We looked specifically at two frequency bands: 0.1-1.0 Hz and 1.0-5.0 Hz. A Wilcoxon rank-sum test showed that ChABC animals had decreased power from baseline within the slow wave frequency range (0.1-1.0 Hz), $z = 5.39$, $p < 0.001$ with a medium effect size ($r = 0.34$) and in the delta frequency range (1.0-5.0 Hz), $z = 2.19$, $p = 0.028$ with a small effect size ($r = 0.08$). In comparison, control animals had similar power values in the slow wave frequency range ($\underline{z} = 0.72$, $p = 0.47$) and the delta frequency band ($z = 1.81$, $p = 0.069$). These results indicate that PNN degradation resulted in a decrease in the power of low frequency activity within the RSC. We also evaluated RMS values as a measure of changes in activity over the time course of spontaneous activity (Figure 9C). We compared change in RMS from baseline to the 1-month time point for both groups. A repeated measures

ANOVA of treatment group and cortical area revealed a main effect of cortical area ($F_{(17, 144)}$ = 1.865, p = 0.026) but no main effect of ChABC ($F_{(1, 144)}$ = 1.647, p = 0.202) and no interaction between the two ($F_{(17, 144)}$ = 0.769, p = 0.727). Post-hoc comparisons did not reveal any significant differences between control and ChABC treated animals in any of the ROIs.

Correlations Between RSC & Other Cortical Areas. To probe the connectivity between the RSC in each hemisphere with other cortical areas, we evaluated correlations between their activity (Figure 10A, B). First, we probed change in correlated activity between the RSC and ipsilateral cortical areas (Figure 10A, bottom), where a two-way ANOVA showed no significant main effect of cortical area ($F_{(15, 128)}$ = 1.656, p = 0.068), treatment ($F_{(1, 128)}$ = 2.260, p = 0.135) and no interaction ($F_{(15, 128)}$ = 0.650, p = 0.829). Comparing changes in correlated activity between the RSC and contralateral areas (Figure 10B, bottom) showed a main effect of cortical area ($F_{(15, 128)}$ = 2.050, p = 0.014), but no main effect of treatment ($F_{(1, 128)}$ = 0.283, p = 0.595) and no interaction between area and treatment ($F_{(15, 128)}$ = 0.92, p = 0.545). These results suggest that PNN degradation within the RSC did not result in significant changes in interconnectivity between cortical areas.

Seed Pixel Analysis. To evaluate common activation with the RSC, we conducted a seed pixel analysis by calculating correlation coefficients between the region of interest pixel and every other brain pixel in the field of view. A two-way repeated measures ANOVA examining the effects of time and treatment on RSC seed pixel maps (Figure 11B, left) showed no main effect of time (F(1, 8) = 2.370, p = 0.163), treatment ($F_{(1, 8)}$ = 0.40, p = 0.544), and no interaction between the two ($F_{(1, 8)}$ = 0.15, p = 0.709). To further corroborate these results and confirm the effect was not specific to the threshold chosen, we tested a less restrictive threshold for establishing a retrosplenial seed pixel (Figure 11B, right). Here, a two-way repeated measures

ANOVA revealed a main effect of time ($F_{(1, 8)} = 6.180$, $p = 0.038$), but no main effect of treatment ($F_{(1, 8)} = 0.020$, $p = 0.885$) and no interaction ($F_{(1, 8)} = 0.060$, $p = 0.807$). Post-hoc comparisons at between time points of either group did not reveal significant differences.

Auditory-Evoked Activity. We evaluated sensory-evoked activity after presentation of an auditory stimulus to evaluate whether PNN degradation might alter sensory processing. First, we analyzed the time-course of activation (Figure 12A) in the auditory cortex of the contralateral hemisphere by assessing peak response amplitude and peak response delay. We utilized paired t-tests to compare each condition from baseline to 1-month. Neither control or ChABC groups showed significant changes between the two time points on peak amplitude (Figure 12B, top; CTRL: $t_{(4)}$=0.061, $p = 0.953$; DOX: $t_{(5)}$=0.258, $p = 0.807$) or peak delay (Figure 12B, middle; CTRL: $t_{(4)}$=0.466, $p = 0.666$; DOX: $t_{(5)}$=0.791, $p = 0.465$). To further evaluate the neural response to the auditory stimulus, we conducted an area under the curve calculation of the activation time course for 15 ms after the stimulus was presented (Figure 12B, bottom). A two-way repeated measures ANOVA for the contralateral hemisphere showed no main effect of time ($F_{(1, 9)} = 0.030$, $p = 0.868$) or treatment ($F_{(1, 9)} = 0.000$, $p = 0.949$), and no interaction between the two ($F_{(1, 9)} = 0.000$, p = 0.973). These results indicate that PNN degradation within the RSC did not have an impact on the evoked activity of the auditory cortex after the presentation of an auditory stimulus.

Discussion

Here, we evaluated whether PNN degradation in the mPFC or RSC would impact performance on several assessments of working memory and utilized optical imaging to evaluate changes in cortical activity and connectivity after their focal disruption. By using viral vectors to express ChABC under the control of a dietary trigger, we allowed for behavioural assessments at

baseline, after 30 days of ChABC expression, and at a final 60-day time point, 30 days after ChABC had been withdrawn. Only in the RSC degradation group did we detect any cognitive changes, with a moderate deficit after 30 days of ChABC expression on the crossmodal object recognition. These moderate deficits are somewhat surprising given the role of the RSC in cognition and immunohistological data that confirmed that our dox-i-ChABC viral vector for ChABC expression was effective at reducing PNNs and showed a decrease in PV+ interneurons the RSC after ChABC expression. Furthermore, we showed using wide-field optical imaging of calcium fluorescence that PNN degradation within the RSC decreased the power of low frequency activity generated from the RSC but did not alter other measures of overt activity or connectivity.

Our findings suggest that PNN degradation within either the mPFC or RSC had no impact on locomotor or exploratory activity within the open field. Despite the well-described role of the RSC in spatial cognition we did not expect to see differences in open field behaviour, although studies of the impact of RSC manipulations on open field behaviour are limited. While outright lesions of the RSC have been shown to impact spontaneous alternation behaviours, these deficits are dependent on additional conditions placed on the task (Cooper & Mizumori, 1999). A consensus is that the RSC is involved in more complex aspects of spatial cognition (Alexander et al., 2023; Miller et al., 2014; Mitchell et al., 2018). Spatial tasks such as those that involve spatial memory, allocentric cue processing or cue-switching, and object location memory have all been shown to be impaired by RSC manipulations (Chen et al., 1994; Pothuizen et al., 2008, 2010). Another example can be drawn from spatial alternation tasks, where simpler forms of the task do not appear sensitive to manipulations of the RSC, but more complex ones which involve additional conditions placed on the task do (Pothuizen et al., 2008). Previous studies utilizing

genetic knockouts of PNN components, such as tenascin or brevican, have shown impairment in spatial memory tasks, including spontaneous alternation (Favuzzi et al., 2017; Montag-Sallaz & Montag, 2003; Stamenkovic et al., 2017). However, these knockouts result in far more global deficits in the formation of the PNNs throughout the brain compared to the more focal degradation utilized here. Given this, the fact that spontaneous alternation is unaltered after PNN degradation at either site is not surprising. We did however observe an increase in the time spent in the perimeter of the arena in animals treated with ChABC at the 60-day time point. While this result is interesting, we would exercise caution in its interpretation. A wide variety of studies have demonstrated that the use of anxiolytic or anxiogenic compounds within the open field assessment utilized here fail to produce predictable results and it is considered best suited for only locomotor and exploratory assessments (Himanshu et al., 2020; Prut & Belzung, 2003).

In the RSC cohort, ChABC animals were unable to perform the crossmodal object recognition task at above chance levels after 30 days of ChABC treatment (whereas controls were significantly better than chance). However, we would note that in our study ChABC animals also showed elevated exploration times in the visual and crossmodal phases of this task, which might indicate that the change in performance on this task was driven by factors other than working memory alone. While the impairment we observed was subtle, this result is consistent with a previous study showing that lesions of the RSC in rats can impact performance on this task (Hindley et al., 2014). Another report from primates indicates that during aging, PNNs surrounding PV+ cells decrease and this decline in PNNs is correlated with poorer performance in object recognition tasks (Gray et al., 2023). Together, these results indicate that the RSC could have a role in working memory beyond just its well-described role in spatial working memory. Interestingly, lesions of the RSC do not affect performance on standard versions of the

spontaneous object recognition task (Ennaceur et al., 1997; Vann & Aggleton, 2002). Manipulations of the RSC shown here, as well as in Hindley et al., (2014) also indicate that unimodal tactile and visual object recognition are spared. These common results indicate that RSC contributes specifically to the cross-modal aspect of this task, which challenges working memory to integrate sensory information from multiple modalities. However, we encourage further replication of this finding to better validate RSC involvement in the crossmodal task.

One function of the RSC that may be involved in crossmodal object recognition is feature binding. Feature binding is the process by which the different attributes or characteristics of an object, which can be drawn from a wide variety of sensory modalities, are integrated. In the crossmodal task, that process is challenged during the crossmodal phase of the test, which requires visual-tactile integration about the features of an object for successful object recognition. Typically, the RSC has thought to play a role in location-based contributions to feature binding, such as is demonstrated in the object-in-place task, though the present data suggests that it's role could be less restricted than previously thought (Aggleton & Nelson, 2020; Vann & Aggleton, 2002) . Further examination of the role of PNN degradation within the RSC in other tasks that depend on feature binding, such as the those evaluating object recency, or object location, would be informative in better describing its role in this process.

A consideration of the connectivity of the RSC is also worthwhile when interpreting our results. While the bulk of connections within the RSC are thought to originate within the RSC itself, it also features a broad network of connectivity with both cortical and subcortical structures (Kobayashi & Amaral, 2003; Mitchell et al., 2018). Notable among this network is connections with areas involved in object recognition and working memory. The RSC is known to share strong reciprocal communication with the parahippocampal region. This region of the

brain, particularly the perirhinal cortex, have shown to have a clear involvement in the crossmodal object recognition task (Inhoff & Ranganath, 2015; Taylor et al., 2006; Winters & Reid, 2010). Similarly, the RSC shares prominent reciprocal connections with the frontal cortex which has a demonstrated involvement in crossmodal object recognition (Amedi et al., 2005; Reid et al., 2014). Given the highly interconnected nature of the RSC and the fact that PNN disruption can alter inhibitory activity patterns, the impairment observed here could also be mediated by altered signaling to other areas involved in working memory or feature binding (Dzyubenko et al., 2021). Another anatomical consideration is the high degree of connectivity of the RSC and other regions of the brain thought to be involved in spatial navigation and spatial memory, such as the hippocampus and secondary motor cortex. While the crossmodal and oddity tasks are not intended to challenge spatial memory, the presence of altered explorations times for animals with PNN degradation in the present study indicate that observed deficits may not be driven solely by working memory impairments.

A third consideration for the observed deficits here is cellular consequences of PNN degradation. The obvious consequences in our data were a significant loss of PV+ interneurons present within the RSC after ChABC treatment. This deficit was quite striking and stands in contrast to previous studies demonstrating that PNN degradation can have consequences for PV+ cell activity and expression but typically does not result in outright cell loss. However, most studies investigating the impact of PNN degradation on PV+ cells typically utilize single administrations of ChABC. Here we utilized prolonged expression over 30 days. Thus, the observed results here may be the due to prolonged expression of ChABC and PNN degradation. Consistent with this, previous studies have indicated that in cells which would typically express a PNN, their sustained absence renders these cells more vulnerable to environmental stressors

(Cabungcal et al., 2013; Ruden et al., 2021; Suttkus et al., 2014). Other studies have demonstrated that ChABC treatment can reduce PV protein and mRNA expression within PV+ cells, making them more difficult to identify (Yamada et al., 2015). In addition to affecting PV+ cell integrity, numerous studies have demonstrated that PNN degradation can have consequences for the activity of PV+ cells. Common findings are that PNN degradation decreases the ability of fast-spiking PV interneurons to maintain high frequency activity and can increase spiking variability (Christensen et al., 2021; Favuzzi et al., 2017; Lensjø et al., 2017; Wingert & Sorg, 2021). PV+ interneurons are also known to play an important role in the generation of gamma oscillatory activity (Antonoudiou et al., 2020; Volman et al., 2011; Vreugdenhil et al., 2003). The impacts of PNN degradation on PV+ cell activity is also apparent within this relationship, where degradation can alter gamma oscillatory activity (Faini et al., 2018; Steullet et al., 2014). These studies demonstrate that PNN degradation can impact both PV+ interneurons and the generation of gamma oscillatory activity, which is particularly relevant to object recognition tasks as gamma oscillations are integral to feature binding processes (Gray & Singer, 1989; Honkanen et al., 2015; Tallon-Baudry & Bertrand, 1999). Given this information, one possible explanation for the crossmodal and oddity deficits observed here could be that they are only indirectly related to PNN disruption, but rather be mediated by a loss of PV+ activity.

PV+ interneurons have diverse roles in generating inhibitory activity within the cortex, but most relevant among them to the present study might be their role in pattern separation (Cayco-Gajic & Silver, 2019). The successful identification of similar, but not identical stimuli requires that these inputs be separated into different patterns of neural activity. PV+ interneurons play a critical role in this process by inhibiting competing assemblies of neurons while discriminating between stimuli. This is well demonstrated in a study of mouse visual processing,

where suppression of PV+ activity increases the overlap of cellular activity in response to different visual inputs (Zhu et al., 2015). This in turn makes it difficult to discriminate between two stimuli. Similarly, the suppression of PV+ interneurons increases the overlap in cellular responses to visual stimuli that previously had a more separate representation in the brain (Agetsuma et al., 2018). Other studies have shown that the role of PV+ interneurons in discriminating different stimuli is not restricted to visual processing. PV+ suppression in the ventral CA1 region of the hippocampus, which is important for social recognition, impairs the ability of animals to discriminate between familiar and novel animals (Deng et al., 2019). These studies demonstrate across multiple modalities that PV+ interneuron activity is important in the discrimination between stimuli. In light of the effects of PNN disruption on PV+ cells, this could indicate that PNN disruption impacts the recruitment of neural assemblies in processing stimuli and leads to overlap or interference in neural encoding (Wingert & Sorg, 2021). In support of this, PNN removal around grid cells, which encode for spatial environments, made previously stable representations of familiar environments susceptible to alterations after being exposed to a novel environment (Christensen et al., 2021). Thus, the loss of PV+ interneurons here may have contributed to impairments in discriminating between familiar and novel stimuli when challenged to integrate this information across sensory modalities. Further study is required to better evaluate the role of PNN degradation and alterations of PV+ activity within the RSC to determine if they contribute to these discriminations like PV+ interneurons have been shown to in other processing systems.

PNN degradation within the mPFC had no effect on open field behaviour, spontaneous alternation, oddity task preference, or crossmodal object recognition in the present study. This stands in contrast to previous work from our laboratory that demonstrated that PNN disruption

via direct infusion of ChABC can impair both oddity object preference and crossmodal object recognition in rats (Paylor et al., 2018). Our results from the crossmodal object recognition task are difficult to interpret given that ChABC animals performed poorly at the task across all three time points. There are numerous factors that could have impacted behavioural outcomes on this task, including the lack of screening with sample phase object exploration measurements, the length and extent of the behavioural battery utilized, and the use of genetic strains and viral vector injections. Despite the limitations of the present study, other studies offer insight into the potential role of PNNs in the mPFC in working memory. Animal studies have indicated a clear role for the mPFC in other test paradigms that evaluate of working memory (Anderson et al., 2020; Benoit et al., 2020; Dexter et al., 2022; Horst & Laubach, 2009; Liu et al., 2014; Yang et al., 2014). However, it's specific involvement in the crossmodal object recognition task is still not clear. In contrast to Paylor et al (2018), a previous lesion study indicated that damage to the mPFC alone are not sufficient to impair crossmodal object recognition (Reid et al., 2014). Further study is required to better evaluate the relationship between mPFC function and crossmodal object recognition.

With regards to the oddity preference task, our lab has previously shown that PNN degradation in the mPFC can decrease oddity preference (Paylor et al., 2018). Moreover, PNN counts within the mPFC were predictive of performance on the task. While the deficits in oddity performance and the relationship between performance and PNN integrity were not replicated here, there are numerous differences that could underlie these this. Firstly, our previous work utilized rats rather than mice. Mice are typically considered to display lower performance than rats in tests of cognition and their performance is more subject to non-cognitive factors such as stress and anxiety (Colacicco et al., 2002; Ellenbroek & Youn, 2016; Whishaw & Tomie, 1996). Mice also

respond differentially to common practices in rat studies such as pre-experimental handling and habituation, which can actually enhance stress and impact behavioural performance (Meijer et al., 2007). In support of this, the mice in the present study had exhibited lower preference for the odd object than we had previously shown in rats. Genetic strains of animals like the mice utilized here, can also have an impact on behavioural performance and should be carefully considered when being used for behavioural experiments (Brooks et al., 2005; Van Der Staay & Steckler, 2002). With regards to the predictive relationship between PNN integrity and performance on the oddity task, we had previously evaluated these two weeks after infusions of ChABC, in contrast to the present study where this comparison was only made 30 days after the trigger for ChABC expression had been withdrawn. Differences could also be attributable to the delivery method of ChABC, where here we used viral expression as opposed to direct infusion of ChABC.

In addition to the behavioural observations we made, our wide field optical imaging of calcium fluorescence indicated that PNN degradation within the RSC had no observable impact on broader cortical activity or interconnectivity between cortical regions. This alone is informative in that it demonstrates that PNN disruption and subsequent PV+ cell loss within the RSC is not sufficient to disrupt broader patterns of activity in the brain. We did however note decreased power of slow wave (0.1-1.0 Hz) and delta (1.0-5.0 Hz) frequency activity within the RSC after PNN degradation. Due to the close relationship between PNNs and PV+ interneurons, research has focused primarily on their impact within high frequency ranges such as the gamma band (40-100 Hz). However, low frequency activity such as delta has been implicated in sensory processing and in diseases that feature sensory integration dysfunction, such as SZ (Hong et al., 2010; Howells et al., 2018; Mäki-Marttunen et al., 2019). People suffering from SZ have reduced task-evoked delta activity and show decreased delta coherence between brain structures when

attending to stimuli (Bates et al., 2009; Ford et al., 2002). Treatment with NMDA antagonists, such as ketamine or MK-801 have also been shown to decrease delta activity (Hong et al., 2010; Hunt et al., 2010; Kiss et al., 2011; Mahdavi et al., 2020). These results pair well with delta abnormalities shown in SZ studies, as NMDA antagonists can induce SZ-like symptoms in human subjects and are widely utilized in animals to model SZ. NMDAR antagonists can also impact parvalbumin expression (Kaushik et al., 2021; Keilhoff et al., 2004; Koh et al., 2016; Matuszko et al., 2017; Venturino et al., 2021; Zhou et al., 2015). Thus, in our data the loss of PNNs and subsequent disruption of PV+ interneurons may have reduced delta power, similar to the consequences of NMDAR antagonism. While these interpretations require scientific study to back them up, a growing body of research suggests that NMDA hypofunction, particularly within PV+ interneuron could have implications for SZ. A more direct link between PV+ cells and delta power has also been demonstrated in healthy contexts. Stimulation of inhibitory interneurons expressing GAD67+, which all PV+ interneurons express, in the parafacial zone can instantly and reliably induce the onset of slow-wave sleep in animals and also increases the power of delta frequency activity (Y. Lu et al., 2018). While the context of slow wave sleep is not applicable in the present study, this against suggests that inhibitory interneuron activity can impact the power of the delta band.

While wide field optical imaging has been sparsely utilized to evaluate changes after PNN degradation, the application is still intriguing for future studies. One previous study utilizing this technique demonstrated that during transitions from rest to locomotion, or vice-versa, most brain nodes examined increased in correlated activity (West et al., 2022). However, during steady states of continuous locomotion, most nodes decreased in correlated activity. In contrast, correlations between the RSC and secondary motor cortex increase during continuous

locomotion. Others have utilized wide field optical imaging to show that the RSC is involved in associating environmental contexts with appropriate motor outputs (Franco & Goard, 2021). These studies demonstrate that the RSC plays a role in determining the appropriate motor activity within environments and are informative when considering the changes in exploratory activity we observed here after manipulation of the RSC. Wide field optical imaging has an exciting potential for evaluating brain activity and connectivity, and further utilization of this technique when evaluating PNN degradation would be insightful. Particularly in the context of investigating CNS disorders like schizophrenia, where aberrant connectivity and PNN loss are noted features, wide field optical imaging offers unique opportunities to evaluate the broader impacts of PNN loss.

Conclusions

The present study demonstrates that PNN degradation within the RSC may have a subtle impact on working memory as demonstrated in the crossmodal object recognition task. However, deficits in the tested constructs of working memory here were also paralleled by changes in exploratory activity which might indicate that PNN disruption impacted more than just working memory. Our observation that PV+ interneurons are reduced after ChABC expression is also interesting, given the important contributions that PV+ interneurons make to discriminating between objects. These outcomes warrant further investigation into the impacts of PNN degradation within the RSC, particularly to evaluate the consequences on cognition, spatial navigation, and exploratory activity. The application of wide field imaging techniques to studies of PNN degradation are also encouraged given that PNN loss and aberrant connectivity after a common feature in certain CNS disorders, such as schizophrenia.

Figures

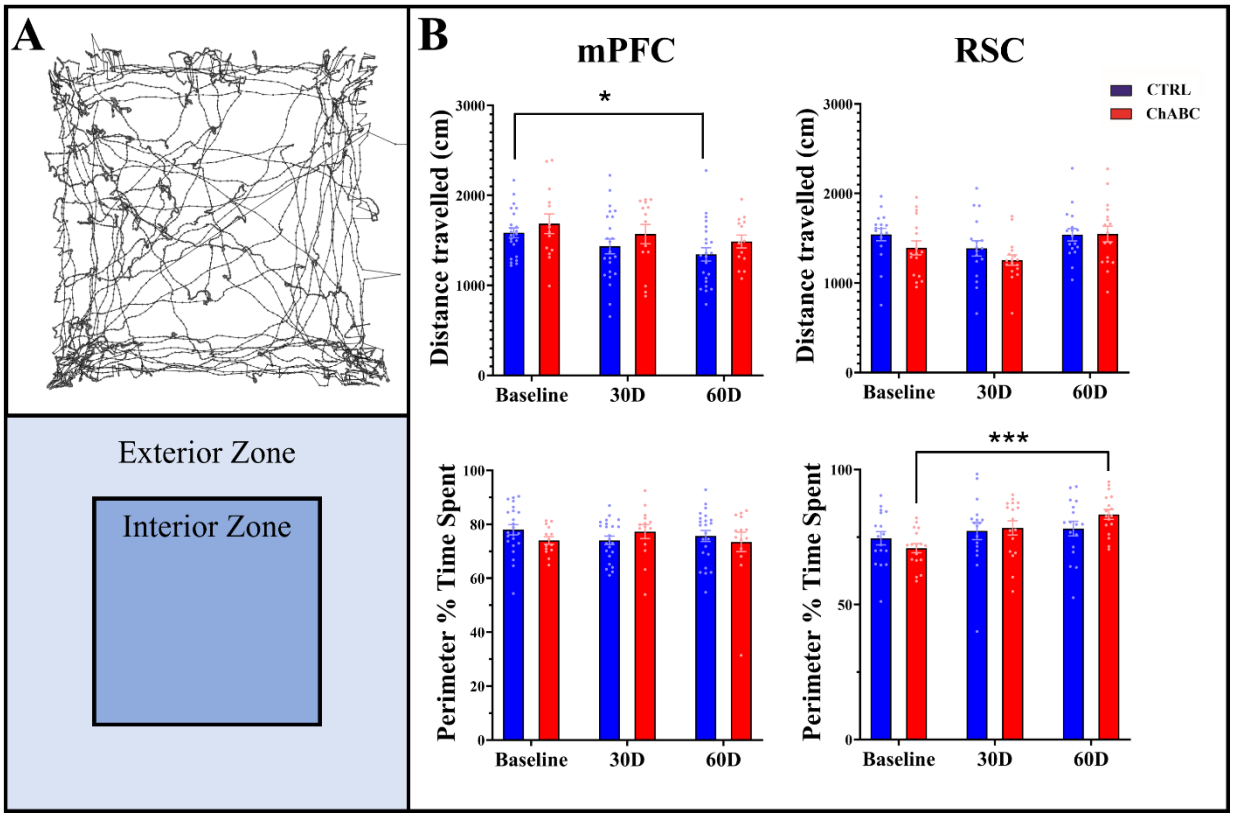
A
Exterior Zone
Interior Zone
B
mPFC
RSC
CTRL
ChABC
Distance travelled (cm)
Perimeter % Time Spent
Baseline
30D
60D
*
***

Figure 4.1. Effects of ChABC treatment on open field and anxiety behaviour. (A) Representative open field tracking of animal behaviour over the course of a 4- minute trial (shown top) and a schematic of zones (shown bottom) utilized for to determine anxiety behaviour in animals. (B) Graphs in the left column describe outcomes for animals in the MPFC group. A repeated-measures ANOVA on distance travelled (top left) showed a main effect of time ($F_{(2, 70)} = 5.295$, $p < 0.01$), but no main effect of treatment and no interaction. Post-hoc comparisons showed a significant decrease in control animals from baseline to 60 days ($t_{(22)} = 2.691$, $p < 0.05$). Time and treatment group had no impact on percentage time spent in the perimeter of the arena (bottom). Graphs in the right column show RSC outcomes. Similar to the mPFC, we observed a main effect of time ($F_{(2, 64)} = 5.409$, $p < 0.01$) although post-hoc comparisons showed no differences between any of the time points within groups. There was no main effect of treatment and no interaction. In the RSC group, there was a main effect of time on time spent in the perimeter $F_{(2, 64)} = 8.022$, $p < 0.01$) but no main effect of treatment and no interaction. Post-hoc comparisons showed that ChABC had a significant decrease in time spent in the perimeter from baseline to 60 days ($t_{(16)}=4.623$, $p < 0.001$). Data presented as mean ± SEM; *, $p < 0.05$, ***, $p < 0.001$; (Legend: CTRL = blue; ChABC = red)

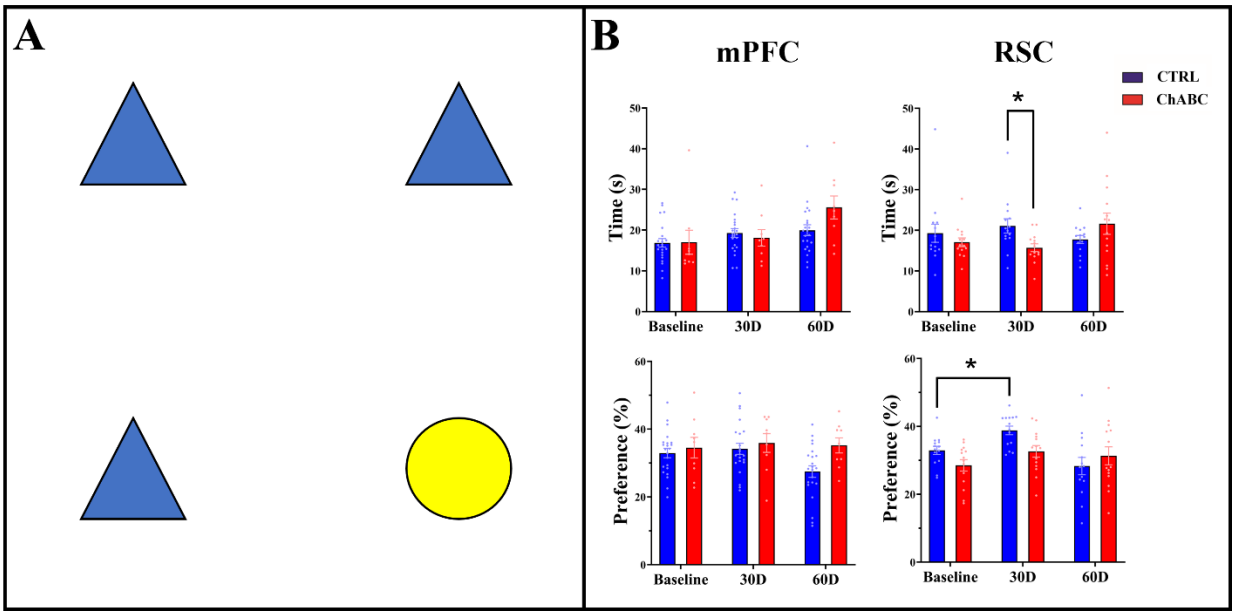
A
B
mPFC
RSC
CTRL
ChABC
Time (s)
Preference (%)
Baseline
30D
60D
*
*

Figure 4.2. ChABC treatment in either of the mPFC or RSC has no impact on oddity object preference. (A) Schematic of the oddity object preference task design. Animals' preference for the 'odd' object among three other identical objects is calculated as a percentage of time spent exploring the odd object. (B) Graphical representation of animal's preference for the odd object at either site. A repeated-measures ANOVA on mean exploration time (top left) for the mPFC showed a main effect of time ($F_{(2, 58)} = 7.336$, $p < 0.01$), but no main effect of treatment and no interaction. Post-hoc comparisons showed no differences between time points in either group. Oddity preference in the mPFC group (bottom left) was also not affected by time or treatment, and there was no interaction between the two. Exploration times for the RSC group (top right) showed an interaction between time and treatment ($F_{(2, 52)} = 4.519$, $p < 0.05$) but no main effect of time or treatment. Post-hoc comparisons showed that ChABC treated animals explored the objects less after 30 days ($t_{(26)}=2.684$, $p < 0.05$). An evaluation of oddity preference in the RSC group showed a main effect of time ($F_{(2, 52)} = 5.254$, $p < 0.05$), but no main effect of treatment and no interaction. Post-hoc comparisons showed a significant increase in exploration between baseline and 30 days for the control group ($t(13) = 3.325$, $p < 0.05$). Data presented as mean ± SEM; *, $p < 0.05$ (Legend: CTRL = blue; ChABC = red).

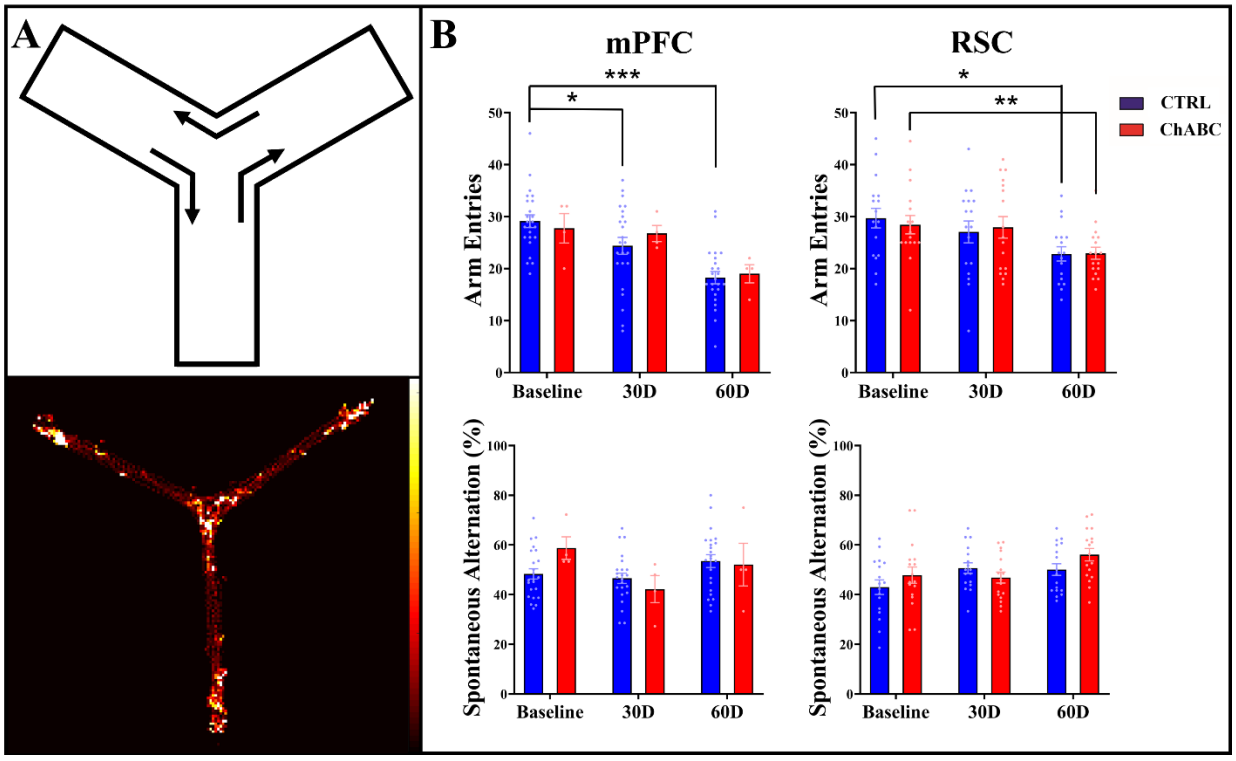
A
B
mPFC
RSC
CTRL
ChABC
Arm Entries
Spontaneous Alternation (%)
Baseline
30D
60D
***
*
**

Figure 4.3. ChABC expression did not impact working memory performance on the spontaneous alternation task. (A) Schematic of the Y-maze utilized for the spontaneous alternation task (shown top). A heat map (shown bottom) from a representative trial of an animal participating in the task. (B) Graphical representation of animal's outcomes from the spontaneous alternation task. The left-column shows data from the mPFC group. A repeated-measures ANOVA on total arm entries (top left) showed a main effect of time ($F_{(2, 52)} = 8.970$, $p < 0.01$) but no main effect of treatment and no interaction. Post-hoc comparisons showed that control animals had significant decreases in exploration time from baseline to 30 days and 60 days (30D: $t_{(22)} = 2.445$, $p < 0.05$; 60D: $t_{(22)} = 6.538$, $p < 0.001$). Spontaneous alternation (bottom left) showed no effect of time, treatment, and no interaction between time and treatment. In the RSC group, a repeated measures ANOVA of total arm entries (top right) showed a main effect of time ($F_{(2, 64)} = 8.242$, $p < 0.01$), but no effect of treatment and no interaction. Post-hoc comparisons showed that both groups of animals had significant reductions in arm entries from baseline to 60 days (CTRL: $t_{(16)} = 3.047$, $p < 0.05$; ChABC: $t_{(16)} = 3.711$, $p < 0.01$). Spontaneous alternation behaviour showed a main effect of time ($F_{(2, 64)} = 4.890$, $p < 0.05$) but no main effect of treatment and no interaction. Post-hoc comparisons did not show any significant differences between time points for either group. Data presented as mean ± SEM; *, $p < 0.05$, ***, $p < 0.001$; (Legend: CTRL = blue; ChABC = red).

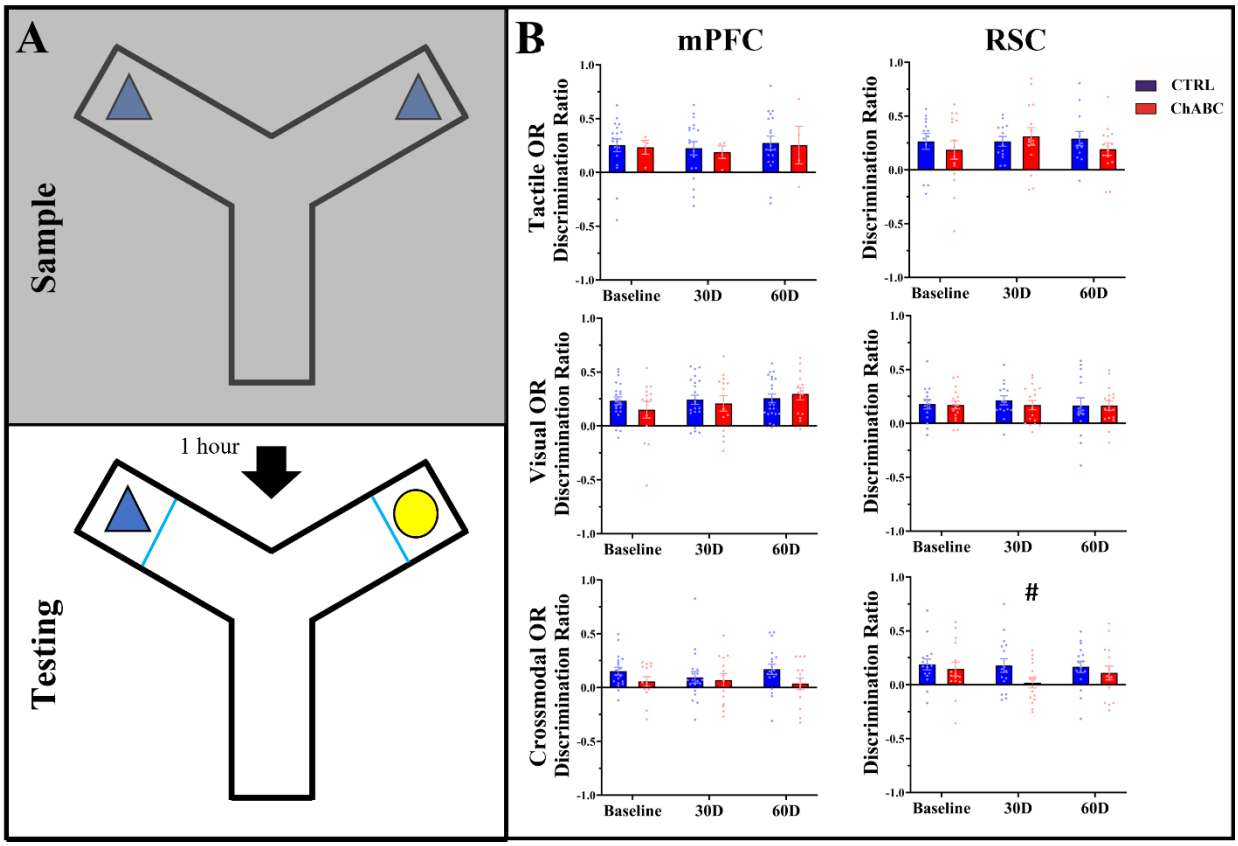
A
Sample
1 hour
Testing
B
mPFC
RSC
CTRL
ChABC
Tactile OR Discrimination Ratio
Visual OR Discrimination Ratio
Crossmodal OR Discrimination Ratio
Discrimination Ratio
Baseline
30D
60D
#

Figure 4.4. ChABC expression in the RSC results in a subtle impairment in crossmodal object recognition. (A) Schematic representation of the Y-maze utilized for the crossmodal object recognition task. This task involved three phases: visual, tactile, and crossmodal (shown). In the visual phase, a glass pane prevents the animal from touching the objects during both the training and testing phase. In the tactile phase, red lights are utilized to limit animals to gathering tactile information about the objects in both the training and testing phase. In the crossmodal phase, animals are trained under red light conditions but tested under visual conditions. (B) Graphical representation of animal's outcomes from all three tasks. Data from the mPFC group is shown in the left-hand column. A repeated-measures ANOVA on discrimination ratios in the visual phase (top left) showed that there was no effect of time, treatment, and no interaction between the two. Similarly, tactile object recognition (middle left) was unaffected by ChABC treatment, time, and there was no interaction. In the crossmodal phase (bottom left), there was a main effect of treatment ($F_{(1, 31)} = 4.622$, $p < 0.05$) but post-hoc comparisons did not show significant differences between groups at any of the three time points. One sample t-tests of the 30-day time point showed that neither control or ChABC animals were able to perform significantly better than chance (CTRL: $t_{(18)} = 1.783$, p = n.s.; DOX: $t_{(13)} = 1.106$, p = n.s.). Data for the RSC group are shown in the right-hand column. A repeated-measures ANOVA showed that visual object recognition (top right) had no main effect of treatment, time, and no interaction. Similarly, tactile object recognition (middle right) was unaffected by time, treatment, and there was no interaction. In the crossmodal phase for the RSC group (bottom right), object recognition was unaffected by treatment, time, and there was no interaction. However, one-sample t-tests showed that ChABC animals were unable to perform significantly better than chance at this task ($t_{(14)}= 0.382$, p = n.s.), whereas control animals could ($t_{(15)}=2.823$, $p < 0.05$). Data presented as mean ± SEM; #, p = n.s., one sample t-test against chance performance (Legend: CTRL = blue; ChABC = red).

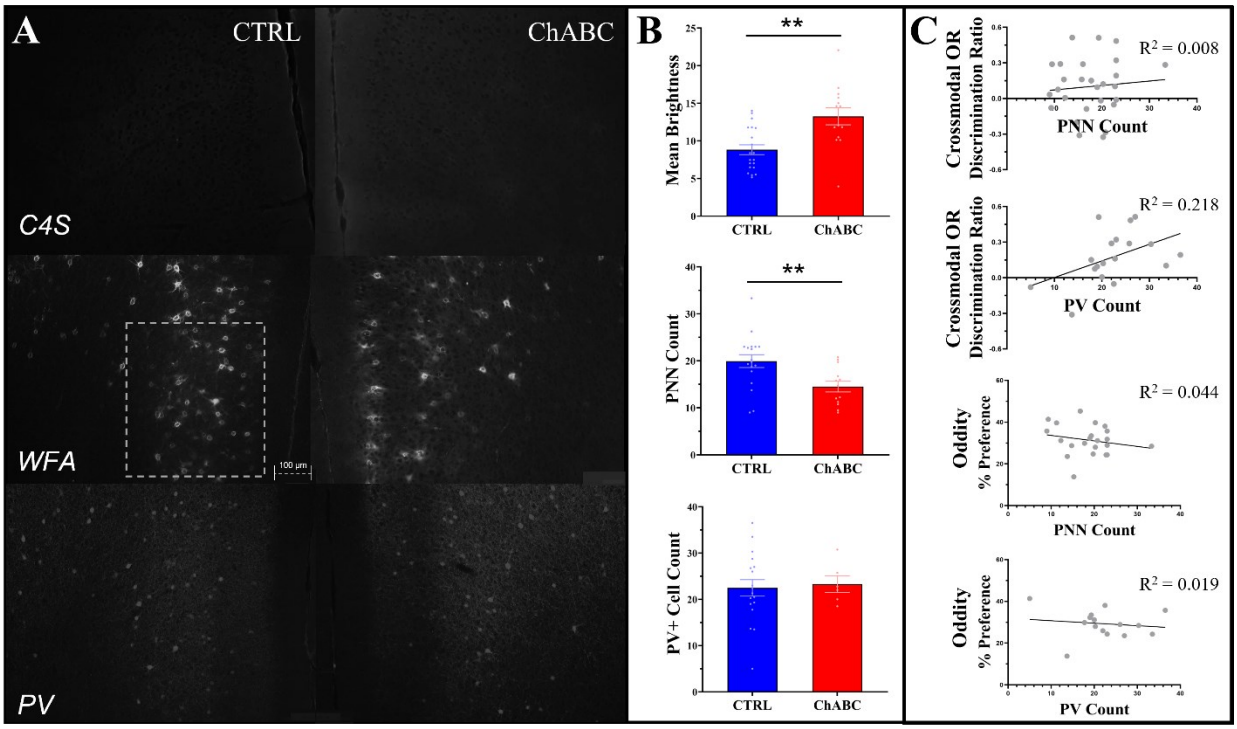
A
CTRL
ChABC
C4S
WFA
PV
100 µm
B
Mean Brightness
**
CTRL
ChABC
PNN Count
**
CTRL
ChABC
PV+ Cell Count
CTRL
ChABC
C
Crossmodal OR Discrimination Ratio
PNN Count
R2 = 0.008
Crossmodal OR Discrimination Ratio
PV Count
R2 = 0.218
Oddity % Preference
PNN Count
R2 = 0.044
Oddity % Preference
PV Count
R2 = 0.019

Figure 4.5. ChABC treatment degrades PNNs within the mPFC, but PV+ interneurons are unaffected. (A) Representative immunostaining for chondroitin-4-sulfate (top), which labels the cleaved components of PNNs, wisteria floribunda agglutinin (middle), which labels intact PNNs, and parvalbumin inhibitory interneurons (bottom). The left-hand column shows control (CTRL) treated animals and the right ChABC animals. (B) Graphical representative of measurements for each stain. ChABC expression resulted in an increase in C4S staining ($p < 0.01$), and a decrease in PNN counts ($p < 0.01$) within the mPFC. PV+ interneurons were unaltered. (C) Correlations between immunostaining and animals' behavioural performance across all animals. No significant relationships were detected between PNNs or PV+ interneurons and crossmodal object recognition performance ((PNN: $R^2 = 0.008$, $p = 0.653$; PV+: $R^2 = 0.218$, $p = 0.051$). Similarly, PNNs and PV+ interneurons had no significant relationship with oddity object performance (PNN: $R^2 = 0.044$, $p = 0.351$; PV+: $R^2 = 0.019$, $p = 0.621$). Data presented as mean ± SEM; *, $p < 0.05$; **, $p < 0.01$ (Legend: CTRL = blue; ChABC = red).

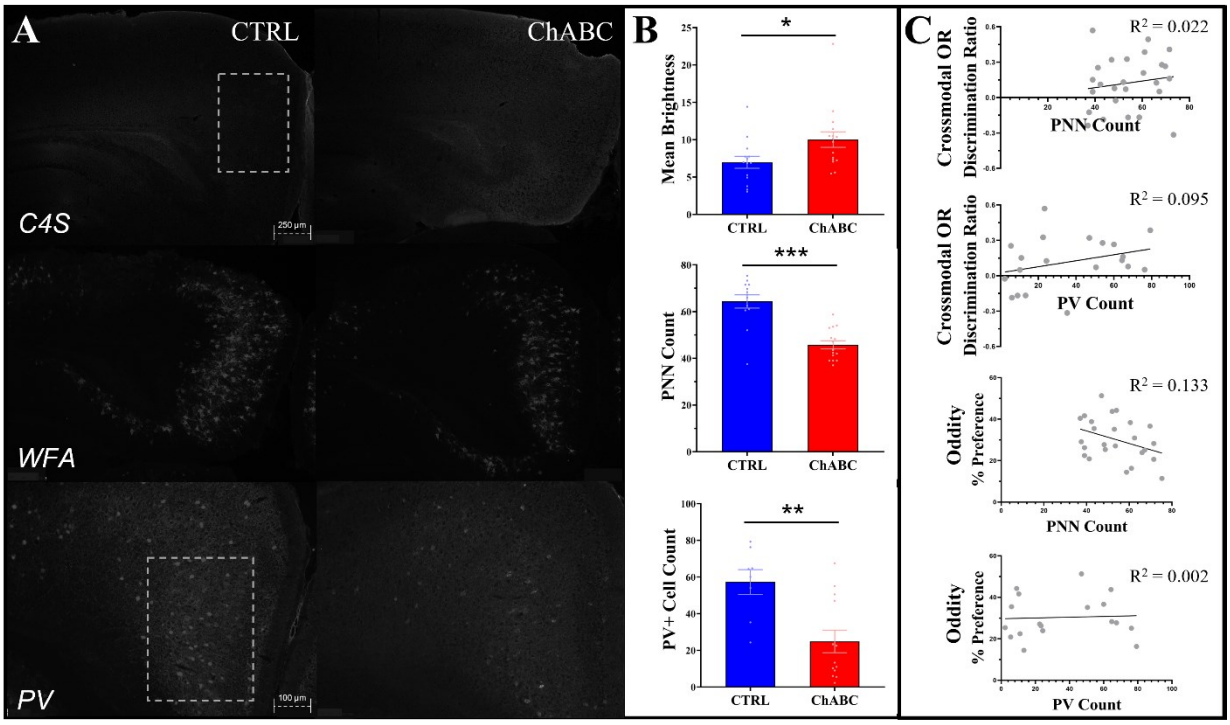
A
CTRL
ChABC
C4S
250 µm
WFA
PV
100 µm
B
Mean Brightness
*
CTRL
ChABC
PNN Count
***
CTRL
ChABC
PV+ Cell Count
**
CTRL
ChABC
C
Crossmodal OR Discrimination Ratio
R2 = 0.022
PNN Count
Crossmodal OR Discrimination Ratio
R2 = 0.095
PV Count
Oddity % Preference
R2 = 0.133
PNN Count
Oddity % Preference
R2 = 0.002
PV Count

Figure 4.6. After dox-i-ChABC injections in the RSC, doxycycline administration results in PNN degradation. (A) Representative immunostaining for chondroitin-4-sulfate (top), which labels the cleaved components of PNNs, wisteria floribunda agglutinin (middle), which labels intact PNNs, and parvalbumin inhibitory interneurons (bottom). The left-hand column shows control (CTRL) treated animals and the right ChABC animals. (B) Graphical representative of measurements for each stain. ChABC expression resulted in an increase in C4S staining ($p < 0.05$), and a decrease in PNN counts ($p < 0.001$) within the mPFC. PV+ interneurons were also reduced in ChABC group ($p < 0.01$). (C) Correlations between immunostaining and animals' behavioural performance. No significant relationships were detected between either of PNNs or PV+ interneurons and crossmodal object recognition performance (PNN: $R^2 = 0.022$, $p = 0.467$; PV+: $R^2 = 0.095$, $p = 0.186$). Similarly, there was no relationship between PNNs or PV+ interneurons and oddity object preference (PNN: $R^2 = 0.133$, $p = 0.073$; PV+: $R^2 = 0.002$, $p = 0.844$). Data presented as mean ± SEM; *, $p < 0.05$; **, $p < 0.01$; ***, $p < 0.001$ (Legend: CTRL = blue; ChABC = red).

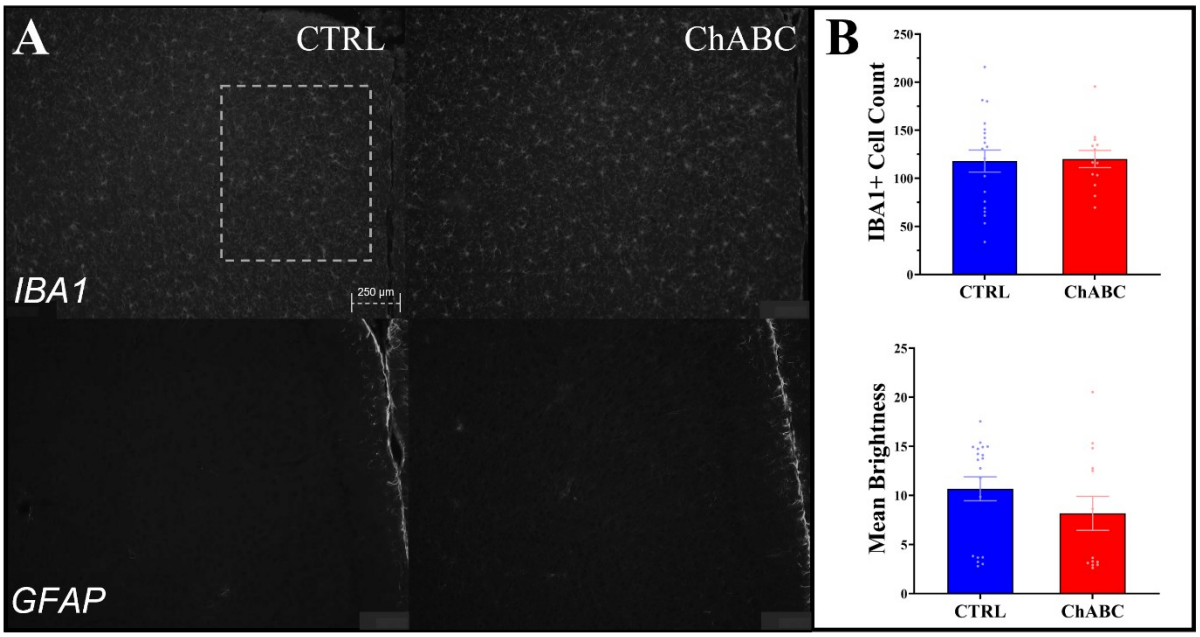
A
CTRL
ChABC
IBA1
250 µm
GFAP
B
IBA1+ Cell Count
250
200
150
100
50
0
CTRL
ChABC
Mean Brightness
25
20
15
10
5
0
CTRL
ChABC

Figure 4.7. ChABC expression via dox-i-ChABC injections into the mPFC does not result in overt inflammation. (A) Representative immunostaining for IBA1 (top), which labels microglia, and GFAP (bottom), which labels astrocytes. The left side images show control (CTRL) treated animals and the right ChABC animals. (B) Graphical representation of measurements for each stain. ChABC did not result in any change in IBA1+ cell counts (top) or GFAP mean brightness (bottom). Data presented as mean ± SEM (Legend: CTRL = blue; DOX = red).

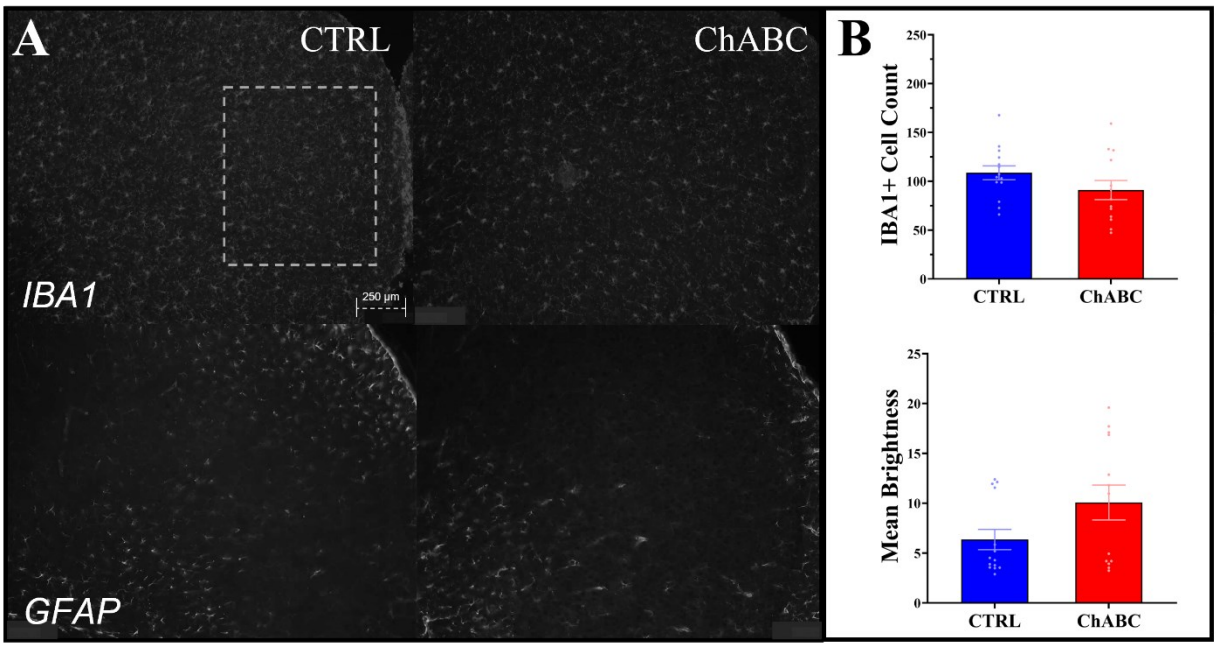
A
CTRL
ChABC
IBA1
250 µm
GFAP
B
IBA1+ Cell Count
250
200
150
100
50
0
CTRL
ChABC
Mean Brightness
25
20
15
10
5
0
CTRL
ChABC

Figure 4.8. ChABC expression via dox-i-ChABC injections into the RSC does not result in overt inflammation. (A) Representative immunostaining for IBA1 (top), which labels microglia, and GFAP (bottom), which labels astrocytes. The left side images show control (CTRL) treated animals and the right ChABC animals. (B) Graphical representation of measurements for each stain. ChABC expression did not result in any change in IBA1+ cell counts (top) or GFAP mean brightness (bottom). Data presented as mean ± SEM (Legend: CTRL = blue; ChABC = red; Regions: AC = Anterior Cingulate; CG = Cingulate; M1 = Primary Motor; M2 = Secondary Motor; FL = Forelimb; HL = Hindlimb; BC = Barrel Cortex; TR = Trunk Region; MO = Mouth Region; NO = Nose Region; S2 = Secondary Somatosensory; PTAa = Parietal Association Area A; PTAb = Parietal Association Area B; RS = Retrosplenial; V1 = Primary Visual; AU = Primary Auditory; TEA = Temporal Association).

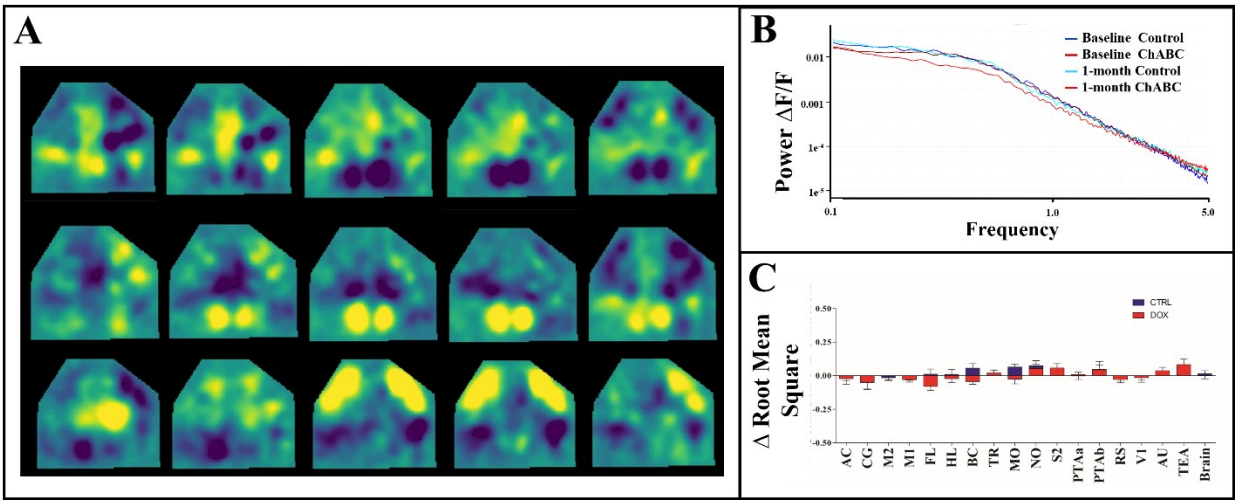
A
B
Baseline Control
Baseline ChABC
1-month Control
1-month ChABC
Power ΔF/F
0.01
0.001
1e-4
1e-5
0.1
1.0
5.0
Frequency
C
Δ Root Mean Square
CTRL
DOX
0.50
0.25
0.00
-0.25
-0.50
AC
CG
M2
M1
FL
HL
BC
TR
MO
NO
S2
PTAa
PTAb
RS
V1
AU
TEA
Brain

Figure 4.9. ChABC expression in the RSC decreases the power of low frequency activity generated from the RSC but does not alter broader patterns of activity in the cortex. (A) Representative time course of 45 ms of spontaneous activity. (B) A power spectrum analysis of activity within the RSC showed that ChABC treatment reduced low frequency power of slow wave (0.1-1.0 Hz; $r = 0.34$) and delta (1.0-5.0 Hz; $r = 0.08$) activity, where as control animals did not. (Wilcoxon rank-sum test; CTRL (0.1-1.0 Hz): $z = 0.72$, p = n.s.; (1.0-5.0 Hz): $z = 1.81$, p = n.s.; ChABC (0.1-1.0 Hz): $z = 5.39$, $p < 0.001$; (1.0-5.0 Hz): $z = 2.19$, $p < 0.05$). (C) Graphical representation of change in (Δ) RMS across the 17 cortical areas examined. A two-way ANOVA on change in RMS showed a main effect of cortical area ($F_{(17, 144)} = 1.865$, $p < 0.05$) but no main effect of treatment and no interaction between treatment and area. Post-hoc comparisons did not show any significant differences between control and ChABC animals within any of the regions of interest. Data presented as mean ± SEM (B Legend: dark blue = baseline control; dark red = baseline ChABC; light blue = 1-month control; light red = 1-month ChABC; C Legend: CTRL = blue; ChABC = red; Regions: AC = Anterior Cingulate; CG = Cingulate; M1 = Primary Motor; M2 = Secondary Motor; FL = Forelimb; HL = Hindlimb; BC = Barrel Cortex; TR = Trunk Region; MO = Mouth Region; NO = Nose Region; S2 = Secondary Somatosensory; PTAa = Parietal Association Area A; PTAb = Parietal Association Area B; RS = Retrosplenial; V1 = Primary Visual; AU = Primary Auditory; TEA = Temporal Association).

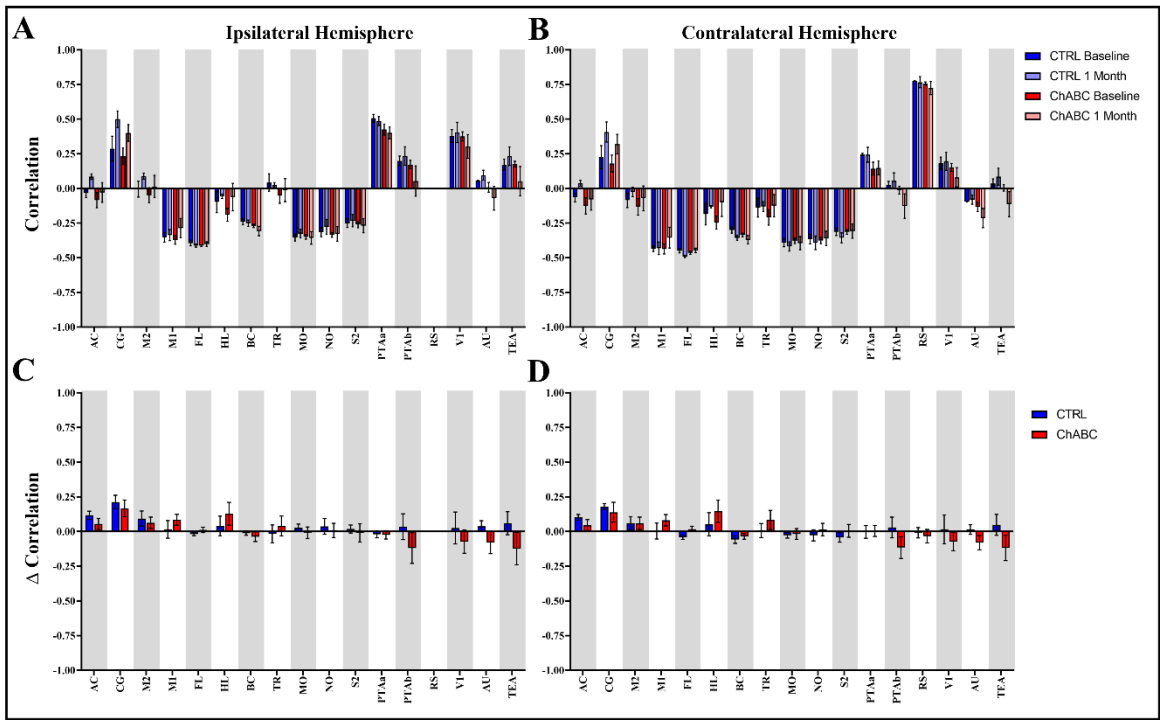
A
Ipsilateral Hemisphere
B
Contralateral Hemisphere
C
D
Correlation
Δ Correlation
CTRL Baseline
CTRL 1 Month
ChABC Baseline
ChABC 1 Month
CTRL
ChABC
AC
CG
M2
M1
FL
HL
BC
TR
MO
NO
S2
PTAa
PTAb
RS
V1
AU
TEA

Figure 4.10. ChABC treatment did not result in broader changes in cortical connectivity between regions. (A) Graphical representation of the raw correlation values for the RSC with cortical areas in the ipsilateral hemisphere. (B) Graphical representation of the raw correlation values for RSC with cortical areas in the contralateral hemisphere. (C) Graphical representation of the change (Δ) in correlated activity from baseline to 1-month for the RSC with ipsilateral cortical areas. A two-way ANOVA on the change in correlation over time for the RSC and ipsilateral areas showed no significant main effect of cortical area ($F_{(15, 128)} = 1.656$, $p = 0.068$), treatment ($F_{(1, 128)} = 2.260$, $p = 0.135$) and no interaction ($F_{(15, 128)} = 0.650$, $p = 0.829$). (D) Graphical representation of the change (Δ) in correlated activity from baseline to 1-month for the RSC with contralateral cortical areas. Change in correlations between the RSC and contralateral areas showed a main effect of cortical area ($F_{(15, 128)} = 2.050$, $p = 0.014$), but no main effect of treatment ($F_{(1, 128)} = 0.283$, $p = 0.595$) and no interaction between area and treatment ($F_{(15, 128)} = 0.92$, $p = 0.545$).

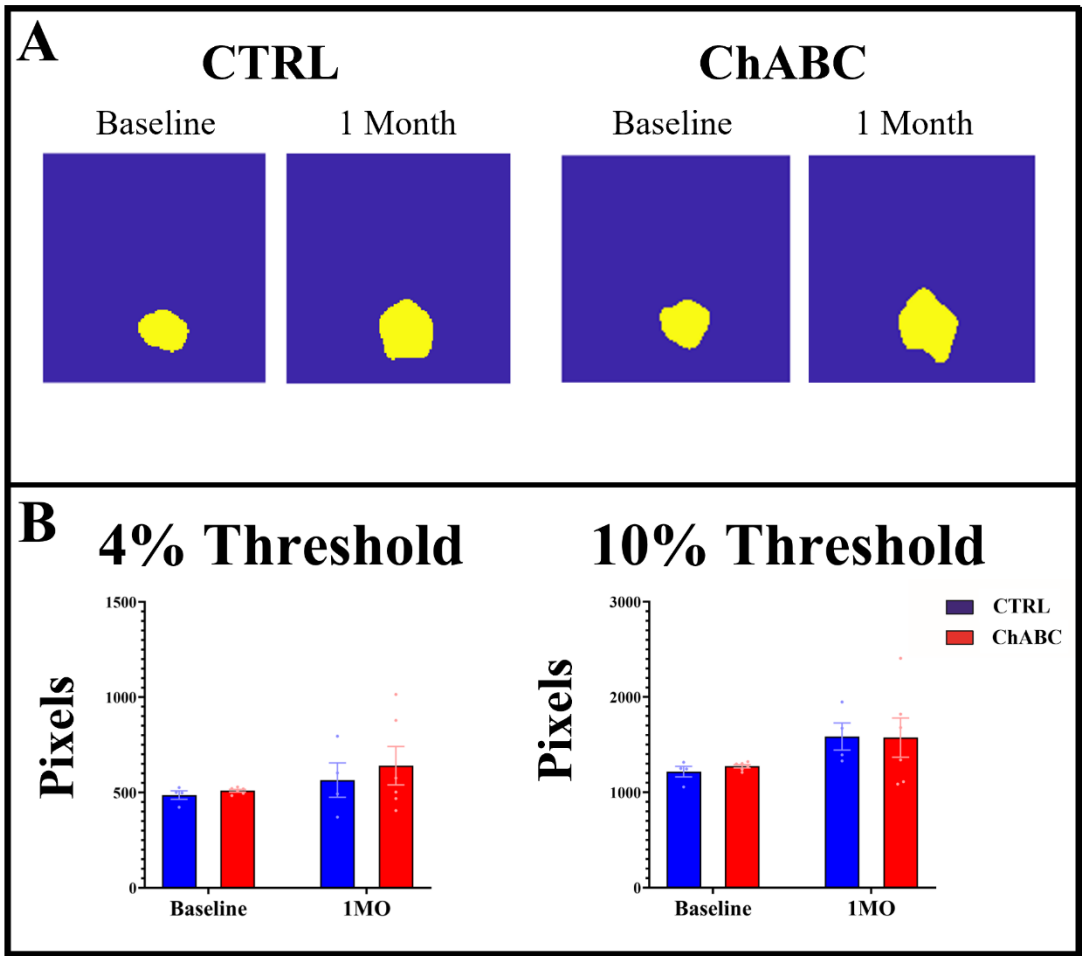
A
CTRL
ChABC
Baseline
1 Month
Baseline
1 Month
B
4% Threshold
10% Threshold
Pixels
1500
1000
500
0
Baseline
1MO
Pixels
3000
2000
1000
0
Baseline
1MO
CTRL
ChABC

Figure 4.11. PNN degradation in the RSC does not alter seed pixel maps of correlated activity. (A) Representative image of a processed seed pixel map from the right hemisphere of a control and ChABC animal across both time points of the experiment. Areas highlighted in yellow show highly correlated activity with the seed pixel. (B) Graphical comparison of seed pixel maps. Seed pixel maps generated based on anatomical estimations of the RSC were not altered after ChABC treatment at either time point. To further corroborate these results were not threshold specific, we tested a less restrictive threshold for establishing a retrosplenial seed pixel. Here, a two-way repeated measures ANOVA revealed a significant main effect of time ($F_{(1,8)}$ = 6.180, p = 0.038) but no main effect of treatment and no interaction. Post-hoc comparisons did not reveal any significant differences between either control or ChABC groups between time points.

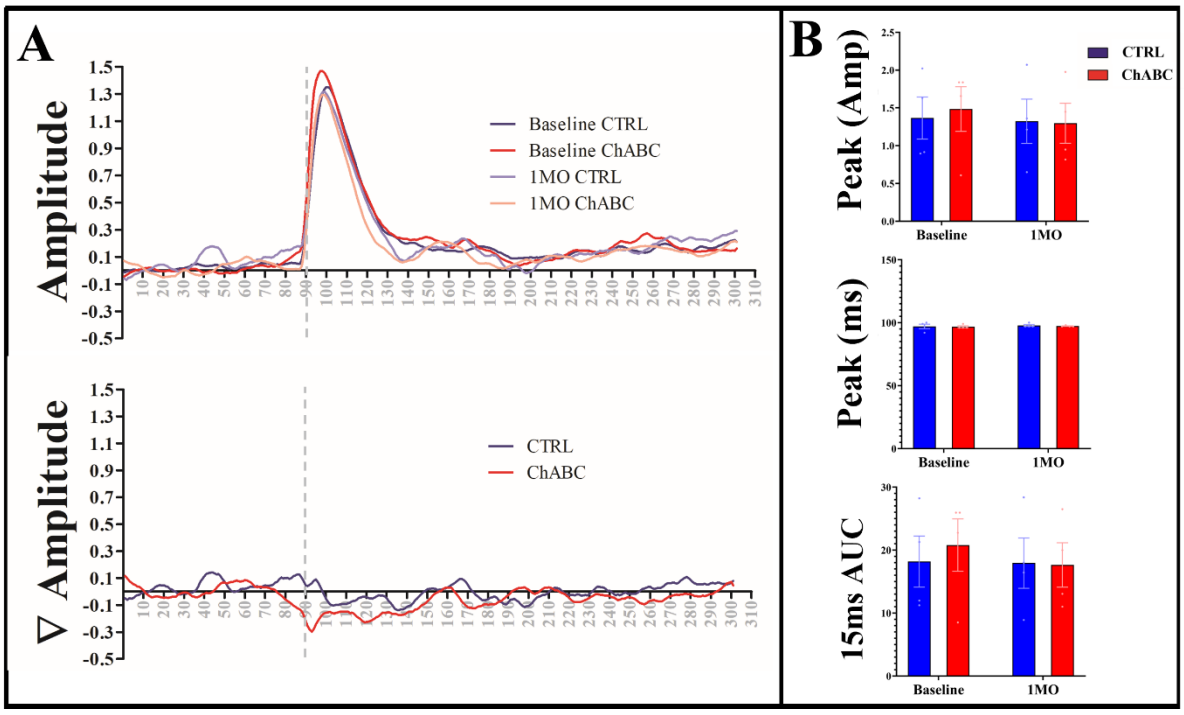
A
Amplitude
Baseline CTRL
Baseline ChABC
1MO CTRL
1MO ChABC
∇ Amplitude
CTRL
ChABC
B
Peak (Amp)
Peak (ms)
15ms AUC
CTRL
ChABC
Baseline
1MO

Figure 4.12. PNN degradation in the RSC does not affect auditory-evoked responses generated in the primary auditory cortex. (A) Plot of the time course of activation in the contralateral hemisphere after the presentation of an auditory stimulus (top) and a plot of the change in activation pattern between baseline and 1-month time points (bottom). (B) Graphical representation of measures of the responses. Peak amplitude of the response was not altered by ChABC treatment at either time point (top) nor was the delay in the peak (middle). An area under the curve calculation for the 15 ms following the presentation of the stimulus was similarly unaffected by ChABC treatment.

Region	Exploration Time (sec)	Treatment	Baseline	30D	60D
mPFC	Tactile Phase	Control	28.41±1.49	33.79±2.08	30.73±2.31
		ChABC	36.18±2.31	34.69±6.29	34.55±1.74
	Visual Phase	Control	26.14±2.41	23.75±1.83	21.03±1.60
		ChABC	26.17±2.27	26.90±1.66	21.04±1.81
	Crossmodal Phase	**Control**	27.46±2.18	29.04±1.51	19.18±1.71**
		ChABC	30.87±1.90	35.40±2.95	24.96±1.70*
RSC	Tactile Phase	Control	23.76±1.77	40.31±3.15***	32.32±1.81**
		ChABC	29.29±2.49	36.97±3.83	38.19±2.49
	Visual Phase	**Control**	20.98±2.10	28.19±2.87*	22.66±2.30
		ChABC	24.10±2.65	32.56±1.70	28.50±2.28
	Crossmodal Phase	**Control**	24.90±1.47	33.12±1.57**	24.27±2.31
		ChABC	28.61±2.89	38.46±2.93**	33.56±3.40

Table 4.1. Crossmodal Object Exploration Times. Here we outline exploration times for both cohorts (mPFC and RSC) in all three phases of the crossmodal object recognition task. For the mPFC cohort (top), tactile exploration times were unaffected by time, treatment, and showed no interaction. In the visual phase, a repeated measures ANOVA on exploration time showed a significant main effect of time ($F_{(2,66)} = 4.434$, $p < 0.05$), but no main effect of treatment and no significant interaction. Post-hoc comparisons did not show any significant differences between the time points for either group. In the crossmodal phase, exploration times showed a significant main effect of time ($F_{(2,62)} = 14.70$, $p < 0.001$) and of treatment ($F_{(1,31)} = 8.06$, $p < 0.01$) but no interaction. Post-hoc comparisons revealed that animals exploration times significantly decreased from baseline to 60 days in both control and ChABC groups (CTRL: $t_{(18)} = 4.018$, $p < 0.01$); ChABC: $t_{(13)} = 2.687$, $p < 0.05$). There were no significant differences between treatment groups at any of the three time points. For animals in the RSC cohort (bottom), repeated measures ANOVAs on tactile exploration time showed a main effect of time ($F_{(2, 52)} = 10.75$, $p < 0.001$) but no main effect of treatment and no interaction. Post-hoc comparisons showed that control animals had significantly increased exploration times at both 30 days and 60 days compared to baseline (30D: $t_{(12)} = 5.011$, $p < 0.001$; 60D, $t_{(12)} = 3.496$, $p < 0.01$). A comparison of visual exploration times showed a main effect of time ($F_{(2, 58)} = 6.020$, $p < 0.01$) and treatment ($F_{(1, 29)} = 4.78$, $p < 0.05$), but no significant interaction. Post-hoc comparisons showed that in ChABC animals there was a significant increase in exploration time from baseline to 30 days ($t_{(16)} = 2.563$, $p < 0.05$). Lastly, evaluating crossmodal exploration times showed a significant main effect of time ($F_{(2, 58)} = 12.08$, $p < 0.001$) and treatment ($F_{(1, 29)} = 4.98$, $p < 0.05$). Post-hoc comparisons did not reveal any significant differences between the treatment groups at any of the three time points, but both control and ChABC animals had increased exploration times at 30

days compared to baseline (CTRL: $t_{(15)} = 3.634$, $p = 0.005$; ChABC: $t_{(16)} = 3.477$, $p = 0.007$). Data presented as mean ± SEM; Bold indicates a significant treatment effect on exploration time in that phase; *, $p < 0.05$; **, $p < 0.01$, ***, $p < 0.001$.

Chapter 5 – Conclusions

In both the healthy and diseased brain there is now widespread recognition that PNNs play a significant role in cognition and behaviour. Genetic knockout studies have demonstrated that manipulations of essential PNN components can enhance or diminish task performance depending on the test and the region of the brain affected (Favuzzi et al., 2017; Romberg et al., 2013; Shi et al., 2019). Similarly, a large and growing body of research shows that targeted manipulation of PNNs using enzymes which degrade them can have similar implications for cognition and behaviour (Domínguez et al., 2019; Gogolla et al., 2009; Hylin et al., 2013; Paylor et al., 2018; Romberg et al., 2013). Together, these studies inform a broader context within which PNN loss and cognitive impairment are shared features of CNS diseases, such as SZ and AD. However, significant limitations remain in the field of PNN research. Thorough characterizations of PNN deficits in animal models to compare against human disease are limited, and where available often examine only select areas of the brain at select ages. Similarly, evaluations of PNN degradation on cognition, learning, and memory has been selective in both the behaviours evaluated and the regions where these manipulations are conducted.

The works here contribute to this body of literature by evaluating the 5xFAD animal model of AD and showing that it is a capable model for demonstrating PNN deficits. The results shown here join one other study demonstrating similar results and warrants use of this model for future evaluations into PNN loss, its consequences, and mechanisms within AD (Crapser et al., 2020). I also showed mixed evidence of PNNs involvement in working memory and cognition. In rats, PNN degradation in the mPFC can result in deficits in working memory as demonstrated in oddity object recognition and crossmodal working memory. By contrast, PNN degradation in the mPFC or RSC of mice had only subtle impacts on working memory, which may be mediated

by alterations in exploratory behaviour rather than memory. I described the impacts of targeted PNN degradation on closely associated PV+ cells across two studies. In the rat or mouse mPFC, PNN degradation had no observable impact on PV+ cell integrity. In the RSC of mice, prolonged PNN degradation resulted in a loss of PV+ cells. This manipulation also resulted in a decrease in the power of low frequency activity generated by the RSC, although broader patterns of cortical activity (spontaneous and evoked) were unaltered.

5.1 Chapter 2 Conclusions

The experiments in Chapter 2 were based on previous observations of PNN loss in the post-mortem tissue of patients who suffered from AD, as shown in the cingulate, entorhinal, frontal, and temporal cortices (Baig et al., 2005; Crapser et al., 2020; Kobayashi et al., 1989; Morawski et al., 2012; Pantazopoulos et al., 2016). However, another post-mortem study had shown sparing of PNNs in AD across several brain regions (Morawski et al., 2012). While reflections on these studies would highlight the differences in PNN-labeling techniques and inherent variability within human post-mortem samples, it nonetheless demonstrates a lack of consistent results of PNN deficits in AD. Animal models of AD also exhibit significant variability in their evaluations of PNNs in the disease (Ajmo et al., 2010; Cattaud et al., 2018; Crapser et al., 2020; Javonillo et al., 2022; Kudo et al., 2023; Morawski et al., 2010; Rey et al., 2022). Again though, these studies utilized models with unique etiological origins, evaluated different and often singular areas of the brain, and the age of animals frequently differed. This inconsistency makes it difficult to interpret whether PNN deficits are a consistent phenomenon in AD or its models. Thus, I evaluated 5xFAD mice which are a commonly utilized model of AD that exhibits many of its pathological features including Aβ plaque deposition, neuroinflammation, and cell death (Oakley et al., 2006). 5xFAD mice also display memory and cognitive impairment that is

consistent with an AD-like phenotype (de Pins et al., 2019; Devi et al., 2015; El Gaamouch et al., 2020). I demonstrate that PNN deficits are apparent in 5xFAD mice as early as 7-months of age in three of the regions examined: the primary motor cortex, CA1 region of the dorsal hippocampus, and RSC. PNN deficits were not detected in the mPFC or entorhinal cortex. Our results join only one other study to our knowledge that has evaluated PNN integrity in the 5xFAD mouse model. In this case, they demonstrated that PNN deficits are also apparent within the subiculum and visual cortex of this strain (Crapser et al., 2020). When comparing these results with post-mortem observations from AD there are notable differences. In my evaluation there was no PNN deficit observed in the mPFC or entorhinal cortex, which contrasts with previous results showing deficits in both the anterior cingulate or entorhinal cortex of post-mortem human tissue (Baig et al., 2005; Morawski et al., 2010; Pantazopoulos & Berretta, 2016). I did observe PNN deficits in the primary motor cortex and retrosplenial cortex but am not aware of studies investigating these areas in post-mortem AD tissue. Similarly in the hippocampus, human observations are lacking but animal models of AD exhibit PNN deficits here (Cattaud et al., 2018). Together, these findings demonstrate that PNN deficits are observed throughout the brains of AD and its models, but they are not universal. Of the regions evaluated in my experiment, the impact of PNN loss observed could underlie some of the deficits observed in 5xFAD animals such as motor impairment, deficits in spatial memory and navigation, and object recognition, although this requires more direct investigation (Bouter et al., 2014; Griñán-Ferré et al., 2016; Jawhar et al., 2012; Oakley et al., 2006; Ohno et al., 2006; O'Leary et al., 2020; O'Leary & Brown, 2022). I also provide additional evidence of impairment in spontaneous alternation and novel object recognition, two tests of memory function. These results join others who have shown significant impairment in both tasks in 5xFAD animals (Devi et al., 2015; Devi

& Ohno, 2016; Grayson et al., 2015; Griñán-Ferré et al., 2018; Jawhar et al., 2012; Kim et al., 2020).

Despite these contributions, there are numerous limitations to the present research and important considerations for future studies. Foremost among them is that the PNN deficits I observed in conjunction with behavioural impairment are not causative. This is particularly relevant with regards to the symptoms of AD given the numerous other significant pathophysiological events that occur in the disease, e.g. Aβ-deposition, tau phosphorylation, neuroinflammation, cell death (Kent et al., 2020; Scheltens et al., 2021; Sengoku, 2020). Thus, PNN loss could simply be an epiphenomenon of the progression of AD that does not play a significant role in the behavioural impairments common to the disease. This does not however diminish the significance of their loss given the breadth of studies showing synaptic, neuronal, and network level alterations after PNN disruption (Fawcett et al., 2022; Wingert & Sorg, 2021). Given recent studies that demonstrate that PNN manipulation can impact cognitive impairment in AD models, continued study utilizing more focal approaches to PNN manipulation in AD would be valuable (Yang et al., 2015, 2021). Another limitation in our study is observations from an expanded range of time points, especially those from earlier stages of 5xFAD disease. Given that Crapser et al. (2020) demonstrated PNN impairments within the subiculum and visual cortex of 5xFAD animals at 4-months of age and 18-months of age, it is possible that the deficits I observed are also apparent at earlier stages of disease, or more severe in later stages of disease. Two timepoints in the progression of PNN loss in 5xFAD are of particular interest. Firstly, do PNN deficits precede, coincide, or follow the onset of cognitive impairment in 5xFAD? For example, spontaneous alternation deficits in 5xFAD animals have been shown as early as 5-months of age (de Pins et al., 2019; Devi et al., 2015; El Gaamouch et al., 2020; Jawhar et al.,

2012; Oakley et al., 2006). An evaluation of PNN integrity within regions involved in this task such as the hippocampus or retrosplenial cortex preceding and following the emergence of this deficit would be informative (Anzalone et al., 2009; Lalonde, 2002). Secondly, given that PV cells loss has been shown in later stages of disease in the subiculum, well after PNN deficits emerge, is this also apparent in other regions of the brain (Crapser et al., 2020)? While this might not be informative for the behavioural symptoms of 5xFAD given that they emerge far earlier, a better understanding of the temporal relationship between PNN loss and subsequent PV+ loss could help better design evaluations of the mechanisms that underlie these alterations.

In addition to the limitations of Chapter 2, I would offer directions for future research into PNNs involvement in AD. Firstly, this experiment is similar only to that of Morawski et al. (2012) in offering a broad characterization of PNN integrity across numerous brain regions. I also evaluated these regions across time points considered within the literature to have modest or robust severities of disease based on their amyloid deposition (Devi et al., 2015; Devi & Ohno, 2010). This design is particularly informative when evaluating the 'where' and 'when' of PNN deficits emergence. I recommend this approach where available to other studies of PNN integrity in AD. While tissue availability is limited for human post-mortem studies, making this approach challenging, animal models of AD could benefit from far more thorough characterizations of pathological observations such as PNN loss in both time and breadth of brain regions examined. Secondly, further investigation is required to elucidate the mechanisms by which PNNs are lost in AD. I would acknowledge significant recent information in this regard by Crapser et al. (2020) demonstrating that microglia play a significant role in PNN loss in the subiculum and visual cortex of 5xFAD animals. Other studies have also highlighted the role of MMPs and ADAMTS as the primary enzymes for degrading PNNs and noted abnormalities in these enzymes in AD

(Bekris et al., 2012; Colciaghi et al., 2002; Kudo et al., 2023; Leake et al., 2000; Lorenzl et al., 2003; Martino Adami et al., 2022). Continued characterization of the relationship between these enzymes, PNNs, and how they might be altered in AD are encouraged. A final direction for future investigations is more focal evaluation of the impact of PNN degradation outside of the contexts of disease models. Given the significant and pervasive pathophysiology of AD, it's challenging to consider the consequences of PNN loss in isolation. Studies designed to manipulate PNNs with more focal areas of the brain might better inform our understanding how their loss contributes to cognitive impairment in AD. Similarly, more precise observations of the consequences of PNN degradation on cortical hyperexcitability, inhibitory networks, PV+ interneurons, and more would be informative to better understand the consequences of their loss in AD.

5.2 Chapter 3 Conclusions

In chapter 3, I demonstrate that targeted PNN degradation in the mPFC of otherwise healthy rats' results in cognitive impairment as measured on two tasks: the oddity preference task and crossmodal object recognition task. This finding is notable for several reasons. Firstly, it demonstrates that more targeted approaches to degrading PNNs within the mPFC can disturb cognition outside of the confounds of disease models. It also shows that some of the features of cognitive impairment observed in the polyI:C model of SZ, which features a much broader pathology, can be induced by degradation of PNNs within the mPFC alone (Ballendine et al., 2015; Howland et al., 2012; Lins et al., 2018). And lastly, it shows that even subtle manipulations of PNNs (~15% loss) can impact cognition. In comparison to the literature regarding mPFC involvement in crossmodal tasks, my results are consistent with human imaging studies that show involvement of the mPFC in crossmodal, multisensory tasks (Adams & Janata,

2002; Laurienti et al., 2003). Evidence of mPFC involvement in crossmodal object recognition in animal studies however is limited. One previous study has shown that lesions of the orbitofrontal cortex, but not mPFC, result in impairments in crossmodal object recognition (Reid et al., 2014). Thus, further studies evaluating mPFC contributions to crossmodal object recognition would prove valuable in reconciling these findings. The neural circuitry underlying the object oddity task is poorly characterized and thus my findings are difficult to evaluate in a broader context. Other studies have identified that the perirhinal cortex may be an area of interest in effective performance in this task (Bartko et al., 2007; Buckley et al., 2001). My results also show that PNN degradation within the mPFC had no observable impact on set-shifting or prepulse inhibition which test behavioural flexibility and sensorimotor gating, respectively. In this case, I demonstrate an absence of an effect of PNN degradation on two tests of cognitive functions that have demonstrated impairment in human subjects suffering from SZ and in the rat model our lab had described mPFC PNN deficits within (Floresco et al., 2009; Ibi et al., 2009; Lins et al., 2018; Paylor et al., 2016; Romero et al., 2010). With regards to prepulse inhibition, previous studies have shown an involvement of the mPFC in this test but there is also a wide array of other brain areas involved (Swerdlow et al., 2001). Similarly, operant set shifting tasks have been shown to involve processing of the mPFC, particularly in the strategy shifting component of the task as opposed to reversal learning (Bissonette et al., 2013; Brady & Floresco, 2015; Braff & Geyer, 1990; Swerdlow et al., 1994). As such, the subtle modulation of PNNs induced here may not have been sufficient to disturb the contributions of the mPFC to these behaviours. Together, these behavioural effects demonstrate the unique contributions of PNNs within the mPFC to impairments seen in animal models of SZ.

In addition to my behavioural results, I also evaluated PV+ interneuron integrity, including their expression of GAD67+ and PV+ protein after PNN degradation. There were no alterations in these measures or in gephyrin+ puncta on mature neuronal cells within the mPFC. Thus, my results are not indicative of disruption of ongoing PV+ cell activity or alterations in a basic assessment of inhibitory connectivity within the area of PNN degradation. Studies in SZ have demonstrated that while PV+ interneurons are typically spared in density, they present with significantly less PV+ protein and expression of GAD67+, an important GABA-synthesizing enzyme (Beasley et al., 2002; Fung et al., 2010; Glausier et al., 2014; Hashimoto et al., 2003; Mellios et al., 2009; Tooney & Chahl, 2004). Moreover, PV+ dysfunction appears central to numerous pathophysiological phenomena in SZ, which includes PNN deficits, and thus warranted this investigation (Gonzalez-Burgos & Lewis, 2012; Lewis et al., 2012). The results here should be interpreted with caution however, given that immunohistochemical staining cannot fully capture the integrity of PV+ interneuron activity. In previous studies utilizing electrophysiological approaches it has been shown that PNN degradation can increase the excitability of PV+ interneurons, decrease their firing rates, and increase their spike variability (Christensen et al., 2021; Lensjø et al., 2017; Liu et al., 2023). A consideration of the electrophysiological properties of PV+ cells within the mPFC after PNN degradation would be informative in this regard. A recent proposal for the mechanism by which PNN loss affects functions like memory was put forward by Fawcett et al., (2019). They suggest that PNN loss increases inhibitory inputs onto PV+ cells, which reduces their inhibitory output and increases the excitability of local networks. While this hypothesis is supported by experimental observations, they are not always consistent between different regions of the brain and warrant

further investigation into the mechanisms by which PNN loss within the mPFC affects performance on the tasks demonstrated here.

5.3 Chapter 4 Conclusions

Within the experiments in Chapter 4 I describe the impact of PNN degradation at two sites, the mPFC and RSC, on a battery of cognitive tests and mesoscale activity in mice. My results indicate that PNN degradation at either site did not have drastic impacts on cognition. Mice with PNN degradation within the RSC exhibited a subtle impairment on the crossmodal object recognition test as demonstrated by their inability to perform at above chance levels after degradation (controls performed better than chance). However, these animals also exhibited increases in exploratory activity during the task indicating factors other than working memory may have been impacted. PNN degradation at both sites had no impact on open field or spontaneous alternation behaviours, which assess locomotor and spatial working memory, respectively. Similarly, neither group showed disruption of their ability to perform the oddity object task. This contrasts results in Chapter 3 where I showed impairments in oddity task preference and crossmodal object recognition after ChABC infusions into the mPFC of rats (Paylor et al., 2018). This discrepancy would suggest that PNN degradation within the mPFC of mice does not have the same deleterious consequences for performance in these two tests as the manipulation does for rats. While I would hesitate to interpret the absence of a crossmodal object recognition deficit here in mice given the poor performance of these animals generally on the task, this is consistent with previous reports suggesting the mPFC is not necessary for this task (Reid et al., 2014). My observations after PNN degradation in the RSC on the crossmodal task are however consistent with a previous study demonstrating that RSC lesions can impair performance on this task (Hindley et al., 2014). A recent study in primates has also demonstrated

that aging related declines in PNNs surrounding PV+ cells within the RSC correlates with object recognition performance (Gray et al., 2023). Together, these studies and the data presented here suggest a role for the RSC in object recognition paradigms that warrants further evaluation.

In addition to my behavioural observations, I also show a deficit in PV+ interneurons within the RSC after PNN degradation. This finding contrasts with what I observed in both mice and rats after PNN degradation in the mPFC, which did not affect PV+ cells. This discrepancy could be due to regional differences in both PNN and PV+ cells. This result is especially interesting in comparison to other studies evaluating PV+ cells after PNN degradation, which most often show spared PV+ cell density but a loss of PV expression within PV cells (Yamada et al., 2015). Notably, in most studies of PNN degradation using enzymes like ChABC the duration of effect is much shorter. Even in the experiment in Chapter 3, I utilized a single injection of ChABC and evaluated immunostaining ~25 days later. Here, I utilized a prolonged duration of ChABC expression. Previous studies have demonstrated that without intact PNNs, neurons typically surrounded by them can become vulnerable to stressors like oxidative stress or other disease related pathologies (Cabungcal et al., 2013; Crapser et al., 2020; Ruden et al., 2021; Suttkus et al., 2014). Thus, our results indicate that in after prolonged absence of PNNs can have consequences for cellular integrity beyond that of one-time disruptive events. These findings warrant further investigation into how PNN disruption can impact host neurons when their exposure is prolonged, which is likely more clinically relevant.

Lastly, I utilized wide field optical imaging to evaluate broader changes in cortical activity and connectivity after PNN degradation within the RSC. This manipulation did not result in changes in spontaneous or evoked activity as measured by calcium fluorescence. To my knowledge, there are no other studies utilizing wide field optical imaging to evaluate changes in

cortical activity after localized PNN degradation. Similarly, other mesoscale imaging techniques such as functional magnetic resonance imaging or diffusion tensor imaging have not been applied in this regard despite their widespread use in disorders featuring PNN loss such as SZ. I would encourage further investigation into PNN degradation with these techniques as they could be insightful into determining the how PNN loss can affect broader cortical activity and connectivity. Despite leaving cortical activity patterns unaltered, I did observe a decrease in the power of low frequency activity after PNN degradation in the RSC, potentially mediated by the loss of PV+ cells I observed. Administration of NMDAR antagonists such as ketamine which can induce SZ-like symptoms and have also been shown to decrease delta activity (Hong et al., 2010; Hunt et al., 2010; Kiss et al., 2011; Mahdavi et al., 2020). Coincidentally, ketamine can also result in PV+ interneuron dysfunction and PNN loss (Kaushik et al., 2021; Keilhoff et al., 2004; Koh et al., 2016; Matuszko et al., 2017; Venturino et al., 2021; Z. Zhou et al., 2015). Thus, a common feature of PNN degradation shown here and NMDAR antagonists might be reductions in PV+ cell activity and their contributions delta activity. Within the broader SZ literature, delta activity is also impaired during task-performance and delta coherence between regions is decreased when attending to auditory stimuli (Bates et al., 2009; Ford et al., 2002). These studies show that decreased delta and PV dysfunction is a common feature among my findings, SZ studies, and in pharmacological treatments that mimic SZ-like symptoms. One possible link between these observations is Reelin, a molecule involved in NMDA receptor organization that is readily integrated into PNNs has been shown to be abnormal in SZ (Grayson et al., 2005; Guidotti et al., 2000; Impagnatiello et al., 1998). These converging findings warrant more focused investigation in the future to describe the relationship between PV+ interneurons and delta activity, and how PNN loss might affect them.

5.4 General Conclusions

While the effects of PNN loss here varied based on species, region, and task, evaluation of my data along with the broader body of PNN literature informs us that their manipulation can impact cognitive function. How this manipulation affects cognition however is less coherent, but nonetheless apparent at the synaptic, cellular, and network level. Firstly, from a synaptic perspective intact PNNs play an important role in receptor clustering and mobility within synapses (Chang et al., 2010; Favuzzi et al., 2017; Lee et al., 2017). Their disruption at this level could affect the extrasynaptic diffusion of receptors, allowing for exchange of desensitized synapses which would otherwise be restricted in the presence of a PNN (Frischknecht et al., 2009). These alterations could underlie the hyperexcitability of interneurons, as new sensitized receptors are recycled into synapses. Similarly, increases in lateral mobility of receptors might underlie the alterations in LTP and LTD observed after PNN degradation (Brakebusch et al., 2002; Zhou et al., 2001). At a cellular level, the loss of PNNs removes an important support for ongoing cellular function. Evidence of PNNs role in cation buffering and ion sorting would suggest that their loss disrupts their contributions to the significant physiological demands of host neurons such as PV cells (Burket et al., 2021; Morawski et al., 2015; Reinert et al., 2022). Their loss may also strip neurons of an important buffer against pathological stressors such as oxidative stress (Cabungcal et al., 2013). The incredibly high firing rates of PV+ cells in particular subject them to significant metabolic and physiological stress, even in healthy conditions (Ruden et al., 2021). This is only further exacerbated in conditions like AD or SZ, where oxidative stress or cellular toxicity (e.g. Aβ and tau accumulation) are elevated. In this case, their absence confers an elevated vulnerability to host neurons in these conditions (Cabungcal et al., 2013; Crapser et al., 2020; Miyata et al., 2007). Consistent with this, PV+ cell

dysfunction is often shared in contexts healthy or otherwise where PNNs are disrupted activity (Enwright et al., 2016; Fujikawa et al., 2021; Kilonzo et al., 2020). PNNs also support the contributions of PV+ cells to network activity. The combined effects of PNN loss on synaptic and cellular activity typically results in a decrease in inhibitory output from PV+ cells (Fawcett et al., 2022; Wingert & Sorg, 2021). This in turn reduces inhibitory drive within networks, tilting the balance of excitation and inhibition towards excitability. Consistent with this, cortical hyperexcitability is observed after PNN degradation and in diseases such as SZ where PNNs are deficient (Daskalakis et al., 2007; Heckers et al., 1998; Hoffman & Cavus, 2002; Wen et al., 2018). The loss of PNN not only affects overall inhibitory activity but also the important network regulating properties of inhibitory activity and PV+ cells. This is readily demonstrated in observations of gamma asynchrony after PNN loss (Cabungcal et al., 2013; Carceller et al., 2020; Lensjø et al., 2017). The disruption of PV+ cell activity here could have significant impacts within local and broader cortical network. Gamma oscillations are integral to the numerous cognitive functions and have been shown to contribute to cognitive impairment in CNS diseases where they are dysfunctional such as AD and SZ (Buzsáki & Wang, 2012; Fries, 2005, 2009; Lesh et al., 2011). Given the support that PNNs provide to the physiological demands of highly active neurons, it is notable that gamma deficits are often more pronounced during task-evoked activity, where neural activity is upregulated (Farzan et al., 2010; Sun et al., 2011; Williams & Boksa, 2010). In summary, PNNs make important contributions to ongoing neural function at multiple levels, ranging from ion buffering and sorting to broader scale synchrony of cortical activity and behavioural outputs. Many of these effects are likely mediated through alterations in host neurons, which are most commonly PV+ interneurons, but also include other inhibitory interneuron types and in some cases pyramidal cells. Continued

investigation into how PNN disruption affects cognition would benefit from localized degradation studies like the ones utilized here. These findings can be readily translated back into animal models of CNS diseases where cognitive impairment and PNN loss are shared features.

Given that I observed object recognition impairments of varying degrees in each of my experiments, it warrants consideration how PNN loss could affect this task specifically. Beyond the general impacts of PNN loss on synaptic, cellular, and network function discussed above in cognition, disruption of PV+ interneurons has also shown to have a direct impact on discrimination tasks. PV+ cell activity is thought to contributes to numerous inhibitory network functions, but particularly relevant to this task are their role in lateral inhibition and pattern separation (Braganza et al., 2020; Espinoza et al., 2018; Guzman et al., 2019; Yang et al., 2017). Lateral inhibition describes the capacity of excited neurons to inhibit neighbouring or competing neural assemblies. In addition to experimental observations of PV+ cells involvement in lateral inhibition, other studies have demonstrated that single EPSPs in a PV+ cell from an impinging pyramidal cell can elicit a response from that PV neuron (Jouhanneau et al., 2018). Given their high degree of local connectivity and perisomatic innervation, they can readily inhibit a significant proportion of local cells, called blanket inhibition (Carceller et al., 2020; Freund & Katona, 2007; Packer & Yuste, 2011). These processes plays a critical role in pattern separation whereby inputs for similar but unique stimuli are transformed into more distinct patterns of activity to facilitate discrimination (Cayco-Gajic & Silver, 2019). In this case, PV+ cells facilitate a theorized ‘winner-takes-all’ firing pattern, whereby the excitation of a neural assembly representing one stimulus inhibits activity within competing assemblies (Kurt et al., 2008; Plenz, 2003; Wingert & Sorg, 2021). Together, these functions are though to play an integral role in discrimination tasks such as object recognition where two potentially similar

objects must be differentiated. The demonstrated impact of PNN loss on PV+ cell activity suggests that their manipulation could impact these inhibitory network functions. In support of this, a recent study showed that PNN degradation around grid cells decreased the stability of neural representations of familiar environments after introduction of a novel environment (Christensen et al., 2021). This suggests that in the absence of PNNs, pattern separation is diminished and competing assemblies of neural activity representing two environments may interfere with each other. The effects of PNN degradation also induce interference in drug-administration paradigms. Rats trained on cocaine self-administration, where one lever press results in one cocaine administration, do not exhibit impairment in cue recall after PNN disruption (Wingert & Sorg, 2021). However, if PNNs are degraded, these animals do exhibit cue recall impairments when the ruleset (e.g., fixed interval of one press becomes random interval) is changed. Studies directly manipulating PV+ cells are also supportive of this role in pattern separation. Work by Zhu et al., (2015) showed that in the visual cortex, patterns of visual activity observed in response to the presentation of visual images could be coded precisely for the specific video frame the animals were currently observing. Thus, the authors could predict the image that the animal was viewing simply by evaluating neural activity (Zhu et al., 2015). However, after optogenetic suppression of PV+ cells, the classification of frames became significantly less reliable, indicating increased overlap between the neural activation patterns for these stimuli. This is consistent with another study within the visual cortex showing that optogenetic suppression of PV+ cells increased both overall activity and the cellular overlap between two representations that were previously dissimilar (Agetsuma et al., 2018). Together, these studies offer a potential mechanism by which PV disruption after PNN degradation could underlie impairments in discriminating between two stimuli. They also offer an intriguing

opportunity to further probe object recognition paradigms with competing or interfering stimuli, which could further exacerbate the deficits observed after PNN loss.

Limitations and Future Directions

Despite both direct and converging evidence that PNNs might play a significant role in the pathophysiology and symptoms of SZ and other CNS diseases, numerous questions about their involvement remain. Firstly, how do PNN deficits develop in disorders like SZ? From the first study demonstrating a reduction of PNNs in the amygdala and entorhinal cortex in SZ, it was observed that there were massive increases in CSPG-rich glial cells within the same regions that deficits were observed (Pantazopoulos et al., 2010). This might be taken as indicative of an active degradation and phagocytosis of PNN that occurs during maturity. Consistent with this, gene profiling studies and gene-wide association scans have identified that genes encoding for enzymes that degrade PNNs such as matrix metalloproteinases (MMPs) and a disintegrin and metalloproteinase with thrombospondin motifs (ADAMTSs) are altered in SZ (Bespalova et al., 2012; Dow et al., 2011; McGrath et al., 2013; Pietersen et al., 2014). Microglia have also been shown to have an important role in the regulation of PNNs and in disease models where PNNs are disrupted, and inhibiting microglia can rescue PNN deficits (Crapser et al., 2020). However, significant evidence also exists to suggest that SZ is a neurodevelopmental disorder (Howes & Shatalina, 2022; Owen et al., 2011; Rapoport et al., 2012). Given the relationship between PNNs and critical periods of plasticity, it is also feasible that disruptions to antecedent developmental steps such as PV+ maturation could result in decreased PNN formation (Dityatev et al., 2007; Takesian & Hensch, 2013). Numerous studies have shown that interventions which impede progression of critical periods of plasticity prior to PNN development can impair their formation (Balmer et al., 2009; McRae et al., 2007a; Sur et al., 1988; Ye & Miao, 2013). In this context,

PNN abnormalities in SZ might be a result of impaired development rather than active degradation (Berretta et al., 2015). Support for this perspective can be drawn from studies suggesting that there is abnormalities in genes encoding for CSPG components of PNNs (Buxbaum et al., 2008; Cichon et al., 2011; Mühleisen et al., 2012; Pantazopoulos et al., 2015). Unfortunately, to date there is no conclusive evidence to support either active degradation or failures in development as the primary mechanisms by which PNNs are deficient in SZ. If the former, developing therapies aimed at preventing this degradation would be applicable not only in SZ but also in other CNS diseases like AD which similarly show elevated levels of MMPs (Gu et al., 2020; Adami et al., 2022; Wang et al., 2014). If the latter is true and PNN deficits are a result of failed formation, then there are limited options available currently. This is one among several outstanding issues within the field of PNN research, which is that we have abundant means to degrade PNNs but few to promote their growth. Genetic strains of animals that overexpress PNN components to increase PNN formation have not been widely demonstrated and would likely be ill suited as therapies in clinical contexts. This is an understudied aspect of PNN research and would significantly undercut future discoveries addressing why PNNs fail to form if we cannot identify means to encourage their healthy development.

In addition to the lack of PNN-promoting strategies currently available, several other limitations are apparent in the field more broadly that are particularly relevant to the work presented here. Foremost among them is the use of ChABC to degrade PNNs. I utilized ChABC in both of my PNN disruption studies and it is likely the most common method applied in the larger body of literature. There are two major issues with this approach. Firstly, ChABC degrades CSPGs by cleaving their CS-GAG chains. While this is highly effective in reducing PNNs it also has a much more generalized impact on the ECM. Other ECM components such as

the interstitial matrix and perinodal matrices are also disrupted by ChABC cleavage, although that is not readily acknowledged in studies utilizing ChABC. This means that the contributions of other ECM structures that are disrupted by ChABC are undervalued and in many cases, may contribute to any consequences observed after treatment. Given estimates that 2% of the total CSPGs in the brain are present within PNNs and the remaining 98% in the diffuse matrix, this issue is significant (Deepa et al., 2006). In this regard, future studies should consider whether other means to degrade PNNs are better suited to their experiments. Endogenous enzymes like MMPs and ADAMTSs are possible candidates (Mohamedi et al., 2020). Among ADAMTSs are enzymes which are thought to degrade specific CSPGs, such as aggrecanases (ADAMTS-4 and -5) that specifically degrade aggrecan (Verma & Dalal, 2011; Westling et al., 2002). This is a particularly appealing target given that aggrecan is expressed in nearly all PNNs (Deepa et al., 2006; Matthews et al., 2002). Other ADAMTSs have also been shown to have varying specificity to CSPGs like versican and brevican and may be well suited to certain studies (Cross et al., 2005; Gary et al., 1998; Nakada et al., 2005; Stanton et al., 2011). Alternative approaches such as overexpression of C6S in animals lacking chondroitin-6-sulfotransferase, which prevents aggrecan accumulation into PNNs, might also be considered as more targeted means to PNN disruption (Miyata et al., 2012; Miyata & Kitagawa, 2016). The second major issue with utilizing ChABC disruption or any PNN degrading enzyme is that these manipulations are often not only a ‘net loss’ but also increase the availability of other molecules within CNS tissues. For example, C4S is cleaved from PNNs after enzymatic degradation and has significant growth-inhibiting properties within CNS tissues. C4S is highly expressed in the adult brain relative to C6S, which is growth-promoting and primarily expressed in development and studies have shown that manipulation the C4S to C6S ratio the brain can impact cortical plasticity (Miyata et al., 2012).

The release of CS chains could also have broader impacts on cognition which is demonstrated by a study that administered Cat316, an antibody against C4S, and found that it had similar effects to that of ChABC in restoring memory loss in a mouse model of tauopathy (Yang et al., 2017). PNNs also bind and sequester numerous other signaling molecules such as neurotrophins, OTX2, semaphorin 3A, and reelin, among others (Beurdeley et al., 2012; Dick et al., 2013; Lensjø et al., 2017; Martínez-Cerdeño & Clascá, 2002; Pesold et al., 1999). Again, the degradation of PNNs in this case could release these molecules into the extracellular milieu with their own neuroactive effects. Together these studies demonstrate that PNN disruption with enzymes like ChABC can have broader effects than simply degrading PNNs and that the degraded components of PNN can exert their own effects within the CNS. These issues should be carefully considered in future studies utilizing ChABC.

Another limitation within the current field is the use of WFA to label and detect PNNs in CNS tissues. While this is by far the most widely utilized technique to identify PNNs, but not all PNNs are detectable with WFA. In studies utilizing broader sets of immunohistochemical markers for PNNs, diverse subpopulations of PNNs have been identified. These markers include Cat315^{+} and Cat316^{+}, 3B3, and other antibodies directly against the CSPG components of PNNs. For example, in the mouse visual cortex, while almost all Cat316^{+} PNNs are also positive for WFA, ~16.5% of PNNs were positive for Cat315^{+} but not labelled with WFA (Miyata et al., 2018). Within WFA-expressing PNNs, those that also expressed Cat315^{+} had significantly lower WFA immunofluorescence than those than co-expressed Cat316^{+}. This suggests that there are subpopulations of PNNs with higher or lower WFA-staining that are labelled by Cat315^{+} and Cat316^{+}, respectively, and there are other PNNs uniquely labelled by Cat315^{+}alone (Miyata et al., 2018). In the lateral nucleus of the human amygdala, WFA labels ~54% and 80% of PNNs that

are also immunoreactive for aggrecan or 3B3, respectively (Pantazopoulos et al., 2015), indicating a significant population of aggrecan-labelled but WFA-labelled PNNs. Another study described a broadly distributed population of brevican positive PNNs that are not labelled with WFA (Ajmo et al., 2008). Together, these observations clearly demonstrate the significant heterogeneity amongst PNNs and show that WFA alone provides an incomplete picture of PNN integrity as whole. Future studies would benefit from consideration of this heterogeneity when selecting markers to identify PNNs. It also warrants further consideration whether these unique PNN compositions are consistently affiliated with specific cell types. As a final comment regarding issues related to PNN-labeling in conventional experimental studies, I would point out the lack of available in vivo imaging techniques for PNNs. Other in vivo imaging tools have seen immense progress over the last several decades but applying these techniques in PNN experiments has suffered from a disconnect between real time imaging of cellular activity and a lack of available PNN detection methods in parallel. However, a very recent publication demonstrating in vivo labeling and imaging of PNNs may have broken ground on this issue (Benbenishty et al., 2023). I would encourage further innovation in this area and challenge future studies evaluating the consequences of PNN degradation in vivo to also make efforts to visualize PNNs.

Conclusion

In summary, the experiments presented here join a growing body of literature which demonstrates PNNs involvement in CNS diseases and demonstrate the subtle, but noticeable impacts they can have on cognitive function. A significant work remains to better describe the unique contributions of PNNs to cognitive functions or behaviours in other domains. I encourage continued study utilizing targeted disruption of PNNs in otherwise healthy animals, as was

demonstrated here. These findings can be translated back into models of disease to describe the functional consequences of PNN loss within them. Additional study into the mechanisms by which PNNs come to be deficient in CNS diseases is also critical, particularly as we consider therapies that might mitigate these effects. I eagerly anticipate future discovery in this regard.

Bibliography

Adams, R. B., & Janata, P. (2002). A Comparison of Neural Circuits Underlying Auditory and Visual Object Categorization. *NeuroImage*, *16*(2), 361–377. https://doi.org/10.1006/nimg.2002.1088

Agetsuma, M., Hamm, J. P., Tao, K., Fujisawa, S., & Yuste, R. (2018). Parvalbumin-Positive Interneurons Regulate Neuronal Ensembles in Visual Cortex. *Cerebral Cortex*, *28*(5), 1831–1845. https://doi.org/10.1093/cercor/bhx169

Aggleton, J. P., Keen, S., Warburton, E. C., & Bussey, T. J. (1997). Extensive Cytotoxic Lesions Involving Both the Rhinal Cortices and Area TE Impair Recognition But Spare Spatial Alternation in the Rat. *Brain Research Bulletin*, *43*(3), 279–287. https://doi.org/10.1016/S0361-9230(97)00007-5

Aggleton, J. P., & Nelson, A. J. D. (2020). Distributed interactive brain circuits for object-in-place memory: A place for time? *Brain and Neuroscience Advances*, *4*, 2398212820933471. https://doi.org/10.1177/2398212820933471

Ajmo, J. M., Bailey, L. A., Howell, M. D., Cortez, L. K., Pennypacker, K. R., Mehta, H. N., Morgan, D., Gordon, M. N., & Gottschall, P. E. (2010). Abnormal post-translational and extracellular processing of brevican in plaque-bearing mice over-expressing APPsw. *Journal of Neurochemistry*, *113*(3), 784–795. https://doi.org/10.1111/j.1471-4159.2010.06647.x

Ajmo, J. M., Eakin, A. K., Hamel, M. G., & Gottschall, P. E. (2008). Discordant localization of WFA reactivity and brevican/ADAMTS-derived fragment in rodent brain. *BMC Neuroscience*, *9*(1), 14. https://doi.org/10.1186/1471-2202-9-14

Akhtar, A., Gupta, S. M., Dwivedi, S., Kumar, D., Shaikh, Mohd. F., & Negi, A. (2022). Preclinical Models for Alzheimer's Disease: Past, Present, and Future Approaches. *ACS Omega*, *7*(51), 47504–47517. https://doi.org/10.1021/acsomega.2c05609

Alcaide, J., Guirado, R., Crespo, C., Blasco-Ibáñez, J. M., Varea, E., Sanjuan, J., & Nacher, J. (2019). Alterations of perineuronal nets in the dorsolateral prefrontal cortex of neuropsychiatric patients. *International Journal of Bipolar Disorders*, *7*(1), 24. https://doi.org/10.1186/s40345-019-0161-0

Alexander, A. S., Place, R., Starrett, M. J., Chrastil, E. R., & Nitz, D. A. (2023). Rethinking retrosplenial cortex: Perspectives and predictions. *Neuron*, *111*(2), 150–175. https://doi.org/10.1016/j.neuron.2022.11.006

Ali, F., Baringer, S. L., Neal, A., Choi, E. Y., & Kwan, A. C. (2019). Parvalbumin-Positive Neuron Loss and Amyloid-β Deposits in the Frontal Cortex of Alzheimer's Disease-Related Mice. *Journal of Alzheimer's Disease: JAD*, *72*(4), 1323–1339. https://doi.org/10.3233/JAD-181190

Alvarado-Alanis, P., León-Ortiz, P., Reyes-Madrigal, F., Favila, R., Rodríguez-Mayoral, O., Nicolini, H., Azcárraga, M., Graff-Guerrero, A., Rowland, L. M., & de la Fuente-Sandoval, C. (2015). Abnormal white matter integrity in antipsychotic-naïve first-episode psychosis patients assessed by a DTI principal component analysis. *Schizophrenia Research*, *162*(1), 14–21. https://doi.org/10.1016/j.schres.2015.01.019

Alzheimer's Association. (2019). 2019 Alzheimer's disease facts and figures. *Alzheimer's & Dementia*, *15*(3), 321–387. https://doi.org/10.1016/j.jalz.2019.01.010

Amedi, A., von Kriegstein, K., van Atteveldt, N. M., Beauchamp, M. S., & Naumer, M. J. (2005). Functional imaging of human crossmodal identification and object recognition.

Experimental Brain Research, *166*(3), 559–571. https://doi.org/10.1007/s00221-005-2396-5

Anderson, M. D., Paylor, J. W., Scott, G. A., Greba, Q., Winship, I. R., & Howland, J. G. (2020). ChABC infusions into medial prefrontal cortex, but not posterior parietal cortex, improve the performance of rats tested on a novel, challenging delay in the touchscreen TUNL task. *Learning & Memory (Cold Spring Harbor, N.Y.)*, *27*(6), 222–235. https://doi.org/10.1101/lm.050245.119

Angelov, D. N., Walther, M., Streppel, M., Guntinas-Lichius, O., Neiss, W. F., Probstmeier, R., & Pesheva, P. (1998). Tenascin-R Is Antiadhesive for Activated Microglia that Induce Downregulation of the Protein after Peripheral Nerve Injury: A New Role in Neuronal Protection. *Journal of Neuroscience*, *18*(16), 6218–6229. https://doi.org/10.1523/JNEUROSCI.18-16-06218.1998

Antonoudiou, P., Tan, Y. L., Kontou, G., Upton, A. L., & Mann, E. O. (2020). Parvalbumin and Somatostatin Interneurons Contribute to the Generation of Hippocampal Gamma Oscillations. *Journal of Neuroscience*, *40*(40), 7668–7687. https://doi.org/10.1523/JNEUROSCI.0261-20.2020

Anzalone, S., Roland, J., Vogt, B., & Savage, L. (2009). Acetylcholine efflux from retrosplenial areas and hippocampal sectors during maze exploration. *Behavioural Brain Research*, *201*(2), 272–278. https://doi.org/10.1016/j.bbr.2009.02.023

Arai, H., Emson, P. C., Mountjoy, C. Q., Carassco, L. H., & Heizmann, C. W. (1987). Loss of parvalbumin-immunoreactive neurones from cortex in Alzheimer-type dementia. *Brain Research*, *418*(1), 164–169. https://doi.org/10.1016/0006-8993(87)90974-7

Aston, C., Jiang, L., & Sokolov, B. P. (2004). Microarray analysis of postmortem temporal cortex from patients with schizophrenia. *Journal of Neuroscience Research*, *77*(6), 858–866. https://doi.org/10.1002/jnr.20208

Bai, W., Xia, M., Liu, T., & Tian, X. (2016). Aβ1-42-induced dysfunction in synchronized gamma oscillation during working memory. *Behavioural Brain Research*, *307*, 112–119. https://doi.org/10.1016/j.bbr.2016.04.003

Baig, S., Wilcock, G. K., & Love, S. (2005a). Loss of perineuronal net N-acetylgalactosamine in Alzheimer's disease. *Acta Neuropathologica*, *110*(4), 393–401. https://doi.org/10.1007/s00401-005-1060-2

Baig, S., Wilcock, G. K., & Love, S. (2005b). Loss of perineuronal net N-acetylgalactosamine in Alzheimer's disease. *Acta Neuropathologica*, *110*(4), 393–401. https://doi.org/10.1007/s00401-005-1060-2

Ballendine, S. A., Greba, Q., Dawicki, W., Zhang, X., Gordon, J. R., & Howland, J. G. (2015a). Behavioral alterations in rat offspring following maternal immune activation and ELR-CXC chemokine receptor antagonism during pregnancy: Implications for neurodevelopmental psychiatric disorders. *Progress in Neuro-Psychopharmacology and Biological Psychiatry*, *57*, 155–165. https://doi.org/10.1016/j.pnpbp.2014.11.002

Ballendine, S. A., Greba, Q., Dawicki, W., Zhang, X., Gordon, J. R., & Howland, J. G. (2015b). Behavioral alterations in rat offspring following maternal immune activation and ELR-CXC chemokine receptor antagonism during pregnancy: Implications for neurodevelopmental psychiatric disorders. *Progress in Neuro-Psychopharmacology and Biological Psychiatry*, *57*, 155–165. https://doi.org/10.1016/j.pnpbp.2014.11.002

Balmer, T. S. (2016). Perineuronal Nets Enhance the Excitability of Fast-Spiking Neurons. *ENeuro*, *3*(4), ENEURO.0112-16.2016. https://doi.org/10.1523/ENEURO.0112-16.2016

Balmer, T. S., Carels, V. M., Frisch, J. L., & Nick, T. A. (2009). Modulation of Perineuronal Nets and Parvalbumin with Developmental Song Learning. *Journal of Neuroscience*, *29*(41), 12878–12885. https://doi.org/10.1523/JNEUROSCI.2974-09.2009

Banerjee, S. B., Gutzeit, V. A., Baman, J., Aoued, H. S., Doshi, N. K., Liu, R. C., & Ressler, K. J. (2017). Perineuronal Nets in the Adult Sensory Cortex Are Necessary for Fear Learning. *Neuron*, *95*(1), 169-179.e3. https://doi.org/10.1016/j.neuron.2017.06.007

Barker, G. R. I., Bird, F., Alexander, V., & Warburton, E. C. (2007). Recognition Memory for Objects, Place, and Temporal Order: A Disconnection Analysis of the Role of the Medial Prefrontal Cortex and Perirhinal Cortex. *Journal of Neuroscience*, *27*(11), 2948–2957. https://doi.org/10.1523/JNEUROSCI.5289-06.2007

Bartko, S. J., Winters, B. D., Cowell, R. A., Saksida, L. M., & Bussey, T. J. (2007a). Perceptual functions of perirhinal cortex in rats: Zero-delay object recognition and simultaneous oddity discriminations. *Journal of Neuroscience*, *27*(10), 2548–2559. https://doi.org/10.1523/JNEUROSCI.5171-06.2007

Bartko, S. J., Winters, B. D., Cowell, R. A., Saksida, L. M., & Bussey, T. J. (2007b). Perceptual Functions of Perirhinal Cortex in Rats: Zero-Delay Object Recognition and Simultaneous Oddity Discriminations. *Journal of Neuroscience*, *27*(10), 2548–2559. https://doi.org/10.1523/JNEUROSCI.5171-06.2007

Bartos, M., & Elgueta, C. (2012). Functional characteristics of parvalbumin- and cholecystokinin-expressing basket cells. *The Journal of Physiology*, *590*(4), 669–681. https://doi.org/10.1113/jphysiol.2011.226175

Basar-Eroglu, C., Brand, A., Hildebrandt, H., Karolina Kedzior, K., Mathes, B., & Schmiedt, C. (2007). Working memory related gamma oscillations in schizophrenia patients. *International Journal of Psychophysiology*, *64*(1), 39–45. https://doi.org/10.1016/j.ijpsycho.2006.07.007

Bates, A. T., Kiehl, K. A., Laurens, K. R., & Liddle, P. F. (2009). Low-frequency EEG oscillations associated with information processing in schizophrenia. *Schizophrenia Research*, *115*(2), 222–230. https://doi.org/10.1016/j.schres.2009.09.036

Baxter, P. S., Bell, K. F. S., Hasel, P., Kaindl, A. M., Fricker, M., Thomson, D., Cregan, S. P., Gillingwater, T. H., & Hardingham, G. E. (2015). Synaptic NMDA receptor activity is coupled to the transcriptional control of the glutathione system. *Nature Communications*, *6*(1), Article 1. https://doi.org/10.1038/ncomms7761

Beasley, C. L., Zhang, Z. J., Patten, I., & Reynolds, G. P. (2002). Selective deficits in prefrontal cortical GABAergic neurons in schizophrenia defined by the presence of calcium-binding proteins. *Biological Psychiatry*, *52*(7), 708–715. https://doi.org/10.1016/S0006-3223(02)01360-4

Bekku, Y., Rauch, U., Ninomiya, Y., & Oohashi, T. (2009). Brevican distinctively assembles extracellular components at the large diameter nodes of Ranvier in the CNS. *Journal of Neurochemistry*, *108*(5), 1266–1276. https://doi.org/10.1111/j.1471-4159.2009.05873.x

Bekku, Y., Saito, M., Moser, M., Fuchigami, M., Maehara, A., Nakayama, M., Kusachi, S., Ninomiya, Y., & Oohashi, T. (2012). Bral2 is indispensable for the proper localization of brevican and the structural integrity of the perineuronal net in the brainstem and cerebellum. *Journal of Comparative Neurology*, *520*(8), 1721–1736. https://doi.org/10.1002/cne.23009

Bekris, L. M., Lutz, F., Li, G., Galasko, D. R., Farlow, M. R., Quinn, J. F., Kaye, J. A., Leverenz, J. B., Tsuang, D. W., Montine, T. J., Peskind, E. R., & Yu, C.-E. (2012). ADAM10 expression and promoter haplotype in Alzheimer's disease. *Neurobiology of Aging*, *33*(9), 2229.e1-2229.e9. https://doi.org/10.1016/j.neurobiolaging.2012.03.013

Belforte, J. E., Zsiros, V., Sklar, E. R., Jiang, Z., Yu, G., Li, Y., Quinlan, E. M., & Nakazawa, K. (2010). Postnatal NMDA receptor ablation in corticolimbic interneurons confers schizophrenia-like phenotypes. *Nature Neuroscience*, *13*(1), Article 1. https://doi.org/10.1038/nn.2447

Benbenishty, A., Peled-Hajaj, S., Krishnaswamy, V. R., Har-Gil, H., Havusha-Laufer, S., Ruggiero, A., Slutsky, I., Blinder, P., & Sagi, I. (2023). Longitudinal in vivo imaging of perineuronal nets. *Neurophotonics*, *10*(1), 015008. https://doi.org/10.1117/1.NPh.10.1.015008

Benoit, L. J., Holt, E. S., Teboul, E., Taliaferro, J. P., Kellendonk, C., & Canetta, S. (2020). Medial prefrontal lesions impair performance in an operant delayed nonmatch to sample working memory task. *Behavioral Neuroscience*, *134*, 187–197. https://doi.org/10.1037/bne0000357

Ben-Shaul, Y. (2017). OptiMouse: A comprehensive open source program for reliable detection and analysis of mouse body and nose positions. *BMC Biology*, *15*(1), 41. https://doi.org/10.1186/s12915-017-0377-3

Berretta, S., Pantazopoulos, H., Markota, M., Brown, C., & Batzianouli, E. T. (2015a). Losing the sugar coating: Potential impact of perineuronal net abnormalities on interneurons in schizophrenia. *Schizophrenia Research*, *167*(1–3), 18–27. https://doi.org/10.1016/j.schres.2014.12.040

Berretta, S., Pantazopoulos, H., Markota, M., Brown, C., & Batzianouli, E. T. (2015b). Losing the sugar coating: Potential impact of perineuronal net abnormalities on interneurons in schizophrenia. *Schizophrenia Research*, *167*(1), 18–27. https://doi.org/10.1016/j.schres.2014.12.040

Bespalova, I. N., Angelo, G. W., Ritter, B. P., Hunter, J., Reyes-Rabanillo, M. L., Siever, L. J., & Silverman, J. M. (2012). Genetic Variations in the ADAMTS12 Gene are Associated with Schizophrenia in Puerto Rican Patients of Spanish Descent. *NeuroMolecular Medicine*, *14*(1), 53–64. https://doi.org/10.1007/s12017-012-8169-y

Beurdeley, M., Spatazza, J., Lee, H. H. C., Sugiyama, S., Bernard, C., Nardo, A. A. D., Hensch, T. K., & Prochiantz, A. (2012). Otx2 Binding to Perineuronal Nets Persistently Regulates Plasticity in the Mature Visual Cortex. *Journal of Neuroscience*, *32*(27), 9429–9437. https://doi.org/10.1523/JNEUROSCI.0394-12.2012

Binette, F., Cravens, J., Kahoussi, B., Haudenschild, D. R., & Goetinck, P. F. (1994). Link protein is ubiquitously expressed in non-cartilaginous tissues where it enhances and stabilizes the interaction of proteoglycans with hyaluronic acid. *Journal of Biological Chemistry*, *269*(29), 19116–19122. https://doi.org/10.1016/S0021-9258(17)32282-2

Bissonette, G. B., Powell, E. M., & Roesch, M. R. (2013a). Neural structures underlying set-shifting: Roles of medial prefrontal cortex and anterior cingulate cortex. *Behavioural Brain Research*, *250*, 91–101. https://doi.org/10.1016/j.bbr.2013.04.037

Bissonette, G. B., Powell, E. M., & Roesch, M. R. (2013b). Neural structures underlying set-shifting: Roles of medial prefrontal cortex and anterior cingulate cortex. *Behavioural Brain Research*, *250*, 91–101. https://doi.org/10.1016/j.bbr.2013.04.037

Bitanihirwe, B. K. Y., & Woo, T.-U. W. (2011). Oxidative stress in schizophrenia: An integrated approach. *Neuroscience & Biobehavioral Reviews*, *35*(3), 878–893. https://doi.org/10.1016/j.neubiorev.2010.10.008

Bitanihirwe, B. K. Y., & Woo, T.-U. W. (2014). Perineuronal nets and schizophrenia: The importance of neuronal coatings. *Neuroscience & Biobehavioral Reviews*, *45*, 85–99. https://doi.org/10.1016/j.neubiorev.2014.03.018

Bitanihirwe, B., Lim, M., Kelley, J., Kaneko, T., & Woo, T. (2009). Glutamatergic deficits and parvalbumin-containing inhibitory neurons in the prefrontal cortex in schizophrenia. *BMC Psychiatry*, *9*(1), 71. https://doi.org/10.1186/1471-244X-9-71

Bitzenhofer, S. H., Pöpplau, J. A., & Hanganu-Opatz, I. (2020). Gamma activity accelerates during prefrontal development. *ELife*, *9*, e56795. https://doi.org/10.7554/eLife.56795

Bluhm, R. L., Miller, J., Lanius, R. A., Osuch, E. A., Boksman, K., Neufeld, R. W. J., Théberge, J., Schaefer, B., & Williamson, P. C. (2009). Retrosplenial cortex connectivity in schizophrenia. *Psychiatry Research: Neuroimaging*, *174*(1), 17–23. https://doi.org/10.1016/j.pscychresns.2009.03.010

Bouter, Y., Kacprowski, T., Weissmann, R., Dietrich, K., Borgers, H., BrauÃŸ, A., Sperling, C., Wirths, O., Albrecht, M., Jensen, L. R., Kuss, A. W., & Bayer, T. A. (2014). Deciphering the Molecular Profile of Plaques, Memory Decline and Neuron Loss in Two Mouse Models for Alzheimerâ€™s Disease by Deep Sequencing. *Frontiers in Aging Neuroscience*, *6*. https://doi.org/10.3389/fnagi.2014.00075

Braak, H., & Braak, E. (1991). Neuropathological stageing of Alzheimer-related changes. *Acta Neuropathologica*, *82*(4), 239–259. https://doi.org/10.1007/BF00308809

Brady, A. M., & Floresco, S. B. (2015). Operant Procedures for Assessing Behavioral Flexibility in Rats. *Journal of Visualized Experiments : JoVE*, *96*, 52387. https://doi.org/10.3791/52387

Brady, D. R., & Mufson, E. J. (1997). Parvalbumin-immunoreactive neurons in the hippocampal formation of Alzheimer's diseased brain. *Neuroscience*, *80*(4), 1113–1125. https://doi.org/10.1016/S0306-4522(97)00068-7

Braff, D. L., & Geyer, M. A. (1990). Sensorimotor Gating and Schizophrenia: Human and Animal Model Studies. *Archives of General Psychiatry*, *47*(2), 181–188. https://doi.org/10.1001/archpsyc.1990.01810140081011

Braganza, O., Mueller-Komorowska, D., Kelly, T., & Beck, H. (2020). Quantitative properties of a feedback circuit predict frequency-dependent pattern separation. *ELife*, *9*, e53148. https://doi.org/10.7554/eLife.53148

Brakebusch, C., Seidenbecher, C. I., Asztely, F., Rauch, U., Matthies, H., Meyer, H., Krug, M., Böckers, T. M., Zhou, X., Kreutz, M. R., Montag, D., Gundelfinger, E. D., & Fässler, R. (2002). Brevican-Deficient Mice Display Impaired Hippocampal CA1 Long-Term Potentiation but Show No Obvious Deficits in Learning and Memory. *Molecular and Cellular Biology*, *22*(21), 7417–7427. https://doi.org/10.1128/MCB.22.21.7417-7427.2002

Brandenburg, C., & Blatt, G. J. (2022). Region-Specific Alterations of Perineuronal Net Expression in Postmortem Autism Brain Tissue. *Frontiers in Molecular Neuroscience*, *15*, 838918. https://doi.org/10.3389/fnmol.2022.838918

Brooks, S. P., Pask, T., Jones, L., & Dunnett, S. B. (2005). Behavioural profiles of inbred mouse strains used as transgenic backgrounds. II: Cognitive tests. *Genes, Brain and Behavior*, *4*(5), 307–317. https://doi.org/10.1111/j.1601-183X.2004.00109.x

Brown, T. E., & Sorg, B. A. (2023). Net gain and loss: Influence of natural rewards and drugs of abuse on perineuronal nets. *Neuropsychopharmacology*, *48*(1), Article 1. https://doi.org/10.1038/s41386-022-01337-x

Brückner, G., Brauer, K., Härtig, W., Wolff, J. R., Rickmann, M. J., Derouiche, A., Delpech, B., Girard, N., Oertel, W. H., & Reichenbach, A. (1993a). Perineuronal nets provide a polyanionic, glia-associated form of microenvironment around certain neurons in many parts of the rat brain. *Glia*, *8*(3), 183–200. https://doi.org/10.1002/glia.440080306

Brückner, G., Brauer, K., Härtig, W., Wolff, J. R., Rickmann, M. J., Derouiche, A., Delpech, B., Girard, N., Oertel, W. H., & Reichenbach, A. (1993b). Perineuronal nets provide a polyanionic, glia-associated form of microenvironment around certain neurons in many parts of the rat brain. *Glia*, *8*(3), 183–200.

Brückner, G., Bringmann, A., Härtig, W., Köppe, G., Delpech, B., & Brauer, K. (1998). Acute and long-lasting changes in extracellular-matrix chondroitin-sulphate proteoglycans induced by injection of chondroitinase ABC in the adult rat brain. *Experimental Brain Research*, *121*(3), 300–310.

Brückner, G., Grosche, J., Schmidt, S., Härtig, W., Margolis, R. U., Delpech, B., Seidenbecher, C. I., Czaniera, R., & Schachner, M. (2000). Postnatal development of perineuronal nets in wild-type mice and in a mutant deficient in tenascin-R. *Journal of Comparative Neurology*, *428*(4), 616–629. https://doi.org/10.1002/1096-9861(20001225)428:4<616::AID-CNE3>3.0.CO;2-K

Brückner, G., Härtig, W., Kacza, J., Seeger, J., Welt, K., & Brauer, K. (1996). Extracellular matrix organization in various regions of rat brain grey matter. *Journal of Neurocytology*, *25*(1), 333–346. https://doi.org/10.1007/BF02284806

Brückner, G., Hausen, D., Härtig, W., Drlicek, M., Arendt, T., & Brauer, K. (1999a). Cortical areas abundant in extracellular matrix chondroitin sulphate proteoglycans are less affected by cytoskeletal changes in Alzheimer's disease. *Neuroscience*, *92*(3), 791–805. https://doi.org/10.1016/s0306-4522(99)00071-8

Brückner, G., Hausen, D., Härtig, W., Drlicek, M., Arendt, T., & Brauer, K. (1999b). Cortical areas abundant in extracellular matrix chondroitin sulphate proteoglycans are less affected by cytoskeletal changes in Alzheimer's disease. *Neuroscience*, *92*(3), 791–805. https://doi.org/10.1016/S0306-4522(99)00071-8

Brun, A., Liu, X., & Erikson, C. (1995). Synapse Loss and Gliosis in the Molecular Layer of the Cerebral Cortex in Alzheimer's Disease and in Frontal Lobe Degeneration. *Neurodegeneration*, *4*(2), 171–177. https://doi.org/10.1006/neur.1995.0021

Bucher, E. A., Collins, J. M., King, A. E., Vickers, J. C., & Kirkcaldie, M. T. K. (2021). Coherenceand cognition in the cortex: The fundamental role of parvalbumin, myelin, and the perineuronal net. *Brain Structure and Function*, *226*(7), 2041–2055. https://doi.org/10.1007/s00429-021-02327-3

Buckley, M. J., Booth, M. C. A., Rolls, E. T., & Gaffan, D. (2001). Selective Perceptual Impairments After Perirhinal Cortex Ablation. *Journal of Neuroscience*, *21*(24), 9824–9836. https://doi.org/10.1523/JNEUROSCI.21-24-09824.2001

Buckner, R. L., & DiNicola, L. M. (2019). The brain's default network: Updated anatomy, physiology and evolving insights. *Nature Reviews Neuroscience*, *20*(10), Article 10. https://doi.org/10.1038/s41583-019-0212-7

Buhl, E. H., Tamás, G., & Fisahn, A. (1998). Cholinergic activation and tonic excitation induce persistent gamma oscillations in mouse somatosensory cortex in vitro. *The Journal of Physiology*, *513*(1), 117–126. https://doi.org/10.1111/j.1469-7793.1998.117by.x

Bukalo, O., Schachner, M., & Dityatev, A. (2007). Hippocampal Metaplasticity Induced by Deficiency in the Extracellular Matrix Glycoprotein Tenascin-R. *Journal of Neuroscience*, *27*(22), 6019–6028. https://doi.org/10.1523/JNEUROSCI.1022-07.2007

Burket, J. A., Webb, J. D., & Deutsch, S. I. (2021). Perineuronal Nets and Metal Cation Concentrations in the Microenvironments of Fast-Spiking, Parvalbumin-Expressing GABAergic Interneurons: Relevance to Neurodevelopment and Neurodevelopmental Disorders. *Biomolecules*, *11*(8), Article 8. https://doi.org/10.3390/biom11081235

Burnside, E. R., De Winter, F., Didangelos, A., James, N. D., Andreica, E.-C., Layard-Horsfall, H., Muir, E. M., Verhaagen, J., & Bradbury, E. J. (2018). Immune-evasive gene switch enables regulated delivery of chondroitinase after spinal cord injury. *Brain*, *141*(8), 2362–2381. https://doi.org/10.1093/brain/awy158

Bussière, T., Giannakopoulos, P., Bouras, C., Perl, D. P., Morrison, J. H., & Hof, P. R. (2003). Progressive degeneration of nonphosphorylated neurofilament protein-enriched pyramidal neurons predicts cognitive impairment in Alzheimer's disease: Stereologic analysis of prefrontal cortex area 9. *Journal of Comparative Neurology*, *463*(3), 281–302. https://doi.org/10.1002/cne.10760

Buxbaum, J. D., Georgieva, L., Young, J. J., Plescia, C., Kajiwara, Y., Jiang, Y., Moskvina, V., Norton, N., Peirce, T., Williams, H., Craddock, N. J., Carroll, L., Corfas, G., Davis, K. L., Owen, M. J., Harroch, S., Sakurai, T., & O'Donovan, M. C. (2008). Molecular dissection of NRG1-ERBB4 signaling implicates PTPRZ1 as a potential schizophrenia susceptibility gene. *Molecular Psychiatry*, *13*(2), Article 2. https://doi.org/10.1038/sj.mp.4001991

Buzsáki, G., & Wang, X.-J. (2012). Mechanisms of Gamma Oscillations. *Annual Review of Neuroscience*, *35*(1), 203–225. https://doi.org/10.1146/annurev-neuro-062111-150444

Cabungcal, J.-H., Steullet, P., Morishita, H., Kraftsik, R., Cuenod, M., Hensch, T. K., & Do, K. Q. (2013a). Perineuronal nets protect fast-spiking interneurons against oxidative stress. *Proceedings of the National Academy of Sciences*, *110*(22), 9130–9135. https://doi.org/10.1073/pnas.1300454110

Cabungcal, J.-H., Steullet, P., Morishita, H., Kraftsik, R., Cuenod, M., Hensch, T. K., & Do, K. Q. (2013b). Perineuronal nets protect fast-spiking interneurons against oxidative stress. *Proceedings of the National Academy of Sciences of the United States of America*, *110*(22), 9130–9135. https://doi.org/10.1073/pnas.1300454110

Cabungcal, J.-H., Steullet, P., Morishita, H., Kraftsik, R., Cuenod, M., Hensch, T. K., & Do, K. Q. (2013c). Perineuronal nets protect fast-spiking interneurons against oxidative stress. *Proceedings of the National Academy of Sciences*, *110*(22), 9130–9135. https://doi.org/10.1073/pnas.1300454110

Caillard, O., Moreno, H., Schwaller, B., Llano, I., Celio, M. R., & Marty, A. (2000). Role of the calcium-binding protein parvalbumin in short-term synaptic plasticity. *Proceedings of the*

National Academy of Sciences, *97*(24), 13372–13377. https://doi.org/10.1073/pnas.230362997

Cameron, B., & Landreth, G. E. (2010). Inflammation, microglia, and alzheimer's disease. *Neurobiology of Disease*, *37*(3), 503–509. https://doi.org/10.1016/j.nbd.2009.10.006

Campo, C. G., Sinagra, M., Verrier, D., Manzoni, O. J., & Chavis, P. (2009). Reelin Secreted by GABAergic Neurons Regulates Glutamate Receptor Homeostasis. *PLOS ONE*, *4*(5), e5505. https://doi.org/10.1371/journal.pone.0005505

Canetta, S., Bolkan, S., Padilla-Coreano, N., Song, L. J., Sahn, R., Harrison, N. L., Gordon, J. A., Brown, A., & Kellendonk, C. (2016). Maternal immune activation leads to selective functional deficits in offspring parvalbumin interneurons. *Molecular Psychiatry*, *21*(7), Article 7. https://doi.org/10.1038/mp.2015.222

Carceller, H., Gramuntell, Y., Klimczak, P., & Nacher, J. (2022). Perineuronal Nets: Subtle Structures with Large Implications. *The Neuroscientist*, 10738584221106346. https://doi.org/10.1177/10738584221106346

Carceller, H., Guirado, R., Ripolles-Campos, E., Teruel-Marti, V., & Nacher, J. (2020). Perineuronal Nets Regulate the Inhibitory Perisomatic Input onto Parvalbumin Interneurons and γ Activity in the Prefrontal Cortex. *Journal of Neuroscience*, *40*(26), 5008–5018. https://doi.org/10.1523/JNEUROSCI.0291-20.2020

Cardis, R., Cabungcal, J.-H., Dwir, D., Do, K. Q., & Steullet, P. (2018). A lack of GluN2A-containing NMDA receptors confers a vulnerability to redox dysregulation: Consequences on parvalbumin interneurons, and their perineuronal nets. *Neurobiology of Disease*, *109*, 64–75. https://doi.org/10.1016/j.nbd.2017.10.006

Caroni, P. (2015). Regulation of Parvalbumin Basket cell plasticity in rule learning. *Biochemical and Biophysical Research Communications*, *460*(1), 100–103. https://doi.org/10.1016/j.bbrc.2015.02.023

Carstens, K. E., Phillips, M. L., Pozzo-Miller, L., Weinberg, R. J., & Dudek, S. M. (2016). Perineuronal Nets Suppress Plasticity of Excitatory Synapses on CA2 Pyramidal Neurons. *Journal of Neuroscience*, *36*(23), 6312–6320. https://doi.org/10.1523/JNEUROSCI.0245-16.2016

Carulli, D., Broersen, R., de Winter, F., Muir, E. M., Mešković, M., de Waal, M., de Vries, Boele, H.-J., & Canto, C. B. (2020). Cerebellar plasticity and associative memories are controlled by perineuronal nets. *Proceedings of the National Academy of Sciences*, *117*(12), 6855–6865.

Carulli, D., Pizzorusso, T., Kwok, J. C. F., Putignano, E., Poli, A., Forostyak, S., Andrews, M. R., Deepa, S. S., Glant, T. T., & Fawcett, J. W. (2010a). Animals lacking link protein have attenuated perineuronal nets and persistent plasticity. *Brain: A Journal of Neurology*, *133*(Pt 8), 2331–2347. https://doi.org/10.1093/brain/awq145

Carulli, D., Pizzorusso, T., Kwok, J. C. F., Putignano, E., Poli, A., Forostyak, S., Andrews, M. R., Deepa, S. S., Glant, T. T., & Fawcett, J. W. (2010b). Animals lacking link protein have attenuated perineuronal nets and persistent plasticity. *Brain*, *133*(8), 2331–2347. https://doi.org/10.1093/brain/awq145

Carulli, D., Pizzorusso, T., Kwok, J. C. F., Putignano, E., Poli, A., Forostyak, S., Andrews, M. R., Deepa, S. S., Glant, T. T., & Fawcett, J. W. (2010c). Animals lacking link protein have attenuated perineuronal nets and persistent plasticity. *Brain*, *133*(8), 2331–2347. https://doi.org/10.1093/brain/awq145

Carulli, D., Rhodes, K. E., Brown, D. J., Bonnert, T. P., Pollack, S. J., Oliver, K., Strata, P., & Fawcett, J. W. (2006). Composition of perineuronal nets in the adult rat cerebellum and the cellular origin of their components. *Journal of Comparative Neurology*, *494*(4), 559–577. https://doi.org/10.1002/cne.20822

Carulli, D., Rhodes, K. E., & Fawcett, J. W. (2007). Upregulation of aggrecan, link protein 1, and hyaluronan synthases during formation of perineuronal nets in the rat cerebellum. *Journal of Comparative Neurology*, *501*(1), 83–94. https://doi.org/10.1002/cne.21231

Carulli, D., & Verhaagen, J. (2021). An Extracellular Perspective on CNS Maturation: Perineuronal Nets and the Control of Plasticity. *International Journal of Molecular Sciences*, *22*(5), 2434. https://doi.org/10.3390/ijms22052434

Cattaud, V., Bezzina, C., Rey, C. C., Lejards, C., Dahan, L., & Verret, L. (2018). Early disruption of parvalbumin expression and perineuronal nets in the hippocampus of the Tg2576 mouse model of Alzheimer's disease can be rescued by enriched environment. *Neurobiology of Aging*, *72*, 147–158. https://doi.org/10.1016/j.neurobiolaging.2018.08.024

Cayco-Gajic, N. A., & Silver, R. A. (2019). Re-evaluating Circuit Mechanisms Underlying Pattern Separation. *Neuron*, *101*(4), 584–602. https://doi.org/10.1016/j.neuron.2019.01.044

Chang, M. C., Park, J. M., Pelkey, K. A., Grabenstatter, H. L., Xu, D., Linden, D. J., Sutula, T. P., McBain, C. J., & Worley, P. F. (2010). Narp regulates homeostatic scaling of excitatory synapses on parvalbumin-expressing interneurons. *Nature Neuroscience*, *13*(9), Article 9. https://doi.org/10.1038/nn.2621

Chen, L. L., Lin, L.-H., Green, E. J., Barnes, C. A., & McNaughton, B. L. (1994). Head-direction cells in the rat posterior cortex. *Experimental Brain Research*, *101*(1), 8–23. https://doi.org/10.1007/BF00243212

Cheung, V., Cheung, C., McAlonan, G. M., Deng, Y., Wong, J. G., Yip, L., Tai, K. S., Khong, P. L., Sham, P., & Chua, S. E. (2008). A diffusion tensor imaging study of structural dysconnectivity in never-medicated, first-episode schizophrenia. *Psychological Medicine*, *38*(6), 877–885. https://doi.org/10.1017/S0033291707001808

Cho, K. K. A., Davidson, T. J., Bouvier, G., Marshall, J. D., Schnitzer, M. J., & Sohal, V. S. (2020). Cross-hemispheric gamma synchrony between prefrontal parvalbumin interneurons supports behavioral adaptation during rule shift learning. *Nature Neuroscience*, *23*(7), Article 7. https://doi.org/10.1038/s41593-020-0647-1

Cho, K. K. A., Hoch, R., Lee, A. T., Patel, T., Rubenstein, J. L. R., & Sohal, V. S. (2015). Gamma Rhythms Link Prefrontal Interneuron Dysfunction with Cognitive Inflexibility in Dlx5/6+/− Mice. *Neuron*, *85*(6), 1332–1343. https://doi.org/10.1016/j.neuron.2015.02.019

Christen, Y. (2000). Oxidative stress and Alzheimer disease. *The American Journal of Clinical Nutrition*, *71*(2), 621S-629S. https://doi.org/10.1093/ajcn/71.2.621s

Christensen, A. C., Lensjø, K. K., Lepperød, M. E., Dragly, S.-A., Sutterud, H., Blackstad, J. S., Fyhn, M., & Hafting, T. (2021). Perineuronal nets stabilize the grid cell network. *Nature Communications*, *12*(1), Article 1. https://doi.org/10.1038/s41467-020-20241-w

Cichon, S., Mühleisen, T. W., Degenhardt, F. A., Mattheisen, M., Miró, X., Strohmaier, J., Steffens, M., Meesters, C., Herms, S., Weingarten, M., Priebe, L., Haenisch, B., Alexander, M., Vollmer, J., Breuer, R., Schmäl, C., Tessmann, P., Moebus, S.,

Wichmann, H.-E., … Nöthen, M. M. (2011). Genome-wide Association Study Identifies Genetic Variation in Neurocan as a Susceptibility Factor for Bipolar Disorder. *The American Journal of Human Genetics*, *88*(3), 372–381. https://doi.org/10.1016/j.ajhg.2011.01.017

Cohen, S. J., Munchow, A. H., Rios, L. M., Zhang, G., Asgeirsdóttir, H. N., & Stackman, R. W. (2013). The rodent hippocampus is essential for nonspatial object memory. *Current Biology: CB*, *23*(17), 1685–1690. https://doi.org/10.1016/j.cub.2013.07.002

Cohen, S. J., & Stackman Jr., R. W. (2015). Assessing rodent hippocampal involvement in the novel object recognition task. A review. *Behavioural Brain Research*, *285*, 105–117. https://doi.org/10.1016/j.bbr.2014.08.002

Colacicco, G., Welzl, H., Lipp, H.-P., & Würbel, H. (2002). Attentional set-shifting in mice: Modification of a rat paradigm, and evidence for strain-dependent variation. *Behavioural Brain Research*, *132*(1), 95–102. https://doi.org/10.1016/S0166-4328(01)00391-6

Colciaghi, F., Borroni, B., Pastorino, L., Marcello, E., Zimmermann, M., Cattabeni, F., Padovani, A., & Di Luca, M. (2002). α-Secretase ADAM10 as Well as αAPPs Is Reduced in Platelets and CSF of Alzheimer Disease Patients. *Molecular Medicine*, *8*(2), 67–74. https://doi.org/10.1007/BF03402076

Cooper, B. G., & Mizumori, S. J. Y. (1999). Retrosplenial cortex inactivation selectively impairs navigation in darkness. *NeuroReport*, *10*(3), 625.

Cornez, G., Collignon, C., Müller, W., Cornil, C. A., Ball, G. F., & Balthazart, J. (2020). Development of Perineuronal Nets during Ontogeny Correlates with Sensorimotor Vocal Learning in Canaries. *ENeuro*, *7*(2), ENEURO.0361-19.2020. https://doi.org/10.1523/ENEURO.0361-19.2020

Cornez, G., Shevchouk, O. T., Ghorbanpoor, S., Ball, G. F., Cornil, C. A., & Balthazart, J. (2020). Testosterone stimulates perineuronal nets development around parvalbumin cells in the adult canary brain in parallel with song crystallization. *Hormones and Behavior*, *119*, 104643. https://doi.org/10.1016/j.yhbeh.2019.104643

Cowan, R. L., Wilson, C. J., Emson, P. C., & Heizmann, C. W. (1990). Parvalbumin-containing gabaergic interneurons in the rat neostriatum. *Journal of Comparative Neurology*, *302*(2), 197–205. https://doi.org/10.1002/cne.903020202

Crapser, J. D., Spangenberg, E. E., Barahona, R. A., Arreola, M. A., Hohsfield, L. A., & Green, K. N. (2020). Microglia facilitate loss of perineuronal nets in the Alzheimer's disease brain. *EBioMedicine*, *58*, 102919. https://doi.org/10.1016/j.ebiom.2020.102919

Crespo, D., Asher, R. A., Lin, R., Rhodes, K. E., & Fawcett, J. W. (2007). How does chondroitinase promote functional recovery in the damaged CNS? *Experimental Neurology*, *206*(2), 159–171. https://doi.org/10.1016/j.expneurol.2007.05.001

Cross, N. a., Chandrasekharan, S., Jokonya, N., Fowles, A., Hamdy, F. c., Buttle, D. j., & Eaton, C. l. (2005). The expression and regulation of ADAMTS-1, -4, -5, -9, and -15, and TIMP-3 by TGFβ1 in prostate cells: Relevance to the accumulation of versican. *The Prostate*, *63*(3), 269–275. https://doi.org/10.1002/pros.20182

Cuenod, M., Steullet, P., Cabungcal, J.-H., Dwir, D., Khadimallah, I., Klauser, P., Conus, P., & Do, K. Q. (2022). Caught in vicious circles: A perspective on dynamic feed-forward loops driving oxidative stress in schizophrenia. *Molecular Psychiatry*, *27*(4), Article 4. https://doi.org/10.1038/s41380-021-01374-w

Curley, A. A., Arion, D., Volk, D. W., Asafu-Adjei, J. K., Sampson, A. R., Fish, K. N., & Lewis, D. A. (2011). Cortical Deficits of Glutamic Acid Decarboxylase 67 Expression in

Schizophrenia: Clinical, Protein, and Cell Type-Specific Features. *American Journal of Psychiatry*, *168*(9), 921–929. https://doi.org/10.1176/appi.ajp.2011.11010052

d'Isa, R., Comi, G., & Leocani, L. (2021). Apparatus design and behavioural testing protocol for the evaluation of spatial working memory in mice through the spontaneous alternation T-maze. *Scientific Reports*, *11*(1), Article 1. https://doi.org/10.1038/s41598-021-00402-7

Dana, H., Chen, T.-W., Hu, A., Shields, B. C., Guo, C., Looger, L. L., Kim, D. S., & Svoboda, K. (2014). Thy1-GCaMP6 Transgenic Mice for Neuronal Population Imaging In Vivo. *PLoS ONE*, *9*(9), e108697. https://doi.org/10.1371/journal.pone.0108697

Daskalakis, Z. J., Fitzgerald, P. B., & Christensen, B. K. (2007). The role of cortical inhibition in the pathophysiology and treatment of schizophrenia. *Brain Research Reviews*, *56*(2), 427–442. https://doi.org/10.1016/j.brainresrev.2007.09.006

Dauth, S., Grevesse, T., Pantazopoulos, H., Campbell, P. H., Maoz, B. M., Berretta, S., & Parker, K. K. (2016). Extracellular matrix protein expression is brain region dependent. *Journal of Comparative Neurology*, *524*(7), 1309–1336. https://doi.org/10.1002/cne.23965

Davies, C. A., Mann, D. M. A., Sumpter, P. Q., & Yates, P. O. (1987). A quantitative morphometric analysis of the neuronal and synaptic content of the frontal and temporal cortex in patients with Alzheimer's disease. *Journal of the Neurological Sciences*, *78*(2), 151–164. https://doi.org/10.1016/0022-510X(87)90057-8

de Araújo Costa Folha, O. A., Bahia, C. P., de Aguiar, G. P. S., Herculano, A. M., Coelho, N. L. G., de Sousa, M. B. C., Shiramizu, V. K. M., de Menezes Galvão, A. C., de Carvalho, W. A., & Pereira, A. (2017). Effect of chronic stress during adolescence in prefrontal cortex structure and function. *Behavioural Brain Research*, *326*, 44–51. https://doi.org/10.1016/j.bbr.2017.02.033

de Landeta, A. B., Medina, J. H., & Katche, C. (2022). Dopamine D1/D5 Receptors in the Retrosplenial Cortex Are Necessary to Consolidate Object Recognition Memory. *Frontiers in Behavioral Neuroscience*, *16*, 922971. https://doi.org/10.3389/fnbeh.2022.922971

de Landeta, A. B., Pereyra, M., Medina, J. H., & Katche, C. (2020). Anterior retrosplenial cortex is required for long-term object recognition memory. *Scientific Reports*, *10*(1), Article 1. https://doi.org/10.1038/s41598-020-60937-z

de Landeta, A. B., Pereyra, M., Miranda, M., Bekinschtein, P., Medina, J. H., & Katche, C. (2021). Functional connectivity of anterior retrosplenial cortex in object recognition memory. *Neurobiology of Learning and Memory*, *186*, 107544. https://doi.org/10.1016/j.nlm.2021.107544

de Lima, M. N., Luft, T., Roesler, R., & Schröder, N. (2006). Temporary inactivation reveals an essential role of the dorsal hippocampus in consolidation of object recognition memory. *Neuroscience Letters*, *405*(1), 142–146. https://doi.org/10.1016/j.neulet.2006.06.044

de Pins, B., Cifuentes-Díaz, C., Thamila Farah, A., López-Molina, L., Montalban, E., Sancho-Balsells, A., López, A., Ginés, S., Delgado-García, J. M., Alberch, J., Gruart, A., Girault, J.-A., & Giralt, A. (2019). Conditional BDNF delivery from astrocytes rescues memory deficits, spine density and synaptic properties in the 5xFAD mouse model of Alzheimer disease. *The Journal of Neuroscience*, 2121–18. https://doi.org/10.1523/JNEUROSCI.2121-18.2019

de Vivo, L., Landi, S., Panniello, M., Baroncelli, L., Chierzi, S., Mariotti, L., Spolidoro, M., Pizzorusso, T., Maffei, L., & Ratto, G. M. (2013a). Extracellular matrix inhibits structural

and functional plasticity of dendritic spines in the adult visual cortex. *Nature Communications*, *4*(1), Article 1. https://doi.org/10.1038/ncomms2491

de Vivo, L., Landi, S., Panniello, M., Baroncelli, L., Chierzi, S., Mariotti, L., Spolidoro, M., Pizzorusso, T., Maffei, L., & Ratto, G. M. (2013b). Extracellular matrix inhibits structural and functional plasticity of dendritic spines in the adult visual cortex. *Nature Communications*, *4*, 1484. https://doi.org/10.1038/ncomms2491

de Winter, F., Kwok, J. C. F., Fawcett, J. W., Vo, T. T., Carulli, D., & Verhaagen, J. (2016). The Chemorepulsive Protein Semaphorin 3A and Perineuronal Net-Mediated Plasticity. *Neural Plasticity*, *2016*, e3679545. https://doi.org/10.1155/2016/3679545

Deepa, S. S., Carulli, D., Galtrey, C., Rhodes, K., Fukuda, J., Mikami, T., Sugahara, K., & Fawcett, J. W. (2006). Composition of Perineuronal Net Extracellular Matrix in Rat Brain: A DIFFERENT DISACCHARIDE COMPOSITION FOR THE NET-ASSOCIATED PROTEOGLYCANS *. *Journal of Biological Chemistry*, *281*(26), 17789–17800. https://doi.org/10.1074/jbc.M600544200

del Rio, J., de Lecea, L., Ferrer, I., & Soriano, E. (1994). The development of parvalbumin-immunoreactivity in the neocortex of the mouse. *Developmental Brain Research*, *81*(2), 247–259. https://doi.org/10.1016/0165-3806(94)90311-5

Delatour, B., & Gisquet-Verrier, P. (1996). Prelimbic cortex specific lesions disrupt delayed-variable response tasks in the rat. *Behavioral Neuroscience*, *110*, 1282–1298. https://doi.org/10.1037/0735-7044.110.6.1282

Deng, X., Gu, L., Sui, N., Guo, J., & Liang, J. (2019). Parvalbumin interneuron in the ventral hippocampus functions as a discriminator in social memory. *Proceedings of the National Academy of Sciences*, *116*(33), 16583–16592. https://doi.org/10.1073/pnas.1819133116

Devi, L., & Ohno, M. (2010). Phospho-eIF2α Level Is Important for Determining Abilities of BACE1 Reduction to Rescue Cholinergic Neurodegeneration and Memory Defects in 5XFAD Mice. *PLOS ONE*, *5*(9), e12974. https://doi.org/10.1371/journal.pone.0012974

Devi, L., & Ohno, M. (2016). Cognitive benefits of memantine in Alzheimer's 5XFAD model mice decline during advanced disease stages. *Pharmacology Biochemistry and Behavior*, *144*, 60–66. https://doi.org/10.1016/j.pbb.2016.03.002

Devi, L., Tang, J., & Ohno, M. (2015). Beneficial Effects of the β-Secretase Inhibitor GRL-8234 in 5XFAD Alzheimer's Transgenic Mice Lessen During Disease Progression. *Current Alzheimer Research*, *12*(1), 13–21.

Dexter, T. D., Palmer, D., Hashad, A. M., Saksida, L. M., & Bussey, T. J. (2022). Decision Making in Mice During an Optimized Touchscreen Spatial Working Memory Task Sensitive to Medial Prefrontal Cortex Inactivation and NMDA Receptor Hypofunction. *Frontiers in Neuroscience*, *16*, 905736. https://doi.org/10.3389/fnins.2022.905736

Dick, G., Tan, C. L., Alves, J. N., Ehlert, E. M. E., Miller, G. M., Hsieh-Wilson, L. C., Sugahara, K., Oosterhof, A., Kuppevelt, T. H. van, Verhaagen, J., Fawcett, J. W., & Kwok, J. C. F. (2013). Semaphorin 3A Binds to the Perineuronal Nets via Chondroitin Sulfate Type E Motifs in Rodent Brains *. *Journal of Biological Chemistry*, *288*(38), 27384–27395. https://doi.org/10.1074/jbc.M111.310029

Dickerson, D. D., Wolff, A. R., & Bilkey, D. K. (2010). Abnormal Long-Range Neural Synchrony in a Maternal Immune Activation Animal Model of Schizophrenia. *Journal of Neuroscience*, *30*(37), 12424–12431. https://doi.org/10.1523/JNEUROSCI.3046-10.2010

Dienel, S. J., Schoonover, K. E., & Lewis, D. A. (2022). Cognitive Dysfunction and Prefrontal Cortical Circuit Alterations in Schizophrenia: Developmental Trajectories. *Biological Psychiatry*, *92*(6), 450–459. https://doi.org/10.1016/j.biopsych.2022.03.002

Dino, M. R., Harroch, S., Hockfield, S., & Matthews, R. T. (2006). Monoclonal antibody Cat-315 detects a glycoform of receptor protein tyrosine phosphatase beta/phosphacan early in CNS development that localizes to extrasynaptic sites prior to synapse formation. *Neuroscience*, *142*(4), 1055–1069. https://doi.org/10.1016/j.neuroscience.2006.07.054

Dityatev, A., Brückner, G., Dityateva, G., Grosche, J., Kleene, R., & Schachner, M. (2007a). Activity-dependent formation and functions of chondroitin sulfate-rich extracellular matrix of perineuronal nets. *Developmental Neurobiology*, *67*(5), 570–588. https://doi.org/10.1002/dneu.20361

Dityatev, A., Brückner, G., Dityateva, G., Grosche, J., Kleene, R., & Schachner, M. (2007b). Activity-dependent formation and functions of chondroitin sulfate-rich extracellular matrix of perineuronal nets. *Developmental Neurobiology*, *67*(5), 570–588. https://doi.org/10.1002/dneu.20361

Dityatev, A., Frischknecht, R., & Seidenbecher, C. I. (2006). Extracellular Matrix and Synaptic Functions. In E. D. Gundelfinger, C. I. Seidenbecher, & B. Schraven (Eds.), *Cell Communication in Nervous and Immune System* (pp. 69–97). Springer. https://doi.org/10.1007/400_025

Dityatev, A., & Rusakov, D. A. (2011). Molecular signals of plasticity at the tetrapartite synapse. *Current Opinion in Neurobiology*, *21*(2), 353–359. https://doi.org/10.1016/j.conb.2010.12.006

Dityatev, A., Seidenbecher, C. I., & Schachner, M. (2010). Compartmentalization from the outside: The extracellular matrix and functional microdomains in the brain. *Trends in Neurosciences*, *33*(11), 503–512. https://doi.org/10.1016/j.tins.2010.08.003

Divac, I., Wikmark, R. G. E., & Gade, A. (1975). Spontaneous alternation in rats with lesions in the frontal lobes: An extension of the frontal lobe syndrome. *Physiological Psychology*, *3*(1), 39–42. https://doi.org/10.3758/BF03326820

Do, K. Q., Cuenod, M., & Hensch, T. K. (2015). Targeting Oxidative Stress and Aberrant Critical Period Plasticity in the Developmental Trajectory to Schizophrenia. *Schizophrenia Bulletin*, *41*(4), 835–846. https://doi.org/10.1093/schbul/sbv065

Domínguez, S., Rey, C. C., Therreau, L., Fanton, A., Massotte, D., Verret, L., Piskorowski, R. A., & Chevaleyre, V. (2019). Maturation of PNN and ErbB4 Signaling in Area CA2 during Adolescence Underlies the Emergence of PV Interneuron Plasticity and Social Memory. *Cell Reports*, *29*(5), 1099-1112.e4. https://doi.org/10.1016/j.celrep.2019.09.044

Donato, F., Chowdhury, A., Lahr, M., & Caroni, P. (2015). Early- and Late-Born Parvalbumin Basket Cell Subpopulations Exhibiting Distinct Regulation and Roles in Learning. *Neuron*, *85*(4), 770–786. https://doi.org/10.1016/j.neuron.2015.01.011

Donato, F., Rompani, S. B., & Caroni, P. (2013). Parvalbumin-expressing basket-cell network plasticity induced by experience regulates adult learning. *Nature*, *504*(7479), Article 7479. https://doi.org/10.1038/nature12866

Dow, D. J., Huxley-Jones, J., Hall, J. M., Francks, C., Maycox, P. R., Kew, J. N. C., Gloger, I. S., Mehta, N. A. L., Kelly, F. M., Muglia, P., Breen, G., Jugurnauth, S., Pederoso, I., St.Clair, D., Rujescu, D., & Barnes, M. R. (2011). ADAMTSL3 as a candidate gene for schizophrenia: Gene sequencing and ultra-high density association analysis by

imputation. *Schizophrenia Research*, *127*(1), 28–34. https://doi.org/10.1016/j.schres.2010.12.009

Du, J., Zhang, L., Weiser, M., Rudy, B., & McBain, C. (1996). Developmental expression and functional characterization of the potassium-channel subunit Kv3.1b in parvalbumin-containing interneurons of the rat hippocampus. *The Journal of Neuroscience*, *16*(2), 506–518. https://doi.org/10.1523/JNEUROSCI.16-02-00506.1996

Dwir, D., Cabungcal, J.-H., Xin, L., Giangreco, B., Parietti, E., Cleusix, M., Jenni, R., Klauser, P., Conus, P., Cuénod, M., Steullet, P., & Do, K. Q. (2021). Timely N-Acetyl-Cysteine and Environmental Enrichment Rescue Oxidative Stress-Induced Parvalbumin Interneuron Impairments via MMP9/RAGE Pathway: A Translational Approach for Early Intervention in Psychosis. *Schizophrenia Bulletin*, *47*(6), 1782–1794. https://doi.org/10.1093/schbul/sbab066

Dzyubenko, E., Fleischer, M., Manrique-Castano, D., Borbor, M., Kleinschnitz, C., Faissner, A., & Hermann, D. M. (2021). Inhibitory control in neuronal networks relies on the extracellular matrix integrity. *Cellular and Molecular Life Sciences*, *78*(14), 5647–5663. https://doi.org/10.1007/s00018-021-03861-3

Egea, J., García, A. G., Verges, J., Montell, E., & López, M. G. (2010). Antioxidant, antiinflammatory and neuroprotective actions of chondroitin sulfate and proteoglycans. *Osteoarthritis and Cartilage*, *18*, S24–S27. https://doi.org/10.1016/j.joca.2010.01.016

Eichhammer, P., Wiegand, R., Kharraz, A., Langguth, B., Binder, H., & Hajak, G. (2004). Cortical excitability in neuroleptic-naive first-episode schizophrenic patients. *Schizophrenia Research*, *67*(2), 253–259. https://doi.org/10.1016/S0920-9964(03)00223-8

El Gaamouch, F., Audrain, M., Lin, W.-J., Beckmann, N., Jiang, C., Hariharan, S., Heeger, P. S., Schadt, E. E., Gandy, S., Ehrlich, M. E., & Salton, S. R. (2020). VGF-derived peptide TLQP-21 modulates microglial function through C3aR1 signaling pathways and reduces neuropathology in 5xFAD mice. *Molecular Neurodegeneration*, *15*(1), 4. https://doi.org/10.1186/s13024-020-0357-x

Ellenbroek, B. A., Budde, S., & Cools, A. R. (1996). Prepulse inhibition and latent inhibition: The role of dopamine in the medial prefrontal cortex. *Neuroscience*, *75*(2), 535–542. https://doi.org/10.1016/0306-4522(96)00307-7

Ellenbroek, B., & Youn, J. (2016). Rodent models in neuroscience research: Is it a rat race? *Disease Models & Mechanisms*, *9*(10), 1079–1087. https://doi.org/10.1242/dmm.026120

Elmore, M. R. P., Hohsfield, L. A., Kramár, E. A., Soreq, L., Lee, R. J., Pham, S. T., Najafi, A. R., Spangenberg, E. E., Wood, M. A., West, B. L., & Green, K. N. (2018). Replacement of microglia in the aged brain reverses cognitive, synaptic, and neuronal deficits in mice. *Aging Cell*, *17*(6), e12832. https://doi.org/10.1111/acel.12832

Ennaceur, A., Neave, N., & Aggleton, J. P. (1997). Spontaneous object recognition and object location memory in rats: The effects of lesions in the cingulate cortices, the medial prefrontal cortex, the cingulum bundle and the fornix: *Experimental Brain Research*, *113*(3), 509–519. https://doi.org/10.1007/PL00005603

Enwright, J. F., Sanapala, S., Foglio, A., Berry, R., Fish, K. N., & Lewis, D. A. (2016a). Reduced labeling of parvalbumin neurons and perineuronal nets in the dorsolateral prefrontal cortex of subjects with schizophrenia. *Neuropsychopharmacology*, *41*(9), 2206–2214.

Enwright, J. F., Sanapala, S., Foglio, A., Berry, R., Fish, K. N., & Lewis, D. A. (2016b). Reduced Labeling of Parvalbumin Neurons and Perineuronal Nets in the Dorsolateral Prefrontal Cortex of Subjects with Schizophrenia. *Neuropsychopharmacology*, *41*(9), Article 9. https://doi.org/10.1038/npp.2016.24

Espinoza, C., Guzman, S. J., Zhang, X., & Jonas, P. (2018). Parvalbumin+ interneurons obey unique connectivity rules and establish a powerful lateral-inhibition microcircuit in dentate gyrus. *Nature Communications*, *9*(1), Article 1. https://doi.org/10.1038/s41467-018-06899-3

Euston, D. R., Gruber, A. J., & McNaughton, B. L. (2012). The Role of Medial Prefrontal Cortex in Memory and Decision Making. *Neuron*, *76*(6), 1057–1070. https://doi.org/10.1016/j.neuron.2012.12.002

Faini, G., Aguirre, A., Landi, S., Lamers, D., Pizzorusso, T., Ratto, G. M., Deleuze, C., & Bacci, A. (2018). Perineuronal nets control visual input via thalamic recruitment of cortical PV interneurons. *ELife*, *7*, e41520. https://doi.org/10.7554/eLife.41520

Farzan, F., Barr, M. S., Levinson, A. J., Chen, R., Wong, W., Fitzgerald, P. B., & Daskalakis, Z. J. (2010). Evidence for gamma inhibition deficits in the dorsolateral prefrontal cortex of patients with schizophrenia. *Brain*, *133*(5), 1505–1514. https://doi.org/10.1093/brain/awq046

Favuzzi, E., Marques-Smith, A., Deogracias, R., Winterflood, C. M., Sánchez-Aguilera, A., Mantoan, L., Maeso, P., Fernandes, C., Ewers, H., & Rico, B. (2017). Activity-Dependent Gating of Parvalbumin Interneuron Function by the Perineuronal Net Protein Brevican. *Neuron*, *95*(3), 639-655.e10. https://doi.org/10.1016/j.neuron.2017.06.028

Fawcett, J. W. (2015). The extracellular matrix in plasticity and regeneration after CNS injury and neurodegenerative disease. In *Progress in Brain Research* (Vol. 218, pp. 213–226). Elsevier. https://doi.org/10.1016/bs.pbr.2015.02.001

Fawcett, J. W., Fyhn, M., Jendelova, P., Kwok, J. C. F., Ruzicka, J., & Sorg, B. A. (2022). The extracellular matrix and perineuronal nets in memory. *Molecular Psychiatry*, *27*(8), Article 8. https://doi.org/10.1038/s41380-022-01634-3

Fawcett, J. W., Oohashi, T., & Pizzorusso, T. (2019). The roles of perineuronal nets and the perinodal extracellular matrix in neuronal function. *Nature Reviews Neuroscience*, *20*(8), Article 8. https://doi.org/10.1038/s41583-019-0196-3

Fino, E., Packer, A. M., & Yuste, R. (2013). The Logic of Inhibitory Connectivity in the Neocortex. *The Neuroscientist*, *19*(3), 228–237. https://doi.org/10.1177/1073858412456743

Fitzsimmons, J., Kubicki, M., & Shenton, M. E. (2013). Review of functional and anatomical brain connectivity findings in schizophrenia. *Current Opinion in Psychiatry*, *26*(2), 172–187. https://doi.org/10.1097/YCO.0b013e32835d9e6a

Floresco, S. B., Block, A. E., & Tse, M. T. L. (2008). Inactivation of the medial prefrontal cortex of the rat impairs strategy set-shifting, but not reversal learning, using a novel, automated procedure. *Behavioural Brain Research*, *190*(1), 85–96. https://doi.org/10.1016/j.bbr.2008.02.008

Floresco, S. B., Zhang, Y., & Enomoto, T. (2009). Neural circuits subserving behavioral flexibility and their relevance to schizophrenia. *Behavioural Brain Research*, *204*(2), 396–409. https://doi.org/10.1016/j.bbr.2008.12.001

Forbes, N. F., Carrick, L. A., McIntosh, A. M., & Lawrie, S. M. (2009). Working memory in schizophrenia: A meta-analysis. *Psychological Medicine*, *39*(6), 889–905. https://doi.org/10.1017/S0033291708004558

Ford, J. M., Mathalon, D. H., Whitfield, S., Faustman, W. O., & Roth, W. T. (2002). Reduced communication between frontal and temporal lobes during talking in schizophrenia. *Biological Psychiatry*, *51*(6), 485–492. https://doi.org/10.1016/S0006-3223(01)01335-X

Forner, S., Kawauchi, S., Balderrama-Gutierrez, G., Kramár, E. A., Matheos, D. P., Phan, J., Javonillo, D. I., Tran, K. M., Hingco, E., da Cunha, C., Rezaie, N., Alcantara, J. A., Baglietto-Vargas, D., Jansen, C., Neumann, J., Wood, M. A., MacGregor, G. R., Mortazavi, A., Tenner, A. J., … Green, K. N. (2021). Systematic phenotyping and characterization of the 5xFAD mouse model of Alzheimer's disease. *Scientific Data*, *8*(1), Article 1. https://doi.org/10.1038/s41597-021-01054-y

Foscarin, S., Raha-Chowdhury, R., Fawcett, J. W., & Kwok, J. C. F. (2017). Brain ageing changes proteoglycan sulfation, rendering perineuronal nets more inhibitory. *Aging (Albany NY)*, *9*(6), 1607–1622. https://doi.org/10.18632/aging.101256

Franco, L. M., & Goard, M. J. (2021). A distributed circuit for associating environmental context with motor choice in retrosplenial cortex. *Science Advances*, *7*(35), eabf9815. https://doi.org/10.1126/sciadv.abf9815

Freund, T. F., & Katona, I. (2007). Perisomatic Inhibition. *Neuron*, *56*(1), 33–42. https://doi.org/10.1016/j.neuron.2007.09.012

Fricker, M., Tolkovsky, A. M., Borutaite, V., Coleman, M., & Brown, G. C. (2018). Neuronal Cell Death. *Physiol Rev*, *98*.

Fries, P. (2005). A mechanism for cognitive dynamics: Neuronal communication through neuronal coherence. *Trends in Cognitive Sciences*, *9*(10), 474–480. https://doi.org/10.1016/j.tics.2005.08.011

Fries, P. (2009). Neuronal Gamma-Band Synchronization as a Fundamental Process in Cortical Computation. *Annual Review of Neuroscience*, *32*(1), 209–224. https://doi.org/10.1146/annurev.neuro.051508.135603

Frischknecht, R., Heine, M., Perrais, D., Seidenbecher, C. I., Choquet, D., & Gundelfinger, E. D. (2009a). Brain extracellular matrix affects AMPA receptor lateral mobility and short-term synaptic plasticity. *Nature Neuroscience*, *12*(7), Article 7. https://doi.org/10.1038/nn.2338

Frischknecht, R., Heine, M., Perrais, D., Seidenbecher, C. I., Choquet, D., & Gundelfinger, E. D. (2009b). Brain extracellular matrix affects AMPA receptor lateral mobility and short-term synaptic plasticity. *Nature Neuroscience*, *12*(7), 897–904. https://doi.org/10.1038/nn.2338

Frydman-Marom, A., Levin, A., Farfara, D., Benromano, T., Scherzer-Attali, R., Peled, S., Vassar, R., Segal, D., Gazit, E., Frenkel, D., & Ovadia, M. (2011). Orally Administrated Cinnamon Extract Reduces β-Amyloid Oligomerization and Corrects Cognitive Impairment in Alzheimer's Disease Animal Models. *PLOS ONE*, *6*(1), e16564. https://doi.org/10.1371/journal.pone.0016564

Fuchs, E. C., Zivkovic, A. R., Cunningham, M. O., Middleton, S., LeBeau, F. E. N., Bannerman, D. M., Rozov, A., Whittington, M. A., Traub, R. D., Rawlins, J. N. P., & Monyer, H. (2007). Recruitment of Parvalbumin-Positive Interneurons Determines Hippocampal

Function and Associated Behavior. *Neuron*, *53*(4), 591–604. https://doi.org/10.1016/j.neuron.2007.01.031

Fujikawa, R., Yamada, J., & Jinno, S. (2021). Subclass imbalance of parvalbumin-expressing GABAergic neurons in the hippocampus of a mouse ketamine model for schizophrenia, with reference to perineuronal nets. *Schizophrenia Research*, *229*, 80–93. https://doi.org/10.1016/j.schres.2020.11.016

Funfschilling, U., Supplie, L. M., Mahad, D., Boretius, S., Saab, A. S., Edgar, J., Brinkmann, B. G., Kassmann, C. M., Tzvetanova, I. D., Mobius, W., Diaz, F., Meijer, D., Suter, U., Hamprecht, B., Sereda, M. W., Moraes, C. T., Frahm, J., Goebbels, S., & Nave, K.-A. (2012). Glycolytic oligodendrocytes maintain myelin and long-term axonal integrity. *Nature*, *485*(7399), 517–521. https://doi.org/10.1038/nature11007

Fung, S. J., Webster, M. J., Sivagnanasundaram, S., Duncan, C., Elashoff, M., & Weickert, C. S. (2010). Expression of Interneuron Markers in the Dorsolateral Prefrontal Cortex of the Developing Human and in Schizophrenia. *American Journal of Psychiatry*, *167*(12), 1479–1488. https://doi.org/10.1176/appi.ajp.2010.09060784

Gail Canter, R., Huang, W.-C., Choi, H., Wang, J., Ashley Watson, L., Yao, C. G., Abdurrob, F., Bousleiman, S. M., Young, J. Z., Bennett, D. A., Delalle, I., Chung, K., & Tsai, L.-H. (2019). 3D mapping reveals network-specific amyloid progression and subcortical susceptibility in mice. *Communications Biology*, *2*(1), Article 1. https://doi.org/10.1038/s42003-019-0599-8

Galtrey, C. M., Kwok, J. C. F., Carulli, D., Rhodes, K. E., & Fawcett, J. W. (2008). Distribution and synthesis of extracellular matrix proteoglycans, hyaluronan, link proteins and

tenascin-R in the rat spinal cord. *European Journal of Neuroscience*, *27*(6), 1373–1390. https://doi.org/10.1111/j.1460-9568.2008.06108.x

Gariano, R. F., & Groves, P. M. (1988). Burst firing induced in midbrain dopamine neurons by stimulation of the medial prefrontal and anterior cingulate cortices. *Brain Research*, *462*(1), 194–198. https://doi.org/10.1016/0006-8993(88)90606-3

Gary, S. C., Kelly, G. M., & Hockfield, S. (1998). BEHAB/brevican: A brain-specific lectican implicated in gliomas and glial cell motility. *Current Opinion in Neurobiology*, *8*(5), 576–581. https://doi.org/10.1016/S0959-4388(98)80083-4

Gervais, N. J., Hamel, L. M., Brake, W. G., & Mumby, D. G. (2016a). Intra-perirhinal cortex administration of estradiol, but not an ERβ agonist, modulates object-recognition memory in ovariectomized rats. *Neurobiology of Learning and Memory*, *133*, 89–99. https://doi.org/10.1016/j.nlm.2016.06.012

Gervais, N. J., Hamel, L. M., Brake, W. G., & Mumby, D. G. (2016b). Intra-perirhinal cortex administration of estradiol, but not an ERβ agonist, modulates object-recognition memory in ovariectomized rats. *Neurobiology of Learning and Memory*, *133*, 89–99. https://doi.org/10.1016/j.nlm.2016.06.012

Girard, S., Baranger, K., Gauthier, C., Jacquet, M., Bernard, A., Escoffier, G., Marchetti, E., Khrestchatisky, M., Rivera, S., & Roman, F. (2012). Evidence for Early Cognitive Impairment Related to Frontal Cortex in the 5XFAD Mouse Model of Alzheimer's Disease. *Journal of Alzheimer's Disease : JAD*, *33*. https://doi.org/10.3233/JAD-2012-120982

Gisquet-Verrier, P., & Delatour, B. (2006). The role of the rat prelimbic/infralimbic cortex in working memory: Not involved in the short-term maintenance but in monitoring and

processing functions. *Neuroscience*, *141*(2), 585–596. https://doi.org/10.1016/j.neuroscience.2006.04.009

Glahn, D. C., Ragland, J. D., Abramoff, A., Barrett, J., Laird, A. R., Bearden, C. E., & Velligan, D. I. (2005). Beyond hypofrontality: A quantitative meta-analysis of functional neuroimaging studies of working memory in schizophrenia. *Human Brain Mapping*, *25*(1), 60–69. https://doi.org/10.1002/hbm.20138

Glausier, J., Fish, K., & Lewis, D. (2014). Altered parvalbumin basket cell inputs in the dorsolateral prefrontal cortex of schizophrenia subjects. *Molecular Psychiatry*, *19*(1), 10.1038/mp.2013.152. https://doi.org/10.1038/mp.2013.152

Glausier, J. R., Fish, K. N., & Lewis, D. A. (2014). Altered parvalbumin basket cell inputs in the dorsolateral prefrontal cortex of schizophrenia subjects. *Molecular Psychiatry*, *19*(1), 30–36. https://doi.org/10.1038/mp.2013.152

Goedert, M., Sisodia, S. S., & Price, D. L. (1991). Neurofibrillary tangles and β-amyloid deposits in Alzheimer's disease. *Current Opinion in Neurobiology*, *1*(3), 441–447. https://doi.org/10.1016/0959-4388(91)90067-H

Gogolla, N., Caroni, P., Lüthi, A., & Herry, C. (2009a). Perineuronal nets protect fear memories from erasure. *Science*, *325*(5945), 1258–1261.

Gogolla, N., Caroni, P., Lüthi, A., & Herry, C. (2009b). Perineuronal Nets Protect Fear Memories from Erasure. *Science*, *325*(5945), 1258–1261. https://doi.org/10.1126/science.1174146

Goldberg, E. M., Clark, B. D., Zagha, E., Nahmani, M., Erisir, A., & Rudy, B. (2008). K+ Channels at the Axon Initial Segment Dampen Near-Threshold Excitability of

Neocortical Fast-Spiking GABAergic Interneurons. *Neuron*, *58*(3), 387–400. https://doi.org/10.1016/j.neuron.2008.03.003

Golgi, C. (1893). Golgi, C. (1893). Intorno all'origine del quarto nervo cerebrale e una questione isto-fisiologica che a questo argomento si collega. Rendiconti della Reale Accademia Del Lincei, 2, 379-389. *Rendiconti Della Reale Accademia Del Lincei*, *2*, 379–389.

Gonzalez-Burgos, G., Hashimoto, T., & Lewis, D. A. (2010). Alterations of Cortical GABA Neurons and Network Oscillations in Schizophrenia. *Current Psychiatry Reports*, *12*(4), 335–344. https://doi.org/10.1007/s11920-010-0124-8

Gonzalez-Burgos, G., & Lewis, D. A. (2012a). NMDA Receptor Hypofunction, Parvalbumin-Positive Neurons, and Cortical Gamma Oscillations in Schizophrenia. *Schizophrenia Bulletin*, *38*(5), 950–957. https://doi.org/10.1093/schbul/sbs010

Gonzalez-Burgos, G., & Lewis, D. A. (2012b). NMDA Receptor Hypofunction, Parvalbumin-Positive Neurons, and Cortical Gamma Oscillations in Schizophrenia. *Schizophrenia Bulletin*, *38*(5), 950–957. https://doi.org/10.1093/schbul/sbs010

Gottschall, P., & Deb, S. (1996). Regulation of Matrix Metalloproteinase Expression in Astrocytes, Microglia and Neurons. *Neuroimmunomodulation*, *3*, 69–75. https://doi.org/10.1159/000097229

Granon, S., Vidal, C., Thinus-Blanc, C., Changeux, J.-P., & Poucet, B. (1994). Working memory, response selection, and effortful processing in rats with medial prefrontal lesions. *Behavioral Neuroscience*, *108*, 883–891. https://doi.org/10.1037/0735-7044.108.5.883

Gray, C. M., & Singer, W. (1989). Stimulus-specific neuronal oscillations in orientation columns of cat visual cortex. *Proceedings of the National Academy of Sciences*, *86*(5), 1698–1702. https://doi.org/10.1073/pnas.86.5.1698

Gray, D. T., Khattab, S., Meltzer, J., McDermott, K., Schwyhart, R., Sinakevitch, I., Härtig, W., & Barnes, C. A. (2023). Retrosplenial cortex microglia and perineuronal net densities are associated with memory impairment in aged rhesus macaques. *Cerebral Cortex*, *33*(8), 4626–4644. https://doi.org/10.1093/cercor/bhac366

Gray, E., Thomas, T. L., Betmouni, S., Scolding, N., & Love, S. (2008). Elevated Matrix Metalloproteinase-9 and Degradation of Perineuronal Nets in Cerebrocortical Multiple Sclerosis Plaques. *Journal of Neuropathology & Experimental Neurology*, *67*(9), 888–899. https://doi.org/10.1097/NEN.0b013e318183d003

Grayson, B., Leger, M., Piercy, C., Adamson, L., Harte, M., & Neill, J. C. (2015). Assessment of disease-related cognitive impairments using the novel object recognition (NOR) task in rodents. *Behavioural Brain Research*, *285*, 176–193. https://doi.org/10.1016/j.bbr.2014.10.025

Grayson, D. R., Jia, X., Chen, Y., Sharma, R. P., Mitchell, C. P., Guidotti, A., & Costa, E. (2005). Reelin promoter hypermethylation in schizophrenia. *Proceedings of the National Academy of Sciences*, *102*(26), 9341–9346. https://doi.org/10.1073/pnas.0503736102

Griñán-Ferré, C., Izquierdo, V., Otero, E., Puigoriol-Illamola, D., Corpas, R., Sanfeliu, C., Ortuño-Sahagún, D., & Pallàs, M. (2018). Environmental Enrichment Improves Cognitive Deficits, AD Hallmarks and Epigenetic Alterations Presented in 5xFAD Mouse Model. *Frontiers in Cellular Neuroscience*, *12*. https://www.frontiersin.org/articles/10.3389/fncel.2018.00224

Griñán-Ferré, C., Sarroca, S., Ivanova, A., Puigoriol-Illamola, D., Aguado, F., Camins, A., Sanfeliu, C., & Pallàs, M. (2016). Epigenetic mechanisms underlying cognitive impairment and Alzheimer disease hallmarks in 5XFAD mice. *Aging (Albany NY)*, *8*(4), 664–684. https://doi.org/10.18632/aging.100906

Gu, D., Liu, F., Meng, M., Zhang, L., Gordon, M. L., Wang, Y., Cai, L., & Zhang, N. (2020). Elevated matrix metalloproteinase-9 levels in neuronal extracellular vesicles in Alzheimer's disease. *Annals of Clinical and Translational Neurology*, *7*(9), 1681–1691. https://doi.org/10.1002/acn3.51155

Guidotti, A., Auta, J., Davis, J. M., Gerevini, V. D., Dwivedi, Y., Grayson, D. R., Impagnatiello, F., Pandey, G., Pesold, C., Sharma, R., Uzunov, D., & Costa, E. (2000). Decrease in Reelin and Glutamic Acid Decarboxylase67 (GAD67) Expression in Schizophrenia and Bipolar Disorder: A Postmortem Brain Study. *Archives of General Psychiatry*, *57*(11), 1061–1069. https://doi.org/10.1001/archpsyc.57.11.1061

Gulyás, A. I., Megías, M., Emri, Z., & Freund, T. F. (1999). Total Number and Ratio of Excitatory and Inhibitory Synapses Converging onto Single Interneurons of Different Types in the CA1 Area of the Rat Hippocampus. *Journal of Neuroscience*, *19*(22), 10082–10097. https://doi.org/10.1523/JNEUROSCI.19-22-10082.1999

Guyon, N., Zacharias, L. R., Oliveira, E. F. de, Kim, H., Leite, J. P., Lopes-Aguiar, C., & Carlén, M. (2021). Network Asynchrony Underlying Increased Broadband Gamma Power. *Journal of Neuroscience*, *41*(13), 2944–2963. https://doi.org/10.1523/JNEUROSCI.2250-20.2021

Guzman, S. J., Schlögl, A., Espinoza, C., Zhang, X., Suter, B., & Jonas, P. (2019). *Fast signaling and focal connectivity of PV+ interneurons ensure efficient pattern separation by lateral*

inhibition in a full-scale dentate gyrus network model (p. 647800). bioRxiv. https://doi.org/10.1101/647800

Haig, A. R., Gordon, E., Wright, J. J., Meares, R. A., & Bahramali, H. (2000). Synchronous cortical gamma-band activity in task-relevant cognition. *NeuroReport*, *11*(4), 669.

Haijima, A., & Ichitani, Y. (2012). Dissociable anterograde amnesic effects of retrosplenial cortex and hippocampal lesions on spontaneous object recognition memory in rats. *Hippocampus*, *22*(9), 1868–1875. https://doi.org/10.1002/hipo.22021

Hameed, M. Q., Hodgson, N., Lee, H. H. C., Pascual-Leone, A., MacMullin, P. C., Jannati, A., Dhamne, S. C., Hensch, T. K., & Rotenberg, A. (2023). N-acetylcysteine treatment mitigates loss of cortical parvalbumin-positive interneuron and perineuronal net integrity resulting from persistent oxidative stress in a rat TBI model. *Cerebral Cortex*, *33*(7), 4070–4084. https://doi.org/10.1093/cercor/bhac327

Hammond, R. S., Tull, L. E., & Stackman, R. W. (2004). On the delay-dependent involvement of the hippocampus in object recognition memory. *Neurobiology of Learning and Memory*, *82*(1), 26–34. https://doi.org/10.1016/j.nlm.2004.03.005

Hannesson, D. K. (2004). Interaction between Perirhinal and Medial Prefrontal Cortex Is Required for Temporal Order But Not Recognition Memory for Objects in Rats. *Journal of Neuroscience*, *24*(19), 4596–4604. https://doi.org/10.1523/JNEUROSCI.5517-03.2004

Hansen, D. V., Hanson, J. E., & Sheng, M. (2018). Microglia in Alzheimer's disease. *Journal of Cell Biology*, *217*(2), 459–472. https://doi.org/10.1083/jcb.201709069

Happel, M. F. K., Niekisch, H., Castiblanco Rivera, L. L., Ohl, F. W., Deliano, M., & Frischknecht, R. (2014). Enhanced cognitive flexibility in reversal learning induced by removal of the extracellular matrix in auditory cortex. *Proceedings of the National*

Academy of Sciences of the United States of America, *111*(7), 2800–2805. https://doi.org/10.1073/pnas.1310272111

Hardy, J., & Allsop, D. (1991). Amyloid deposition as the central event in the aetiology of Alzheimer's disease. *Trends in Pharmacological Sciences*, *12*, 383–388. https://doi.org/10.1016/0165-6147(91)90609-V

Harris, L. W., Lockstone, H. E., Khaitovich, P., Weickert, C. S., Webster, M. J., & Bahn, S. (2009). Gene expression in the prefrontal cortex during adolescence: Implications for the onset of schizophrenia. *BMC Medical Genomics*, *2*(1), Article 1. https://doi.org/10.1186/1755-8794-2-28

Härtig, W., Brauer, K., & Brückner, G. (1992). Wisteria floribunda agglutinin-labelled nets surround parvalbumin-containing neurons. *Neuroreport*, *3*(10), 869–872.

Härtig, W., Derouiche, A., Welt, K., Brauer, K., Grosche, J., Mäder, M., Reichenbach, A., & Brückner, G. (1999a). Cortical neurons immunoreactive for the potassium channel Kv3.1b subunit are predominantly surrounded by perineuronal nets presumed as a buffering system for cations. *Brain Research*, *842*(1), 15–29. https://doi.org/10.1016/S0006-8993(99)01784-9

Härtig, W., Derouiche, A., Welt, K., Brauer, K., Grosche, J., Mäder, M., Reichenbach, A., & Brückner, G. (1999b). Cortical neurons immunoreactive for the potassium channel Kv3.1b subunit are predominantly surrounded by perineuronal nets presumed as a buffering system for cations. *Brain Research*, *842*(1), 15–29. https://doi.org/10.1016/S0006-8993(99)01784-9

Hashimoto, T., Volk, D. W., Eggan, S. M., Mirnics, K., Pierri, J. N., Sun, Z., Sampson, A. R., & Lewis, D. A. (2003). Gene Expression Deficits in a Subclass of GABA Neurons in the

Prefrontal Cortex of Subjects with Schizophrenia. *The Journal of Neuroscience*, *23*(15), 6315–6326. https://doi.org/10.1523/JNEUROSCI.23-15-06315.2003

Hayani, H., Song, I., & Dityatev, A. (2018). Increased Excitability and Reduced Excitatory Synaptic Input Into Fast-Spiking CA2 Interneurons After Enzymatic Attenuation of Extracellular Matrix. *Frontiers in Cellular Neuroscience*, *12*. https://www.frontiersin.org/articles/10.3389/fncel.2018.00149

Heckers, S., Rauch, S., Goff, D., Savage, C., Schacter, D., Fischman, A., & Alpert, N. (1998). Impaired recruitment of the hippocampus during conscious recollection in schizophrenia. *Nature Neuroscience*, *1*(4), Article 4. https://doi.org/10.1038/1137

Heine, M., Groc, L., Frischknecht, R., Beique, J., Lounis, B., Rumbaugh, G., Huganir, R., Cognet, L., & Choquet, D. (2008). Surface mobility of AMPARs tunes synaptic transmission. *Science*, *320*(5873), 201–205.

Hendry, S. H., Jones, E. G., Hockfield, S., & McKay, R. D. (1988). Neuronal populations stained with the monoclonal antibody Cat-301 in the mammalian cerebral cortex and thalamus. *Journal of Neuroscience*, *8*(2), 518–542. https://doi.org/10.1523/JNEUROSCI.08-02-00518.1988

Hensch, T. K. (2005). Critical period plasticity in local cortical circuits. *Nature Reviews Neuroscience*, *6*(11), 877–888. https://doi.org/10.1038/nrn1787

Hijazi, S., Heistek, T. S., Scheltens, P., Neumann, U., Shimshek, D. R., Mansvelder, H. D., Smit, A. B., & van Kesteren, R. E. (2020). Early restoration of parvalbumin interneuron activity prevents memory loss and network hyperexcitability in a mouse model of Alzheimer's disease. *Molecular Psychiatry*, *25*(12), Article 12. https://doi.org/10.1038/s41380-019-0483-4

Himanshu, Dharmila, Sarkar, D., & Nutan. (2020). A Review of Behavioral Tests to Evaluate Different Types of Anxiety and Anti-anxiety Effects. *Clinical Psychopharmacology and Neuroscience*, *18*(3), 341–351. https://doi.org/10.9758/cpn.2020.18.3.341

Hindley, E. L., Nelson, A. J. D., Aggleton, J. P., & Vann, S. D. (2014). Dysgranular retrosplenial cortex lesions in rats disrupt cross-modal object recognition. *Learning & Memory*, *21*(3), 171–179. https://doi.org/10.1101/lm.032516.113

Hirono, M., Watanabe, S., Karube, F., Fujiyama, F., Kawahara, S., Nagao, S., Yanagawa, Y., & Misonou, H. (2018). Perineuronal Nets in the Deep Cerebellar Nuclei Regulate GABAergic Transmission and Delay Eyeblink Conditioning. *Journal of Neuroscience*, *38*(27), 6130–6144. https://doi.org/10.1523/JNEUROSCI.3238-17.2018

Hockfield, S., & McKay, R. D. (1983). A surface antigen expressed by a subset of neurons in the vertebrate central nervous system. *Proceedings of the National Academy of Sciences*, *80*(18), 5758–5761.

Hof, P. R., Cox, K., Young, W. G., Celio, M. R., Rogers, J., & Morrison, J. H. (1991). Parvalbumin-immunoreactive neurons in the neocortex are resistant to degeneration in Alzheimer's disease. *Journal of Neuropathology and Experimental Neurology*, *50*(4), 451–462. https://doi.org/10.1097/00005072-199107000-00006

Hoffman, R. E., & Cavus, I. (2002). Slow Transcranial Magnetic Stimulation, Long-Term Depotentiation, and Brain Hyperexcitability Disorders. *American Journal of Psychiatry*, *159*(7), 1093–1102. https://doi.org/10.1176/appi.ajp.159.7.1093

Homayoun, H., & Moghaddam, B. (2007). NMDA Receptor Hypofunction Produces Opposite Effects on Prefrontal Cortex Interneurons and Pyramidal Neurons. *Journal of Neuroscience*, *27*(43), 11496–11500. https://doi.org/10.1523/JNEUROSCI.2213-07.2007

Hong, L. E., Summerfelt, A., Buchanan, R. W., O'Donnell, P., Thaker, G. K., Weiler, M. A., & Lahti, A. C. (2010). Gamma and Delta Neural Oscillations and Association with Clinical Symptoms under Subanesthetic Ketamine. *Neuropsychopharmacology*, *35*(3), Article 3. https://doi.org/10.1038/npp.2009.168

Hong, S., Beja-Glasser, V. F., Nfonoyim, B. M., Frouin, A., Li, S., Ramakrishnan, S., Merry, K. M., Shi, Q., Rosenthal, A., Barres, B. A., Lemere, C. A., Selkoe, D. J., & Stevens, B. (2016). Complement and microglia mediate early synapse loss in Alzheimer mouse models. *Science*, *352*(6286), 712–716. https://doi.org/10.1126/science.aad8373

Honkanen, R., Rouhinen, S., Wang, S. H., Palva, J. M., & Palva, S. (2015). Gamma Oscillations Underlie the Maintenance of Feature-Specific Information and the Contents of Visual Working Memory. *Cerebral Cortex*, *25*(10), 3788–3801. https://doi.org/10.1093/cercor/bhu263

Horst, N. K., & Laubach, M. (2009). The role of rat dorsomedial prefrontal cortex in spatial working memory. *Neuroscience*, *164*(2), 444–456. https://doi.org/10.1016/j.neuroscience.2009.08.004

Howells, F. M., Temmingh, H. S., Hsieh, J. H., van Dijen, A. V., Baldwin, D. S., & Stein, D. J. (2018). Electroencephalographic delta/alpha frequency activity differentiates psychotic disorders: A study of schizophrenia, bipolar disorder and methamphetamine-induced psychotic disorder. *Translational Psychiatry*, *8*(1), Article 1. https://doi.org/10.1038/s41398-018-0105-y

Howes, O. D., & Shatalina, E. (2022). Integrating the Neurodevelopmental and Dopamine Hypotheses of Schizophrenia and the Role of Cortical Excitation-Inhibition Balance. *Biological Psychiatry*, *92*(6), 501–513. https://doi.org/10.1016/j.biopsych.2022.06.017

Howland, J. G., Cazakoff, B. N., & Zhang, Y. (2012a). Altered object-in-place recognition memory, prepulse inhibition, and locomotor activity in the offspring of rats exposed to a viral mimetic during pregnancy. *Neuroscience*, *201*, 184–198. https://doi.org/10.1016/j.neuroscience.2011.11.011

Howland, J. G., Cazakoff, B. N., & Zhang, Y. (2012b). Altered object-in-place recognition memory, prepulse inhibition, and locomotor activity in the offspring of rats exposed to a viral mimetic during pregnancy. *Neuroscience*, *201*, 184–198. https://doi.org/10.1016/j.neuroscience.2011.11.011

Hrabětová, S., Masri, D., Tao, L., Xiao, F., & Nicholson, C. (2009). Calcium diffusion enhanced after cleavage of negatively charged components of brain extracellular matrix by chondroitinase ABC. *The Journal of Physiology*, *587*(16), 4029–4049. https://doi.org/10.1113/jphysiol.2009.170092

Hsieh, T.-H., Lee, H. H. C., Hameed, M. Q., Pascual-Leone, A., Hensch, T. K., & Rotenberg, A. (2017). Trajectory of Parvalbumin Cell Impairment and Loss of Cortical Inhibition in Traumatic Brain Injury. *Cerebral Cortex (New York, N.Y.: 1991)*, *27*(12), 5509–5524. https://doi.org/10.1093/cercor/bhw318

Hu, H., Gan, J., & Jonas, P. (2014). Fast-spiking, parvalbumin $^{+}$ GABAergic interneurons: From cellular design to microcircuit function. *Science*, *345*(6196), 1255263. https://doi.org/10.1126/science.1255263

HUANG, W.-J., ZHANG, X., & CHEN, W.-W. (2016). Role of oxidative stress in Alzheimer's disease. *Biomedical Reports*, *4*(5), 519–522. https://doi.org/10.3892/br.2016.630

Hull, C., Isaacson, J. S., & Scanziani, M. (2009). Postsynaptic Mechanisms Govern the Differential Excitation of Cortical Neurons by Thalamic Inputs. *Journal of Neuroscience*, *29*(28), 9127–9136. https://doi.org/10.1523/JNEUROSCI.5971-08.2009

Hunt, M., Falinska, M., & Kasicki, S. (2010). Local injection of MK801 modifies oscillatory activity in the nucleus accumbens in awake rats. *Journal of Psychopharmacology*, *24*(6), 931–941. https://doi.org/10.1177/0269881109102539

Hunt, M. J., Kopell, N. J., Traub, R. D., & Whittington, M. A. (2017). Aberrant Network Activity in Schizophrenia. *Trends in Neurosciences*, *40*(6), 371–382. https://doi.org/10.1016/j.tins.2017.04.003

Hylin, M. J., Orsi, S. A., Moore, A. N., & Dash, P. K. (2013). Disruption of the perineuronal net in the hippocampus or medial prefrontal cortex impairs fear conditioning. *Learning & Memory*, *20*(5), 267–273. https://doi.org/10.1101/lm.030197.112

Iafrati, J., Orejarena, M. J., Lassalle, O., Bouamrane, L., & Chavis, P. (2014). Reelin, an extracellular matrix protein linked to early onset psychiatric diseases, drives postnatal development of the prefrontal cortex via GluN2B-NMDARs and the mTOR pathway. *Molecular Psychiatry*, *19*(4), 417–426. https://doi.org/10.1038/mp.2013.66

Ibi, D., Nagai, T., Kitahara, Y., Mizoguchi, H., Koike, H., Shiraki, A., Takuma, K., Kamei, H., Noda, Y., Nitta, A., Nabeshima, T., Yoneda, Y., & Yamada, K. (2009). Neonatal polyI:C treatment in mice results in schizophrenia-like behavioral and neurochemical abnormalities in adulthood. *Neuroscience Research*, *64*(3), 297–305. https://doi.org/10.1016/j.neures.2009.03.015

Impagnatiello, F., Guidotti, A. R., Pesold, C., Dwivedi, Y., Caruncho, H., Pisu, M. G., Uzunov, D. P., Smalheiser, N. R., Davis, J. M., Pandey, G. N., Pappas, G. D., Tueting, P., Sharma,

R. P., & Costa, E. (1998). A decrease of reelin expression as a putative vulnerability factor in schizophrenia. *Proceedings of the National Academy of Sciences*, *95*(26), 15718–15723. https://doi.org/10.1073/pnas.95.26.15718

Inhoff, M. C., & Ranganath, C. (2015). Significance of objects in the perirhinal cortex. *Trends in Cognitive Sciences*, *19*(6), 302–303. https://doi.org/10.1016/j.tics.2015.04.008

Jacklin, D. L., Cloke, J. M., Potvin, A., Garrett, I., & Winters, B. D. (2016a). The Dynamic Multisensory Engram: Neural Circuitry Underlying Crossmodal Object Recognition in Rats Changes with the Nature of Object Experience. *Journal of Neuroscience*, *36*(4), 1273–1289. https://doi.org/10.1523/JNEUROSCI.3043-15.2016

Jacklin, D. L., Cloke, J. M., Potvin, A., Garrett, I., & Winters, B. D. (2016b). The Dynamic Multisensory Engram: Neural Circuitry Underlying Crossmodal Object Recognition in Rats Changes with the Nature of Object Experience. *Journal of Neuroscience*, *36*(4), 1273–1289. https://doi.org/10.1523/JNEUROSCI.3043-15.2016

Jadi, M. P., Behrens, M. M., & Sejnowski, T. J. (2016). Abnormal Gamma Oscillations in N-Methyl-D-Aspartate Receptor Hypofunction Models of Schizophrenia. *Biological Psychiatry*, *79*(9), 716–726. https://doi.org/10.1016/j.biopsych.2015.07.005

Jäger, C., Lendvai, D., Seeger, G., Brückner, G., Matthews, R. T., Arendt, T., Alpár, A., & Morawski, M. (2013). Perineuronal and perisynaptic extracellular matrix in the human spinal cord. *Neuroscience*, *238*, 168–184. https://doi.org/10.1016/j.neuroscience.2013.02.014

Javonillo, D. I., Tran, K. M., Phan, J., Hingco, E., Kramár, E. A., da Cunha, C., Forner, S., Kawauchi, S., Milinkeviciute, G., Gomez-Arboledas, A., Neumann, J., Banh, C. E., Huynh, M., Matheos, D. P., Rezaie, N., Alcantara, J. A., Mortazavi, A., Wood, M. A.,

Tenner, A. J., … LaFerla, F. M. (2022). Systematic Phenotyping and Characterization of the 3xTg-AD Mouse Model of Alzheimer's Disease. *Frontiers in Neuroscience*, *15*. https://www.frontiersin.org/articles/10.3389/fnins.2021.785276

Jawhar, S., Trawicka, A., Jenneckens, C., Bayer, T. A., & Wirths, O. (2012). Motor deficits, neuron loss, and reduced anxiety coinciding with axonal degeneration and intraneuronal Aβ aggregation in the 5XFAD mouse model of Alzheimer's disease. *Neurobiology of Aging*, *33*(1), 196.e29-196.e40. https://doi.org/10.1016/j.neurobiolaging.2010.05.027

Jiang, Z., Cowell, R., & Nakazawa, K. (2013). Convergence of genetic and environmental factors on parvalbumin-positive interneurons in schizophrenia. *Frontiers in Behavioral Neuroscience*, *7*. https://www.frontiersin.org/articles/10.3389/fnbeh.2013.00116

Jobson, D. D., Hase, Y., Clarkson, A. N., & Kalaria, R. N. (2021). The role of the medial prefrontal cortex in cognition, ageing and dementia. *Brain Communications*, *3*(3), fcab125. https://doi.org/10.1093/braincomms/fcab125

John, N., Krügel, H., Frischknecht, R., Smalla, K.-H., Schultz, C., Kreutz, M. R., Gundelfinger, E. D., & Seidenbecher, C. I. (2006). Brevican-containing perineuronal nets of extracellular matrix in dissociated hippocampal primary cultures. *Molecular and Cellular Neuroscience*, *31*(4), 774–784. https://doi.org/10.1016/j.mcn.2006.01.011

Johnson, C. T., Olton, D. S., Gage, F. H., & Jenko, P. G. (1977). Damage to hippocampus and hippocampal connections: Effects on DRL and spontaneous alternation. *Journal of Comparative and Physiological Psychology*, *91*(3), 508–522. https://doi.org/10.1037/h0077346

Jouhanneau, J.-S., Kremkow, J., & Poulet, J. F. A. (2018). Single synaptic inputs drive high-precision action potentials in parvalbumin expressing GABA-ergic cortical neurons in

vivo. *Nature Communications*, *9*(1), Article 1. https://doi.org/10.1038/s41467-018-03995-2

Kamiński, J., Sullivan, S., Chung, J. M., Ross, I. B., Mamelak, A. N., & Rutishauser, U. (2017). Persistently active neurons in human medial frontal and medial temporal lobe support working memory. *Nature Neuroscience*, *20*(4), 590–601. https://doi.org/10.1038/nn.4509

Kann, O., Papageorgiou, I. E., & Draguhn, A. (2014). Highly Energized Inhibitory Interneurons are a Central Element for Information Processing in Cortical Networks. *Journal of Cerebral Blood Flow & Metabolism*, *34*(8), 1270–1282. https://doi.org/10.1038/jcbfm.2014.104

Karnani, M. M., Agetsuma, M., & Yuste, R. (2014). A blanket of inhibition: Functional inferences from dense inhibitory connectivity. *Current Opinion in Neurobiology*, *26*, 96–102. https://doi.org/10.1016/j.conb.2013.12.015

Karube, F., Kubota, Y., & Kawaguchi, Y. (2004). Axon Branching and Synaptic Bouton Phenotypes in GABAergic Nonpyramidal Cell Subtypes. *Journal of Neuroscience*, *24*(12), 2853–2865. https://doi.org/10.1523/JNEUROSCI.4814-03.2004

Kaushik, R., Lipachev, N., Matuszko, G., Kochneva, A., Dvoeglazova, A., Becker, A., Paveliev, M., & Dityatev, A. (2021). Fine structure analysis of perineuronal nets in the ketamine model of schizophrenia. *European Journal of Neuroscience*, *53*(12), 3988–4004. https://doi.org/10.1111/ejn.14853

Keilhoff, G., Becker, A., Grecksch, G., Wolf, G., & Bernstein, H.-G. (2004). Repeated application of ketamine to rats induces changes in the hippocampal expression of parvalbumin, neuronal nitric oxide synthase and cFOS similar to those found in human

schizophrenia. *Neuroscience*, *126*(3), 591–598. https://doi.org/10.1016/j.neuroscience.2004.03.039

Kent, S. A., Spires-Jones, T. L., & Durrant, C. S. (2020). The physiological roles of tau and Aβ: Implications for Alzheimer's disease pathology and therapeutics. *Acta Neuropathologica*, *140*(4), 417–447. https://doi.org/10.1007/s00401-020-02196-w

Khoo, G. H., Lin, Y.-T., Tsai, T.-C., & Hsu, K.-S. (2019). Perineuronal Nets Restrict the Induction of Long-Term Depression in the Mouse Hippocampal CA1 Region. *Molecular Neurobiology*, *56*(9), 6436–6450. https://doi.org/10.1007/s12035-019-1526-1

Kilonzo, V. W., Sweet, R. A., Glausier, J. R., & Pitts, M. W. (2020). Deficits in Glutamic Acid Decarboxylase 67 Immunoreactivity, Parvalbumin Interneurons, and Perineuronal Nets in the Inferior Colliculus of Subjects With Schizophrenia. *Schizophrenia Bulletin*, *46*(5), 1053–1059. https://doi.org/10.1093/schbul/sbaa082

Kim, D.-H., Kim, H.-A., Han, Y. S., Jeon, W. K., & Han, J.-S. (2020). Recognition memory impairments and amyloid-beta deposition of the retrosplenial cortex at the early stage of 5XFAD mice. *Physiology & Behavior*, *222*, 112891. https://doi.org/10.1016/j.physbeh.2020.112891

Kim, J., Kim, J., Huang, Z., Goo, N., Bae, H. J., Jeong, Y., Park, H. J., Cai, M., Cho, K., Jung, S. Y., Bae, S. K., & Ryu, J. H. (2019). Theracurmin Ameliorates Cognitive Dysfunctions in 5XFAD Mice by Improving Synaptic Function and Mitigating Oxidative Stress. *Biomolecules & Therapeutics*, *27*(3), 327–335. https://doi.org/10.4062/biomolther.2019.046

Kim, T., Thankachan, S., McKenna, J. T., McNally, J. M., Yang, C., Choi, J. H., Chen, L., Kocsis, B., Deisseroth, K., Strecker, R. E., Basheer, R., Brown, R. E., & McCarley, R.

W. (2015). Cortically projecting basal forebrain parvalbumin neurons regulate cortical gamma band oscillations. *Proceedings of the National Academy of Sciences*, *112*(11), 3535–3540. https://doi.org/10.1073/pnas.1413625112

Kimoto, S., Bazmi, H. H., & Lewis, D. A. (2014). Lower Expression of Glutamic Acid Decarboxylase 67 in the Prefrontal Cortex in Schizophrenia: Contribution of Altered Regulation by Zif268. *American Journal of Psychiatry*, *171*(9), 969–978. https://doi.org/10.1176/appi.ajp.2014.14010004

Kimura, R., & Ohno, M. (2009). Impairments in remote memory stabilization precede hippocampal synaptic and cognitive failures in 5XFAD Alzheimer mouse model. *Neurobiology of Disease*, *33*(2), 229–235. https://doi.org/10.1016/j.nbd.2008.10.006

Kinney, J. W., Davis, C. N., Tabarean, I., Conti, B., Bartfai, T., & Behrens, M. M. (2006). A Specific Role for NR2A-Containing NMDA Receptors in the Maintenance of Parvalbumin and GAD67 Immunoreactivity in Cultured Interneurons. *Journal of Neuroscience*, *26*(5), 1604–1615. https://doi.org/10.1523/JNEUROSCI.4722-05.2006

Kirkby, R. J., Stein, D. G., Kimble, R. J., & Kimble, D. P. (1967). Effects of hippocampal lesions and duration of sensory input on spontaneous alternation. *Journal of Comparative and Physiological Psychology*, *64*(2), 342–345. https://doi.org/10.1037/h0088012

Kiss, T., Hoffmann, W. E., & Hajós, M. (2011). Delta oscillation and short-term plasticity in the rat medial prefrontal cortex: Modelling NMDA hypofunction of schizophrenia. *International Journal of Neuropsychopharmacology*, *14*(1), 29–42. https://doi.org/10.1017/S1461145710000271

Kitagawa, H., Tsutsumi, K., Tone, Y., & Sugahara, K. (1997). Developmental Regulation of the Sulfation Profile of Chondroitin Sulfate Chains in the Chicken Embryo Brain *. *Journal*

of Biological Chemistry, *272*(50), 31377–31381. https://doi.org/10.1074/jbc.272.50.31377

Klausberger, T., & Somogyi, P. (2008). Neuronal Diversity and Temporal Dynamics: The Unity of Hippocampal Circuit Operations. *Science*, *321*(5885), 53–57. https://doi.org/10.1126/science.1149381

Kobayashi, K., Emson, P. C., & Mountjoy, C. Q. (1989). Vicia villosa lectin-positive neurones in human cerebral cortex. Loss in Alzheimer-type dementia. *Brain Research*, *498*(1), 170–174. https://doi.org/10.1016/0006-8993(89)90416-2

Kobayashi, Y., & Amaral, D. G. (2003). Macaque monkey retrosplenial cortex: II. Cortical afferents. *Journal of Comparative Neurology*, *466*(1), 48–79. https://doi.org/10.1002/cne.10883

Kochlamazashvili, G., Henneberger, C., Bukalo, O., Dvoretskova, E., Senkov, O., Lievens, P. M.-J., Westenbroek, R., Engel, A. K., Catterall, W. A., Rusakov, D. A., Schachner, M., & Dityatev, A. (2010). The Extracellular Matrix Molecule Hyaluronic Acid Regulates Hippocampal Synaptic Plasticity by Modulating Postsynaptic L-Type Ca2+ Channels. *Neuron*, *67*(1), 116–128. https://doi.org/10.1016/j.neuron.2010.05.030

Koh, M. T., Shao, Y., Sherwood, A., & Smith, D. R. (2016). Impaired hippocampal-dependent memory and reduced parvalbumin-positive interneurons in a ketamine mouse model of schizophrenia. *Schizophrenia Research*, *171*(1), 187–194. https://doi.org/10.1016/j.schres.2016.01.023

Koppe, G., Bruckner, G., Hartig, W., Delpech, B., & Bigl, V. (1997). Characterization of proteoglycan-containing perineuronal nets by enzymatic treatments of rat brain sections. *The Histochemical Journal*, *29*(1), 11–20. https://doi.org/10.1023/A:1026408716522

Kubota, T., Matsumoto, H., & Kirino, Y. (2016). Ameliorative effect of membrane-associated estrogen receptor G protein coupled receptor 30 activation on object recognition memory in mouse models of Alzheimer's disease. *Journal of Pharmacological Sciences*, *131*(3), 219–222. https://doi.org/10.1016/j.jphs.2016.06.005

Kudo, T., Takuwa, H., Takahashi, M., Urushihata, T., Shimojo, M., Sampei, K., Yamanaka, M., Tomita, Y., Sahara, N., Suhara, T., & Higuchi, M. (2023). Selective dysfunction of fast-spiking inhibitory interneurons and disruption of perineuronal nets in a tauopathy mouse model. *IScience*, *26*(4), 106342. https://doi.org/10.1016/j.isci.2023.106342

Kurt, S., Deutscher, A., Crook, J. M., Ohl, F. W., Budinger, E., Moeller, C. K., Scheich, H., & Schulze, H. (2008). Auditory Cortical Contrast Enhancing by Global Winner-Take-All Inhibitory Interactions. *PLOS ONE*, *3*(3), e1735. https://doi.org/10.1371/journal.pone.0001735

Kwok, J. C. F., Carulli, D., & Fawcett, J. W. (2010). In vitro modeling of perineuronal nets: Hyaluronan synthase and link protein are necessary for their formation and integrity. *Journal of Neurochemistry*, *114*(5), 1447–1459. https://doi.org/10.1111/j.1471-4159.2010.06878.x

Kwok, J. C. F., Dick, G., Wang, D., & Fawcett, J. W. (2011). Extracellular matrix and perineuronal nets in CNS repair. *Developmental Neurobiology*, *71*(11), 1073–1089. https://doi.org/10.1002/dneu.20974

Kwok, J. C. F., Foscarin, S., & Fawcett, J. W. (2015). Perineuronal Nets: A Special Structure in the Central Nervous System Extracellular Matrix. In J. B. Leach & E. M. Powell (Eds.), *Extracellular Matrix* (pp. 23–32). Springer. https://doi.org/10.1007/978-1-4939-2083-9_3

LaFerla, F. M., Green, K. N., & Oddo, S. (2007). Intracellular amyloid-β in Alzheimer's disease. *Nature Reviews Neuroscience*, *8*(7), 499–509. https://doi.org/10.1038/nrn2168

Lakatos, P., Schroeder, C. E., Leitman, D. I., & Javitt, D. C. (2013). Predictive Suppression of Cortical Excitability and Its Deficit in Schizophrenia. *Journal of Neuroscience*, *33*(28), 11692–11702. https://doi.org/10.1523/JNEUROSCI.0010-13.2013

Lalonde, R. (2002). The neurobiological basis of spontaneous alternation. *Neuroscience & Biobehavioral Reviews*, *26*(1), 91–104. https://doi.org/10.1016/S0149-7634(01)00041-0

Lander, C., Kind, P., Maleski, M., & Hockfield, S. (1997). A Family of Activity-Dependent Neuronal Cell-Surface Chondroitin Sulfate Proteoglycans in Cat Visual Cortex. *Journal of Neuroscience*, *17*(6), 1928–1939. https://doi.org/10.1523/JNEUROSCI.17-06-01928.1997

Lander, C., Zhang, H., & Hockfield, S. (1998). Neurons Produce a Neuronal Cell Surface-Associated Chondroitin Sulfate Proteoglycan. *Journal of Neuroscience*, *18*(1), 174–183. https://doi.org/10.1523/JNEUROSCI.18-01-00174.1998

Lasek, A. W., Chen, H., & Chen, W.-Y. (2018). Releasing Addiction Memories Trapped in Perineuronal Nets. *Trends in Genetics*, *34*(3), 197–208. https://doi.org/10.1016/j.tig.2017.12.004

Latif-Hernandez, A., Shah, D., Ahmed, T., Lo, A. C., Callaerts-Vegh, Z., Van der Linden, A., Balschun, D., & D'Hooge, R. (2016). Quinolinic acid injection in mouse medial prefrontal cortex affects reversal learning abilities, cortical connectivity and hippocampal synaptic plasticity. *Scientific Reports*, *6*(1). https://doi.org/10.1038/srep36489

Lau, L. W., Cua, R., Keough, M. B., Haylock-Jacobs, S., & Yong, V. W. (2013). Pathophysiology of the brain extracellular matrix: A new target for remyelination. *Nature Reviews Neuroscience*, *14*(10), Article 10. https://doi.org/10.1038/nrn3550

Laurienti, P. J., Wallace, M. T., Maldjian, J. A., Susi, C. M., Stein, B. E., & Burdette, J. H. (2003). Cross-modal sensory processing in the anterior cingulate and medial prefrontal cortices. *Human Brain Mapping*, *19*(4), 213–223. https://doi.org/10.1002/hbm.10112

Lavigne, K. M., Kanagasabai, K., & Palaniyappan, L. (2022). Ultra-high field neuroimaging in psychosis: A narrative review. *Frontiers in Psychiatry*, *13*, 994372. https://doi.org/10.3389/fpsyt.2022.994372

Leake, A., Morris, C. M., & Whateley, J. (2000). Brain matrix metalloproteinase 1 levels are elevated in Alzheimer's disease. *Neuroscience Letters*, *291*(3), 201–203. https://doi.org/10.1016/s0304-3940(00)01418-x

LeBeau, F. E. N., Towers, S. K., Traub, R. D., Whittington, M. A., & Buhl, E. H. (2002). Fast network oscillations induced by potassium transients in the rat hippocampus in vitro. *The Journal of Physiology*, *542*(1), 167–179. https://doi.org/10.1113/jphysiol.2002.015933

Lee, S.-J., Wei, M., Zhang, C., Maxeiner, S., Pak, C., Botelho, S. C., Trotter, J., Sterky, F. H., & Südhof, T. C. (2017). Presynaptic Neuronal Pentraxin Receptor Organizes Excitatory and Inhibitory Synapses. *Journal of Neuroscience*, *37*(5), 1062–1080. https://doi.org/10.1523/JNEUROSCI.2768-16.2016

Lee, Y., Morrison, B. M., Li, Y., Lengacher, S., Farah, M. H., Hoffman, P. N., Liu, Y., Tsingalia, A., Jin, L., Zhang, P.-W., Pellerin, L., Magistretti, P. J., & Rothstein, J. D. (2012). Oligodendroglia metabolically support axons and contribute to neurodegeneration. *Nature*, *487*(7408), 443–448. https://doi.org/10.1038/nature11314

Lehéricy, S., Hirsch, E. C., Cervera, P., Hersh, L. B., Hauw, J. J., Ruberg, M., & Agid, Y. (1989). Selective loss of cholinergic neurons in the ventral striatum of patients with Alzheimer disease. *Proceedings of the National Academy of Sciences*, *86*(21), 8580–8584. https://doi.org/10.1073/pnas.86.21.8580

Lener, M. S., Wong, E., Tang, C. Y., Byne, W., Goldstein, K. E., Blair, N. J., Haznedar, M. M., New, A. S., Chemerinski, E., Chu, K.-W., Rimsky, L. S., Siever, L. J., Koenigsberg, H. W., & Hazlett, E. A. (2015). White Matter Abnormalities in Schizophrenia and Schizotypal Personality Disorder. *Schizophrenia Bulletin*, *41*(1), 300–310. https://doi.org/10.1093/schbul/sbu093

Lensjø, K. K., Christensen, A. C., Tennøe, S., Fyhn, M., & Hafting, T. (2017). Differential Expression and Cell-Type Specificity of Perineuronal Nets in Hippocampus, Medial Entorhinal Cortex, and Visual Cortex Examined in the Rat and Mouse. *ENeuro*, *4*(3), ENEURO.0379-16.2017. https://doi.org/10.1523/ENEURO.0379-16.2017

Lensjø, K. K., Lepperød, M. E., Dick, G., Hafting, T., & Fyhn, M. (2017a). Removal of Perineuronal Nets Unlocks Juvenile Plasticity Through Network Mechanisms of Decreased Inhibition and Increased Gamma Activity. *The Journal of Neuroscience*, *37*(5), 1269–1283. https://doi.org/10.1523/JNEUROSCI.2504-16.2016

Lensjø, K. K., Lepperød, M. E., Dick, G., Hafting, T., & Fyhn, M. (2017b). Removal of Perineuronal Nets Unlocks Juvenile Plasticity Through Network Mechanisms of Decreased Inhibition and Increased Gamma Activity. *The Journal of Neuroscience*, *37*(5), 1269–1283. https://doi.org/10.1523/JNEUROSCI.2504-16.2016

Lensjø, K. K., Lepperød, M. E., Dick, G., Hafting, T., & Fyhn, M. (2017c). Removal of Perineuronal Nets Unlocks Juvenile Plasticity Through Network Mechanisms of

Decreased Inhibition and Increased Gamma Activity. *Journal of Neuroscience*, *37*(5), 1269–1283. https://doi.org/10.1523/JNEUROSCI.2504-16.2016

Lesh, T. A., Niendam, T. A., Minzenberg, M. J., & Carter, C. S. (2011). Cognitive Control Deficits in Schizophrenia: Mechanisms and Meaning. *Neuropsychopharmacology*, *36*(1), Article 1. https://doi.org/10.1038/npp.2010.156

Lett, T. A., Voineskos, A. N., Kennedy, J. L., Levine, B., & Daskalakis, Z. J. (2014). Treating Working Memory Deficits in Schizophrenia: A Review of the Neurobiology. *Biological Psychiatry*, *75*(5), 361–370. https://doi.org/10.1016/j.biopsych.2013.07.026

Leuba, G., Kraftsik, R., & Saini, K. (1998). Quantitative Distribution of Parvalbumin, Calretinin, and Calbindin D-28k Immunoreactive Neurons in the Visual Cortex of Normal and Alzheimer Cases. *Experimental Neurology*, *152*(2), 278–291. https://doi.org/10.1006/exnr.1998.6838

Leung, L. S., & Ma, J. (2018). Medial septum modulates hippocampal gamma activity and prepulse inhibition in an N-methyl-d-aspartate receptor antagonist model of schizophrenia. *Schizophrenia Research*, *198*, 36–44. https://doi.org/10.1016/j.schres.2017.07.053

Lewis, D. A. (2014). Inhibitory neurons in human cortical circuits: Substrate for cognitive dysfunction in schizophrenia. *Current Opinion in Neurobiology*, *26*, 22–26. https://doi.org/10.1016/j.conb.2013.11.003

Lewis, D. A., Curley, A. A., Glausier, J. R., & Volk, D. W. (2012). Cortical parvalbumin interneurons and cognitive dysfunction in schizophrenia. *Trends in Neurosciences*, *35*(1), 57–67. https://doi.org/10.1016/j.tins.2011.10.004

Liang, M., Zhou, Y., Jiang, T., Liu, Z., Tian, L., Liu, H., & Hao, Y. (2006). Widespread functional disconnectivity in schizophrenia with resting-state functional magnetic resonance imaging. *NeuroReport*, *17*(2), 209.

Liao, H., Bu, W., Wang, T.-H., Ahmed, S., & Xiao, Z.-C. (2005). Tenascin-R Plays a Role in Neuroprotection via Its Distinct Domains That Coordinate to Modulate the Microglia Function *. *Journal of Biological Chemistry*, *280*(9), 8316–8323. https://doi.org/10.1074/jbc.M412730200

Lim, L., Mi, D., Llorca, A., & Marín, O. (2018). Development and Functional Diversification of Cortical Interneurons. *Neuron*, *100*(2), 294–313. https://doi.org/10.1016/j.neuron.2018.10.009

Lins, B. R., Hurtubise, J. L., Roebuck, A. J., Marks, W. N., Zabder, N. K., Scott, G. A., Greba, Q., Dawicki, W., Zhang, X., Rudulier, C. D., Gordon, J. R., & Howland, J. G. (2018a). Prospective Analysis of the Effects of Maternal Immune Activation on Rat Cytokines during Pregnancy and Behavior of the Male Offspring Relevant to Schizophrenia. *Eneuro*, *5*(4), ENEURO.0249-18.2018. https://doi.org/10.1523/ENEURO.0249-18.2018

Lins, B. R., Hurtubise, J. L., Roebuck, A. J., Marks, W. N., Zabder, N. K., Scott, G. A., Greba, Q., Dawicki, W., Zhang, X., Rudulier, C. D., Gordon, J. R., & Howland, J. G. (2018b). Prospective Analysis of the Effects of Maternal Immune Activation on Rat Cytokines during Pregnancy and Behavior of the Male Offspring Relevant to Schizophrenia. *ENeuro*, *5*(4), ENEURO.0249-18.2018. https://doi.org/10.1523/ENEURO.0249-18.2018

Lins, B. R., Marks, W. N., Phillips, A. G., & Howland, J. G. (2017). Dissociable effects of the d- and l- enantiomers of govadine on the disruption of prepulse inhibition by MK-801 and

apomorphine in male Long-Evans rats. *Psychopharmacology*, *234*(7), 1079–1091. https://doi.org/10.1007/s00213-017-4540-x

Lipachev, N., Arnst, N., Melnikova, A., Jäälinoja, H., Kochneva, A., Zhigalov, A., Kulesskaya, N., Aganov, A. V., Mavlikeev, M., Rauvala, H., Kiyasov, A. P., & Paveliev, M. (2019). Quantitative changes in perineuronal nets in development and posttraumatic condition. *Journal of Molecular Histology*, *50*(3), 203–216. https://doi.org/10.1007/s10735-019-09818-y

Liu, D., Gu, X., Zhu, J., Zhang, X., Han, Z., Yan, W., Cheng, Q., Hao, J., Fan, H., Hou, R., Chen, Z., Chen, Y., & Li, C. T. (2014). Medial prefrontal activity during delay period contributes to learning of a working memory task. *Science*, *346*(6208), 458–463.

Liu, L., Xu, H., Wang, J., Li, J., Tian, Y., Zheng, J., He, M., Xu, T.-L., Wu, Z.-Y., Li, X.-M., Duan, S.-M., & Xu, H. (2020). Cell type–differential modulation of prefrontal cortical GABAergic interneurons on low gamma rhythm and social interaction. *Science Advances*, *6*(30), eaay4073. https://doi.org/10.1126/sciadv.aay4073

Liu, L., Zhang, Y., Men, S., Li, X., Hou, S.-T., & Ju, J. (2023). Elimination of perineuronal nets in CA1 disrupts GABA release and long-term contextual fear memory retention. *Hippocampus*, *n/a*(n/a). https://doi.org/10.1002/hipo.23503

Locci, A., Orellana, H., Rodriguez, G., Gottliebson, M., McClarty, B., Dominguez, S., Keszycki, R., & Dong, H. (2021). Comparison of memory, affective behavior, and neuropathology in APPNLGF knock-in mice to 5xFAD and APP/PS1 mice. *Behavioural Brain Research*, *404*, 113192. https://doi.org/10.1016/j.bbr.2021.113192

Lodge, D. J., Behrens, M. M., & Grace, A. A. (2009). A Loss of Parvalbumin-Containing Interneurons Is Associated with Diminished Oscillatory Activity in an Animal Model of

Schizophrenia. *Journal of Neuroscience*, *29*(8), 2344–2354. https://doi.org/10.1523/JNEUROSCI.5419-08.2009

Lorenzl, S., Albers, D. S., Relkin, N., Ngyuen, T., Hilgenberg, S. L., Chirichigno, J., Cudkowicz, M. E., & Beal, M. F. (2003). Increased plasma levels of matrix metalloproteinase-9 in patients with Alzheimer's disease. *Neurochemistry International*, *43*(3), 191–196. https://doi.org/10.1016/S0197-0186(03)00004-4

Lorke, D. E., Lu, G., Cho, E., & Yew, D. T. (2006). Serotonin 5-HT2A and 5-HT6 receptors in the prefrontal cortex of Alzheimer and normal aging patients. *BMC Neuroscience*, *7*(1), 36. https://doi.org/10.1186/1471-2202-7-36

Lu, H., Zou, Q., Gu, H., Raichle, M. E., Stein, E. A., & Yang, Y. (2012). Rat brains also have a default mode network. *Proceedings of the National Academy of Sciences*, *109*(10), 3979–3984. https://doi.org/10.1073/pnas.1200506109

Lu, Y., Zhu, Z.-G., Ma, Q.-Q., Su, Y.-T., Han, Y., Wang, X., Duan, S., & Yu, Y.-Q. (2018). A Critical Time-Window for the Selective Induction of Hippocampal Memory Consolidation by a Brief Episode of Slow-Wave Sleep. *Neuroscience Bulletin*, *34*(6), 1091–1099. https://doi.org/10.1007/s12264-018-0303-x

Lupori, L., Totaro, V., Cornuti, S., Ciampi, L., Carrara, F., Grilli, E., Viglione, A., Tozzi, F., Putignano, E., Mazziotti, R., Amato, G., Gennaro, C., Tognini, P., & Pizzorusso, T. (2023). *A Comprehensive Atlas of Perineuronal Net Distribution and Colocalization with Parvalbumin in the Adult Mouse Brain* [Preprint]. Neuroscience. https://doi.org/10.1101/2023.01.24.525313

MacKay, M.-A. B., Paylor, J. W., Wong, J. T. F., Winship, I. R., Baker, G. B., & Dursun, S. M. (2018). Multidimensional Connectomics and Treatment-Resistant Schizophrenia: Linking

Phenotypic Circuits to Targeted Therapeutics. *Frontiers in Psychiatry*, *9*. https://www.frontiersin.org/articles/10.3389/fpsyt.2018.00537

Mahdavi, A., Qin, Y., Aubry, A.-S., Cornec, D., Kulikova, S., & Pinault, D. (2020). A single psychotomimetic dose of ketamine decreases thalamocortical spindles and delta oscillations in the sedated rat. *Schizophrenia Research*, *222*, 362–374. https://doi.org/10.1016/j.schres.2020.04.029

Majewska, A., & Sur, M. (2003). Motility of dendritic spines in visual cortex in vivo: Changes during the critical period and effects of visual deprivation. *Proceedings of the National Academy of Sciences*, *100*(26), 16024–16029. https://doi.org/10.1073/pnas.2636949100

Mäki-Marttunen, T., Krull, F., Bettella, F., Hagen, E., Næss, S., Ness, T. V., Moberget, T., Elvsåshagen, T., Metzner, C., Devor, A., Edwards, A. G., Fyhn, M., Djurovic, S., Dale, A. M., Andreassen, O. A., & Einevoll, G. T. (2019). Alterations in Schizophrenia-Associated Genes Can Lead to Increased Power in Delta Oscillations. *Cerebral Cortex*, *29*(2), 875–891. https://doi.org/10.1093/cercor/bhy291

Martino Adami, P. V., Orellana, A., García, P., Kleineidam, L., Alarcón-Martín, E., Montrreal, L., Aguilera, N., Espinosa, A., Abdelnour, C., Rosende-Roca, M., Pablo Tartari, J., Vargas, L., Mauleón, A., Esteban-De Antonio, E., López-Cuevas, R., Dalmasso, M. C., Campos Martin, R., Parveen, K., Andrade Fuentes, V. M., … Ramírez, A. (2022). Matrix metalloproteinase 10 is linked to the risk of progression to dementia of the Alzheimer's type. *Brain*, *145*(7), 2507–2517. https://doi.org/10.1093/brain/awac024

Martínez-Cerdeño, V., & Clascá, F. (2002). Reelin immunoreactivity in the adult neocortex: A comparative study in rodents, carnivores, and non-human primates. *Brain Research Bulletin*, *57*(3), 485–488. https://doi.org/10.1016/S0361-9230(01)00718-3

Masliah, E., Mallory, M., Alford, M., DeTeresa, R., Hansen, L. A., McKeel, D. W., & Morris, J. C. (2001). Altered expression of synaptic proteins occurs early during progression of Alzheimer's disease. *Neurology*, *56*(1), 127–129. https://doi.org/10.1212/WNL.56.1.127

Matta, J. A., Ashby, M. C., Sanz-Clemente, A., Roche, K. W., & Isaac, J. T. R. (2011). MGluR5 and NMDA Receptors Drive the Experience- and Activity-Dependent NMDA Receptor NR2B to NR2A Subunit Switch. *Neuron*, *70*(2), 339–351. https://doi.org/10.1016/j.neuron.2011.02.045

Matthews, R. T., Kelly, G. M., Zerillo, C. A., Gray, G., Tiemeyer, M., & Hockfield, S. (2002). Aggrecan glycoforms contribute to the molecular heterogeneity of perineuronal nets. *The Journal of Neuroscience: The Official Journal of the Society for Neuroscience*, *22*(17), 7536–7547. https://doi.org/10.1523/JNEUROSCI.22-17-07536.2002

Matuszko, G., Curreli, S., Kaushik, R., Becker, A., & Dityatev, A. (2017). Extracellular matrix alterations in the ketamine model of schizophrenia. *Neuroscience*, *350*, 13–22. https://doi.org/10.1016/j.neuroscience.2017.03.010

Mauney, S. A., Athanas, K. M., Pantazopoulos, H., Shaskan, N., Passeri, E., Berretta, S., & Woo, T.-U. W. (2013a). Developmental pattern of perineuronal nets in the human prefrontal cortex and their deficit in schizophrenia. *Biological Psychiatry*, *74*(6), 427–435. https://doi.org/10.1016/j.biopsych.2013.05.007

Mauney, S. A., Athanas, K. M., Pantazopoulos, H., Shaskan, N., Passeri, E., Berretta, S., & Woo, T.-U. W. (2013b). Developmental Pattern of Perineuronal Nets in the Human Prefrontal Cortex and Their Deficit in Schizophrenia. *Biological Psychiatry*, *74*(6), 427–435. https://doi.org/10.1016/j.biopsych.2013.05.007

McGee, A. W., Yang, Y., Fischer, Q. S., Daw, N. W., & Strittmatter, S. M. (2005). Experience-Driven Plasticity of Visual Cortex Limited by Myelin and Nogo Receptor. *Science*, *309*(5744), 2222–2226. https://doi.org/10.1126/science.1114362

McGlothan, J. L., Karcz-Kubicha, M., & Guilarte, T. R. (2008). Developmental lead exposure impairs extinction of conditioned fear in young adult rats. *NeuroToxicology*, *29*(6), 1127–1130. https://doi.org/10.1016/j.neuro.2008.06.010

McGrath, L. M., Cornelis, M. C., Lee, P. H., Robinson, E. B., Duncan, L. E., Barnett, J. H., Huang, J., Gerber, G., Sklar, P., Sullivan, P., Perlis, R. H., & Smoller, J. W. (2013). Genetic predictors of risk and resilience in psychiatric disorders: A cross-disorder genome-wide association study of functional impairment in major depressive disorder, bipolar disorder, and schizophrenia. *American Journal of Medical Genetics Part B: Neuropsychiatric Genetics*, *162*(8), 779–788. https://doi.org/10.1002/ajmg.b.32190

McNally, J. M., Aguilar, D. D., Katsuki, F., Radzik, L. K., Schiffino, F. L., Uygun, D. S., McKenna, J. T., Strecker, R. E., Deisseroth, K., Spencer, K. M., & Brown, R. E. (2021). Optogenetic manipulation of an ascending arousal system tunes cortical broadband gamma power and reveals functional deficits relevant to schizophrenia. *Molecular Psychiatry*, *26*(7), Article 7. https://doi.org/10.1038/s41380-020-0840-3

McRae, P. A., & Porter, B. E. (2012a). The Perineuronal Net Component of the Extracellular Matrix in Plasticity and Epilepsy. *Neurochemistry International*, *61*(7), 963–972. https://doi.org/10.1016/j.neuint.2012.08.007

McRae, P. A., & Porter, B. E. (2012b). The Perineuronal Net Component of the Extracellular Matrix in Plasticity and Epilepsy. *Neurochemistry International*, *61*(7), 963–972. https://doi.org/10.1016/j.neuint.2012.08.007

McRae, P. A., Rocco, M. M., Kelly, G., Brumberg, J. C., & Matthews, R. T. (2007a). Sensory Deprivation Alters Aggrecan and Perineuronal Net Expression in the Mouse Barrel Cortex. *Journal of Neuroscience*, *27*(20), 5405–5413. https://doi.org/10.1523/JNEUROSCI.5425-06.2007

McRae, P. A., Rocco, M. M., Kelly, G., Brumberg, J. C., & Matthews, R. T. (2007b). Sensory Deprivation Alters Aggrecan and Perineuronal Net Expression in the Mouse Barrel Cortex. *Journal of Neuroscience*, *27*(20), 5405–5413. https://doi.org/10.1523/JNEUROSCI.5425-06.2007

Means, L. W., David Leander, J., & Isaacson, R. L. (1971). The effects of hippocampectomy on alternation behavior and response to novelty. *Physiology & Behavior*, *6*(1), 17-IN1. https://doi.org/10.1016/0031-9384(71)90006-0

Meijer, M. K., Sommer, R., Spruijt, B. M., van Zutphen, L. F. M., & Baumans, V. (2007). Influence of environmental enrichment and handling on the acute stress response in individually housed mice. *Laboratory Animals*, *41*(2), 161–173. https://doi.org/10.1258/002367707780378168

Mellios, N., Huang, H.-S., Baker, S. P., Galdzicka, M., Ginns, E., & Akbarian, S. (2009). Molecular Determinants of Dysregulated GABAergic Gene Expression in the Prefrontal Cortex of Subjects with Schizophrenia. *Biological Psychiatry*, *65*(12), 1006–1014. https://doi.org/10.1016/j.biopsych.2008.11.019

Mercerón-Martínez, D., Ibaceta-González, C., Salazar, C., Almaguer-Melian, W., Bergado, J., & Palacios, A. (2021). Alzheimer's Disease, Neural Plasticity, and Functional Recovery. *Journal of Alzheimer's Disease*, *82*, 1–14. https://doi.org/10.3233/JAD-201178

Mesulam, M.-M. (2000). A Plasticity-Based Theory of the Pathogenesis of Alzheimer's Disease. *Annals of the New York Academy of Sciences*, *924*(1), 42–52. https://doi.org/10.1111/j.1749-6632.2000.tb05559.x

Micheva, K. D., Wolman, D., Mensh, B. D., Pax, E., Buchanan, J., Smith, S. J., & Bock, D. D. (2016). A large fraction of neocortical myelin ensheathes axons of local inhibitory neurons. *ELife*, *5*, e15784. https://doi.org/10.7554/eLife.15784

Milev, P., Maurel, P., Chiba, A., Mevissen, M., Popp, S., Yamaguchi, Y., Margolis, R. K., & Margolis, R. U. (1998). Differential Regulation of Expression of Hyaluronan-Binding Proteoglycans in Developing Brain: Aggrecan, Versican, Neurocan, and Brevican. *Biochemical and Biophysical Research Communications*, *247*(2), 207–212. https://doi.org/10.1006/bbrc.1998.8759

Miller, A. M. P., Vedder, L. C., Law, L. M., & Smith, D. M. (2014). Cues, context, and long-term memory: The role of the retrosplenial cortex in spatial cognition. *Frontiers in Human Neuroscience*, *8*. https://www.frontiersin.org/articles/10.3389/fnhum.2014.00586

Miller, B., Sheppard, A. M., Bicknese, A. R., & Pearlman, A. L. (1995). Chondroitin sulfate proteoglycans in the developing cerebral cortex: The distribution of neurocan distinguishes forming afferent and efferent axonal pathways. *Journal of Comparative Neurology*, *355*(4), 615–628. https://doi.org/10.1002/cne.903550410

Mitchell, A. S., Czajkowski, R., Zhang, N., Jeffery, K., & Nelson, A. J. D. (2018). Retrosplenial cortex and its role in spatial cognition. *Brain and Neuroscience Advances*, *2*, 2398212818757098. https://doi.org/10.1177/2398212818757098

Mitchell, J. B., & Laiacona, J. (1998). The medial frontal cortex and temporal memory: Tests using spontaneous exploratory behaviour in the rat. *Behavioural Brain Research*, *97*(1), 107–113. https://doi.org/10.1016/S0166-4328(98)00032-1

Miyata, S., & Kitagawa, H. (2016). Chondroitin 6-Sulfation Regulates Perineuronal Net Formation by Controlling the Stability of Aggrecan. *Neural Plasticity*, *2016*, e1305801. https://doi.org/10.1155/2016/1305801

Miyata, S., Komatsu, Y., Yoshimura, Y., Taya, C., & Kitagawa, H. (2012). Persistent cortical plasticity by upregulation of chondroitin 6-sulfation. *Nature Neuroscience*, *15*(3), Article 3. https://doi.org/10.1038/nn.3023

Miyata, S., Nadanaka, S., Igarashi, M., & Kitagawa, H. (2018). Structural Variation of Chondroitin Sulfate Chains Contributes to the Molecular Heterogeneity of Perineuronal Nets. *Frontiers in Integrative Neuroscience*, *12*. https://www.frontiersin.org/articles/10.3389/fnint.2018.00003

Miyata, S., Nishimura, Y., Hayashi, N., & Oohira, A. (2005). Construction of perineuronal net-like structure by cortical neurons in culture. *Neuroscience*, *136*(1), 95–104. https://doi.org/10.1016/j.neuroscience.2005.07.031

Miyata, S., Nishimura, Y., & Nakashima, T. (2007). Perineuronal nets protect against amyloid β-protein neurotoxicity in cultured cortical neurons. *Brain Research*, *1150*, 200–206. https://doi.org/10.1016/j.brainres.2007.02.066

Mohamedi, Y., Fontanil, T., Cobo, T., Cal, S., & Obaya, A. J. (2020). New Insights into ADAMTS Metalloproteases in the Central Nervous System. *Biomolecules*, *10*(3), Article 3. https://doi.org/10.3390/biom10030403

Monko, M. E., & Heilbronner, S. R. (2021). Retrosplenial Cortical Connectivity with Frontal Basal Ganglia Networks. *Journal of Cognitive Neuroscience*, *33*(6), 1096–1105. https://doi.org/10.1162/jocn_a_01699

Montag-Sallaz, M., & Montag, D. (2003). Severe cognitive and motor coordination deficits in Tenascin-R-deficient mice. *Genes, Brain and Behavior*, *2*(1), 20–31. https://doi.org/10.1034/j.1601-183X.2003.00003.x

Morawski, M., Brückner, G., Jäger, C., Seeger, G., & Arendt, T. (2010a). Neurons associated with aggrecan-based perineuronal nets are protected against tau pathology in subcortical regions in Alzheimer's disease. *Neuroscience*, *169*(3), 1347–1363. https://doi.org/10.1016/j.neuroscience.2010.05.022

Morawski, M., Brückner, G., Jäger, C., Seeger, G., & Arendt, T. (2010b). Neurons associated with aggrecan-based perineuronal nets are protected against tau pathology in subcortical regions in Alzheimer's disease. *Neuroscience*, *169*(3), 1347–1363. https://doi.org/10.1016/j.neuroscience.2010.05.022

Morawski, M., Brückner, G., Jäger, C., Seeger, G., Matthews, R. T., & Arendt, T. (2012). Involvement of Perineuronal and Perisynaptic Extracellular Matrix in Alzheimer's Disease Neuropathology. *Brain Pathology*, *22*(4), 547–561. https://doi.org/10.1111/j.1750-3639.2011.00557.x

Morawski, M., Brückner, M. K., Riederer, P., Brückner, G., & Arendt, T. (2004a). Perineuronal nets potentially protect against oxidative stress. *Experimental Neurology*, *188*(2), 309–315. https://doi.org/10.1016/j.expneurol.2004.04.017

Morawski, M., Brückner, M. K., Riederer, P., Brückner, G., & Arendt, T. (2004b). Perineuronal nets potentially protect against oxidative stress. *Experimental Neurology*, *188*(2), 309–315. https://doi.org/10.1016/j.expneurol.2004.04.017

Morawski, M., Pavlica, S., Seeger, G., Grosche, J., Kouznetsova, E., Schliebs, R., Brückner, G., & Arendt, T. (2010). Perineuronal nets are largely unaffected in Alzheimer model Tg2576 mice. *Neurobiology of Aging*, *31*(7), 1254–1256. https://doi.org/10.1016/j.neurobiolaging.2008.07.023

Morawski, M., Reinert, T., Brückner, G., Wagner, F., Arendt, T., & Tröger, W. (2004). The Binding of Iron to Perineuronal Nets: A Combined Nuclear Microscopy and Mössbauer Study. *Hyperfine Interactions*, *159*, 719–725. https://doi.org/10.1007/3-540-30924-1_116

Morawski, M., Reinert, T., Meyer-Klaucke, W., Wagner, F. E., Tröger, W., Reinert, A., Jäger, C., Brückner, G., & Arendt, T. (2015). Ion exchanger in the brain: Quantitative analysis of perineuronally fixed anionic binding sites suggests diffusion barriers with ion sorting properties. *Scientific Reports*, *5*(1), Article 1. https://doi.org/10.1038/srep16471

Morellini, F., Sivukhina, E., Stoenica, L., Oulianova, E., Bukalo, O., Jakovcevski, I., Dityatev, A., Irintchev, A., & Schachner, M. (2010a). Improved Reversal Learning and Working Memory and Enhanced Reactivity to Novelty in Mice with Enhanced GABAergic Innervation in the Dentate Gyrus. *Cerebral Cortex*, *20*(11), 2712–2727. https://doi.org/10.1093/cercor/bhq017

Morellini, F., Sivukhina, E., Stoenica, L., Oulianova, E., Bukalo, O., Jakovcevski, I., Dityatev, A., Irintchev, A., & Schachner, M. (2010b). Improved Reversal Learning and Working Memory and Enhanced Reactivity to Novelty in Mice with Enhanced GABAergic

Innervation in the Dentate Gyrus. *Cerebral Cortex*, *20*(11), 2712–2727. https://doi.org/10.1093/cercor/bhq017

Morris, R., Pandya, D. N., & Petrides, M. (1999). Fiber system linking the mid-dorsolateral frontal cortex with the retrosplenial/presubicular region in the rhesus monkey. *Journal of Comparative Neurology*, *407*(2), 183–192. https://doi.org/10.1002/(SICI)1096-9861(19990503)407:2<183::AID-CNE3>3.0.CO;2-N

Mu, L., Cai, J., Gu, B., Yu, L., Li, C., Liu, Q.-S., & Zhao, L. (2022). Treadmill Exercise Prevents Decline in Spatial Learning and Memory in 3×Tg-AD Mice through Enhancement of Structural Synaptic Plasticity of the Hippocampus and Prefrontal Cortex. *Cells*, *11*(2), Article 2. https://doi.org/10.3390/cells11020244

Mueser, K. T., Bellack, A. S., & Brady, E. U. (1990). Hallucinations in schizophrenia. *Acta Psychiatrica Scandinavica*, *82*(1), 26–29. https://doi.org/10.1111/j.1600-0447.1990.tb01350.x

Mühleisen, T. W., Mattheisen, M., Strohmaier, J., Degenhardt, F., Priebe, L., Schultz, C. C., Breuer, R., Meier, S., Hoffmann, P., Rivandeneira, F., Hofman, A., Uitterlinden, A. G., Moebus, S., Gieger, C., Emeny, R., Ladwig, K.-H., Wichmann, H.-E., Schwarz, M., Kammerer-Ciernioch, J., … Cichon, S. (2012). Association between schizophrenia and common variation in neurocan (NCAN), a genetic risk factor for bipolar disorder. *Schizophrenia Research*, *138*(1), 69–73. https://doi.org/10.1016/j.schres.2012.03.007

Murphy, M. P., & LeVine, H. (2010). Alzheimer's Disease and the β-Amyloid Peptide. *Journal of Alzheimer's Disease : JAD*, *19*(1), 311. https://doi.org/10.3233/JAD-2010-1221

Nakada, M., Miyamori, H., Kita, D., Takahashi, T., Yamashita, J., Sato, H., Miura, R., Yamaguchi, Y., & Okada, Y. (2005). Human glioblastomas overexpress ADAMTS-5 that

degrades brevican. *Acta Neuropathologica*, *110*(3), 239–246. https://doi.org/10.1007/s00401-005-1032-6

Nakagawa, F., Schulte, B. A., Wu, J.-Y., & Spicer, S. S. (1987). Postnatal Appearance of Glycoconjugate with Terminal N-Acetylgalactosamine on the Surface of Selected Neurons in Mouse Brain. *Developmental Neuroscience*, *9*(1), 53–60. https://doi.org/10.1159/000111608

Narr, K. L., & Leaver, A. M. (2015). Connectome and schizophrenia. *Current Opinion in Psychiatry*, *28*(3), 229. https://doi.org/10.1097/YCO.0000000000000157

Nelson, A. J. D., Powell, A. L., Holmes, J. D., Vann, S. D., & Aggleton, J. P. (2015). What does spatial alternation tell us about retrosplenial cortex function? *Frontiers in Behavioral Neuroscience*, *9*. https://www.frontiersin.org/articles/10.3389/fnbeh.2015.00126

Nicholson, C., & Syková, E. (1998). Extracellular space structure revealed by diffusion analysis. *Trends in Neurosciences*, *21*(5), 207–215. https://doi.org/10.1016/S0166-2236(98)01261-2

Nihei, M. K., Desmond, N. L., McGlothan, J. L., Kuhlmann, A. C., & Guilarte, T. R. (2000). N-methyl-d-aspartate receptor subunit changes are associated with lead-induced deficits of long-term potentiation and spatial learning. *Neuroscience*, *99*(2), 233–242. https://doi.org/10.1016/S0306-4522(00)00192-5

Nordberg, A., & Winblad, B. (1986). Reduced number of [3H]nicotine and [3H]acetylcholine binding sites in the frontal cortex of Alzheimer brains. *Neuroscience Letters*, *72*(1), 115–120. https://doi.org/10.1016/0304-3940(86)90629-4

Nörenberg, A., Hu, H., Vida, I., Bartos, M., & Jonas, P. (2010). Distinct nonuniform cable properties optimize rapid and efficient activation of fast-spiking GABAergic

interneurons. *Proceedings of the National Academy of Sciences*, *107*(2), 894–899. https://doi.org/10.1073/pnas.0910716107

Nowicka, D., Soulsby, S., Skangiel-Kramska, J., & Glazewski, S. (2009). Parvalbumin-containing neurons, perineuronal nets and experience-dependent plasticity in murine barrel cortex. *European Journal of Neuroscience*, *30*(11), 2053–2063. https://doi.org/10.1111/j.1460-9568.2009.06996.x

Nusser, Z. (1996). Differential synaptic localization of two major gamma-aminobutyric acid type A receptor alpha subunits on hippocampal pyramidal cells. *Proceedings of the National Academy of Sciences*, *93*, 11939–11944. https://doi.org/10.1073/pnas.93.21.11939

NyÍri, G., Stephenson, F. A., Freund, T. F., & Somogyi, P. (2003). Large variability in synaptic n-methyl-d-aspartate receptor density on interneurons and a comparison with pyramidal-cell spines in the rat hippocampus. *Neuroscience*, *119*(2), 347–363. https://doi.org/10.1016/S0306-4522(03)00157-X

Oakley, H., Cole, S. L., Logan, S., Maus, E., Shao, P., Craft, J., Guillozet-Bongaarts, A., Ohno, M., Disterhoft, J., Van Eldik, L., Berry, R., & Vassar, R. (2006). Intraneuronal beta-Amyloid Aggregates, Neurodegeneration, and Neuron Loss in Transgenic Mice with Five Familial Alzheimer's Disease Mutations: Potential Factors in Amyloid Plaque Formation. *Journal of Neuroscience*, *26*(40), 10129–10140. https://doi.org/10.1523/JNEUROSCI.1202-06.2006

Oblak, A. L., Lin, P. B., Kotredes, K. P., Pandey, R. S., Garceau, D., Williams, H. M., Uyar, A., O'Rourke, R., O'Rourke, S., Ingraham, C., Bednarczyk, D., Belanger, M., Cope, Z. A., Little, G. J., Williams, S.-P. G., Ash, C., Bleckert, A., Ragan, T., Logsdon, B. A., … Lamb, B. T. (2021). Comprehensive Evaluation of the 5XFAD Mouse Model for

Preclinical Testing Applications: A MODEL-AD Study. *Frontiers in Aging Neuroscience*, *13*. https://www.frontiersin.org/articles/10.3389/fnagi.2021.713726

Ohno, M., Chang, L., Tseng, W., Oakley, H., Citron, M., Klein, W. L., Vassar, R., & Disterhoft, J. F. (2006). Temporal memory deficits in Alzheimer's mouse models: Rescue by genetic deletion of BACE1. *European Journal of Neuroscience*, *23*(1), 251–260. https://doi.org/10.1111/j.1460-9568.2005.04551.x

Ojima, H., Sakai, M., & Ohyama, J. (1998). Molecular heterogeneity of Vicia villosa-recognized perineuronal nets surrounding pyramidal and nonpyramidal neurons in the guinea pig cerebral cortex. *Brain Research*, *786*(1–2), 274–280. https://doi.org/10.1016/s0006-8993(97)01564-3

Okamoto, M., Mori, S., & Endo, H. (1994). A protective action of chondroitin sulfate proteoglycans against neuronal cell death induced by glutamate. *Brain Research*, *637*(1–2), 57–67. https://doi.org/10.1016/0006-8993(94)91217-3

Okamoto, M., Mori, S., Ichimura, M., & Endo, H. (1994). Chondroitin sulfate proteoglycans protect cultured rat's cortical and hippocampal neurons from delayed cell death induced by excitatory amino acids. *Neuroscience Letters*, *172*(1), 51–54. https://doi.org/10.1016/0304-3940(94)90660-2

O'Leary, T. P., & Brown, R. E. (2022). Visuo-spatial learning and memory impairments in the 5xFAD mouse model of Alzheimer's disease: Effects of age, sex, albinism, and motor impairments. *Genes, Brain and Behavior*, *21*(4), e12794. https://doi.org/10.1111/gbb.12794

O'Leary, T. P., Mantolino, H. M., Stover, K. R., & Brown, R. E. (2020). Age-related deterioration of motor function in male and female 5xFAD mice from 3 to 16 months of age. *Genes, Brain and Behavior*, *19*(3), e12538. https://doi.org/10.1111/gbb.12538

Oohashi, T., Edamatsu, M., Bekku, Y., & Carulli, D. (2015). The hyaluronan and proteoglycan link proteins: Organizers of the brain extracellular matrix and key molecules for neuronal function and plasticity. *Experimental Neurology*, *274*, 134–144. https://doi.org/10.1016/j.expneurol.2015.09.010

Orlando, C., Ster, J., Gerber, U., Fawcett, J. W., & Raineteau, O. (2012a). Perisynaptic Chondroitin Sulfate Proteoglycans Restrict Structural Plasticity in an Integrin-Dependent Manner. *Journal of Neuroscience*, *32*(50), 18009–18017. https://doi.org/10.1523/JNEUROSCI.2406-12.2012

Orlando, C., Ster, J., Gerber, U., Fawcett, J. W., & Raineteau, O. (2012b). Perisynaptic Chondroitin Sulfate Proteoglycans Restrict Structural Plasticity in an Integrin-Dependent Manner. *Journal of Neuroscience*, *32*(50), 18009–18017. https://doi.org/10.1523/JNEUROSCI.2406-12.2012

Owen, M. J., O'Donovan, M. C., Thapar, A., & Craddock, N. (2011). Neurodevelopmental hypothesis of schizophrenia. *The British Journal of Psychiatry*, *198*(3), 173–175. https://doi.org/10.1192/bjp.bp.110.084384

Packer, A. M., & Yuste, R. (2011). Dense, Unspecific Connectivity of Neocortical Parvalbumin-Positive Interneurons: A Canonical Microcircuit for Inhibition? *The Journal of Neuroscience*, *31*(37), 13260–13271. https://doi.org/10.1523/JNEUROSCI.3131-11.2011

Pajevic, S., Basser, P. J., & Fields, R. D. (2014). Role of myelin plasticity in oscillations and synchrony of neuronal activity. *Neuroscience*, *276*, 135–147. https://doi.org/10.1016/j.neuroscience.2013.11.007

Pantazopoulos, H., & Berretta, S. (2016a). In Sickness and in Health: Perineuronal Nets and Synaptic Plasticity in Psychiatric Disorders. *Neural Plasticity*, *2016*, 1–23. https://doi.org/10.1155/2016/9847696

Pantazopoulos, H., & Berretta, S. (2016b). In Sickness and in Health: Perineuronal Nets and Synaptic Plasticity in Psychiatric Disorders. *Neural Plasticity*, *2016*, 1–23. https://doi.org/10.1155/2016/9847696

Pantazopoulos, H., Boyer-Boiteau, A., Holbrook, E. H., Jang, W., Hahn, C.-G., Arnold, S. E., & Berretta, S. (2013). Proteoglycan abnormalities in olfactory epithelium tissue from subjects diagnosed with schizophrenia. *Schizophrenia Research*, *150*(2), 366–372. https://doi.org/10.1016/j.schres.2013.08.013

Pantazopoulos, H., Lange, N., Hassinger, L., & Berretta, S. (2006). Subpopulations of neurons expressing parvalbumin in the human amygdala. *Journal of Comparative Neurology*, *496*(5), 706–722. https://doi.org/10.1002/cne.20961

Pantazopoulos, H., Markota, M., Jaquet, F., Ghosh, D., Wallin, A., Santos, A., Caterson, B., & Berretta, S. (2015). Aggrecan and chondroitin-6-sulfate abnormalities in schizophrenia and bipolar disorder: A postmortem study on the amygdala. *Translational Psychiatry*, *5*(1), Article 1. https://doi.org/10.1038/tp.2014.128

Pantazopoulos, H., Tsung-Ung, W., Maribel, P., Lange, N., & Berretta, S. (2010). Extracellular matrix-glial abnormalities in the amygdala and entorhinal cortex of subjects diagnosed with schizophrenia. *Archives of General Psychiatry*, *67*(2), 155–166.

Pantazopoulos, H., Woo, T.-U. W., Lim, M. P., Lange, N., & Berretta, S. (2010). Extracellular Matrix-Glial Abnormalities in the Amygdala and Entorhinal Cortex of Subjects Diagnosed With Schizophrenia. *Archives of General Psychiatry*, *67*(2), 155–166. https://doi.org/10.1001/archgenpsychiatry.2009.196

Papadia, S., Soriano, F. X., Léveillé, F., Martel, M.-A., Dakin, K. A., Hansen, H. H., Kaindl, A., Sifringer, M., Fowler, J., Stefovska, V., Mckenzie, G., Craigon, M., Corriveau, R., Ghazal, P., Horsburgh, K., Yankner, B. A., Wyllie, D. J. A., Ikonomidou, C., & Hardingham, G. E. (2008). Synaptic NMDA receptor activity boosts intrinsic antioxidant defenses. *Nature Neuroscience*, *11*(4), Article 4. https://doi.org/10.1038/nn2071

Patel, A. R., Ritzel, R., McCullough, L. D., & Liu, F. (2013). Microglia and ischemic stroke: A double-edged sword. *International Journal of Physiology, Pathophysiology and Pharmacology*, *5*(2), 73–90.

Paxinos, G., & Watson, C. (2007). *The rat brain in stereotaxic coordinates* (6th ed). Academic Press/Elsevier.

Paylor, J. W., Lins, B. R., Greba, Q., Moen, N., de Moraes, R. S., Howland, J. G., & Winship, I. R. (2016a). Developmental disruption of perineuronal nets in the medial prefrontal cortex after maternal immune activation. *Scientific Reports*, *6*, 37580. https://doi.org/10.1038/srep37580

Paylor, J. W., Lins, B. R., Greba, Q., Moen, N., de Moraes, R. S., Howland, J. G., & Winship, I. R. (2016b). Developmental disruption of perineuronal nets in the medial prefrontal cortex after maternal immune activation. *Scientific Reports*, *6*, 37580. https://doi.org/10.1038/srep37580

Paylor, J. W., Wendlandt, E., Freeman, T. S., Greba, Q., Marks, W. N., Howland, J. G., & Winship, I. R. (2018). Impaired Cognitive Function after Perineuronal Net Degradation in the Medial Prefrontal Cortex. *ENeuro*, *5*(6), ENEURO.0253-18.2018. https://doi.org/10.1523/ENEURO.0253-18.2018

Pearlman, A. L., & Sheppard, A. M. (1996). Chapter 9 Extracellular matrix in early cortical development. In R. R. Mize & R. S. Erzurumlu (Eds.), *Progress in Brain Research* (Vol. 108, pp. 119–134). Elsevier. https://doi.org/10.1016/S0079-6123(08)62536-4

Pérez-Iglesias, R., Tordesillas-Gutiérrez, D., Barker, G. J., McGuire, P. K., Roiz-Santiañez, R., Mata, I., de Lucas, E. M., Quintana, F., Vazquez-Barquero, J. L., & Crespo-Facorro, B. (2010). White matter defects in first episode psychosis patients: A voxelwise analysis of diffusion tensor imaging. *NeuroImage*, *49*(1), 199–204. https://doi.org/10.1016/j.neuroimage.2009.07.016

Perkins, D. O., Jeffries, C. D., & Do, K. Q. (2020). Potential Roles of Redox Dysregulation in the Development of Schizophrenia. *Biological Psychiatry*, *88*(4), 326–336. https://doi.org/10.1016/j.biopsych.2020.03.016

Perry, V. H., Nicoll, J. A. R., & Holmes, C. (2010). Microglia in neurodegenerative disease. *Nature Reviews Neurology*, *6*(4), Article 4. https://doi.org/10.1038/nrneurol.2010.17

Pesold, C., Impagnatiello, F., Pisu, M. G., Uzunov, D. P., Costa, E., Guidotti, A., & Caruncho, H. J. (1998). Reelin is preferentially expressed in neurons synthesizing γ-aminobutyric acid in cortex and hippocampus of adult rats. *Proceedings of the National Academy of Sciences*, *95*(6), 3221–3226. https://doi.org/10.1073/pnas.95.6.3221

Pesold, C., Liu, W. S., Guidotti, A., Costa, E., & Caruncho, H. J. (1999). Cortical bitufted, horizontal, and Martinotti cells preferentially express and secrete reelin into perineuronal

nets, nonsynaptically modulating gene expression. *Proceedings of the National Academy of Sciences*, *96*(6), 3217–3222. https://doi.org/10.1073/pnas.96.6.3217

Pietersen, C. Y., Mauney, S. A., Kim, S. S., Passeri, E., Lim, M. P., Rooney, R. J., Goldstein, J. M., Petreyshen, T. L., Seidman, L. J., Shenton, M. E., Mccarley, R. W., Sonntag, K.-C., & Woo, T.-U. W. (2014). Molecular Profiles of Parvalbumin-Immunoreactive Neurons in the Superior Temporal Cortex in Schizophrenia. *Journal of Neurogenetics*, *28*(1–2), 70–85. https://doi.org/10.3109/01677063.2013.878339

Pizzorusso, T., Medini, P., Berardi, N., Chierzi, S., Fawcett, J. W., & Maffei, L. (2002a). Reactivation of Ocular Dominance Plasticity in the Adult Visual Cortex. *Science*, *298*(5596), 1248–1251. https://doi.org/10.1126/science.1072699

Pizzorusso, T., Medini, P., Berardi, N., Chierzi, S., Fawcett, J. W., & Maffei, L. (2002b). Reactivation of Ocular Dominance Plasticity in the Adult Visual Cortex. *Science*, *298*(5596), 1248–1251. https://doi.org/10.1126/science.1072699

Pizzorusso, T., Medini, P., Landi, S., Baldini, S., Berardi, N., & Maffei, L. (2006a). Structural and functional recovery from early monocular deprivation in adult rats. *Proceedings of the National Academy of Sciences*, *103*(22), 8517–8522.

Pizzorusso, T., Medini, P., Landi, S., Baldini, S., Berardi, N., & Maffei, L. (2006b). Structural and functional recovery from early monocular deprivation in adult rats. *Proceedings of the National Academy of Sciences*, *103*(22), 8517–8522. https://doi.org/10.1073/pnas.0602657103

Plenz, D. (2003). When inhibition goes incognito: Feedback interaction between spiny projection neurons in striatal function. *Trends in Neurosciences*, *26*(8), 436–443. https://doi.org/10.1016/S0166-2236(03)00196-6

Pollock, E., Everest, M., Brown, A., & Poulter, M. O. (2014a). Metalloproteinase inhibition prevents inhibitory synapse reorganization and seizure genesis. *Neurobiology of Disease*, *70*, 21–31.

Pollock, E., Everest, M., Brown, A., & Poulter, M. O. (2014b). Metalloproteinase inhibition prevents inhibitory synapse reorganization and seizure genesis. *Neurobiology of Disease*, *70*, 21–31. https://doi.org/10.1016/j.nbd.2014.06.003

Pothuizen, H. H. J., Aggleton, J. P., & Vann, S. D. (2008). Do rats with retrosplenial cortex lesions lack direction? *European Journal of Neuroscience*, *28*(12), 2486–2498. https://doi.org/10.1111/j.1460-9568.2008.06550.x

Pothuizen, H. H. J., Davies, M., Aggleton, J. P., & Vann, S. D. (2010). Effects of selective granular retrosplenial cortex lesions on spatial working memory in rats. *Behavioural Brain Research*, *208*(2), 566–575. https://doi.org/10.1016/j.bbr.2010.01.001

Powell, S. B., Sejnowski, T. J., & Behrens, M. M. (2012). Behavioral and neurochemical consequences of cortical oxidative stress on parvalbumin-interneuron maturation in rodent models of schizophrenia. *Neuropharmacology*, *62*(3), 1322–1331. https://doi.org/10.1016/j.neuropharm.2011.01.049

Prut, L., & Belzung, C. (2003). The open field as a paradigm to measure the effects of drugs on anxiety-like behaviors: A review. *European Journal of Pharmacology*, *463*(1), 3–33. https://doi.org/10.1016/S0014-2999(03)01272-X

Raichle, M. E. (2015). The Brain's Default Mode Network. *Annual Review of Neuroscience*, *38*(1), 433–447. https://doi.org/10.1146/annurev-neuro-071013-014030

Raichle, M. E., MacLeod, A. M., Snyder, A. Z., Powers, W. J., Gusnard, D. A., & Shulman, G. L. (2001). A default mode of brain function. *Proceedings of the National Academy of Sciences*, *98*(2), 676–682. https://doi.org/10.1073/pnas.98.2.676

Ramirez, J. J., & Stein, D. G. (1984). Sparing and recovery of spatial alternation performance after entorhinal cortex lesions in rats. *Behavioural Brain Research*, *13*(1), 53–61. https://doi.org/10.1016/0166-4328(84)90029-9

Ramsaran, A. I., Wang, Y., Golbabaei, A., Yeung, B. A., de, M. L., Rashid, A. J., Awasthi, A., Lau, J., Tran, L. M., Ko, S. Y., Abegg, A., Duan, L. C., McKenzie, C., Gallucci, J., Ahmed, M., Kaushik, R., Dityatev, A., Josselyn, S. A., & Frankland, P. W. (2023). *A shift in the mechanisms controlling hippocampal engram formation during brain maturation*.

Rapoport, J. L., Giedd, J. N., & Gogtay, N. (2012). Neurodevelopmental model of schizophrenia: Update 2012. *Molecular Psychiatry*, *17*(12), Article 12. https://doi.org/10.1038/mp.2012.23

Rauch, U. (2007). Brain matrix: Structure, turnover and necessity. *Biochemical Society Transactions*, *35*(Pt 4), 656–660. https://doi.org/10.1042/bst0350656

Reh, R. K., Dias, B. G., Nelson, C. A., Kaufer, D., Werker, J. F., Kolb, B., Levine, J. D., & Hensch, T. K. (2020). Critical period regulation across multiple timescales. *Proceedings of the National Academy of Sciences*, *117*(38), 23242–23251. https://doi.org/10.1073/pnas.1820836117

Reichelt, A. C., Hare, D. J., Bussey, T. J., & Saksida, L. M. (2019). Perineuronal Nets: Plasticity, Protection, and Therapeutic Potential. *Trends in Neurosciences*, *42*(7), 458–470. https://doi.org/10.1016/j.tins.2019.04.003

Reid, J. M., Jacklin, D. L., & Winters, B. D. (2014a). Delineating Prefrontal Cortex Region Contributions to Crossmodal Object Recognition in Rats. *Cerebral Cortex*, *24*(8), 2108–2119. https://doi.org/10.1093/cercor/bht061

Reid, J. M., Jacklin, D. L., & Winters, B. D. (2014b). Delineating Prefrontal Cortex Region Contributions to Crossmodal Object Recognition in Rats. *Cerebral Cortex*, *24*(8), 2108–2119. https://doi.org/10.1093/cercor/bht061

Reimers, S., Hartlage-Rübsamen, M., Brückner, G., & Roßner, S. (2007). Formation of perineuronal nets in organotypic mouse brain slice cultures is independent of neuronal glutamatergic activity. *European Journal of Neuroscience*, *25*(9), 2640–2648. https://doi.org/10.1111/j.1460-9568.2007.05514.x

Reinert, A., Reinert, T., Arendt, T., & Morawski, M. (2022). High Iron and Iron Household Protein Contents in Perineuronal Net-Ensheathed Neurons Ensure Energy Metabolism with Safe Iron Handling. *International Journal of Molecular Sciences*, *23*(3), Article 3. https://doi.org/10.3390/ijms23031634

Reinhard, S. M., Abundez-Toledo, M., Espinoza, K., & Razak, K. A. (2019). Effects of developmental noise exposure on inhibitory cell densities and perineuronal nets in A1 and AAF of mice. *Hearing Research*, *381*, 107781. https://doi.org/10.1016/j.heares.2019.107781

Rey, C. C., Robert, V., Bouisset, G., Loisy, M., Lopez, S., Cattaud, V., Lejards, C., Piskorowski, R. A., Rampon, C., Chevaleyre, V., & Verret, L. (2022). Altered inhibitory function in hippocampal CA2 contributes in social memory deficits in Alzheimer's mouse model. *IScience*, *25*(3), 103895. https://doi.org/10.1016/j.isci.2022.103895

Rice, R. A., Spangenberg, E. E., Yamate-Morgan, H., Lee, R. J., Arora, R. P. S., Hernandez, M. X., Tenner, A. J., West, B. L., & Green, K. N. (2015). Elimination of Microglia Improves Functional Outcomes Following Extensive Neuronal Loss in the Hippocampus. *The Journal of Neuroscience: The Official Journal of the Society for Neuroscience*, *35*(27), 9977–9989. https://doi.org/10.1523/JNEUROSCI.0336-15.2015

Richard, A. D., Tian, X.-L., El-Saadi, M. W., & Lu, X.-H. (2018). Erasure of striatal chondroitin sulfate proteoglycan–associated extracellular matrix rescues aging-dependent decline of motor learning. *Neurobiology of Aging*, *71*, 61–71. https://doi.org/10.1016/j.neurobiolaging.2018.07.008

Rogers, S. L., Rankin-Gee, E., Risbud, R. M., Porter, B. E., & Marsh, E. D. (2018). Normal Development of the Perineuronal Net in Humans; In Patients with and without Epilepsy. *Neuroscience*, *384*, 350–360. https://doi.org/10.1016/j.neuroscience.2018.05.039

Romberg, C., Yang, S., Melani, R., Andrews, M. R., Horner, A. E., Spillantini, M. G., Bussey, T. J., Fawcett, J. W., Pizzorusso, T., & Saksida, L. M. (2013a). Depletion of Perineuronal Nets Enhances Recognition Memory and Long-Term Depression in the Perirhinal Cortex. *Journal of Neuroscience*, *33*(16), 7057–7065. https://doi.org/10.1523/JNEUROSCI.6267-11.2013

Romberg, C., Yang, S., Melani, R., Andrews, M. R., Horner, A. E., Spillantini, M. G., Bussey, T. J., Fawcett, J. W., Pizzorusso, T., & Saksida, L. M. (2013b). Depletion of Perineuronal Nets Enhances Recognition Memory and Long-Term Depression in the Perirhinal Cortex. *Journal of Neuroscience*, *33*(16), 7057–7065. https://doi.org/10.1523/JNEUROSCI.6267-11.2013

Romero, E., Guaza, C., Castellano, B., & Borrell, J. (2010). Ontogeny of sensorimotor gating and immune impairment induced by prenatal immune challenge in rats: Implications for the etiopathology of schizophrenia. *Molecular Psychiatry*, *15*(4), Article 4. https://doi.org/10.1038/mp.2008.44

Roopun, A. K., Cunningham, M. O., Racca, C., Alter, K., Traub, R. D., & Whittington, M. A. (2008). Region-Specific Changes in Gamma and Beta2 Rhythms in NMDA Receptor Dysfunction Models of Schizophrenia. *Schizophrenia Bulletin*, *34*(5), 962–973. https://doi.org/10.1093/schbul/sbn059

Rotaru, D. C., Yoshino, H., Lewis, D. A., Ermentrout, G. B., & Gonzalez-Burgos, G. (2011). Glutamate Receptor Subtypes Mediating Synaptic Activation of Prefrontal Cortex Neurons: Relevance for Schizophrenia. *Journal of Neuroscience*, *31*(1), 142–156. https://doi.org/10.1523/JNEUROSCI.1970-10.2011

Rowlands, D., Lensjø, K. K., Dinh, T., Yang, S., Andrews, M. R., Hafting, T., Fyhn, M., Fawcett, J. W., & Dick, G. (2018). Aggrecan Directs Extracellular Matrix-Mediated Neuronal Plasticity. *The Journal of Neuroscience*, *38*(47), 10102–10113. https://doi.org/10.1523/JNEUROSCI.1122-18.2018

Rubinov, M., & Bullmore, Ed. (2013). Schizophrenia and abnormal brain network hubs. *Dialogues in Clinical Neuroscience*, *15*(3), 339–349. https://doi.org/10.31887/DCNS.2013.15.3/mrubinov

Ruden, J. B., Dugan, L. L., & Konradi, C. (2021). Parvalbumin interneuron vulnerability and brain disorders. *Neuropsychopharmacology*, *46*(2), 279–287. https://doi.org/10.1038/s41386-020-0778-9

Rudy, B., Fishell, G., Lee, S., & Hjerling-Leffler, J. (2011). Three groups of interneurons account for nearly 100% of neocortical GABAergic neurons. *Developmental Neurobiology*, *71*(1), 45–61. https://doi.org/10.1002/dneu.20853

Saiz-Sanchez, D., De La Rosa-Prieto, C., Ubeda-Bañon, I., & Martinez-Marcos, A. (2013). Interneurons and Beta-Amyloid in the Olfactory Bulb, Anterior Olfactory Nucleus and Olfactory Tubercle in APPxPS1 Transgenic Mice Model of Alzheimer's Disease. *The Anatomical Record*, *296*(9), 1413–1423. https://doi.org/10.1002/ar.22750

Saiz-Sanchez, D., De la Rosa-Prieto, C., Ubeda-Banon, I., & Martinez-Marcos, A. (2015). Interneurons, tau and amyloid-β in the piriform cortex in Alzheimer's disease. *Brain Structure and Function*, *220*(4), 2011–2025. https://doi.org/10.1007/s00429-014-0771-3

Salami, M., Itami, C., Tsumoto, T., & Kimura, F. (2003). Change of conduction velocity by regional myelination yields constant latency irrespective of distance between thalamus and cortex. *Proceedings of the National Academy of Sciences*, *100*(10), 6174–6179. https://doi.org/10.1073/pnas.0937380100

Scheltens, P., De Strooper, B., Kivipelto, M., Holstege, H., Chételat, G., Teunissen, C. E., Cummings, J., & van der Flier, W. M. (2021). Alzheimer's disease. *The Lancet*, *397*(10284), 1577–1590. https://doi.org/10.1016/S0140-6736(20)32205-4

Schneider, F., Baldauf, K., Wetzel, W., & Reymann, K. G. (2014). Behavioral and EEG changes in male 5xFAD mice. *Physiology & Behavior*, *135*, 25–33. https://doi.org/10.1016/j.physbeh.2014.05.041

Schüppel, K., Brauer, K., Härtig, W., Grosche, J., Earley, B., Leonard, B. E., & Brückner, G. (2002). Perineuronal nets of extracellular matrix around hippocampal interneurons resist

destruction by activated microglia in trimethyltin-treated rats. *Brain Research*, *958*(2), 448–453. https://doi.org/10.1016/S0006-8993(02)03569-2

Seeger, G., Brauer, K., Härtig, W., & Brückner, G. (1994). Mapping of perineuronal nets in the rat brain stained by colloidal iron hydroxide histochemistry and lectin cytochemistry. *Neuroscience*, *58*(2), 371–388. https://doi.org/10.1016/0306-4522(94)90044-2

Seibenhener, M. L., & Wooten, M. C. (2015). Use of the Open Field Maze to Measure Locomotor and Anxiety-like Behavior in Mice. *Journal of Visualized Experiments : JoVE*, *96*, 52434. https://doi.org/10.3791/52434

Seidenbecher, C. I., Smalla, K.-H., Fischer, N., Gundelfinger, E. D., & Kreutz, M. R. (2002). Brevican isoforms associate with neural membranes. *Journal of Neurochemistry*, *83*(3), 738–746. https://doi.org/10.1046/j.1471-4159.2002.01183.x

Sekiguchi, H., Pavey, G., & Dean, B. (2019). Altered levels of dopamine transporter in the frontal pole and dorsal striatum in schizophrenia. *Npj Schizophrenia*, *5*(1), Article 1. https://doi.org/10.1038/s41537-019-0087-7

Selkoe, D. J., & Hardy, J. (2016). The amyloid hypothesis of Alzheimer's disease at 25 years. *EMBO Molecular Medicine*, *8*(6), 595–608. https://doi.org/10.15252/emmm.201606210

Sengoku, R. (2020). Aging and Alzheimer's disease pathology. *Neuropathology*, *40*(1), 22–29. https://doi.org/10.1111/neup.12626

Senkowski, D., & Gallinat, J. (2015). Dysfunctional Prefrontal Gamma-Band Oscillations Reflect Working Memory and Other Cognitive Deficits in Schizophrenia. *Biological Psychiatry*, *77*(12), 1010–1019. https://doi.org/10.1016/j.biopsych.2015.02.034

Sesack, S. R., & Carr, D. B. (2002). Selective prefrontal cortex inputs to dopamine cells: Implications for schizophrenia. *Physiology & Behavior*, *77*(4), 513–517. https://doi.org/10.1016/S0031-9384(02)00931-9

Shi, S., Grothe, S., Zhang, Y., O'Connor-McCourt, M. D., Poole, A. R., Roughley, P. J., & Mort, J. S. (2004). Link Protein Has Greater Affinity for Versican than Aggrecan *. *Journal of Biological Chemistry*, *279*(13), 12060–12066. https://doi.org/10.1074/jbc.M310091200

Shi, W., Wei, X., Wang, X., Du, S., Liu, W., Song, J., & Wang, Y. (2019a). Perineuronal nets protect long-term memory by limiting activity-dependent inhibition from parvalbumin interneurons. *Proceedings of the National Academy of Sciences*, *116*(52), 27063–27073. https://doi.org/10.1073/pnas.1902680116

Shi, W., Wei, X., Wang, X., Du, S., Liu, W., Song, J., & Wang, Y. (2019b). Perineuronal nets protect long-term memory by limiting activity-dependent inhibition from parvalbumin interneurons. *Proceedings of the National Academy of Sciences*, *116*(52), 27063–27073. https://doi.org/10.1073/pnas.1902680116

Shibata, S., Fukada, K., Imai, H., Abe, T., & Yamashita, Y. (2003). In situ hybridization and immunohistochemistry of versican, aggrecan and link protein, and histochemistry of hyaluronan in the developing mouse limb bud cartilage. *Journal of Anatomy*, *203*(4), 425–432. https://doi.org/10.1046/j.1469-7580.2003.00226.x

Shin, S.-W., Kim, D.-H., Jeon, W. K., & Han, J.-S. (2020). 4-Hydroxynonenal Immunoreactivity Is Increased in the Frontal Cortex of 5XFAD Transgenic Mice. *Biomedicines*, *8*(9), Article 9. https://doi.org/10.3390/biomedicines8090326

Sigal, Y. M., Bae, H., Bogart, L. J., Hensch, T. K., & Zhuang, X. (2019). Structural maturation of cortical perineuronal nets and their perforating synapses revealed by superresolution

imaging. *Proceedings of the National Academy of Sciences*, *116*(14), 7071–7076. https://doi.org/10.1073/pnas.1817222116

Sik, A., Penttonen, M., Ylinen, A., & Buzsaki, G. (1995). Hippocampal CA1 interneurons: An in vivo intracellular labeling study. *Journal of Neuroscience*, *15*(10), 6651–6665. https://doi.org/10.1523/JNEUROSCI.15-10-06651.1995

Slaker, M., Blacktop, J. M., & Sorg, B. A. (2016). Caught in the Net: Perineuronal Nets and Addiction. *Neural Plasticity*, *2016*, e7538208. https://doi.org/10.1155/2016/7538208

Slaker, M., Churchill, L., Todd, R. P., Blacktop, J. M., Zuloaga, D. G., Raber, J., Darling, R. A., Brown, T. E., & Sorg, B. A. (2015). Removal of Perineuronal Nets in the Medial Prefrontal Cortex Impairs the Acquisition and Reconsolidation of a Cocaine-Induced Conditioned Place Preference Memory. *Journal of Neuroscience*, *35*(10), 4190–4202. https://doi.org/10.1523/JNEUROSCI.3592-14.2015

Smucny, J., Dienel, S. J., Lewis, D. A., & Carter, C. S. (2022). Mechanisms underlying dorsolateral prefrontal cortex contributions to cognitive dysfunction in schizophrenia. *Neuropsychopharmacology*, *47*(1), Article 1. https://doi.org/10.1038/s41386-021-01089-0

Sohal, V. S., Zhang, F., Yizhar, O., & Deisseroth, K. (2009). Parvalbumin neurons and gamma rhythms enhance cortical circuit performance. *Nature*, *459*(7247), Article 7247. https://doi.org/10.1038/nature07991

Solodkin, A., Veldhuizen, S. D., & Hoesen, G. W. V. (1996). Contingent Vulnerability of Entorhinal Parvalbumin-Containing Neurons in Alzheimer's Disease. *Journal of Neuroscience*, *16*(10), 3311–3321. https://doi.org/10.1523/JNEUROSCI.16-10-03311.1996

Son, Y., Kim, J. S., Jeong, Y. J., Jeong, Y. K., Kwon, J. H., Choi, H.-D., Pack, J.-K., Kim, N., Lee, Y.-S., & Lee, H.-J. (2018). Long-term RF exposure on behavior and cerebral glucose metabolism in 5xFAD mice. *Neuroscience Letters*, *666*, 64–69. https://doi.org/10.1016/j.neulet.2017.12.042

Song, I., & Dityatev, A. (2018). Crosstalk between glia, extracellular matrix and neurons. *Brain Research Bulletin*, *136*, 101–108. https://doi.org/10.1016/j.brainresbull.2017.03.003

Sorg, B. A., Berretta, S., Blacktop, J. M., Fawcett, J. W., Kitagawa, H., Kwok, J. C. F., & Miquel, M. (2016a). Casting a Wide Net: Role of Perineuronal Nets in Neural Plasticity. *The Journal of Neuroscience*, *36*(45), 11459–11468. https://doi.org/10.1523/JNEUROSCI.2351-16.2016

Sorg, B. A., Berretta, S., Blacktop, J. M., Fawcett, J. W., Kitagawa, H., Kwok, J. C. F., & Miquel, M. (2016b). Casting a Wide Net: Role of Perineuronal Nets in Neural Plasticity. *The Journal of Neuroscience*, *36*(45), 11459–11468. https://doi.org/10.1523/JNEUROSCI.2351-16.2016

Sos, K. E., Mayer, M. I., Takács, V. T., Major, A., Bardóczi, Z., Beres, B. M., Szeles, T., Saito, T., Saido, T. C., Mody, I., Freund, T. F., & Nyiri, G. (2020). Amyloid β induces interneuron-specific changes in the hippocampus of APPNL-F mice. *PLOS ONE*, *15*(5), e0233700. https://doi.org/10.1371/journal.pone.0233700

Speers, L. J., & Bilkey, D. K. (2021). Disorganization of Oscillatory Activity in Animal Models of Schizophrenia. *Frontiers in Neural Circuits*, *15*. https://www.frontiersin.org/articles/10.3389/fncir.2021.741767

Spencer, K. M., Niznikiewicz, M. A., Nestor, P. G., Shenton, M. E., & McCarley, R. W. (2009). Left auditory cortex gamma synchronization and auditory hallucination symptoms in schizophrenia. *BMC Neuroscience*, *10*(1), 85. https://doi.org/10.1186/1471-2202-10-85

Spires-Jones, T., & Knafo, S. (2011). Spines, Plasticity, and Cognition in Alzheimer's Model Mice. *Neural Plasticity*, *2012*, e319836. https://doi.org/10.1155/2012/319836

Spreng, R. N., Mar, R. A., & Kim, A. S. N. (2009). The Common Neural Basis of Autobiographical Memory, Prospection, Navigation, Theory of Mind, and the Default Mode: A Quantitative Meta-analysis. *Journal of Cognitive Neuroscience*, *21*(3), 489–510. https://doi.org/10.1162/jocn.2008.21029

Stacho, M., & Manahan-Vaughan, D. (2022). Mechanistic flexibility of the retrosplenial cortex enables its contribution to spatial cognition. *Trends in Neurosciences*, *45*(4), 284–296. https://doi.org/10.1016/j.tins.2022.01.007

Stamenkovic, V., Milenkovic, I., Galjak, N., Todorovic, V., & Andjus, P. (2017). Enriched environment alters the behavioral profile of tenascin-C deficient mice. *Behavioural Brain Research*, *331*, 241–253. https://doi.org/10.1016/j.bbr.2017.05.047

Stanton, H., Melrose, J., Little, C. B., & Fosang, A. J. (2011). Proteoglycan degradation by the ADAMTS family of proteinases. *Biochimica et Biophysica Acta (BBA) - Molecular Basis of Disease*, *1812*(12), 1616–1629. https://doi.org/10.1016/j.bbadis.2011.08.009

Steullet, P., Cabungcal, J., Coyle, J., Didriksen, M., Gill, A., Grace, A., Hensch, T., LaMantia, A., Lindemann, L., Maynard, T., Meyer, U., Morishita, H., Puhl, M., Cuenod, M., & Do, K. (2017). Oxidative stress-driven parvalbumin interneuron impairment as a common mechanism in models of schizophrenia. *Molecular Psychiatry*, *22*, 936–943.

Steullet, P., Cabungcal, J.-H., Bukhari, S. A., Ardelt, M. I., Pantazopoulos, H., Hamati, F., Salt, T. E., Cuenod, M., Do, K. Q., & Berretta, S. (2018). The thalamic reticular nucleus in schizophrenia and bipolar disorder: Role of parvalbumin-expressing neuron networks and oxidative stress. *Molecular Psychiatry*, *23*(10), Article 10. https://doi.org/10.1038/mp.2017.230

Steullet, P., Cabungcal, J.-H., Coyle, J., Didriksen, M., Gill, K., Grace, A. A., Hensch, T. K., LaMantia, A.-S., Lindemann, L., Maynard, T. M., Meyer, U., Morishita, H., O'Donnell, P., Puhl, M., Cuenod, M., & Do, K. Q. (2017). Oxidative stress-driven parvalbumin interneuron impairment as a common mechanism in models of schizophrenia. *Molecular Psychiatry*, *22*(7), Article 7. https://doi.org/10.1038/mp.2017.47

Steullet, P., Cabungcal, J.-H., Cuénod, M., & Do, K. Q. (2014). Fast oscillatory activity in the anterior cingulate cortex: Dopaminergic modulation and effect of perineuronal net loss. *Frontiers in Cellular Neuroscience*, *8*. https://www.frontiersin.org/articles/10.3389/fncel.2014.00244

Steullet, P., Cabungcal, J.-H., Cuenod, M., & Do, K. Q. (2014). Fast oscillatory activity in the anterior cingulate cortex: Dopaminergic modulation and effect of perineuronal net loss. *Frontiers in Cellular Neuroscience*, *8*. https://doi.org/10.3389/fncel.2014.00244

Stevens, R., & Cowey, A. (1973). Effects of dorsal and ventral hippocampal lesions on spontaneous alternation, learned alternation and probability learning in rats. *Brain Research*, *52*, 203–224. https://doi.org/10.1016/0006-8993(73)90659-8

Strekalova, T. (2002). Fibronectin Domains of Extracellular Matrix Molecule Tenascin-C Modulate Hippocampal Learning and Synaptic Plasticity. *Molecular and Cellular Neuroscience*, *21*(1), 173–187. https://doi.org/10.1006/mcne.2002.1172

Sun, Q., Zhang, J., Li, A., Yao, M., Liu, G., Chen, S., Luo, Y., Wang, Z., Gong, H., Li, X., & Luo, Q. (2022). Acetylcholine deficiency disrupts extratelencephalic projection neurons in the prefrontal cortex in a mouse model of Alzheimer's disease. *Nature Communications*, *13*(1), Article 1. https://doi.org/10.1038/s41467-022-28493-4

Sun, Y., Farzan, F., Barr, M. S., Kirihara, K., Fitzgerald, P. B., Light, G. A., & Daskalakis, Z. J. (2011). Gamma oscillations in schizophrenia: Mechanisms and clinical significance. *Brain Research*, *1413*, 98–114. https://doi.org/10.1016/j.brainres.2011.06.065

Sun, Z. Y., Bozzelli, P. L., Caccavano, A., Allen, M., Balmuth, J., Vicini, S., Wu, J.-Y., & Conant, K. (2018). Disruption of perineuronal nets increases the frequency of sharp wave ripple events. *Hippocampus*, *28*(1), 42–52. https://doi.org/10.1002/hipo.22804

Sur, M., Frost, D. O., & Hockfield, S. (1988). Expression of a surface-associated antigen on Y-cells in the cat lateral geniculate nucleus is regulated by visual experience. *Journal of Neuroscience*, *8*(3), 874–882. https://doi.org/10.1523/JNEUROSCI.08-03-00874.1988

Suttkus, A., Holzer, M., Morawski, M., & Arendt, T. (2016). The neuronal extracellular matrix restricts distribution and internalization of aggregated Tau-protein. *Neuroscience*, *313*, 225–235. https://doi.org/10.1016/j.neuroscience.2015.11.040

Suttkus, A., Morawski, M., & Arendt, T. (2016). Protective Properties of Neural Extracellular Matrix. *Molecular Neurobiology*, *53*(1), 73–82. https://doi.org/10.1007/s12035-014-8990-4

Suttkus, A., Rohn, S., Jäger, C., Arendt, T., & Morawski, M. (2012). Neuroprotection against iron-induced cell death by perineuronal nets-an in vivo analysis of oxidative stress. *American Journal of Neurodegenerative Disease*, *1*(2), 122.

Suttkus, A., Rohn, S., Weigel, S., Glöckner, P., Arendt, T., & Morawski, M. (2014). Aggrecan, link protein and tenascin-R are essential components of the perineuronal net to protect neurons against iron-induced oxidative stress. *Cell Death & Disease*, *5*(3), Article 3. https://doi.org/10.1038/cddis.2014.25

Swerdlow, N., Geyer, M., & Braff, D. (2001a). Neural circuit regulation of prepulse inhibition of startle in the rat: Current knowledge and future challenges. *Psychopharmacology*, *156*(2–3), 194–215. https://doi.org/10.1007/s002130100799

Swerdlow, N., Geyer, M., & Braff, D. (2001b). Neural circuit regulation of prepulse inhibition of startle in the rat: Current knowledge and future challenges. *Psychopharmacology*, *156*(2), 194–215. https://doi.org/10.1007/s002130100799

Swerdlow, N. R., Braff, D. L., Taaid, N., & Geyer, M. A. (1994). Assessing the Validity of an Animal Model of Deficient Sensorimotor Gating in Schizophrenic Patients. *Archives of General Psychiatry*, *51*(2), 139–154. https://doi.org/10.1001/archpsyc.1994.03950020063007

Swerdlow, N. R., Light, G. A., Sprock, J., Calkins, M. E., Green, M. F., Greenwood, T. A., Gur, R. E., Gur, R. C., Lazzeroni, L. C., Nuechterlein, K. H., Radant, A. D., Ray, A., Seidman, L. J., Siever, L. J., Silverman, J. M., Stone, W. S., Sugar, C. A., Tsuang, D. W., Tsuang, M. T., … Braff, D. L. (2014). Deficient prepulse inhibition in schizophrenia detected by the multi-site COGS. *Schizophrenia Research*, *152*(2), 503–512. https://doi.org/10.1016/j.schres.2013.12.004

Tajerian, M., Hung, V., Nguyen, H., Lee, G., Joubert, L.-M., Malkovskiy, A. V., Zou, B., Xie, S., Huang, T.-T., & Clark, J. D. (2018). The hippocampal extracellular matrix regulates

pain and memory after injury. *Molecular Psychiatry*, *23*(12), Article 12. https://doi.org/10.1038/s41380-018-0209-z

Takahashi, H., Brasnjevic, I., Rutten, B. P. F., Van Der Kolk, N., Perl, D. P., Bouras, C., Steinbusch, H. W. M., Schmitz, C., Hof, P. R., & Dickstein, D. L. (2010). Hippocampal interneuron loss in an APP/PS1 double mutant mouse and in Alzheimer's disease. *Brain Structure and Function*, *214*(2), 145–160. https://doi.org/10.1007/s00429-010-0242-4

Takesian, A. E., & Hensch, T. K. (2013a). Balancing plasticity/stability across brain development. In *Progress in Brain Research* (Vol. 207, pp. 3–34). Elsevier. https://doi.org/10.1016/B978-0-444-63327-9.00001-1

Takesian, A. E., & Hensch, T. K. (2013b). Balancing Plasticity/Stability Across Brain Development. In *Progress in Brain Research* (Vol. 207, pp. 3–34). Elsevier. https://doi.org/10.1016/B978-0-444-63327-9.00001-1

Tallon-Baudry, C., & Bertrand, O. (1999). Oscillatory gamma activity in humans and its role in object representation. *Trends in Cognitive Sciences*, *3*(4), 151–162. https://doi.org/10.1016/S1364-6613(99)01299-1

Tamamaki, N., Yanagawa, Y., Tomioka, R., Miyazaki, J.-I., Obata, K., & Kaneko, T. (2003). Green fluorescent protein expression and colocalization with calretinin, parvalbumin, and somatostatin in the GAD67-GFP knock-in mouse. *Journal of Comparative Neurology*, *467*(1), 60–79. https://doi.org/10.1002/cne.10905

Taylor, K. I., Moss, H. E., Stamatakis, E. A., & Tyler, L. K. (2006). Binding crossmodal object features in perirhinal cortex. *Proceedings of the National Academy of Sciences*, *103*(21), 8239–8244. https://doi.org/10.1073/pnas.0509704103

Testa, D., Prochiantz, A., & Di Nardo, A. A. (2019). Perineuronal nets in brain physiology and disease. *Seminars in Cell & Developmental Biology*, *89*, 125–135. https://doi.org/10.1016/j.semcdb.2018.09.011

Thai, C. A., Zhang, Y., & Howland, J. G. (2013). Effects of acute restraint stress on set-shifting and reversal learning in male rats. *Cognitive, Affective, & Behavioral Neuroscience*, *13*(1), 164–173. https://doi.org/10.3758/s13415-012-0124-8

Thompson, E. H., Lensjø, K. K., Wigestrand, M. B., Malthe-Sørenssen, A., Hafting, T., & Fyhn, M. (2018). Removal of perineuronal nets disrupts recall of a remote fear memory. *Proceedings of the National Academy of Sciences*, *115*(3), 607–612. https://doi.org/10.1073/pnas.1713530115

Thompson, M., Weickert, C. S., Wyatt, E., & Webster, M. J. (2009). Decreased glutamic acid decarboxylase67 mRNA expression in multiple brain areas of patients with schizophrenia and mood disorders. *Journal of Psychiatric Research*, *43*(11), 970–977. https://doi.org/10.1016/j.jpsychires.2009.02.005

Tian, Y., Yang, C., Cui, Y., Su, F., Wang, Y., Wang, Y., Yuan, P., Shang, S., Li, H., Zhao, J., Zhu, D., Tang, S., Cao, P., Liu, Y., Wang, X., Wang, L., Zeng, W., Jiang, H., Zhao, F., … Zhang, C. (2018). An Excitatory Neural Assembly Encodes Short-Term Memory in the Prefrontal Cortex. *Cell Reports*, *22*(7), 1734–1744. https://doi.org/10.1016/j.celrep.2018.01.050

Tooney, P. A., & Chahl, L. A. (2004). Neurons expressing calcium-binding proteins in the prefrontal cortex in schizophrenia. *Progress in Neuro-Psychopharmacology and Biological Psychiatry*, *28*(2), 273–278. https://doi.org/10.1016/j.pnpbp.2003.10.004

Torres-Flores, M., & Peña-Ortega, F. (2022). Amyloid Beta Alters Prefrontal-dependent Functions Along with its Excitability and Synaptic Plasticity in Male Rats. *Neuroscience*, *498*, 260–279. https://doi.org/10.1016/j.neuroscience.2022.07.006

Trask, S., & Fournier, D. I. (2022). Examining a role for the retrosplenial cortex in age-related memory impairment. *Neurobiology of Learning and Memory*, *189*, 107601. https://doi.org/10.1016/j.nlm.2022.107601

Traub, R. D., Whittington, M. A., Colling, S. B., Buzsáki, G., & Jefferys, J. G. (1996). Analysis of gamma rhythms in the rat hippocampus in vitro and in vivo. *The Journal of Physiology*, *493*(2), 471–484. https://doi.org/10.1113/jphysiol.1996.sp021397

Tremblay, M.-È., Stevens, B., Sierra, A., Wake, H., Bessis, A., & Nimmerjahn, A. (2011). The role of microglia in the healthy brain. *The Journal of Neuroscience: The Official Journal of the Society for Neuroscience*, *31*(45), 16064–16069. https://doi.org/10.1523/JNEUROSCI.4158-11.2011

Troy Harker, K., & Whishaw, I. Q. (2004). A reaffirmation of the retrosplenial contribution to rodent navigation: Reviewing the influences of lesion, strain, and task. *Neuroscience & Biobehavioral Reviews*, *28*(5), 485–496. https://doi.org/10.1016/j.neubiorev.2004.06.005

Tsien, R. Y. (2013). Very long-term memories may be stored in the pattern of holes in the perineuronal net. *Proceedings of the National Academy of Sciences*, *110*(30), 12456–12461. https://doi.org/10.1073/pnas.1310158110

Tukker, J. J., Lasztóczi, B., Katona, L., Roberts, J. D. B., Pissadaki, E. K., Dalezios, Y., Márton, L., Zhang, L., Klausberger, T., & Somogyi, P. (2013). Distinct Dendritic Arborization and In Vivo Firing Patterns of Parvalbumin-Expressing Basket Cells in the Hippocampal

Area CA3. *Journal of Neuroscience*, *33*(16), 6809–6825. https://doi.org/10.1523/JNEUROSCI.5052-12.2013

Ueno, H., Suemitsu, S., Okamoto, M., Matsumoto, Y., & Ishihara, T. (2017). Sensory experience-dependent formation of perineuronal nets and expression of Cat-315 immunoreactive components in the mouse somatosensory cortex. *Neuroscience*, *355*, 161–174. https://doi.org/10.1016/j.neuroscience.2017.04.041

Uhlhaas, P. J., Haenschel, C., Nikolić, D., & Singer, W. (2008). The Role of Oscillations and Synchrony in Cortical Networks and Their Putative Relevance for the Pathophysiology of Schizophrenia. *Schizophrenia Bulletin*, *34*(5), 927–943. https://doi.org/10.1093/schbul/sbn062

Uhlhaas, P. J., & Singer, W. (2015). Oscillations and Neuronal Dynamics in Schizophrenia: The Search for Basic Symptoms and Translational Opportunities. *Biological Psychiatry*, *77*(12), 1001–1009. https://doi.org/10.1016/j.biopsych.2014.11.019

Urano, T., & Tohda, C. (2010). Icariin improves memory impairment in Alzheimer's disease model mice (5xFAD) and attenuates amyloid β-induced neurite atrophy. *Phytotherapy Research*, *24*(11), 1658–1663. https://doi.org/10.1002/ptr.3183

Van Der Staay, F. J., & Steckler, T. (2002). The fallacy of behavioral phenotyping without standardisation. *Genes, Brain and Behavior*, *1*(1), 9–13. https://doi.org/10.1046/j.1601-1848.2001.00007.x

Vann, S. D., & Aggleton, J. P. (2002). Extensive cytotoxic lesions of the rat retrosplenial cortex reveal consistent deficits on tasks that tax allocentric spatial memory. *Behavioral Neuroscience*, *116*, 85–94. https://doi.org/10.1037/0735-7044.116.1.85

Vann, S. D., Aggleton, J. P., & Maguire, E. A. (2009). What does the retrosplenial cortex do? *Nature Reviews Neuroscience*, *10*(11), Article 11. https://doi.org/10.1038/nrn2733

Végh, M. J., Heldring, C. M., Kamphuis, W., Hijazi, S., Timmerman, A. J., Li, K. W., van Nierop, P., Mansvelder, H. D., Hol, E. M., Smit, A. B., & van Kesteren, R. E. (2014). Reducing hippocampal extracellular matrix reverses early memory deficits in a mouse model of Alzheimer's disease. *Acta Neuropathologica Communications*, *2*(1), 76. https://doi.org/10.1186/s40478-014-0076-z

Venturino, A., Schulz, R., De Jesús-Cortés, H., Maes, M. E., Nagy, B., Reilly-Andújar, F., Colombo, G., Cubero, R. J. A., Schoot Uiterkamp, F. E., Bear, M. F., & Siegert, S. (2021). Microglia enable mature perineuronal nets disassembly upon anesthetic ketamine exposure or 60-Hz light entrainment in the healthy brain. *Cell Reports*, *36*(1), 109313. https://doi.org/10.1016/j.celrep.2021.109313

Verma, P., & Dalal, K. (2011). ADAMTS-4 and ADAMTS-5: Key enzymes in osteoarthritis. *Journal of Cellular Biochemistry*, *112*(12), 3507–3514. https://doi.org/10.1002/jcb.23298

Verret, L., Mann, E. O., Hang, G. B., Barth, A. M. I., Cobos, I., Ho, K., Devidze, N., Masliah, E., Kreitzer, A. C., Mody, I., Mucke, L., & Palop, J. J. (2012). Inhibitory Interneuron Deficit Links Altered Network Activity and Cognitive Dysfunction in Alzheimer Model. *Cell*, *149*(3), 708–721. https://doi.org/10.1016/j.cell.2012.02.046

Volk, D. W., Austin, M. C., Pierri, J. N., Sampson, A. R., & Lewis, D. A. (2000). Decreased Glutamic Acid Decarboxylase67 Messenger RNA Expression in a Subset of Prefrontal Cortical ^{3}-Aminobutyric Acid Neurons in Subjects With Schizophrenia. *ARCH GEN PSYCHIATRY*, *57*, 9.

Volman, V., Behrens, M. M., & Sejnowski, T. J. (2011). Downregulation of Parvalbumin at Cortical GABA Synapses Reduces Network Gamma Oscillatory Activity. *Journal of Neuroscience*, *31*(49), 18137–18148. https://doi.org/10.1523/JNEUROSCI.3041-11.2011

Vorhees, C. V., Graham, D. L., Braun, A. A., Schaefer, T. L., Skelton, M. R., Richtand, N. M., & Williams, M. T. (2015). Prenatal immune challenge in rats: Effects of polyinosinic–polycytidylic acid on spatial learning, prepulse inhibition, conditioned fear, and responses to MK-801 and amphetamine. *Neurotoxicology and Teratology*, *47*, 54–65. https://doi.org/10.1016/j.ntt.2014.10.007

Vreugdenhil, M., Jefferys, J. G. R., Celio, M. R., & Schwaller, B. (2003). Parvalbumin-Deficiency Facilitates Repetitive IPSCs and Gamma Oscillations in the Hippocampus. *Journal of Neurophysiology*, *89*(3), 1414–1422. https://doi.org/10.1152/jn.00576.2002

Wang, D., & Fawcett, J. (2012a). The perineuronal net and the control of CNS plasticity. *Cell and Tissue Research*, *349*(1), 147–160. https://doi.org/10.1007/s00441-012-1375-y

Wang, D., & Fawcett, J. (2012b). The perineuronal net and the control of CNS plasticity. *Cell and Tissue Research*, *349*(1), 147–160. https://doi.org/10.1007/s00441-012-1375-y

Wang, D.-S., Dickson, D. W., & Malter, J. S. (2006). β -Amyloid Degradation and Alzheimer's Disease. *Journal of Biomedicine and Biotechnology*, *2006*, 1–12. https://doi.org/10.1155/JBB/2006/58406

Wang, H., Katagiri, Y., McCann, T. E., Unsworth, E., Goldsmith, P., Yu, Z.-X., Tan, F., Santiago, L., Mills, E. M., Wang, Y., Symes, A. J., & Geller, H. M. (2008). Chondroitin-4-sulfation negatively regulates axonal guidance and growth. *Journal of Cell Science*, *121*(18), 3083–3091. https://doi.org/10.1242/jcs.032649

Wang, H.-X., & Gao, W.-J. (2009). Cell Type-Specific Development of NMDA Receptors in the Interneurons of Rat Prefrontal Cortex. *Neuropsychopharmacology*, *34*(8), Article 8. https://doi.org/10.1038/npp.2009.20

Wang, W.-Y., Tan, M.-S., Yu, J.-T., & Tan, L. (2015). Role of pro-inflammatory cytokines released from microglia in Alzheimer's disease. *Annals of Translational Medicine*, *3*(10), 136. https://doi.org/10.3978/j.issn.2305-5839.2015.03.49

Wang, X.-X., Tan, M.-S., Yu, J.-T., & Tan, L. (2014). Matrix Metalloproteinases and Their Multiple Roles in Alzheimer's Disease. *BioMed Research International*, *2014*, 908636. https://doi.org/10.1155/2014/908636

Weber, P., Bartsch, U., Rasband, M. N., Czaniera, R., Lang, Y., Bluethmann, H., Margolis, R. U., Levinson, S. R., Shrager, P., Montag, D., & Schachner, M. (1999). Mice Deficient for Tenascin-R Display Alterations of the Extracellular Matrix and Decreased Axonal Conduction Velocities in the CNS. *Journal of Neuroscience*, *19*(11), 4245–4262. https://doi.org/10.1523/JNEUROSCI.19-11-04245.1999

Wen, T. H., Afroz, S., Reinhard, S. M., Palacios, A. R., Tapia, K., Binder, D. K., Razak, K. A., & Ethell, I. M. (2018). Genetic Reduction of Matrix Metalloproteinase-9 Promotes Formation of Perineuronal Nets Around Parvalbumin-Expressing Interneurons and Normalizes Auditory Cortex Responses in Developing Fmr1 Knock-Out Mice. *Cerebral Cortex*, *28*(11), 3951–3964. https://doi.org/10.1093/cercor/bhx258

Wen, T. H., Binder, D. K., Ethell, I. M., & Razak, K. A. (2018). The Perineuronal 'Safety' Net? Perineuronal Net Abnormalities in Neurological Disorders. *Frontiers in Molecular Neuroscience*, *11*. https://www.frontiersin.org/articles/10.3389/fnmol.2018.00270

West, S. L., Aronson, J. D., Popa, L. S., Feller, K. D., Carter, R. E., Chiesl, W. M., Gerhart, M. L., Shekhar, A. C., Ghanbari, L., Kodandaramaiah, S. B., & Ebner, T. J. (2022). Wide-Field Calcium Imaging of Dynamic Cortical Networks during Locomotion. *Cerebral Cortex*, *32*(12), 2668–2687. https://doi.org/10.1093/cercor/bhab373

Westling, J., Fosang, A. J., Last, K., Thompson, V. P., Tomkinson, K. N., Hebert, T., McDonagh, T., Collins-Racie, L. A., LaVallie, E. R., Morris, E. A., & Sandy, J. D. (2002). ADAMTS4 Cleaves at the Aggrecanase Site (Glu373-Ala374) and Secondarily at the Matrix Metalloproteinase Site (Asn341-Phe342) in the Aggrecan Interglobular Domain *. *Journal of Biological Chemistry*, *277*(18), 16059–16066. https://doi.org/10.1074/jbc.M108607200

Whishaw, I. Q., & Tomie, J.-A. (1996). Of Mice and Mazes: Similarities Between Mice and Rats on Dry Land But Not Water Mazes. *Physiology & Behavior*, *60*(5), 1191–1197. https://doi.org/10.1016/S0031-9384(96)00176-X

White, T., Magnotta, V. A., Bockholt, H. J., Williams, S., Wallace, S., Ehrlich, S., Mueller, B. A., Ho, B.-C., Jung, R. E., Clark, V. P., Lauriello, J., Bustillo, J. R., Schulz, S. C., Gollub, R. L., Andreasen, N. C., Calhoun, V. D., & Lim, K. O. (2011). Global White Matter Abnormalities in Schizophrenia: A Multisite Diffusion Tensor Imaging Study. *Schizophrenia Bulletin*, *37*(1), 222–232. https://doi.org/10.1093/schbul/sbp088

Whitfield-Gabrieli, S., Thermenos, H. W., Milanovic, S., Tsuang, M. T., Faraone, S. V., McCarley, R. W., Shenton, M. E., Green, A. I., Nieto-Castanon, A., LaViolette, P., Wojcik, J., Gabrieli, J. D. E., & Seidman, L. J. (2009). Hyperactivity and hyperconnectivity of the default network in schizophrenia and in first-degree relatives of

persons with schizophrenia. *Proceedings of the National Academy of Sciences*, *106*(4), 1279–1284. https://doi.org/10.1073/pnas.0809141106

Whittington, M. A., Traub, R. D., Kopell, N., Ermentrout, B., & Buhl, E. H. (2000). Inhibition-based rhythms: Experimental and mathematical observations on network dynamics. *International Journal of Psychophysiology*, *38*(3), 315–336. https://doi.org/10.1016/S0167-8760(00)00173-2

Williams, S., & Boksa, P. (2010). Gamma oscillations and schizophrenia. *Journal of Psychiatry and Neuroscience*, *35*(2), 75–77. https://doi.org/10.1503/jpn.100021

Wingert, J. C., & Sorg, B. A. (2021). Impact of Perineuronal Nets on Electrophysiology of Parvalbumin Interneurons, Principal Neurons, and Brain Oscillations: A Review. *Frontiers in Synaptic Neuroscience*, *13*. https://www.frontiersin.org/articles/10.3389/fnsyn.2021.673210

Winship, I. R., Dursun, S. M., Baker, G. B., Balista, P. A., Kandratavicius, L., Maia-de-Oliveira, J. P., Hallak, J., & Howland, J. G. (2018). An Overview of Animal Models Related to Schizophrenia. *The Canadian Journal of Psychiatry*, 070674371877372. https://doi.org/10.1177/0706743718773728

Winters, B. D., & Reid, J. M. (2010a). A Distributed Cortical Representation Underlies Crossmodal Object Recognition in Rats. *Journal of Neuroscience*, *30*(18), 6253–6261. https://doi.org/10.1523/JNEUROSCI.6073-09.2010

Winters, B. D., & Reid, J. M. (2010b). A Distributed Cortical Representation Underlies Crossmodal Object Recognition in Rats. *Journal of Neuroscience*, *30*(18), 6253–6261. https://doi.org/10.1523/JNEUROSCI.6073-09.2010

Wolff, A. R., & Bilkey, D. K. (2008). Immune activation during mid-gestation disrupts sensorimotor gating in rat offspring. *Behavioural Brain Research*, *190*(1), 156–159. https://doi.org/10.1016/j.bbr.2008.02.021

Wolff, A. R., Cheyne, K. R., & Bilkey, D. K. (2011). Behavioural deficits associated with maternal immune activation in the rat model of schizophrenia. *Behavioural Brain Research*, *225*(1), 382–387. https://doi.org/10.1016/j.bbr.2011.07.033

Woo, T.-U. W., Walsh, J. P., & Benes, F. M. (2004). Density of Glutamic Acid Decarboxylase 67 Messenger RNA–ContainingNeurons That Express the N-Methyl-D-AspartateReceptor Subunit NR2A in the Anterior Cingulate Cortex in Schizophreniaand Bipolar Disorder. *Archives of General Psychiatry*, *61*(7), 649–657. https://doi.org/10.1001/archpsyc.61.7.649

Xu, D., Hopf, C., Reddy, R., Cho, R. W., Guo, L., Lanahan, A., Petralia, R. S., Wenthold, R. J., O'Brien, R. J., & Worley, P. (2003). Narp and NP1 Form Heterocomplexes that Function in Developmental and Activity-Dependent Synaptic Plasticity. *Neuron*, *39*(3), 513–528. https://doi.org/10.1016/S0896-6273(03)00463-X

Xue, Y.-X., Xue, L.-F., Liu, J.-F., He, J., Deng, J.-H., Sun, S.-C., Han, H.-B., Luo, Y.-X., Xu, L.-Z., Wu, P., & Lu, L. (2014). Depletion of Perineuronal Nets in the Amygdala to Enhance the Erasure of Drug Memories. *Journal of Neuroscience*, *34*(19), 6647–6658. https://doi.org/10.1523/JNEUROSCI.5390-13.2014

Yamada, J., Ohgomori, T., & Jinno, S. (2015). Perineuronal nets affect parvalbumin expression in GABAergic neurons of the mouse hippocampus. *European Journal of Neuroscience*, *41*(3), 368–378. https://doi.org/10.1111/ejn.12792

Yamaguchi, Y. (2000). Lecticans: Organizers of the brain extracellular matrix. *Cellular and Molecular Life Sciences CMLS*, *57*(2), 276–289. https://doi.org/10.1007/PL00000690

Yang, J.-W., Prouvot, P.-H., Reyes-Puerta, V., Stüttgen, M. C., Stroh, A., & Luhmann, H. J. (2017). Optogenetic Modulation of a Minor Fraction of Parvalbumin-Positive Interneurons Specifically Affects Spatiotemporal Dynamics of Spontaneous and Sensory-Evoked Activity in Mouse Somatosensory Cortex in Vivo. *Cerebral Cortex*, *27*(12), 5784–5803. https://doi.org/10.1093/cercor/bhx261

Yang, S., Cacquevel, M., Saksida, L. M., Bussey, T. J., Schneider, B. L., Aebischer, P., Melani, R., Pizzorusso, T., Fawcett, J. W., & Spillantini, M. G. (2015). Perineuronal net digestion with chondroitinase restores memory in mice with tau pathology. *Experimental Neurology*, *265*, 48–58. https://doi.org/10.1016/j.expneurol.2014.11.013

Yang, S., Gigout, S., Molinaro, A., Naito-Matsui, Y., Hilton, S., Foscarin, S., Nieuwenhuis, B., Tan, C. L., Verhaagen, J., Pizzorusso, T., Saksida, L. M., Bussey, T. M., Kitagawa, H., Kwok, J. C. F., & Fawcett, J. W. (2021). Chondroitin 6-sulphate is required for neuroplasticity and memory in ageing. *Molecular Psychiatry*, *26*(10), Article 10. https://doi.org/10.1038/s41380-021-01208-9

Yang, S., Hilton, S., Alves, J. N., Saksida, L. M., Bussey, T., Matthews, R. T., Kitagawa, H., Spillantini, M. G., Kwok, J. C. F., & Fawcett, J. W. (2017). Antibody recognizing 4-sulfated chondroitin sulfate proteoglycans restores memory in tauopathy-induced neurodegeneration. *Neurobiology of Aging*, *59*, 197–209. https://doi.org/10.1016/j.neurobiolaging.2017.08.002

Yang, S.-T., Shi, Y., Wang, Q., Peng, J.-Y., & Li, B.-M. (2014a). Neuronal representation of working memory in the medial prefrontal cortex of rats. *Molecular Brain*, *7*(1), 61. https://doi.org/10.1186/s13041-014-0061-2

Yang, S.-T., Shi, Y., Wang, Q., Peng, J.-Y., & Li, B.-M. (2014b). Neuronal representation of working memory in the medial prefrontal cortex of rats. *Molecular Brain*, *7*(1), 61. https://doi.org/10.1186/s13041-014-0061-2

Yang, S.-T., Shi, Y., Wang, Q., Peng, J.-Y., & Li, B.-M. (2014c). Neuronal representation of working memory in the medial prefrontal cortex of rats. *Molecular Brain*, *7*(1). https://doi.org/10.1186/s13041-014-0061-2

Yang, Y., Mufson, E. J., & Herrup, K. (2003). Neuronal Cell Death Is Preceded by Cell Cycle Events at All Stages of Alzheimer's Disease. *Journal of Neuroscience*, *23*(7), 2557–2563. https://doi.org/10.1523/JNEUROSCI.23-07-02557.2003

Yao, J. K., & Reddy, R. (2011). Oxidative Stress in Schizophrenia: Pathogenetic and Therapeutic Implications. *Antioxidants & Redox Signaling*, *15*(7), 1999–2002. https://doi.org/10.1089/ars.2010.3646

Ye, Q., & Miao, Q. (2013). Experience-dependent development of perineuronal nets and chondroitin sulfate proteoglycan receptors in mouse visual cortex. *Matrix Biology*, *32*(6), 352–363. https://doi.org/10.1016/j.matbio.2013.04.001

Yutsudo, N., & Kitagawa, H. (2015). Involvement of chondroitin 6-sulfation in temporal lobe epilepsy. *Experimental Neurology*, *274*, 126–133. https://doi.org/10.1016/j.expneurol.2015.07.009

Zallo, F., Gardenal, E., Verkhratsky, A., & Rodríguez, J. J. (2018). Loss of calretinin and parvalbumin positive interneurones in the hippocampal CA1 of aged Alzheimer's disease mice. *Neuroscience Letters*, *681*, 19–25. https://doi.org/10.1016/j.neulet.2018.05.027

Zhang, L., Gao, Y.-Z., Zhao, C.-J., Xia, J.-Y., Yang, J.-J., & Ji, M.-H. (2023). Reduced inhibitory and excitatory input onto parvalbumin interneurons mediated by perineuronal net might contribute to cognitive impairments in a mouse model of sepsis-associated encephalopathy. *Neuropharmacology*, *225*, 109382. https://doi.org/10.1016/j.neuropharm.2022.109382

Zhang, Y., Cazakoff, B. N., Thai, C. A., & Howland, J. G. (2012a). Prenatal exposure to a viral mimetic alters behavioural flexibility in male, but not female, rats. *Neuropharmacology*, *62*(3), 1299–1307. https://doi.org/10.1016/j.neuropharm.2011.02.022

Zhang, Y., Cazakoff, B. N., Thai, C. A., & Howland, J. G. (2012b). Prenatal exposure to a viral mimetic alters behavioural flexibility in male, but not female, rats. *Neuropharmacology*, *62*(3), 1299–1307. https://doi.org/10.1016/j.neuropharm.2011.02.022

Zhou, X.-H., Brakebusch, C., Matthies, H., Oohashi, T., Hirsch, E., Moser, M., Krug, M., Seidenbecher, C. I., Boeckers, T. M., Rauch, U., Buettner, R., Gundelfinger, E. D., & Fässler, R. (2001). Neurocan Is Dispensable for Brain Development. *Molecular and Cellular Biology*, *21*(17), 5970–5978. https://doi.org/10.1128/MCB.21.17.5970-5978.2001

Zhou, Z., Zhang, G., Li, X., Liu, X., Wang, N., Qiu, L., Liu, W., Zuo, Z., & Yang, J. (2015). Loss of Phenotype of Parvalbumin Interneurons in Rat Prefrontal Cortex Is Involved in Antidepressant- and Propsychotic-Like Behaviors Following Acute and Repeated

Ketamine Administration. *Molecular Neurobiology*, *51*(2), 808–819. https://doi.org/10.1007/s12035-014-8798-2

Zhu, Y., Qiao, W., Liu, K., Zhong, H., & Yao, H. (2015). Control of response reliability by parvalbumin-expressing interneurons in visual cortex. *Nature Communications*, *6*(1), Article 1. https://doi.org/10.1038/ncomms7802

Zimmermann, D. R., & Dours-Zimmermann, M. T. (2008). Extracellular matrix of the central nervous system: From neglect to challenge. *Histochemistry and Cell Biology*, *130*(4), 635–653. https://doi.org/10.1007/s00418-008-0485-9